JUL 8 1946

VOLUME 103 NUMBER 3

THE ASTROPHYSICAL JOURNAL

AN INTERNATIONAL REVIEW OF SPECTROSCOPY AND ASTRONOMICAL PHYSICS

Founded in 1895 by GEORGE E. HALE *and* JAMES E. KEELER

Edited by

OTTO STRUVE
Managing Editor

S. CHANDRASEKHAR
Associate Managing Editor

Yerkes Observatory of the University of Chicago

PAUL W. MERRILL
Mount Wilson Observatory of the Carnegie Institution of Washington

HARLOW SHAPLEY
Harvard College Observatory
Cambridge, Massachusetts

N. U. MAYALL
Lick Observatory
University of California

MAY 1946

THE CORRELATION OF MAGNETIC DISTURBANCES WITH INTENSE EMISSION REGIONS OF THE SOLAR CORONA . . . . *A. H. Shapley and W. O. Roberts* 257

ATOMIC LINES IN THE SPECTRUM OF R LEONIS . . . . . *Paul W. Merrill* 275

THE PHOTOGRAPHIC DETERMINATION OF STELLAR PARALLAXES WITH THE 60- AND 100-INCH REFLECTORS. TWENTIETH SERIES . . *Adriaan van Maanen* 289

THE ECLIPSING STAR RT ANDROMEDAE . . . . . *Cecilia Payne-Gaposchkin* 291

THE SYSTEM OF RX CASSIOPEIAE . . . . . *Cecilia Payne Gaposchkin* 299

ON THE NATURE OF THE ECLIPSES OF ζ AURIGAE . . . . . *Zdeněk Kopal* 310

APPLICATION OF THE MULTIPLIER PHOTOTUBE TO ASTRONOMICAL PHOTOELECTRIC PHOTOMETRY . . . . . *Gerald E. Kron* 326

NEAR THERMODYNAMIC RADIATIVE EQUILIBRIUM . . . . . *L. G. Henyey* 332

ON THE RADIATIVE EQUILIBRIUM OF A STELLAR ATMOSPHERE. X *S. Chandrasekhar* 351

THE SPECTRUM OF CLUSTER-TYPE CEPHEIDS *Guido Münch and Luis Rivera Terrazas* 371

NOTES

MICROWAVE RADIATION FROM THE SUN AND MOON . . *Robert H. Dicke and Robert Beringer* 375

THE NEAR-ECLIPSING SPECTROSCOPIC BINARIES AS A MEANS FOR STUDYING PECULIAR PHENOMENA IN CLOSE DOUBLE STARS . . . . . *Gerald E. Kron* 376

NEW $H\alpha$ EMISSION STARS . . . . . *W. W. Morgan and W. P. Bidelman* 378

Be STARS SHOWING BRIGHT LINES OF *Fe* II . . . . . *W. W. Morgan and Irene Hansen* 379

ON THE POLARIZATION OF THE CONTINUOUS RADIATION OF EARLY-TYPE STARS *Edith M. Janssen* 380

REVIEWS 381

ERRATA 383

NOTICE 384

INDEX 385

THE UNIVERSITY OF CHICAGO PRESS
CHICAGO, ILLINOIS, U.S.A.

May 1946 Vol. 103, No. 3

THE ASTROPHYSICAL JOURNAL

AN INTERNATIONAL REVIEW OF SPECTROSCOPY AND ASTRONOMICAL PHYSICS

Edited by

OTTO STRUVE
Managing Editor

S. CHANDRASEKHAR
Associate Managing Editor

Yerkes Observatory of the University of Chicago

PAUL W. MERRILL
Mount Wilson Observatory of the Carnegie Institution of Washington

HARLOW SHAPLEY
Harvard College Observatory
Cambridge, Massachusetts

N. U. MAYALL
Lick Observatory
University of California

With the Collaboration of the American Astronomical Society

Collaborating Editors:

1944-46	1945-47	1946-49
JOEL STEBBINS Washburn Observatory	CECILIA H. PAYNE-GAPOSCHKIN Harvard College Observatory	C. S. BEALS Dominion Astrophysical Observatory, Victoria
A. N. VYSSOTSKY Leander McCormick Observatory	H. N. RUSSELL Princeton University	LUIS E. ERRO Astrophysical Observatory, Tonanzintla
W. W. MORGAN Yerkes Observatory	R. H. BAKER University of Illinois	O. C. WILSON Mount Wilson Observatory

The Astrophysical Journal is published bimonthly by the University of Chicago at the University of Chicago Press, 5750 Ellis Avenue, Chicago, Illinois, during July, September, November, January, March, and May. ¶The subscription price is $10.00 a year; the price of single copies is $2.00. Orders for service of less than a full year will be charged at the single-copy rate. ¶Postage is prepaid by the publishers on all orders from the United States and its possessions, Argentina, Bolivia, Brazil, Chile, Colombia, Costa Rica, Cuba, Dominican Republic, Ecuador, Guatemala, Haiti, Republic of Honduras, Mexico, Morocco (Spanish Zone), Nicaragua, Panama, Paraguay, Peru, Rio de Oro, El Salvador, Spain (including Balearic Islands, Canary Islands, and the Spanish Offices in Northern Africa; Andorra), Spanish Guinea, Uruguay, and Venezuela. ¶Postage is charged extra as follows: for Canada and Newfoundland, 42 cents on annual subscriptions (total $10.42); on single copies, 7 cents (total $2.07); for all other countries in the Postal Union, 96 cents on annual subscriptions (total $10.96), on single copies 16 cents (total $2.16). ¶Patrons are requested to make all remittances payable to The University of Chicago Press, in United States currency or its equivalent by postal or express money orders or bank drafts.

The following are authorized agents:

For the British Empire, except North America, India, and Australasia: The Cambridge University Press, Bentley House, 200 Euston Road, London, N.W. 1, England. Prices of yearly subscriptions and of single copies may be had on application.

Claims for missing numbers should be made within the month following the regular month of publication. The publishers expect to supply missing numbers free only when losses have been sustained in transit, and when the reserve stock will permit.

Business correspondence should be addressed to The University of Chicago Press, Chicago 37, Illinois.

Communications for the editors and manuscripts should be addressed to: Otto Struve, Editor of THE ASTROPHYSICAL JOURNAL, Yerkes Observatory, Williams Bay, Wisconsin.

Line drawings and photographs should be made by the author, and all marginal notes such as co-ordinates, wave lengths, etc., should be included in the cuts. It will not be possible to set up such material in type.

One copy of the corrected galley proof should be returned as soon as possible to the editor, Yerkes Observatory, Williams Bay, Wisconsin. Authors should take notice that the manuscript will not be sent to them with the proof.

The cable address is "Observatory, Williamsbay, Wisconsin."

The articles in this journal are indexed in the *International Index to Periodicals*, New York, N.Y.

Applications for permission to quote from this journal should be addressed to The University of Chicago Press, and will be freely granted.

Entered as second-class matter, July 31, 1940, at the Post-Office at Chicago, Ill., under the act of March 3, 1879.
Acceptance for mailing at special rate of postage provided for in United States Postal Act of October 3, 1917, Section 1103, amended February 28, 1925.

[PRINTED IN U.S.A.]

THE ASTROPHYSICAL JOURNAL

AN INTERNATIONAL REVIEW OF SPECTROSCOPY AND ASTRONOMICAL PHYSICS

VOLUME 103 MAY 1946 NUMBER 3

THE CORRELATION OF MAGNETIC DISTURBANCES WITH INTENSE EMISSION REGIONS OF THE SOLAR CORONA[1]

A. H. SHAPLEY AND W. O. ROBERTS

Department of Terrestrial Magnetism, Carnegie Institution of Washington, and Harvard College Observatory, Fremont Pass Station, Climax, Colorado

Received March 25, 1946

ABSTRACT

Correlation analyses of coronal and magnetic data, during the period August, 1942—July, 1944, show that, on the average, magnetic disturbance occurred when intense emission regions of the solar corona were situated in the eastern hemisphere of the visible solar disk. Some specific comparisons are cited with regard to the correspondence of coronal-emission regions and M-regions. Although there are some valid criticisms of the methods of correlation used thus far, the results demonstrate that a correlation does exist and that more refined and complete analysis is indicated to realize fully the value of coronal observations as applied to short-term forecasts of disturbance. The observing procedure used at the Coronagraph Station of the Harvard College Observatory at Climax, Colorado, and the uncertainties of observation are detailed in the appendix.

I. INTRODUCTION

In view of the conditions supposed to exist in the solar corona, it would not be surprising to find a positive correlation between the existence on the sun of regions of intense coronal emission and the occurrence of magnetic disturbances on the earth. Until recently little observational evidence was available to test such a relationship. In 1939, Waldmeier[2] offered fragmentary experimental evidence for such a correlation. In 1942, steps were taken, as a part of a program of war research sponsored by the Wave Propagation Committee of the Combined Communications Board and co-ordinated at the Department of Terrestrial Magnetism of the Carnegie Institution of Washington (D.T.M. C.I.W.), to utilize coronal observations made with the Harvard College Observatory (H.C.O.) coronagraph in connection with the co-ordinated solar program of forecasting magnetic and ionospheric disturbances. A preliminary account of the results of this study, disclosing the form of a relationship between the corona and magnetic activity, appeared in the final report of N.D.R.C. Project C-53.[3] The conclusions were rather strikingly different from the expected results in that the time relationship indicated between

[1] This investigation was initiated and accomplished through the co-operation and support of the Navy Department. This paper was prepared as a restricted report, on April 30, 1945, but is now declassified.

[2] Max Waldmeier, *Zs. f. Ap.*, **19**, 21, 1939.

[3] A. H. Shapley and H. W. Wells, *Correlation of Solar and Geomagnetic Observations with Conditions of the Ionosphere: Final Report NDRC Project C-53*, 1943.

solar and terrestrial effects was not like that suggested by Waldmeier or like that sometimes found for large sunspot groups. The correlation between intense coronal-emission regions and moderate magnetic disturbances has been used in the preparation of short-term forecasts of radio-propagation conditions issued by the Interservice Radio Propagation Laboratory (I.R.P.L.). The purpose of this paper is to collect and present the evidence from which the coronal-magnetic correlation was derived, to add corroborating evidence from newer observations, and to point out the practical advantages and limitations of the correlation when applied to forecasting short-term disturbances.

Unusual activity on the sun may be detected by examination of any of the visible features of the sun, though the different visible features do not always show disturbance in the same regions of the sun's surface or to the same extent. The smoothly granulated appearance of the sun's undisturbed disk may be marred by dark sunspots or by bright faculae, which can be seen in an ordinary telescope, or by the irregular bright and dark areas frequently discernible with a spectroheliograph and known as "plages" and "filaments" (both of which have sometimes been called "flocculi"). In addition, disturbances of the sun may be detected by observation of the regions just beyond the perimeter of the sun's bright disk. With suitable spectroheliographic or coronagraphic apparatus, artificial total eclipses of the sun may be produced and the prominences and corona observed. Brilliant and changeable prominences are indices of solar disturbance, as are regions of intense coronal emission. All these disturbance phenomena of the sun follow the general eleven-year sunspot-cycle. In individual cases, however, strong disturbance in one of the solar features will frequently be unaccompanied by disturbance in the others.

It is well known that magnetic disturbances of considerable severity may occur when no visible or significant sunspot disturbances are present on the sun's disk. Likewise, all attempts to ascertain for the other solar features a one-to-one relationship with magnetic disturbances have failed. One of the purposes of the co-ordinated solar program has been to investigate the various observable solar phenomena in their relationship to disturbances of terrestrial magnetism and to pursue in detail the extension of the analyses to ionospheric conditions for the indices of solar activity that exhibit the most promise of correlation with disturbance. Fluctuations of the intensity of the emission regions of the solar corona, as mentioned in the earlier report to which we have already referred,[3] appear to be among the most promising criteria of solar activity in relation to magnetic disturbances. Consequently, this report will stress the analysis done with respect to the solar corona.

II. CORONAL DATA

During the summer of 1930, Bernard Lyot, of France, as the climax to over half a century of unsuccessful instrumental researches by other astronomers, succeeded in photographing the solar corona and its spectrum without a total solar eclipse. The reasons for his success where others had failed are now easy to understand. Lyot had investigated all sources of instrumental scattering of light in a telescope and had completely eliminated or greatly reduced all of these by the development of an entirely new type of telescope, now known as the "Lyot-type coronagraph." Since the development of Lyot's instrument, two others have been established. One was installed at Arosa, Switzerland, by the Confederated Observatory of Zurich and has been operated by Max Waldmeier. The other was erected by Harvard College Observatory in the United States at Climax, Colorado, in the Rocky Mountains at an altitude of 11,500 feet above sea-level. The Harvard coronagraph-installation was supervised by D. H. Menzel, and the station has been operated since its establishment by W. O. Roberts.

Observations of the solar corona without eclipse are extremely difficult even with modern coronagraphic equipment. High-altitude observatories are necessary in order to supply the requisite clean, dry atmosphere; and highly developed techniques are required for the manufacture and maintenance of a coronagraph objective lens to insure the high-

est possible standards of purity of glass and lens polish and to make certain that the lens is cleaned to the necessary exacting standards at all times. This last requirement is a surprisingly difficult problem, and the success of the coronagraph depends on the degree to which it succeeds.

In so far as the solar-terrestrial research program co-ordinated under the D.T.M. C.I.W. is concerned, the function of the Harvard coronagraph has been to supply day-to-day observations of the location, extent, and intensity of the regions of bright coronal emission of the sun in the light of two prominent lines of the coronal spectrum, the green

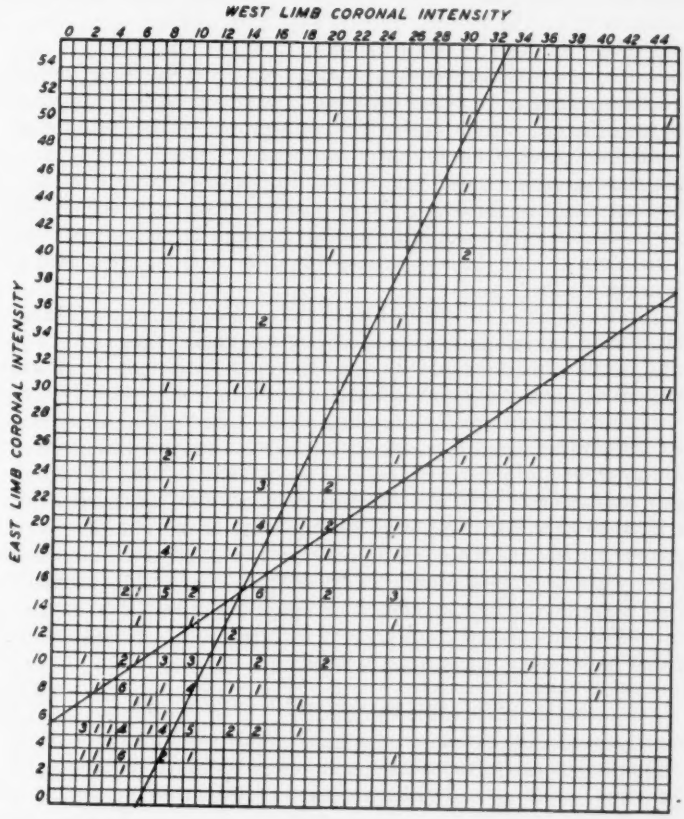

FIG. 1.—Correlation table of east-limb coronal intensity and west-limb intensity 14 days later, August 1, 1942—April 30, 1944, unrevised data (coefficient of linear correlation, 0.58 ± 0.04).

line at 5303 A and the red line at 6374 A. Incidentally, observations of the size, shape, location, and intensity of the prominences present on the sun have been supplied in a routine fashion, together with photographs of all prominences. The coronal data have been derived from visual and photographic observations of the coronal lines displayed in a grating spectrograph used as an adjunct to the Lyot-type coronagraph. The problem is substantially one of photometry of spectrum lines from a spectrograph wherein a curved slit is used. The image of the coronal regions under study is focused upon the curved slit, so that portions of the coronal image reproduced on the spectrograph plate represent conditions at some distance above the sun's limb but at different position angles around the limb.

Experiment has indicated that the magnitude of the fluctuations of coronal intensity is very great. Consequently, it has been possible to evaluate roughly the course of the fluctuations of intensity with relatively crude photometric procedures. An arbitrary scale of coronal intensities has been established, according to which the normal range of intensity varies from about 1 or 2 for the faintest measured intensities to perhaps 30 for the greatest intensities now encountered. The scale is established simply by the routine observational procedure. The accuracy of the measurements of intensity depends on the precision with which the routine is duplicated from day to day. Many of these practices require revision, but it seems highly improbable that more exact photometric methods would substantially alter the general results of the determinations. The standard observational procedure is given in the appendix.

The coronal-intensity estimates are tabulated for 5° intervals of position angle completely around the perimeter of the solar disk at a standard height from the limb, for both the green and the red coronal lines. These observations are obtained at a minimum of once daily, weather permitting, and are transmitted immediately to the co-ordinating office for use in short-term forecasts and for use in the researches detailed in this report. No observations are made of the heights of intense-emission regions of the corona, though the knowledge of this quantity would be useful. A birefringent monochromator is being built, which will permit this determination, together with simpler and more accurate photometric studies of the corona.

The observations obtained suffice to locate the approximate solar latitude and longitude of regions of intense coronal emission when these regions pass either the west or the east solar limbs as the sun rotates on its axis. In general, coronal regions are sufficiently stable from day to day and week to week that the main features of the coronal distribution as they pass either limb are duplicated 2 weeks later as the same features pass the other limb. As shown in Figure 1, a correlation exists between the observations of east-limb coronal intensities and west-limb intensities of 14 days later. The data used in this figure are older measurements of the maximum intensities, since revised measures, including solar latitude, are not completed for the west limb. The period covered by the data is not quite the same as for the other analyses in this paper. The coefficient of linear correlation is $r = 0.58 \pm 0.04$, indicating a considerable degree of stability in the corona. The true correlation may be higher, since this figure also reflects errors of measurement. The coefficient will be calculated from revised coronal data comparable to the data used in the rest of this paper when these are available.

III. GEOMAGNETIC AND IONOSPHERIC DATA

Disturbances in geomagnetic and ionospheric conditions are exceedingly complicated in behavior. Disturbances occur at times in some observable phenomena and not in others, and at some locations and not at others. Often, however, simultaneous disturbances of all geomagnetic and ionospheric phenomena occur at all parts of the earth. The greatest magnetic "storms" are of this character, and the more frequent disturbances of lesser severity are generally accompanied by ionospheric upsets of one type or another. In comparing solar and terrestrial phenomena, it is advisable, for simplicity, to use as an indicator of terrestrial disturbance one that is free from local anomalies and one that does not overemphasize any one particular type of disturbance. If, through the use of world-wide average indices of this sort, we can uncover a significant correlation with solar phenomena, then more detailed investigation of the relationship with regard to specific types of terrestrial disturbance may prove still more profitable.

For comparison with daily solar observations a world-wide terrestrial index averaged over a half-day or a whole day seems most satisfactory. A character-figure of this sort describing ionospheric disturbances has yet to be developed, but, for some time, average magnetic character-figures from combined observations of widely scattered stations have been available. In general, the ionospheric character-figures and the magnetic indices

correlate rather well,[4] and any solar-terrestrial relationship discovered for the magnetic indices must perforce also be valid for the ionospheric.

The indicator of magnetic disturbance used in this paper is derived from the "Reports of Geomagnetic Activity," prepared weekly by D.T.M. C.I.W. Table 1 of those Reports gives magnetic character-figures for the first and second half of each Greenwich day on a scale of increasing disturbance from 0.0 to 2.0, based on combined estimates of the degree of disturbance at seven widely separated magnetic observatories. Ten times the sum of the two half-daily character-figures is a daily indicator of magnetic disturbance, which we have designated by the symbol 20 C_A. The extreme range is obviously 0–40, and the mean value during the period August, 1942—July, 1944, was 8.6. This indicator is nearly proportional to the American magnetic character-figure C_A, published quarterly in the *Journal of Terrestrial Magnetism and Atmospheric Electricity*.

Since many workers in this field are accustomed to the K-indices, which measure magnetic activity on a scale of 0–9 at 3-hourly Greenwich intervals, we show in Figure 2 the correlation during the period August, 1942—July, 1944, between 20 C_A and the daily sum of the K_A-indices given in Table 2 of the "Reports of Geomagnetic Activity." The coefficient of linear correlation, $+0.965 \pm 0.002$, is very high, and analyses comparing solar data with 20 C_A will have approximately the same significance as with the daily sum of K_A.

IV. CORRELATION ANALYSIS AND RESULTS

A) Superposed-epoch analysis.—Shortly after the inception of the co-ordinated solar-terrestrial program, and, indeed, even before it, different workers connected with the program noticed that there seemed to be a significant increase in the probability of magnetic or ionospheric disturbance from one to a few days following the appearance at the east limb of the sun of a region of intense coronal emission. A considerable amount of preliminary analysis was performed more or less independently by members of the staff at D.T.M. C.I.W. and by those at the Climax station. This foundation work indicated not only that there was promise of a significant correlation being derived from more detailed statistical work but also that the relationship between coronal-emission regions and world-wide average magnetic conditions was not a one-to-one relationship. The report,[3] already referred to, summarized preliminary results of further detailed statistical analysis, which was performed at D.T.M. C.I.W.

The method used in comparing coronal and magnetic data is similar to the superposed-epoch method developed by Chree to test and verify the 27-day recurrence tendency of magnetic storms. The advantage of this method is that it removes all suspicion of preconceived opinions as to the time lag between solar and terrestrial phenomena and derives this value in a completely unbiased manner. In addition, the method gives some notion of the value of the correlations which it may reveal.

In our adaptation of the method, days on which the corona was significantly bright on the east solar limb were chosen as the zero-days with reference to which the succeeding days were numbered ordinally. A table was prepared in which a row was assigned to each zero-day derived from the coronal observations, and a column was assigned to all ordinally numbered days from -4 to $+15$ or more with respect to that zero. The appropriate values of 20 C_A were entered in the columns of the table by counting from the actual date of each zero-day. Arithmetic means of the values tabulated in each column of the table were then calculated; these means indicate the average course of the magnetic activity following the bright coronal emission which took place on the zero-day. If there were no correlation between the bright corona and magnetic activity, the means of the successive columns would display a random distribution about the mean value for all days in the table. The existence of a real correlation would be shown by some significant

[4] A. H. Shapley, *The Application of Solar and Geomagnetic Data to Short-Term Forecasts*, restricted report (now declassified, to be published in *J. Terr. Mag.*, 51, June, 1946).

departure from randomness in these successive means. In general, a significant correlation would give rise to a distribution of means, whose values, when plotted vertically against the ordinal numbers of the columns, would fall upon a relatively smooth curve rising above and below the mean value for all days. The magnitude of the departure from the mean value of this curve and its smoothness, together with other considerations, would establish the significance of the correlation.

This procedure was followed in our work, using as zero-days all days on which the Observatory at Climax reported that the corona on the east limb was brighter than 10 units, on the arbitrary scale of 0–30. The coronal observations, unfortunately, are not complete.

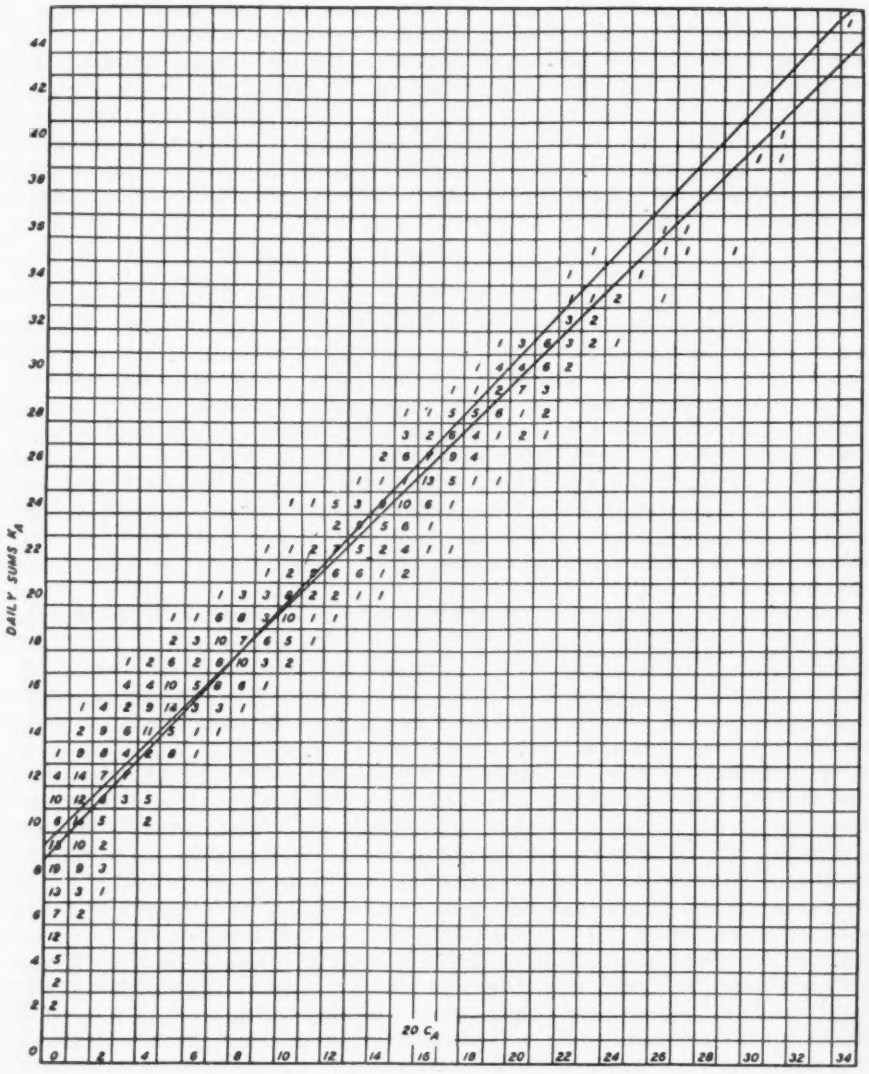

FIG. 2.—Correlation table of magnetic character-figure, $20C_A$, and daily sum of K_A, August, 1942—July, 1944 (coefficient of linear correlation 0.965 ± 0.002).

Conditions of weather permitted observations on only 424 out of the 731 days in the period August 1, 1942—July 31, 1944. Many days on which the corona was probably bright did not appear in the tabulations. Errors were also introduced by the fact that the scale of coronal intensities was inadequately standardized, so that the observations in borderline cases probably did not correctly assign the zero-days of bright east-limb coronal intensity.

In this analysis only the observations of the green coronal line at the east solar limb were used. West-limb observations and red-line observations at either limb have not yet

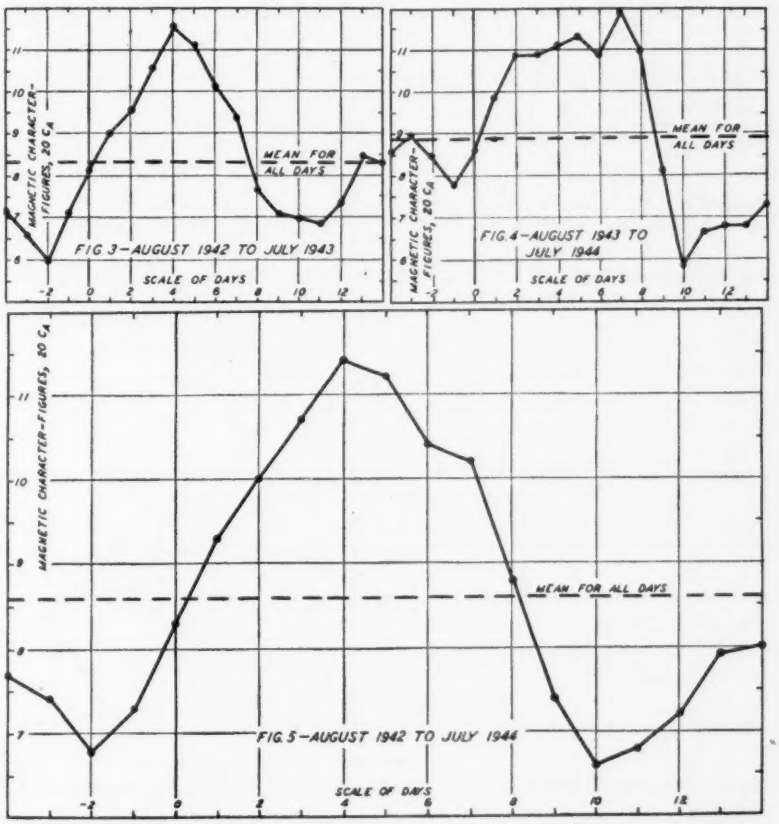
MAGNETIC CHARACTER-FIGURES, 20 Cs
MEAN FOR ALL DAYS
FIG. 3—AUGUST 1942 TO JULY 1943
SCALE OF DAYS
FIG. 4—AUGUST 1943 TO JULY 1944
FIG. 5—AUGUST 1942 TO JULY 1944

FIGS. 3, 4, and 5.—Mean magnetic character of days with reference to day of observation of bright east-limb corona.

been utilized in this way. The range of intensity of the red line is smaller than that of the green line, though there is some indication that red-line values may be somewhat better determined on days when observing conditions are poor.

Figures 3 and 4 show the mean magnetic character-values derived from successive columns of the work table and plotted vertically against the number of days before or after the zero-day of bright east-limb green-line coronal intensity. The data have been divided into two groups, and the correlation studied independently in each. In both, a significant correlation seems to exist, with greater-than-average magnetic disturbance appearing shortly after the zero-coronal date and continuing through the eighth or ninth

day, with a maximum somewhere between the fourth and the seventh days, on the average. In both periods the magnetic activity is lower than average after about the eighth day, for 5 or more days. In Figure 5 both sets of data are combined.

In the procedure followed above, an intense magnetic storm will tend to dominate the mean curves, not only because of the very large mean character-figures but also because of the long duration usual for such disturbances. This tendency can be reduced by dividing all days into two categories according to whether their magnetic character is greater,

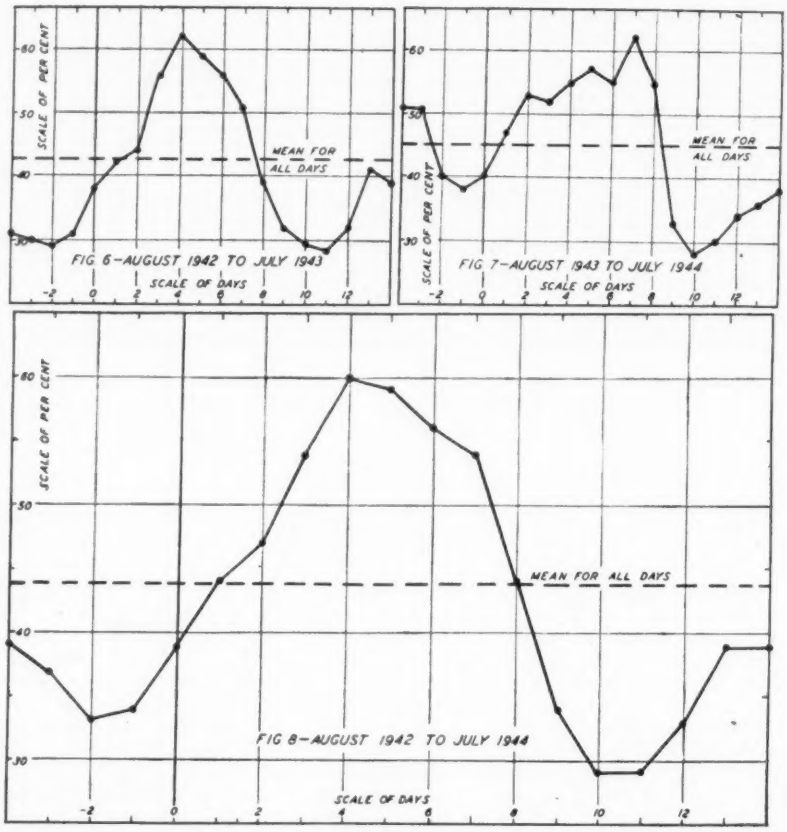
SCALE OF PER CENT
MEAN FOR ALL DAYS
FIG 6—AUGUST 1942 TO JULY 1943
SCALE OF DAYS
FIG 7—AUGUST 1943 TO JULY 1944
FIG 8—AUGUST 1942 TO JULY 1944

FIGS. 6, 7, and 8.—Occurrence frequency of days of magnetic character-figures, 20 C_A, $\geqslant 9$, with reference to day of observation of bright east-limb corona.

or less, than some arbitrary limit, and then plotting superposed-epoch graphs, in which the tabular entries are simply checks for disturbed days and blanks for undisturbed and in which the ordinate of the final graph is simply the number of checks in each column or some number proportional to this. Such occurrence-frequency graphs may be plotted for any chosen arbitrary limits of magnetic disturbance.

The results shown in Figures 6–8 were obtained with the same coronal limit as above (that is, coronal intensity $\geqslant 10$), and when a disturbed day was defined as one with magnetic character-figure 20 C_A of 9 or more. By this definition, 44 per cent of the days in the whole period were disturbed. The ordinates are percentage of days called disturbed according to the chosen arbitrary definition of disturbance. The results in Figures 9–11

were obtained in a similar fashion, except that 15 on the scale of 20 C_A was taken as the arbitrary lower limit for disturbance. According to this definition, 26 per cent of all days were disturbed.

The significant feature of all these graphs and the strikingly new conception to be derived from them are that the probability of geomagnetic disturbance was very markedly greater while the regions of brilliant coronal emission were located somewhere on the eastern half of the solar disk and that, by the time they had reached the central meridian

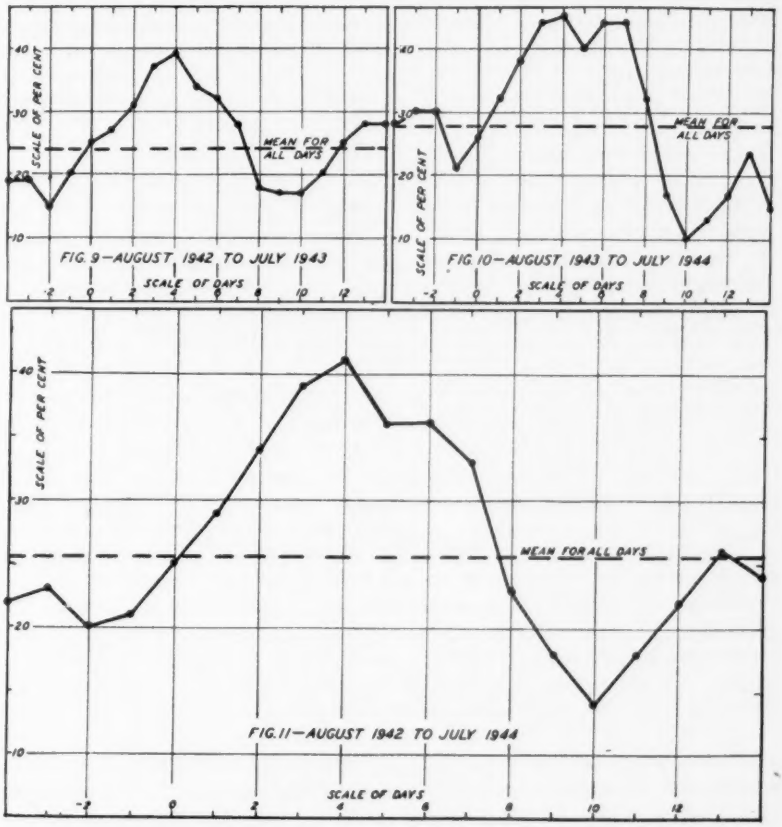
SCALE OF PER CENT
MEAN FOR ALL DAYS
FIG. 9—AUGUST 1942 TO JULY 1943
SCALE OF DAYS
FIG. 10—AUGUST 1943 TO JULY 1944
FIG. 11—AUGUST 1942 TO JULY 1944

FIGS. 9, 10, and 11.—Occurrence frequency of days of magnetic character-figures, 20 C_A, $\geqslant$ 15 with reference to day of observation of bright east-limb corona.

of the sun, the probability of disturbance had definitely begun to drop and, still further, that about 2–5 days after central-meridian passage of these coronal regions the disturbance probabilities were markedly decreased. By the tenth day after any given zero-day in the period examined, the probability of disturbance, as shown by Figures 8 and 11, had dropped to one-half and one-third, respectively, that of the fourth day. This result is in marked contrast to the form of the coronal relationship proposed by Waldmeier[2] on the basis of his comparisons with the Potsdam magnetic observations, namely, that the probability of magnetic disturbance was significantly increased 8 days after the east-limb passage of regions of bright coronal emission. Of course, his observations and ours

do not cover the same intervals of time, but it seems unlikely that the form of the relationship would have differed markedly in these two periods.

All the analyses thus far described have utilized superposed-epoch techniques based on consideration of all days on which the corona was brighter than intensity 10 on the arbitrary Climax scale. Active solar regions are, however, frequently large in extent and take several days to pass the limb. On these occasions a high coronal intensity will be recorded for several consecutive days, each of which will appear in the tables as a zero-day. Therefore, a coronal region of large surface area will have a much larger weight than more sharply defined smaller regions, though from the latter it is reasonable to expect a better definition of the time relationship between appearance of corona and occurrence of magnetic disturbance. For the purpose of forecasting disturbances it would be advantageous

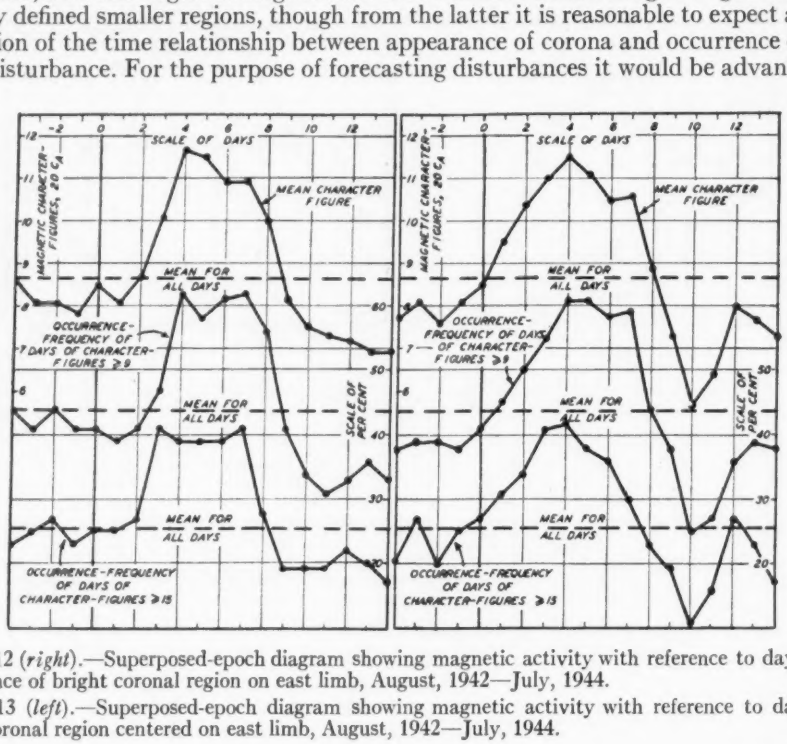
SCALE OF DAYS
MAGNETIC CHARACTER-FIGURES, 20 Cs
MEAN CHARACTER FIGURE
MEAN FOR ALL DAYS
OCCURRENCE-FREQUENCY OF 7 DAYS OF CHARACTER-FIGURES ≥ 9
SCALE OF PER CENT
OCCURRENCE-FREQUENCY OF DAYS OF CHARACTER-FIGURES ≥ 13

FIG. 12 (*right*).—Superposed-epoch diagram showing magnetic activity with reference to day of first appearance of bright coronal region on east limb, August, 1942—July, 1944.

FIG. 13 (*left*).—Superposed-epoch diagram showing magnetic activity with reference to day when bright coronal region centered on east limb, August, 1942—July, 1944.

to find the relationship between the day of first appearance of a bright coronal region on the east limb and the commencement of magnetic disturbance. This would permit issuance of forecasts somewhat further in advance.

Interruptions of the daily series of coronal observations because of vagaries of weather make accurate identification of the days of first appearance of regions of intense coronal emission sometimes uncertain. We have, however, carried out a superposed-epoch analysis, using for zero-days the day of first appearance of bright east-limb corona after a period in which faint corona was observed, regardless of discontinuities in the observations. Figure 12 shows the result of this analysis, which reveals that generally there was an abrupt increase in magnetic disturbance on the third or fourth day after the zero-day. The greater sharpness of this peak and the longer time from zero-day to disturbance conditions make this a more appropriate form of the coronal-terrestrial relationship for use in short-term forecasting of geomagnetic phenomena.

A representation of the average position on the solar disk of bright coronal regions at the time of magnetic disturbance is given if the zero-day is taken as the day when the intensity of a coronal region passing the east limb is a maximum. The results of superposed-

epoch analysis carried out thus are shown in Figure 13. This analysis establishes that maximum magnetic disturbances occurred when the most intense portions of the bright coronal region were situated about 40° of solar longitude east of the central meridian of the sun.

B) Comparison of specific disturbances with specific solar phenomena.—For over a decade those engaged in research relating to the correlation of magnetic and solar activity have followed the suggestion of Bartels[5] in ascribing the cause of the magnetic storms which recur with a 27-day period to hypothetical "M-regions" on the sun. Numerous attempts have been made to associate these M-regions with visible features of the sun, such as sunspot groups, faculae, or plages. It has been customary to consider that an M-region must be near the central meridian of the sun when it emits the radiation which produces magnetic disturbances on the earth. The transmission time of this disturbing radiation has been thought to be of the order of 1 day for large magnetic storms, but C. W. Allen suggests that it may be longer for minor recurrent disturbances.[6] Attempts to identify the M-region with some visible feature of the sun's disk have failed.

It is of interest to compare M-regions with the regions of bright coronal-line emission. Allen, Waldmeier, and others have suggested that M-regions may prove identical with coronal-emission regions. Allen[6] points out that the M-region maximum about 2 years before sunspot minimum indicates a possible coronal origin, since at this time coronal regions are presumably nearer the equator and presumably more effective. Besides this, the continued existence of M-regions through sunspot minimum indicates that they can occur independently of sunspots.

Waldmeier has stated that M-regions are identical with regions of bright-green coronal-line emission[2] and that the terrestrial effect takes place about 1 day after the region of bright corona has passed the central meridian of the sun. Our work indicates that a different relationship obtained during the period analyzed and thus that the M-regions, if they are to be identified with regions of bright coronal emission, are located on the solar disk in such a position that their influence is noticed at the earth several days before they reach the central meridian of the sun.

Several supporting observations tend to strengthen our confidence in the possibility that M-regions and coronal-emission regions may be the same. First, M-regions are most intense and persistent about 1 or 2 years before sunspot minimum, when the corona has its maximum equatorial extension;[6] and, second, coronal regions tend to exhibit a considerable degree of permanence on the solar disk, even when no sunspots are present, with 6 months' duration not uncommon—also a characteristic of M-regions according to Allen.[6] As emphasized in an earlier report,[3] the number of magnetic disturbances is comparable to the number of bright coronal maxima. Still further, many disturbances and coronal regions tended to be spaced 14 days apart in time, or 180° apart on the sun.

As a test of these notions, we have considered the magnetic phenomena for the year 1943 as summarized by H. W. Newton.[7] According to Newton, the most pronounced feature of the Bartels diagram of magnetic phenomena of 1943 is a broad vertical sequence of symbols, indicating the existence of a long-continued series of recurrent disturbances with their definite initiation on August 29, though with some slight indication of their presence for two or three rotations prior. These recurrent disturbances Newton attributed to a pronounced M-region on the sun from August 29, 1943, through January 11, 1944. To the M-region he ascribed a fairly abrupt front, corresponding in time of terrestrial effect to the dates shown in Table 1.

One of the most striking features of the coronal results for the year of 1943 is the definite sequence of stable coronal-emission maxima, for which sharp rises in intensity first passed the east limb of the sun on the dates shown in Table 2.

[5] *J. Terr. Mag.*, **37**, 1, 1932, and **39**, 201, 1934.

[6] C. W. Allen, *MN*, **104**, 13, 1944.

[7] *Observatory*, **65**, 177, 1944.

On July 3, 1943, there was a similar peak on the east limb, but it was of low intensity as compared with the others. The peaks of November and December were most pronounced. The peak in January was poorly established because of incomplete observations, and a poorly established peak was located in February. In March, because of bad weather, no significant observations were possible.

The distribution with latitude of the coronal emission associated with this M-region is of interest. The coronal emission was strongest at approximately 10°–20° north of the equator at the east limb. However, a statistical study would be needed to determine whether this represents the zone at which coronal maxima are most effective in producing terrestrial disturbance.

Figure 14 shows the relationship of average coronal intensities in the zone 10°–25° north of the equator to the date given by Newton for the M-region front, taken as zero-day. The average curve shows that the highest coronal intensity occurred on the zero-day, but a significant rise in coronal intensity appears 3 days earlier. The September coronal peak came earlier with respect to the zero-day than the others. These specific comparisons are in agreement with the statistical result of the preceding section, best exhibited in Figure 12, where it is also shown that intense coronal regions first appear at

TABLE 1

August 29, 1943.....	October 24, 1943	December 16, 1943
September 26, 1943.....	November 19, 1943	January 11, 1944

TABLE 2

August 1, 1943 (cloudy preceding days)	November 19, 1943
August 28, 1943	December 15, 1943
September 23, 1943	January 12, 1944 (cloudy preceding days)
October 24, 1943 (cloudy preceding days)	

the east limb approximately 3 days before a sudden increase in the probability of magnetic disturbance. The peak shown in the average curve (Fig. 14, *B*) at the zero-day does not indicate that the coronal intensity was at maximum on the same day that the magnetic activity was at maximum. It means simply that the coronal intensity reached maximum on the day that the magnetic disturbance commenced. Since the duration of these recurrent disturbances was approximately 8 days, it is clear that the coronal-emission region was situated between the east limb and the central meridian of the sun during the disturbance.

This type of specific comparison could profitably be extended to more data. The example cited here is included to indicate that a detailed comparison of M-regions and coronal regions is in accord with our statistical results. Further work should be done to determine whether the direct association of these stable coronal regions with the stable M-regions postulated to explain recurrent magnetic phenomena is sufficient to explain the statistical correlation of coronal emission and magnetic disturbance or whether bright coronal emission also accompanies the frequently very intense nonrecurrent magnetic storms sometimes encountered.

V. DISCUSSION OF RESULTS

A) *Short-term magnetic and ionospheric forecasting.*—The basic objective of the solar-terrestrial correlation study co-ordinated under the D.T.M. C.I.W. is to improve the techniques of short-term forecasts of the behavior of ionospheric layers for use in radio

communication and allied problems. For the successful attainment of this objective the coronal data have definite usefulness. The significance of the statistical relationship between bright coronal emission at the east solar limb and the occurrence, 3–4 days later, of disturbances of geomagnetic conditions, and thus of ionospheric conditions, can be evaluated by reference to Figures 8 and 11. The application of the principles implicit in the construction of the superposed-epoch graph to predictions would have produced, in the test period, success in six out of ten predictions of disturbance, and in four of these

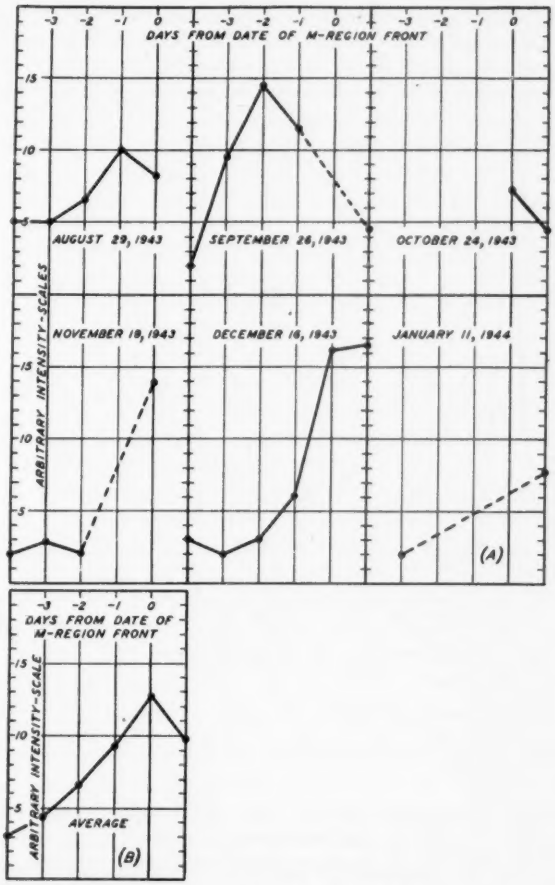

FIG. 14.—Average intensity of corona in zone +10° to +25° heliographic latitude with reference to (*A*) date of six M-region fronts, 1943–44, and (*B*) average for all six cases.

six the magnetic conditions could have been predicted to be of considerable severity, with character 20 C_A equaling 15 or greater. It should be noted, however, that disturbances of this magnitude are still definitely moderate, as compared to what has classically been regarded as disturbed, although they still have a significant effect on the properties of the ionospheric layers.

Forecasts made simply on the basis of the well-known 27-day recurrence tendency of magnetic activity will achieve considerable success, especially near minimum epoch of solar activity. Figure 15, *A* shows the mean activity following days with magnetic char-

acter 20 $C_A \geqslant 15$, during an 8-month interval when the recurrence tendency was marked, derived by the superposed-epoch method. The recurrence is clearly shown, with activity peaked 26–29 days after the disturbed zero-day. If the recurrence were exact, the peaks centered at zero and at 27 days would be similar. The broad recurrence peak indicates that periods slightly different from 27 days existed. During May–December, 1944, the recurrence was less well marked, as shown in Figure 15, *B*. During this time, recurrence tendency was of little use in forecasting disturbed conditions.

The first disturbance of a recurrence sequence obviously cannot be anticipated by such a method of forecasting. This, together with changes in timing and intensity of recurrent activity, must be estimated from solar observations. The coronal-magnetic rela-

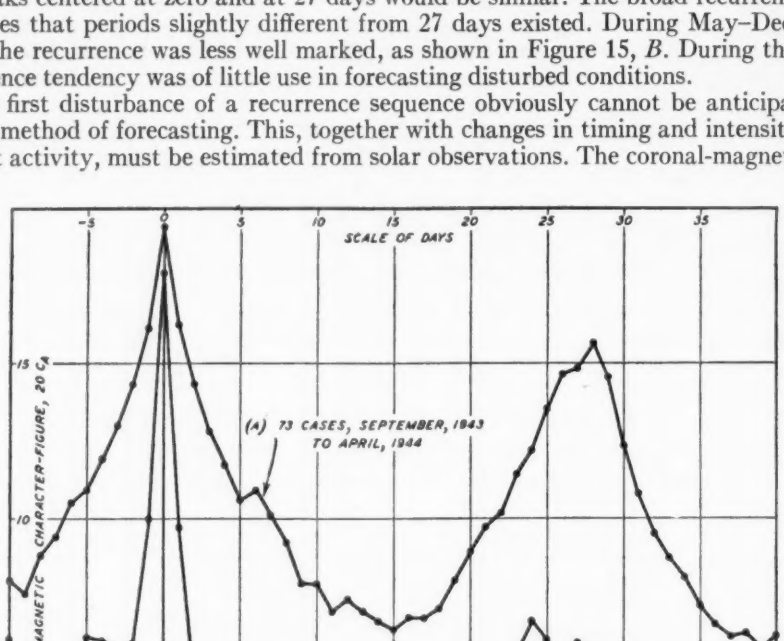

FIG. 15.—Mean magnetic character of days with reference to days with magnetic character, 20 C_A, $\geqslant 15$

tionship, as noted above, is an example of the way in which solar observations can be used to anticipate disturbance several days ahead of time.

Forecasts made only by strict application of the 27-day recurrence tendency or only by the coronal relationship achieve about equal success. In practice, coronal information is combined with a knowledge of other solar data, especially on calcium plages and with a knowledge of recurrence phenomena, and forecasts are prepared by the I.R.P.L. with the collaboration of D.T.M. C.I.W. by qualitative consideration of all observations.

There is, however, still considerable uncertainty in the coronal data and in the use that it is so far possible to make of them. It is hoped that further analyses will result in better methods of forecasting through improved knowledge. A study of the effect of latitude distribution on the nature of the correlation is perhaps the most important of these, inasmuch as the active solar regions encountered during the test period were predominantly in low latitude, belonging to the waning cycle, whereas regions of the new cycle, in high latitude, have since become more numerous. This study, together with studies using observations of the red coronal line, is currently in progress, but the analyses have

not proceeded far enough for a statement of results. These investigations are directed toward determining criteria from coronal observations to account for times when the relationship differed from the average. For instance, there are cases in the period analyzed when a series of disturbed days began only 1–2 days after the first east-limb appearance of bright coronal regions, and in other cases the disturbances did not start until 5 or more days after the east-limb appearance. In many cases, too, the correlation broke down completely, and no disturbance followed bright east-limb coronal observations. However, only very rarely in the 2-year period covered by the analysis was there any significant geomagnetic activity without there also being a significantly bright coronal region located on the eastern half of the visible solar disk

It is obvious that forecasts using present methods based on the present incomplete coronal data alone are not entirely trustworthy. It is also strongly indicated that we cannot remove all shortcomings of forecasts made according to present methods of coronal analysis simply by obtaining complete and more accurate coronal data, much as these would help. Probably, we can never obtain completely trustworthy forecasts from coronal observations. But, since we have derived a correlation that seems to have a higher significance than those derived from other solar phenomena and since there is some reason to expect that the physical conditions of the solar corona can influence those of the ionosphere, the authors believe that investigation of the coronal-magnetic relationship merits further intensive study, including improvement and extension of coronagraphic observations, as well as more detailed statistical analysis.

B) Physical meaning of results.—While a detailed discussion of the physical meaning of the results of the analysis presented here is beyond the scope of this paper, a few remarks may be appropriate. In the past it has been customary to attribute solar influences on magnetic and ionospheric-disturbance phenomena to either or both of two possible physical mechanisms: we have thought that the sun must produce its action either by generation of unusually intense ultraviolet action at times, or by emission of unusually strong or concentrated neutral streams of charged corpuscles which travel with a velocity less than that of light. The ultraviolet action, it is generally believed, produces the sudden complete radio fadeouts which are confined to the visible hemisphere of the earth. The effect is chiefly increased ionization resulting in absorption in the *D*-layer, with higher layers relatively unaffected. The corpuscular streams are thought to produce magnetic storms and disturbances in all regions of the ionosphere, especially the higher layers. These occur on both the bright and the dark terrestrial hemispheres, and especially at high latitudes.

If bright coronal-emission areas are the cause of these magnetic and ionospheric storms, the physical process involved in directing the particle streams to the earth from the east half of the visible disk is rather difficult to visualize. Two forms of evidence have been used to support the belief that the particle streams require approximately 1 day to come from the sun to the earth. First, there appears to be a tendency for a magnetic storm to follow about 24 hours after a sudden radio fadeout. Since the latter is supposed to have been due to radiation propagated with the velocity of light (ultraviolet), perhaps originating in a "chromospheric flare," and since it is reasonable to ascribe a common origin to the two phenomena when they are regularly associated, the 1-day lag between them has been ascribed to the transmission time of the particles in transit between the sun and the earth. Second, great magnetic storms frequently occur 1 day after large sunspot groups have passed the central meridian of the sun. It has been conventional to assume that the particles were emitted radially from the sun when the spot groups were on the central meridian.

The results of our analysis are not necessarily in discord with these conclusions. We are faced with the following two alternatives: (1) The magnetic storms to which the conclusions of the above paragraph refer are the "great" magnetic storms, of which there are few, if any, examples in our test period and for which different physical processes

may be postulated from those operating with the lesser magnetic disturbances mainly concerned in our coronal analysis; or (2) a hitherto undiscovered relationship must exist between the location of a sunspot group and the presence of a region of intense coronal emission following the sunspot group approximately 40° in longitude.

If the first-mentioned alternative is correct, we are not bound, in speculating on the physical meaning of the coronal relationship, to include in an explanation the observed statistical correlation of central-meridian passage of large sunspot groups with the day-later magnetic storms. In support of this alternative, the only great magnetic disturbance in the test period occurred April 1–3, 1944, when the coronal observations were seriously incomplete because of bad conditions of weather at Climax.

If the second alternative is correct, we have a more difficult physical situation. The second alternative appeals because it does not require the development of two different explanations for magnetic storms, depending on whether they are greater or less than some certain magnitude. It is, of course, impossible to derive from coronal observations any knowledge of the transmission time from sun to earth of the radiation or corpuscles responsible for magnetic storms, without some assumption as to the direction in which the corpuscles or radiation are emitted and travel or without some other method of determining the time at which they leave the sun. With the coronal correlation we have derived, neither the practically instantaneous transmission of ultraviolet nor the 1-day transit time ascribed to corpuscles seems to simplify the physical interpretation. If we have reason to believe that a transit time of about 1 day from sun to earth is correct from physical theory or from other observations, then we are faced with the necessity of finding a mechanism by which the disturbing corpuscles are ejected from the east half of the sun's visible disk at an angle of roughly 45° forward with respect to solar rotation. That is, if a 1-day or less transit time is correct, the ejection must be directed toward the earth when the effective coronal region is several days east of the central meridian but not when it is correspondingly west of the central meridian, unless we discover that another geomagnetic influence takes place when coronal regions are at some preferred position in the west half of the solar disk. Such a possibility seems ruled out by our preliminary studies.

C) Shortcomings of the present correlation analysis.—Valid objections of several sorts may be brought to bear upon the superposed-epoch analysis presented herein. The work which has been done thus far must admittedly be classed as preliminary. It is our purpose, at some future time, to present the coronal-magnetic analysis in a more complete form, with more detailed statistical results.

The superposed-epoch graphs presented here were made in an effort to determine accurately the usefulness of the coronal data for making forecasts of the geomagnetic-disturbance character-figures. As such they serve their purpose adequately and indicate that further work is desirable. Furthermore, they leave us no uncertainty about the reality of the correlation of corona and geomagnetism.

One important objection to our superposed-epoch analysis is that even the coronal and magnetic data which are used are very incompletely utilized, and the correlations derived are thus weakened. In the case of occurrence-frequency graphs like those of Figures 6–13, the two continuously variable quantities—the coronal intensity and the magnetic character—are divided arbitrarily according to whether the measured values are above or below chosen limits. Without the construction of large families of such graphs much of the observational information contained in the magnitudes of the observed data is thereby discarded. A more desirable treatment would be the construction of actual correlation tables and the derivation of correlation coefficients between corona and magnetic character for different numbers-of-days' lapse between east-limb coronal observations and magnetic observations. To cover in this fashion the lag for a large number of days, as is readily done in the superposed-epoch analysis, would entail greater labor than we have yet been able to expend. A start at such analysis has been made, however. The problem is readily adaptable to punch-card Hollerith machine study.

A serious criticism of our results is that no significance tests of the correlations have been derived, except the probabilities expressed in Figures 8 and 11. These probabilities have not been compared with probabilities derived from other solar data, to show whether or not the coronal observations are superior, for example, to sunspot data used for the same purpose.[4]

Still another criticism of the present analysis is that not all the available observational data have been considered. Coronal observations for the west limb and for the red line 6374 A have not been utilized in the analysis, though they are used to some extent in the actual methods of forecast. Nor has any considerable use been made of the important latitude-distribution data and their relationship to the changing heliographic latitude of the earth. Quantitative study of the degree of stability of coronal regions should be made with the same coronal data as were used for the superposed-epoch studies. This information is of importance if coronal regions are actually identifiable with the hypothetical solar M-regions.

In spite of the obvious shortcomings of the results, we feel considerable confidence in the reality of the new coronal-terrestrial relationship set forth herein. The superposed-epoch graphs have the virtue of being entirely objective. No preconceived notions of the form of the relationship can be inserted into them. And, though actual tests of significance have not been carried out, the strikingly high probability of magnetic disturbance 4 days after east-limb coronal maxima, as compared with the probability of disturbance 2 days before or 10 days after east-limb maxima, is indubitably significant.

APPENDIX

The standardization of the coronal scale of intensities observed at Climax in the test period has been accomplished simply by preserving the uniformity of the routine of operations involved in the observations. A statement of this routine is given in this appendix. Since the end of the test period, certain of the procedures have been improved to permit better standardization of the photographic operations.

Six exposures daily are made at different solar position angles on Eastman Spectroscopic plates, Type 103-*F*. These are exposed in the spectrograph-coronagraph system (of approximately *f*/30 effective aperture) with a standard exposure time of 1 minute, with a yellow filter in the system (Eastman Kodak Company Wratten K-2) and with a spectrograph-slit opening of 0.002 inch. The spectrograph is of Littrow design, with 96-inch focal length, producing a dispersion of 8 A per mm at $H\alpha$ by means of a metal grating ruled by R. W. Wood with 14,000 lines per inch and designed to concentrate a large percentage of the total incident light in the first order of the grating. Within the optical system are twenty air-glass surfaces and two reflections, one from a front-surfaced aluminum mirror and the other from the grating.

Development of the photographic plates is uniform; fresh solutions of Eastman Kodak Company formula No. D-19 are used with 8-minute development at 65° F, giving $\gamma = 2.5$. The coronal-line intensities derived from the finished plates are estimated by interpolation against artificial lines of various intensities preserved on a test plate which is stored and used for all determinations. These artificial lines were recorded in the laboratory in such a manner that their appearance closely resembles the real coronal lines in apparent width and color of image. The intensities so derived are compared with visual-intensity estimates made earlier with an eye piece used directly at the spectrograph. The agreement is generally acceptable, the values usually being within 20 per cent of each other.

All estimates of intensity, with a very few exceptions, and all plate exposures prior to October, 1944, with the same few exceptions, were made by W. O. Roberts. Since October, 1944, plates have been exposed according to the standard observing procedure by an additional observer. Plates have been developed according to the standard procedure by four different workers.

Some of the obvious sources of error affecting the accuracy of the intensity estimates thus derived may be listed as follows:

1. *Variations of photographic emulsions.*—Several different coatings of the Eastman 103-*F* plate have been used, but large numbers of plates of a given emulsion are generally obtained at one time. Some evaluation is made of the magnitude of the effect encountered during a change

from one coating to another by duplicating observations for the same coronal intensities with both coatings.

2. *Variations of handling and development of photographic plates.*—Different persons may agitate the plates differently in development; the timing of development may be in error; the activity of different solutions may differ; temperatures of developer may be different from day to day.

3. *Variations of plate sensitivity with plate age, ambient temperature, and humidity at exposure.*—Storage of plates is carefully regulated to maintain conditions recommended by the film manufacturer. No control of ambient temperature or humidity at exposure is attempted.

4. *Variations of apparent line-intensity with changes in plate-background intensity arising from changes in sky-background brightness with differences in dust, moisture, and smoke conditions in the atmosphere.*—The coronal lines are superposed on this variable background so that apparent changes in intensity can arise through actual fluctuations in line-density for a given coronal intensity and through subjective factors. This is complicated, for the green line, by the fact that the line falls partially onto a faint absorption line of the Fraunhofer spectrum of the sun.

5. *Variations arising from interpolation against artificial comparison lines whose appearance never exactly duplicates that of the real coronal lines.*—In spite of careful preparation of the comparison lines, some differences in appearance between real coronal lines and the comparison lines arise with changes in the background density of the plates and with other factors. If the difference is great, it is difficult to obtain unambiguous coronal-intensity determinations.

6. *Variations arising from minute misadjustments of the optical system of the coronagraph and spectrograph.*—Small errors of this nature may result from vignetting, changes of focus, errors of slit-width adjustment, etc., which are difficult to eliminate from the present optical arrangements.

7. *Variations from errors in spectrograph-slit positioning relative to the sun's image thereupon.*—This error will produce readings on different days which are not taken from the same height above the sun's limb.

But, in spite of these sources of error, some of which can be corrected and some of which it will be difficult to eliminate without new equipment, the magnitude of all such effects combined cannot reasonably cause fluctuations which are at all comparable to the observed range of changes of coronal intensity.

ATOMIC LINES IN THE SPECTRUM OF R LEONIS*

PAUL W. MERRILL

Mount Wilson Observatory

Received February 25, 1946

ABSTRACT

The spectrum of the Me long-period variable R Leonis was photographed as far into the ultraviolet as λ 3450. Variations with phase in the light-cycle were studied. Identifications and displacements of numerous atomic lines are recorded in some detail.

Dark lines.—The region shortward from *Hδ* is especially favorable for the study of atomic lines because it is rich in lines of common metals and because the interference of molecular lines is negligible. Because of the low temperature, lines whose lower levels have excitation potentials less than 0.5 volts are emphasized. A survey of the behavior of various multiplets includes the elements *Mg* I, *Al* I, *K* I, *Ca* I, *Ca* II, *Sc* I, *Sc* II, *Ti* I, *V* I, *Cr* I, *Mn* I, *Fe* I, *Co* I, *Ni* I, *Sr* I, *Sr* II, *Y* I, *Y* II, *Zr* I.

Bright lines.—The data confirm and extend previous observations of Me variables and make possible some detailed comparisons with R Hydrae. Displacements of lines of the following elements were studied: *H*, *Fe* I, *Mg* I, *Si* I, *In* I, *Ca* II, *Fe* II, *Ti* II, *Mn* II. In two multiplets of *Fe* I the only bright lines observed are from the upper level $z^3G_4^0$. The identification of bright lines of *Fe* II and *Ti* II is certain; that of *Mn* II highly probable. The behavior of the curious displaced emission of H and K of *Ca* II parallels that previously described in R Hydrae.

General.—As spectroscopic observations of long-period variables become more extensive, the great complexity of the phenomena in these objects is clearly exhibited. The characteristic behavior pattern is gradually being determined in greater and greater detail.

The brightness of R Leonis, 094211, was found to vary by D. Koch in 1782. Since then the periodic changes in light have been followed by many observers, and the star has become one of the four best-known long-period variables. The period is 309 days, magnitude range from 5.0 to 10.5, spectral type at maximum M8e. The spectroscopic behavior is typical of advanced Me variables.

In the present investigation of the spectrum with rather high dispersion, 10.3 A/mm, the star was fairly well observed during the brighter portions of the light-cycles associated with two maxima, those of March 6 and of December 30, 1943. Spectrograms were obtained also at one epoch in both the preceding and the following cycle. The journal of observations is in Table 1, the light-curve in Figure 1. I am indebted to Mr. Leon Campbell of the Harvard Observatory for the photometric data. This *Contribution* is the third in a series on the spectra of long-period variables observed with the coudé spectrograph. The material is more extensive, especially in the spectral region shortward[1] from H and K, than that for the Me variables previously described.[2,3]

ABSORPTION LINES

Because of the considerable extension of the photographed spectrum into the ultraviolet, the atomic lines in the spectrum of R Leonis can be studied more comprehensively than those in Me stars previously observed. Except for a single observation of emission lines of *Fe* II near λ 3280, the limit of the recorded spectrum is λ 3440. The whole region shortward from *Hδ*, λ 4101A, is especially favorable for atomic lines because it is rich in lines of common metals and because the interference of molecular bands is negligible. From *Hδ* longward, as interference by the *TiO* bands gradually increases, a general study of the intensities and displacements of atomic lines becomes more and more

* *Contributions from the Mount Wilson Observatory, Carnegie Institution of Washington*, No. 720.

[1] A coined word for "toward shorter wave lengths."

[2] U Ori, R Ser, R Aql, R Cas, *Mt. W. Contr.*, No. 713; *Ap. J.*, **102**, 347, 1945.

[3] R Hya, *Mt. W. Contr.*, No. 717; *Ap. J.*, **103**, 6, 1946.

unsatisfactory. Beyond $H\gamma$, λ 4340A, atomic lines are so buried that only a few of the strongest can be readily identified.

A brief survey of the lines of various elements may be valuable for reference. Because of the low temperature of the reversing layer—say, 2300° at maximum—there will be little ionization, and the atoms will be highly concentrated in the states of low excitation (see Table 2). This means that, within the astronomically observable range of wave lengths, the only lines to be expected are those of the metallic elements. Great emphasis will be placed on those lines whose lower levels have excitation potentials less than 0.5

TABLE 1

JOURNAL OF OBSERVATIONS

Plate Ce	Date	JD 243	Mag.	Phase (Days)	Rad. Vel. from Abs. Lines	
					Km/Sec	No. Lines
2766	1942 Apr. 4	0454	7.4	− 21	+12.2	42
2768	Apr. 6	0456	7.3	− 19	.....	.....
2939	Dec. 27	0721	9.2	− 69	+12.2	26
2958	1943 Feb. 25	0781	6.4	− 9	+12.2	70
2970	Mar. 23	0807	6.3	+ 17	+14.3	110
2973	Mar. 24	0808	6.3	+ 18	+14.6	48
3017	Apr. 24	0839	6.9	+ 49	+15.4	368
3020	Apr. 25	0840	6.9	+ 50	+15.3	23
3021	Apr. 25	0840	6.9	+ 50	.....	.....
3029	May 18	0863	7.5	+ 73	+14.0	36
3033	May 19	0864	7.5	+ 74	+15.6	25
3051	May 25	0870	7.7	+ 80	+14.9	21
3054	May 26	0871	7.7	+ 81	+14.6	17
3059	June 10	0886	8.2	+ 96	.....	.....
3316	Dec. 12	1071	6.6	− 18	+11.5	135
3323	Dec. 14	1073	6.5	− 16	+13.8	20
3360	1944 Jan. 15	1105	6.1	+ 16	+11.8	113
3361	Jan. 15	1105	6.1	+ 16	.....	.....
3366	Jan. 16	1106	6.1	+ 17	+12.5	76
3385	Feb. 8	1129	6.8	+ 40	.....	.....
3387	Feb. 9	1130	6.8	+ 41	.....	.....
3389	Feb. 10	1131	6.9	+ 42	+11.1	72
3401	Apr. 7	1188	8.5	+ 99	.....	.....
3405	Apr. 9	1190	8.6	+101	+11.0	13
3423	May 11	1222	9.1	+133	.....	.....
3689	1945 Jan. 1	1457	6.5	+ 65	+12.1	54
3694	Jan. 2	1458	6.6	+ 66	.....	.....

volts. Ionized lines, except those of abundant elements having low ionization potentials, will be weak or absent. Plates IX and X show the spectrum 49 days after maximum.

Lines of Mg I.—The only observable line from the ground level is the intercombination line λ 4571, $^1S_0 - {}^3P_1^o$. At and before maximum it appears as an absorption line of moderate intensity with a trace of emission on the shortward edge. After maximum the absorption gradually disappears, while the emission fringe increases in intensity until at phase about +60 days it becomes measurable as a distinct bright line. Thereafter the bright line rapidly becomes outstanding; toward minimum it may be the strongest feature in the whole photographic spectrum.

The ultraviolet triplet λλ 3829, 3832, 3838, E.P. 2.70 volts, is visible in emission on practically all the plates (see Pls. X and XII). Early in each cycle there may be weak ab-

PLATE IX

SPECTROGRAM OF R LEONIS, λλ 3410–3770

Plate Ce 3017. April 24, 1943; magnitude 6.9; 49 days after maximum

PLATE X

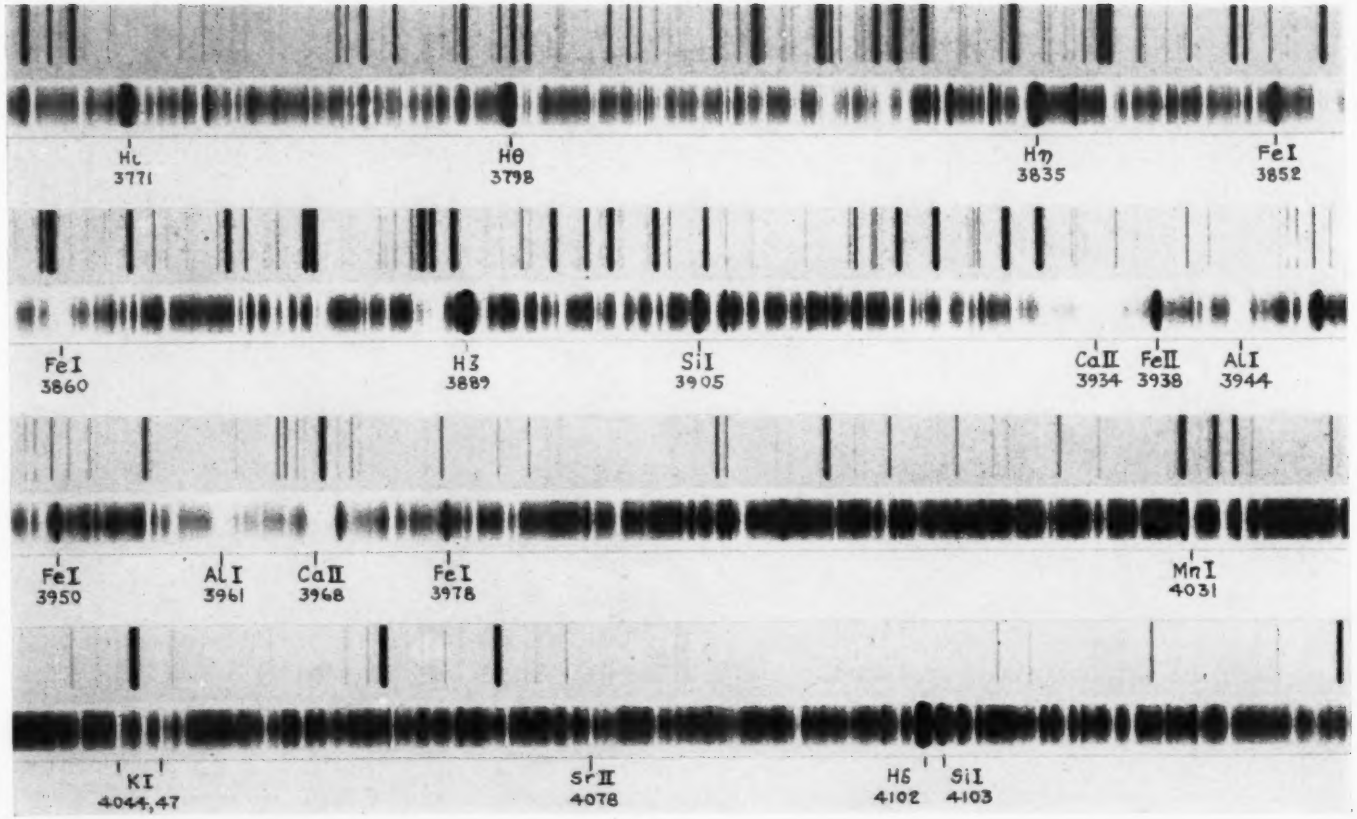

SPECTROGRAM OF R LEONIS, λλ 3760–4130

Plate Ce 3017. April 24, 1943; magnitude 6.9; 49 days after maximum

sorption on the longward edges of the bright lines, but the identification is not entirely certain.

Lines of Al I.—The ultimate lines λ 3944 and λ 3961 are very strong. On a few plates taken at or before maximum they are closely comparable to H and K of *Ca* II; on other plates they are definitely narrower. After maximum the comparison is complicated by the appearance of emission on the shortward sides of the *Ca* II lines. Near maximum the average residual in radial velocity of the two *Al* I lines is about −2 km/sec, but after maximum a residual of about +9 km/sec develops. This positive residual may be caused by a slight strengthening of the shortward border by incipient emission—a phenomenon qualitatively like that which develops so prominently in the H and K lines during the

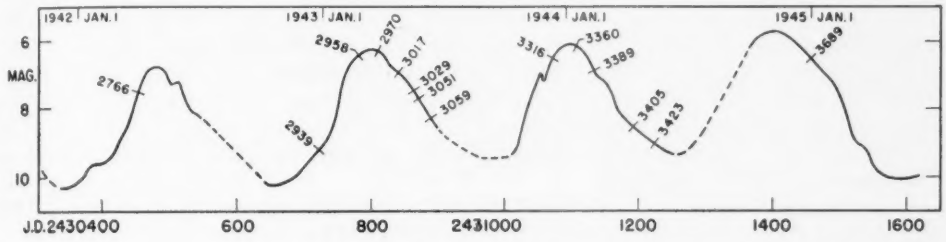

FIG. 1.—Light-curve of R Leonis showing dates of spectrograms (see Table 1)

TABLE 2

BOLTZMANN DISTRIBUTION OF ATOMS AT LOW TEMPERATURES

TEMP.	EXCITATION POTENTIAL IN VOLTS								
	0.00	0.25	0.50	0.75	1.00	1.25	1.50	1.75	2.00
2600°	1000	328.	107.	35.	12.	3.8	1.2	0.40	0.13
2400	1000	298.	89.	27.	7.9	2.4	0.71	0.21	0.063
2200	1000	267.	72.	19.	5.1	1.4	0.37	0.098	0.026
2000	1000	234.	55.	13.	3.0	0.71	0.17	0.039	0.0091
1800	1000	200.	40.	7.9	1.6	0.32	0.063	0.013	0.0025
1600	1000	163.	27.	4.3	0.71	0.12	0.019	0.0031	0.00050

post-maximum phase. The same behavior is suspected in a few strong lines of other elements; in numerous relatively *weak* dark lines, emission on the shortward border develops into a well-marked narrow bright line.

Multiplet (2) of the Revised Multiplet Table,[4] which falls near the short-wave-length limit of the photographed spectrum, was not definitely identified; its lines, if present, must be weak.

Lines of K I.—The violet pair of *K* I lines λ 4044, λ 4047, is well marked on plates at all the observed phases. As would be expected from the low ionization potential of 4.3 volts, the lines are very sensitive to temperature, being weaker at the somewhat higher photospheric temperature near maximum light. In R Leonis they are much stronger than in stars of less advanced spectral type, such as α Herculis or ο Ceti (normal maximum).

[4] Charlotte E. Moore, "A Multiplet Table of Astrophysical Interest," rev. ed., *Contributions from the Princeton Observatory*, No. 20, 1945.

The residual in radial velocity is −3.6 km/sec, agreeing closely with the average residuals in other Me variables.[2,3]

Lines of Ca I.—The ultimate line λ 4226 is extremely strong and wide, being the strongest single line in the whole observed spectrum. On strongly exposed plates, especially those taken near maximum light, when the line has its least intensity, its center can be measured with fair accuracy. The average residual, −0.4 km/sec, shows that within errors of measurement the displacement is the same as that of weaker lines.

Multiplets R.M.T.[5] (4) and (5), which lie in the banded regions where identifications are difficult, appear to be represented by their strongest lines. Multiplets (6) and (9) are present in moderate intensity; the lines are sharp, the velocity residuals small.

Lines of Ca II.—The ionized lines, H and K, although not nearly so intense as the ultimate neutral line λ 4227, are strong and wide; the greatest intensities occur near maximum light. Measurements on one or two strongly exposed plates taken near maximum yield displacements which do not differ appreciably from that corresponding to the mean absorption-line velocity. After maximum the dark lines become unsymmetrical because of the appearance of emission within the shortward wings. This phenomenon will be discussed in the section on emission lines.

Lines of Sc I.—Multiplets (6), (7), and (8) are present in moderate intensity. The displacements have small residuals.

Lines of Sc II.—Multiplets (2) and (3) appear to be represented by weak lines. It is surprising that enough scandium atoms, I.P. 6.7 volts, are ionized to produce observable lines.

Lines of Ti I.—Ultimate lines are numerous and strong. Multiplets (12)–(21) are represented, with the exception of the weak $^3F - {}^5G$ multiplet (16). Multiplets (20) and (21) are weak. Multiplet (83), E.P. 1.1 volts, may be present in low intensity, although multiplet (80), of the same excitation potential, is apparently absent.

Lines of V I.—Multiplets (7) and (9) are strong; (8), (22), (27), (28), and (29) are easily identified.

Lines of Cr I.—Ultimate lines are remarkably strong. The lines of multiplet (4), λλ 3578, 3593, 3605, are outstanding, being exceeded in intensity only by λ 4227 *Ca* I; λ 3933, λ 3968 *Ca* II; λ 3944, λ 3961 *Al* I. The better-known multiplet (1), λλ 4254, 4275, 4290, is strong; multiplets (2) and (3) are well marked. Multiplet (23), E.P. 1.0 volts, also is well marked, but (38), E.P. 2.5 volts, is apparently absent.

Lines of Mn I.—The behavior of the strong ultimate multiplet (2) λλ 4030, 4033, 4034 is remarkably complex. Before maximum the lines are wholly in absorption, but later in the cycle strong emission components develop. It is hoped later to make a special comparative study of this multiplet in the spectra of several long-period variables. The line λ 4041 of multiplet (5), E.P. 2.1 volts, is present in moderate strength without noticeable emission.

Lines of Fe I.—The behavior of multiplets (2) and (3), E.P. 0.0 volts, varies with phase in a complicated manner; the lines, some of which are present in absorption near maximum, develop strong emission during the decline of light. A comparative study of these multiplets in several variables is planned. Multiplets (4) and (5), in absorption only, are extremely strong; (6) also is well marked.

Lines of multiplets (18) and (19), E.P. 0.9, are of moderate intensity without emission. Lines of (20), (21), (22), (23), and (24) are quite strong; during the decline of light many of the weaker ones develop emission on the shortward edge. The strongest line of (25), λ 3452.27, is a weak dark line. Several lines of multiplet (41), E.P. 1.5 volts, are recognizable in the complicated band structure; emission is weak or absent. The behavior of (42) is very complicated; most of the lines are of moderate intensity in absorption, but

[5] Revised Multiplet Table (see n. 4). Throughout the present *Contribution*, multiplet numbers in parentheses are those of the Revised Multiplet Table.

λ 4202 and λ 4308 are outstanding bright lines in the post-maximum phase. Lines of (43) and (45) are regularly observed in absorption in moderate intensity; a few lines of (43) develop weak emission edges.

Six or seven multiplets of higher excitation potential are represented only by bright lines; absorption components are very weak or absent. For a survey of the general behavior of multiplets of *Fe* I see page 285.

Lines of Co I.—Among multiplets from the a^4F term, E.P. 0.0 volts, (1), (3), (4), (5), and (6) are present; (2) is doubtful. From b^4F, E.P. 0.4 volts, the following have been measured: (16), (17), (18), (19), (21), (22), and (23); (20) is probably present, although its identification is interfered with by blends. From a^2F, E.P. 0.9 volts, the following multiplets have been identified: (28), (29), (31)?, (32)?, (33), (34), (35), and (36). Lines of higher excitation potential are weak or absent; λ 3732.39 and λ 3730.48 of multiplet (62) are probably present in very low intensity.

Lines of Ni I.—From the term a^3F, E.P. 0.0 volts, multiplets (1)–(8) inclusive are represented, with the exception of (7), which is outside the observed range of wave lengths. From a^3D, E.P. 0.1 volts, are found (15), (16), (17), (18), (19), and (20); from a^1D, E.P. 0.4 volts, (29), (30), (31), (32), (33), (35), and (36).

Lines of Sr.—The ultimate line of *Sr* I, λ 4607, is barely recognizable in the midst of heavy band absorption. One or both of the ionized lines λ 4077 and λ 4215 are measurable on practically all the plates; their displacements yield in the mean a small positive residual. These lines are somewhat stronger near the time of maximum light.

Lines of Y I.—Multiplets (5), (6), and (8) seem to be represented by very weak lines. There is little evidence either for or against multiplet (7).

Lines of Y II.—The evidence, although not wholly convincing, indicates that the strongest transitions from the ^1S and the ^3D terms are systematically represented by extremely weak lines. In view of the weakness of the lines of *Y* I, it is surprising that enough yttrium atoms, I.P. 6.5 volts, are ionized to produce observable lines. The lines of *Y* II, as well as those of *Sc* II, seem remarkably persistent. The identifications of these faint lines are subject to confirmation either by observations with higher dispersion or by a very detailed study of the spectra of several variables.

Lines of Zr I.—The strongest lines of multiplets (12) and (13) are believed to be present in very low intensity.

Displacements of lines.—On the strongly exposed plate Ce 3017 nearly all the dark lines in the region free from molecular bands were measured—a total of 506 shortward from λ 4227. In addition, 14 strong atomic lines were measured in the banded region from λ 4227 to λ 4576. The measured displacements of 368 of these lines were used in forming the mean velocity. The distribution among various chemical elements is shown in the accompanying tabulation. On most of the other plates, measurement was limited

Fe I	110	*Ti* I	44
Co I	66	*Cr* I	15
Ni I	50	*Mn* I	6
V I	49	Misc.	28
		Total	368

to selected lines. The adopted velocities and the number of lines on which each depends are given in Table 1.

The velocities show little variation throughout the observed phases, which include about half the light-cycle (Fig. 2). The over-all mean is +13.3 ± 0.3 km/sec, which is nearly the same as the mean for 1920–1921, +13.8 ± 0.8 km/sec.[6] In 1926–1928, however,

[6] *Mt. W. Contr.* No. 264; *Ap. J.*, **58**, 215, 1923.

the value was $+7.4 \pm 0.8$ km/sec.[7] In 1943 the post-maximum values were slightly greater than in other years, averaging $+15.0 \pm 0.1$ km/sec. It thus appears that the difference between various cycles may be greater than the amplitude in any one cycle. Future measurements throughout a longer portion of the light-cycle are desirable.

The residuals yielded by lines of the various chemical elements are similar to those in Me stars previously measured (Table 3).

As in other Me stars, the displacements of lines of *Fe* I exhibit a dependence on ex-

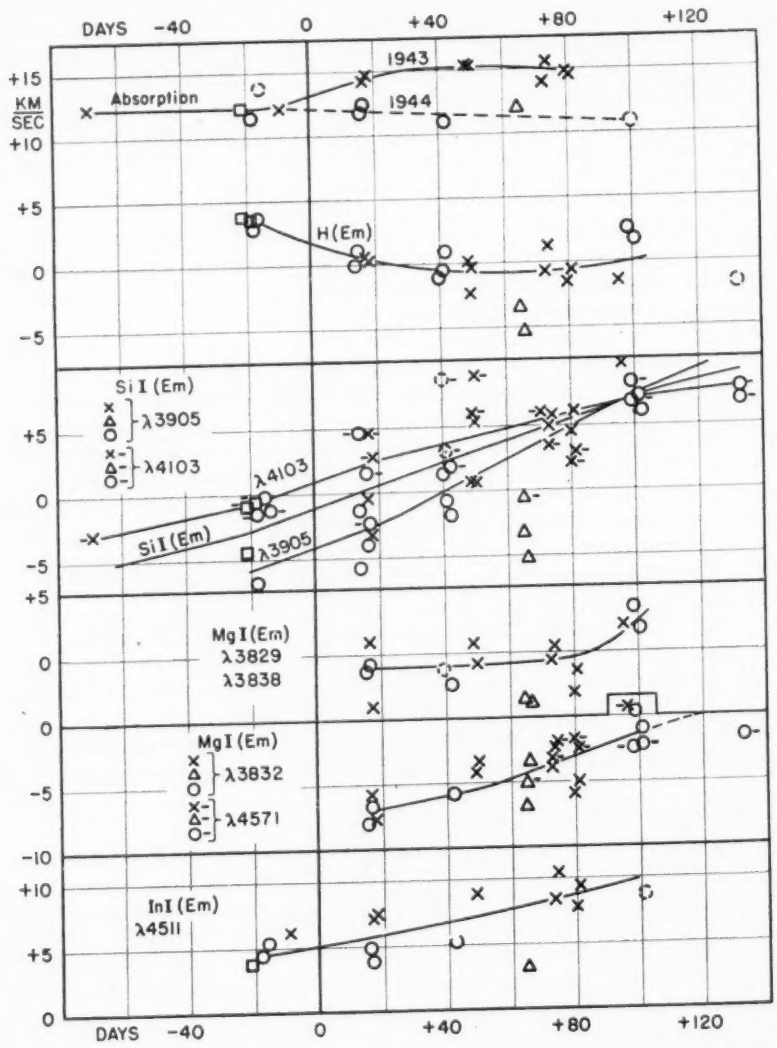

FIG. 2.—Velocity-curves derived from absorption and emission lines. Observations in various years are indicated as follows: *squares*, 1942; *crosses*, 1943; *circles*, 1944; *triangles*, 1945.

[7] *Mt. W. Contr.* No. 649; *Ap. J.*, 94, 171, 1941.

citation potential, the displacement at E.P. 1.0 volts being about 3 km/sec greater algebraically than at 0.0 volts. There is also a weak correlation of displacement with intensity, the stronger lines having algebraically smaller velocities; this result depends largely (perhaps wholly) upon the fact that the low-level lines have the greater mean intensity. A similar dependence of displacement on excitation potential probably prevails generally among the lines of other metals; it is fairly well exhibited by *V* I and *Co* I.

Two questions concerning displacements remain to be answered by future work, preferably with higher dispersion: (1) Do all lines of a given multiplet yield the same displacement regardless of intensity? (2) Is the displacement the same for all multiplets arising from a given lower level? In many lines the interpretation of the measured displacement is complicated by the presence of an emission edge; the difficulty becomes less serious with high dispersion.

TABLE 3

DISPLACEMENTS OF ABSORPTION LINES
(Residuals in Km/Sec)

Element	R Leo	R Hya	Four Me Stars
Al I	.....	−0.2	.....
K I	−3.6	−3.3	−3.3
Ca I	−0.4	.....	.....
Sc I	+1.0	+2.0	+0.5
Ti I	−0.3	−1.0	−0.1
V I	−0.1	−0.2	−0.5
Cr I	−1.4	−1.1	−1.1
Mn I	−1.1	(+0.5)	(−0.6)
Fe I	+0.7	+0.8	+0.4
Co I	0.0	−0.1	0.0
Ni I	−0.5	+0.5	+0.2
Sr II	+1.8	(+1.7)	(−0.5)

EMISSION LINES

In the regions of Me spectra not disturbed by bands, the absorption lines are those corresponding to a normal reversing layer in thermal equilibrium with a low-temperature photosphere. Superposed on this rich dark-line spectrum, especially during the post-maximum phase, are many bright lines, some of great intensity, whose behavior is highly complex and enigmatic. Although much is already known concerning a number of these lines, additional information seems necessary if we are ever to understand their origin and their relationship to the more general phenomena of light-variability.

The data yielded by the present spectrograms of R Leonis make possible some interesting comparisons with R Hydrae.[3] The following notes will be supplemented later, I hope, by intercomparisons of several variables.

Lines of hydrogen.—The intensities vary with phase in the usual way. The lines tend to become narrower and to assume their normal (laboratory) relative intensities as the cycle advances. A striking example is offered by the behavior of $H\epsilon$, which is absent on plate Ce 2970, phase +17 days, but is well developed a month later on Ce 3017, phase +49 days. The intensity of the Balmer series as a whole is no greater on the later plate; hence the difference in $H\epsilon$ appears to be due to decreased effective absorption by the *Ca* II line H, which has apparently become somewhat narrower. At a later phase the

bright *Hε* line becomes still stronger (see Pl. XII). From phase −20 days to +40 days the velocity-curve (Table 4; Fig. 2) drops about 4 km/sec. Thereafter, until the lines disappear, the curve is nearly flat, individual points showing considerable scatter.

Lines of Fe I.—The bright lines of *Fe* I in R Leonis may be discussed in three groups:

I. The outstanding lines λλ 3852, 4202, 4308. These lines are abnormally strong compared to other lines in the same multiplets.

II. The low-excitation intercombination multiplets (2) and (3).

III. The high-excitation (upper level about 5.4 volts) multiplets (72)–(78).

TABLE 4

DISPLACEMENTS OF BRIGHT LINES
(Km/Sec)

Plate Ce	Phase (Days)	*H*	*Si* I		*Mg* I				*In* I
			λ 3905	λ 4103	λ 3829	λ 3832	λ 3838	λ 4571	λ 4511
2766	− 21	+3.8 (2)	−4.4	−0.9	(−9.5)	(−7.2)	.....	.....	+ 3.8
2768	− 19	+3.7 (1)	.....	−0.6	.....	.....	.....	.....	.....
2939	− 69	?	.....	−3.0	.....	.....	.....	.....	.....
2958	− 9	?	.....	.....	.....	.....	.....	.....	+ 6.1
2970	+ 17	+0.5 (4)	−0.5	+4.5	−0.2	−5.7	+2.1	.....	+ 7.1
2973	+ 18	+0.3 (2)	−3.1	+2.7	−5.2	−7.6	−2.9	.....	+ 7.4
3017	+ 49	+0.2 (6)	+0.7	+5.9	−0.3	−4.2	+1.6	.....	+ 8.9
3020	+ 50	−0.2 (13)	(+5.3)	+8.9	−1.1	−3.4	−0.4	.....	.....
3021	+ 50	−2.3 (3)	+0.6	.....	.....	.....	.....	.....	.....
3029	+ 73	−0.6 (20)	+5.0	+3.3	−2.2	−3.8	+0.9	−2.7	+ 8.3
3033	+ 74	+1.9 (18)	+5.7	+6.2	−0.6	−2.2	+1.6	−2.0	+10.3
3051	+ 80	−1.4 (11)	+4.5	+2.1	−2.7	−5.8	−3.5	−1.7	+ 7.9
3054	+ 81	−0.5 (14)	+6.1	+3.0	−1.8	−5.0	−1.1	−2.3	+ 9.4
3059	+ 96	−1.3 (5)	+9.9	.....	+2.0	.....	+1.9	+0.6	.....
3316	− 18	+3.2 (2)	−6.8	−1.5	.....	.....	.....	.....	+ 4.4
3323	− 16	+3.8 (2)	−0.3	−0.4	.....	.....	.....	.....	+ 5.3
3360	+ 16	+0.4 (3)	−5.8	+4.7	−2.3	−6.8	+0.1	.....	+ 4.9
3361	+ 16	+0.6 (4)	−1.4	+1.5	.....	.....	.....	.....	.....
3366	+ 17	+0.8 (4)	−4.0	−2.4	−2.8	−6.7	+1.1	.....	+ 3.8
3385	+ 40	−1.0 (5)	+1.3	(+8.6)	(+0.5)	(−0.3)	(−2.7)	.....	.....
3387	+ 41	−0.5 (5)	−0.7	(+3.1)	.....	.....	.....	.....	.....
3389	+ 42	+1.0 (11)	−1.9	+1.9	−2.8	−5.9	−2.0	.....	+ 5.2
3401	+ 99	+2.7 (5)	+6.8	+8.3	+3.5	+0.3	+3.4	−2.3	.....
3405	+101	+1.9 (8)	+7.0	+6.2	+1.3	−1.0	+2.1	−2.2	(+ 8.7)
3423	+133	(−1.5)(3)	+7.9	+6.9	.....	.....	.....	−1.5	.....
3689	+ 65	−3.4 (14)	−3.2	−0.6	−4.5	−6.8	−2.8	−5.0	+ 3.3
3694	+ 66	−5.2 (4)	−3.6	.....	−5.6	−3.3	−1.7	.....	.....

I. The three strongest bright *Fe* I lines λλ 3852, 4202, 4308 behave much as in R Hydrae, except that λ 3852 and λ 4202 first appear considerably later in the cycle. The velocity-curves of the three lines are remarkably similar in the two stars.

The identification of λ 3852 with *Fe* I 3852.574 of multiplet (73), although probable, is not yet wholly certain. The measured wave length both in R Hydrae and in R Leonis may be a few hundredths greater than the laboratory value. This difference appears to

PLATE XI

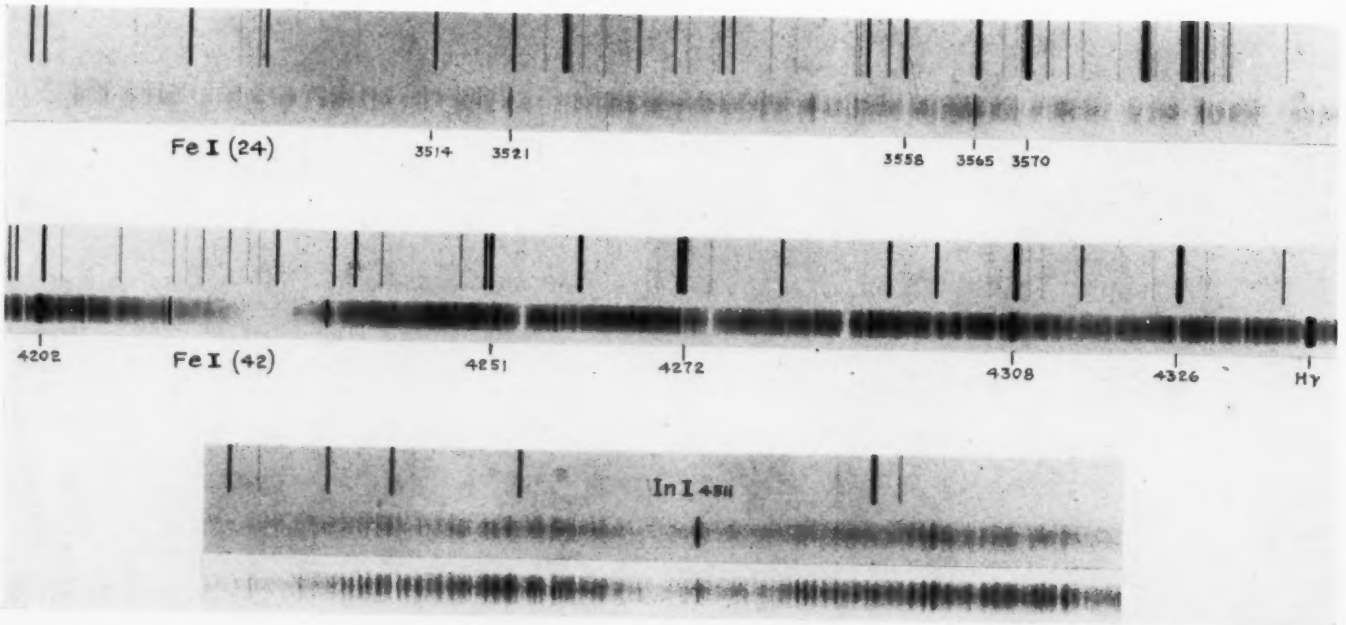

BRIGHT LINES IN THE SPECTRUM OF R LEONIS

Upper, multiplet R.M.T. (24) of *Fe* I; Plate Ce 3689. *Center*, multiplet R.M.T. (42) of *Fe* I; Plate Ce 3689. *Lower*, *In* I λ 4511; Plates Ce 2766, phase −21 days, and Ce 2970, phase +17 days.

PLATE XII

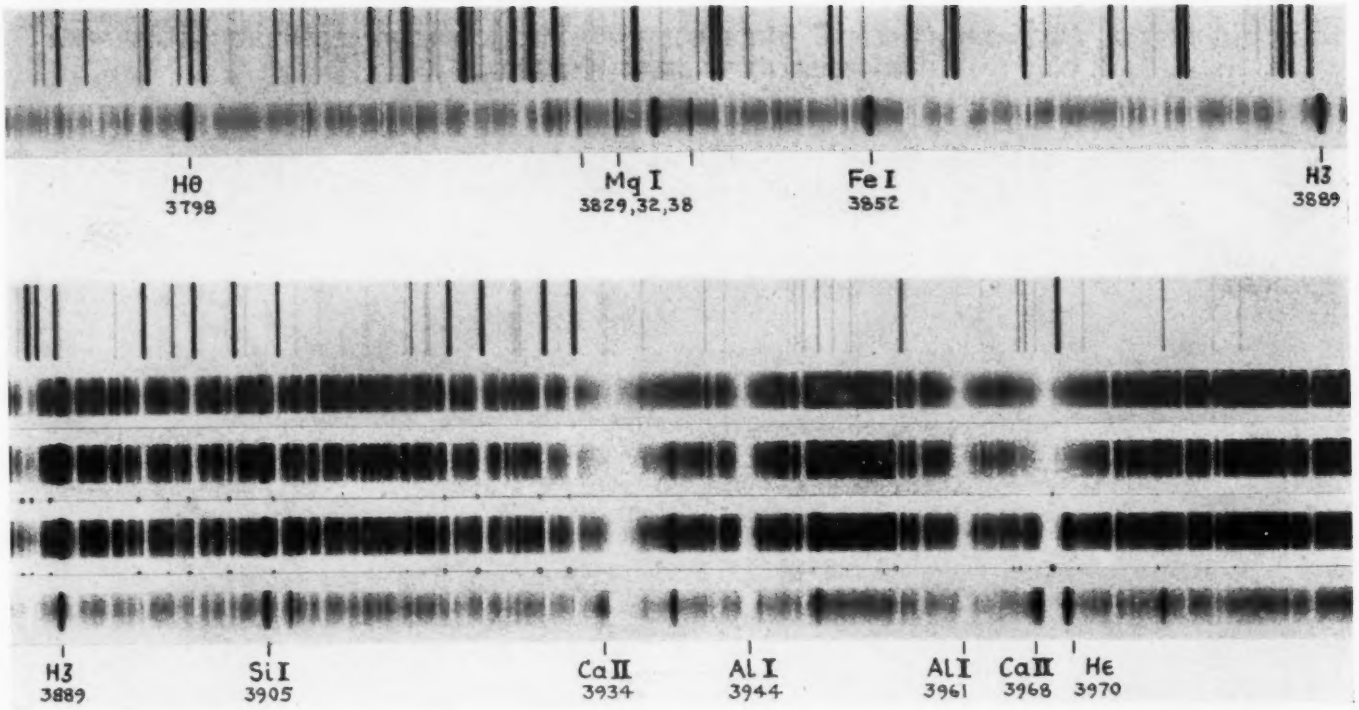

SPECTROGRAMS OF R LEONIS

Upper, region of $H\eta$; Plate Ce 3029. *Lower*, development of emission component in H and K lines of *Ca* II: Plates Ce 3316, phase −18 days; Ce 2970, +17 days; Ce 3017, +49 days; Ce 3051, +80 days.

be greater than the error of measurement, especially in R Leonis, where the line is narrower. The companion line of slightly longer wave length, suspected in R Hydrae, if present at all in R Leonis, is weaker. The only other *Fe* I lines having the same upper level, $w^5D^\circ_4$, are λ 3171.353 of multiplet (52), outside the observed spectral region, and λ 4373.563 of multiplet (214). The λ 4373 line has not been observed; its position is almost exactly 1 A longward from the well-known but unidentified bright line λ 4372.57, in a region of molecular lines of moderate intensity.

TABLE 5

DISPLACEMENTS OF BRIGHT LINES OF IRON AND TITANIUM
(Km/Sec)

PLATE CE	PHASE (DAYS)	*Fe* I				*Fe* II	*Ti* II
		λ 3852	λ 4202	λ 4308	Mean*		
2939	− 69	.....	.....	.....	.....	+12.6 (1)	.....
2970	+ 17	− 0.3	−3.9	.....	+0.8 (3)	+ 8.2 (3)	.....
2973	+ 18	− 1.4	−2.1	.....	−0.3 (1)	+ 9.1 (1)	.....
3017	+ 49	+ 1.9	−2.7	.....	−1.8 (23)	(+ 4.5)(2)	+0.4 (3)
3020	+ 50	+ 0.3	−0.6	−8.2	−1.5 (7)	+ 6.5 (3)	.....
3021	+ 50	+ 1.0	.....	.....	.....	.....	.....
3029	+ 73	+ 7.0	−1.8	−6.6	−2.6 (20)	+ 3.5 (8)	+1.2 (3)
3033	+ 74	+ 1.5	−0.6	−5.9	−2.0 (17)	+ 3.5 (4)	+1.2 (3)
3051	+ 80	+ 6.5	−1.5	−3.5	−3.1 (17)	+ 2.6 (4)	−0.1 (3)
3054	+ 81	+ 6.6	−0.6	−4.1	−2.6 (11)	+ 3.1 (4)	+1.0 (2)
3059	+ 96	+10.3	+0.1	+2.2	−4.3 (6)	+ 1.5 (5)	.....
3360	+ 16	− 2.2	.....	.....	.....	+ 8.1 (3)	.....
3361	+ 16	(+ 1.5)	(−7.4)	.....	.....	.....	.....
3366	+ 17	− 0.4	−3.4	.....	−0.8 (1)	+ 8.1 (3)	−1.2 (2)
3385	+ 40	− 1.1	−3.6	.....	.....	.....	.....
3387	+ 41	− 0.7	.....	.....	.....	.....	.....
3389	+ 42	− 1.2	−3.1	.....	−3.9 (3)	+ 4.6 (3)	−1.6 (3)
3401	+ 99	+ 4.1	+1.1	+1.9	+0.4 (5)	+ 6.6 (2)	.....
3405	+101	+ 5.1	+0.5	+1.3	+0.8 (7)	+ 6.9 (5)	+5.8 (2)
3423	+133	+ 5.3	+3.1	+0.9	−3.9 (5)	+ 6.1 (1)	.....
3689	+ 65	+ 0.4	−5.1	−7.2	−4.4 (14)	+ 2.2 (3)	−5.6 (3)
3694	+ 66	− 0.8	.....	.....	.....	.....	.....

* Excluding λλ 3852, 4202, 4308.

The lines λ 4202 and λ 4308, multiplet (42), have the same upper level, $z^3G^\circ_4$. Other multiplets which have this upper level are (24) and (169), the latter in the red, where bands prevent the recognition of atomic lines. A partial comparison of multiplets (24) and (42) in 1937 yielded an interesting result,[8] which is confirmed and extended by the recent spectrograms of R Leonis (Table 6).

The lines λ 3521 and λ 3565 of multiplet (24) follow the well-known pattern of behavior of λ 4202 and λ 4308 of multiplet (42); they develop in emission about 50 days after maximum light and thereafter become outstanding bright lines. The strong line of the same multiplet, λ 3570.10, does not appear in emission. No line of multiplets (24) or (42) appears in emission unless its upper level is $z^3G^\circ_4$, and of the lines from this level the

[8] Merrill and Thackeray, *Pub. A.S.P.*, **49**, 120, 1937.

only one unobserved is the very weak line λ 3466.50. The dependence on a particular upper level evidently supersedes the ordinary multiplet relationships. The suggestion[9] that this upper level is excited by *Mg* II λ 2795.52 is not easy to prove.

II. The stronger lines of multiplets (2) and (3) are well marked in absorption near the time of maximum; as the cycle advances, emission, appearing first on the shortward edges of the lines, gradually becomes predominant. Toward minimum, numerous emission lines of these multiplets are present in relative intensities approximating those in the laboratory. The observed intensities of these lines are affected by the *TiO* bands; hence in a later detailed intercomparison it is planned to include the S-type variable R Andromedae.

TABLE 6

INCOMPLETE MULTIPLETS OF *Fe* I*

(24) $a^5F - z^5G^\circ$				(42) $a^3F - z^3G^\circ$			
I.A.	Int.	J	Emission in Me Stars	I.A.	Int.	J	Emission in Me Stars
3513.82	30	5–5		4271.76	35	4–5	
3521.26	25	4–4	×	4307.91	35	3–4	×
3526.17	15	3–3		4325.76	35	2–3	
3466.50	3	5–4		4202.03	30	4–4	×
3483.01	3	4–3		4250.79	25	3–3	
3570.10	100R	4–5		4147.67	10	4–3	
3565.38	60r	3–4	×				
3558.52	30	2–3					

* See Pl. XI.

III. Numerous emission lines of multiplets (72)–(78) appear mostly in low intensities for an interval after maximum. Their time of maximum intensity is decidedly earlier in the cycle than that of multiplets (2) and (3). The following notes refer to plate Ce 3017, phase +49 days:

Multiplet	
(72)	The four strongest lines are present
(73)	The four strongest lines are present; of these λ 3852.57 is inordinately intense
(74), (75), (76)	Probably present in low intensity
(77)	No evidence of presence
(78)	Two strongest lines possibly present

On most post-maximum plates, especially those taken in 1943, 10 or 20 emission lines of *Fe* I are sufficiently well marked for accurate measurement. The mean velocities (Table 5) yield a curve which is nearly flat (Fig. 3). The pattern of individual points has a rather remarkable resemblance to that for *Fe* II, although the group as a whole lies definitely lower. The similarity of patterns suggests that this group of bright lines of *Fe* I may arise from the recombination of iron ions with electrons. The general relative displacement may be caused by absorption on the redward sides of the *Fe* I lines.

[9] A. D. Thackeray, *Mt. W. Contr.*, No. 580; *Ap. J.*, **86**, 499, 1937.

Survey of multiplets of Fe I.—The general behavior of the observed multiplets of *Fe* I is indicated in the following brief summary, which includes both absorption and emission lines, but in which some minor details are disregarded:

Lower term a^5D, E.P. 0.0 volts

(2), (3).....Absorption at maximum, changing to emission as phase advances toward minimum
(4), (5), (6).....Absorption only

Lower term a^5F, E.P. 0.9 volts

(18), (19).....Absorption only
(20), (21), (22), (23)....Absorption at maximum; emission develops on the shortward edge during declining phase
(24).....Lines from the upper level $z^3G_4^0$ outstanding in emission during the declining phase

Lower term a^3F, E.P. 1.5 volts

(41).....Absorption only
(42).....Lines from the upper level $z^3G_4^0$ outstanding in emission during the declining phase
(43).....Absorption with weak emission edges after maximum
(45).....Absorption

Lower term a^5P, E.P. 2.2 volts

No absorption lines certainly observed; emission after maximum
(72).....Emission
(73).....Emission; λ 3852 inordinately strong
(74), (75), (76).....Probably in emission in low intensity
(77).....Not seen
(78).....Possibly in emission in low intensity

Lines of Mg I.—The general behavior of multiplets (1) and (3) resembles that in R Hydrae, except that the bright lines do not appear until somewhat later in the light-cycle. The velocity-curves are in Figure 2.

Lines of Si I.—The lines λ 3905 and λ 4103 are stronger than in R Hydrae. The velocity-curves (Fig. 2) rise steadily as the phase advances, individual points exhibiting considerable scatter.

The line λ 4511—This line, probably due to *In* I, is present throughout all the observed portions of the light-cycle (Pl. XI). It undergoes a slight longward shift as the phase advances (Fig. 2). On plate Ce 2939, phase −69 days, a notch in *Hδ* similar to that previously reported in U Orionis,[2] measured at λ 4101.8, may correspond to *In* I λ 4101.77. On most of the plates, *Hδ* is either too badly overexposed or too narrow to allow a useful measure of the absorption line.

Lines of Fe II.—Several bright lines of *Fe* II are present on nearly all the spectrograms. Those most frequently measured are λλ 3938, 4173, 4179, 4233, 4352, 4584. The line λ 4173 exhibits some irregularities in behavior, perhaps because of *TiO* absorption. On plate Ce 3689, phase +65 days, λ 3277 of multiplet (1) is clearly present, accompanied by traces of λ 3281 and λ 3295.

As in *o* Ceti and R Hydrae, the velocity-curve derived from bright lines of *Fe* II lies between that from the absorption lines and that from the bright *H* lines (Figs. 3, 4).

Lines of Ti II.—Three of the strongest lines of *Ti* II λλ 3685, 3759, 3761 of multiplets (13) and (14) were measured as bright lines on most of the well-exposed post-maximum plates. The mean displacement is −0.1 km/sec, compared with 0.0 for *H* and +4.5 for *Fe* II on the same plates. Multiplet (15) may be present in low intensity.

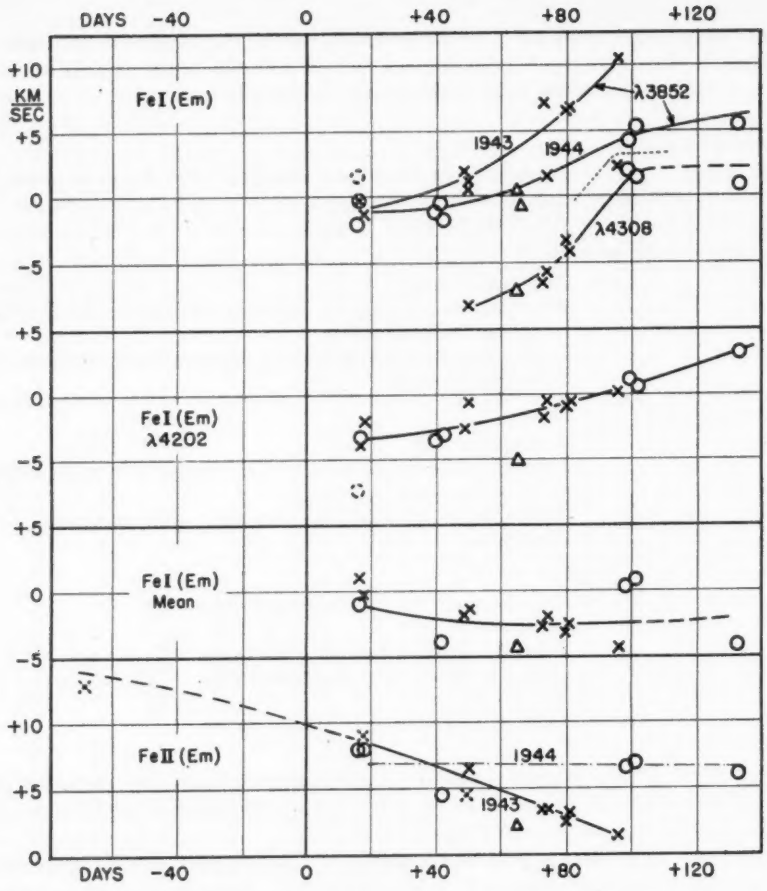

FIG. 3.—Velocity-curves derived from bright iron lines. Observations in various years are indicated as follows: *crosses*, 1943; *circles*, 1944; *triangles*, 1945.

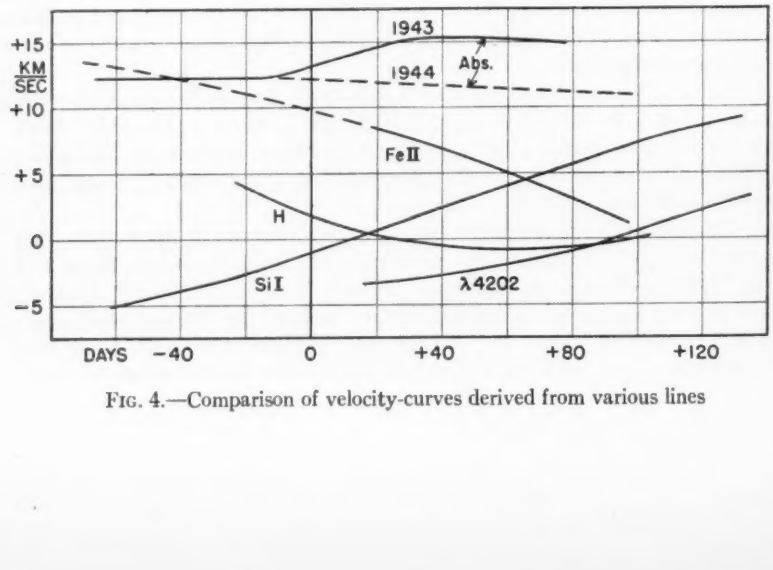

FIG. 4.—Comparison of velocity-curves derived from various lines

Lines of Mn II.—Lines λ 3438.98 and λ 3460.04 of multiplet (1) are present in emission at the shortward end of the strongly exposed plate Ce 3017, phase +49 days. The following notes indicate the probable presence of multiplet (3), although the apparent intensities of the lines do not correspond too well with those given in the Revised Multiplet Table.

λ 3441.98.....Weak
λ 3460.31.....Well marked; stronger than λ 3460.04 of multiplet (1) from which it is only partially resolved
λ 3474.12, λ 3474.04.....Not seen; in the wing of a strong dark line of *Fe* I and nearly coincident with a dark line of moderate intensity of *Co* I
λ 3482.90.....Strong
λ 3488.68.....Weak or absent
λλ 3497.81, 3497.54, 3495.83....Probably present in low intensity; near strong dark lines of *Fe* I and *Co* I

The identification of bright lines of *Fe* II and *Ti* II is certain; that of *Mn* II, highly probable.

TABLE 7

DISPLACEMENTS OF BROAD *Ca* II EMISSION LINES WITH RESPECT TO DARK LINES

Plate Ce	Phase (Days)	H (Km/Sec)	K (Km/Sec)	Plate Ce	Phase (Days)	H (Km/Sec)	K (Km/Sec)
3017.....	+49	−100	−122	3401.....	+ 99	−65	.....
3029.....	+73	− 79	−100	3405.....	+101	−61	.....
3033.....	+74	− 82	−103	3423.....	+133	−43	.....
3051.....	+80	− 76	− 93				
3054.....	+81	− 76	− 98	3689.....	+ 65	−78	−97
3059.....	+96	− 63	.....				

TABLE 8

DISPLACEMENTS OF THE BRIGHT LINE λ 4372.54

Plate Ce	Phase (Days)	Rad. Vel. (Km/Sec)	Rad. Vel. *Fe* II (Km/Sec)	Plate Ce	Phase (Days)	Rad. Vel. (Km/Sec)	Rad. Vel. *Fe* II (Km/Sec)
3029.....	+73	+4.0	+3.5	3401.....	+ 99	+7.6	+8.7
3033.....	+74	+6.8	+3.5	3405.....	+101	+7.7	+6.9
3051.....	+80	+4.3	+2.6				
3054.....	+81	+5.1	+3.1	3689.....	+ 65	(+7.6)	+2.2
3059.....	+96	+3.2	.....				

Displaced lines of Ca II.—About 40 or 50 days after maximum, the H and K lines develop displaced diffuse emission (Pl. XII) whose behavior is similar to that previously described in the spectrum of R Hydrae.[3] The shortward displacements measured in R Leonis (Table 7) are approximately 8 km/sec greater (arithmetically) than the displacements in R Hydrae at corresponding phases. In both stars the negative displacements decrease (arithmetically) with advancing phase. The mean difference H *minus* K is about +21 km/sec in R Leonis, +16 km/sec in R Hydrae.

Unidentified lines.—A number of emission lines, of which about fifteen are well marked, lack positive identification. The interpretation of these lines will possibly be assisted by a future study of the rich bright-line spectra of R Andromedae and χ Cygni.

One of the most important of the unidentified lines is λ 4373. The displacements in Table 8 have been obtained from R Leonis on the assumption that the normal wave length is λ 4372.54. Adjusted to give the same mean displacement as the *Fe* II lines on the same plates, the wave length is 4372.57.

As spectroscopic observations of long-period variables become more extensive and more detailed, the complexity of the phenomena in the atmospheres of these objects is clearly exhibited. Because many features vary somewhat from star to star and even from cycle to cycle in the same star, generalizations must be made with caution. Nevertheless, the characteristic behavior pattern is gradually emerging in greater and greater detail.

More thorough observations of individual cycles of several variables will eventually be required—a very heavy task. In the meantime the intercomparison of variables can be carried somewhat further. It is hoped, next, to include a study of the spectrum of the Se variable R Andromedae.

THE PHOTOGRAPHIC DETERMINATION OF STELLAR PARALLAXES WITH THE 60- AND 100-INCH REFLECTORS*

TWENTIETH SERIES

ADRIAAN VAN MAANEN
Mount Wilson Observatory
Received April 8, 1946

ABSTRACT

Trigonometric parallaxes determined with the 60- and 100-inch reflectors are given for 25 fields, including 28 stars. As in the other recent series, most of the stars were placed on the program on account of their large proper motions.

The present paper gives the trigonometric parallaxes of 28 stars in 25 fields, measured by Dr. van Maanen during the illness which culminated in his death on January 26, 1946. The material was prepared for publication by A. Louise Lowen and R. E. Wilson. The work was carried out in the same way as for the previously published series;[1] it completes the parallaxes in 500 fields, measured by van Maanen on plates taken with the 60- and 100-inch reflectors.

Ross 882, like the companion of Lalande 21258, appears to be a variable of very faint absolute magnitude. With a normal photographic magnitude of 13.1–13.3, it appeared as bright as 11.8 on two plates taken on March 11, 1943. Its absolute magnitude based upon the measured parallax has a minimum range of from +12.6 to +14.1. Its spectral type, determined by A. H. Joy, is M4e; G. P. Kuiper gives M6.

Ross 476, m_{pg} 16.0, appears to be a distant companion of the white dwarf, Wolf 485, m_{pg} 12.5.[2]

Merrill's faint Wolf-Rayet star (No. 209, *Bordeaux carte du ciel*, Pl. +16°516), has a radial velocity of +196 km/sec.[3] Its visual magnitude was estimated as approximately 10.0 at the times the spectrograms were taken. The object is probably distant and may be considerably reddened.

Two stars in the table should be added to the list[4] of stars with photographic absolute magnitudes 15.0 or fainter. They are L 1305-10, +15.4, and Ross 486 B, +15.6.

* *Contributions from the Mount Wilson Observatory, Carnegie Institution of Washington*, No. 721.

[1] *Mt. W. Contr.*, Nos. 111, 1916; 136, 1917; 158, 1918; 182, 1920; 204, 1921; 237, 1922; 270, 1923; 290, 1925; 321, 1926; 356, 1928; 391, 1929; 435, 1931; 468, 1933; 506, 1935; 553, 1936 (*Ap. J.*, **84**, 409); 590, 1938 (*Ap. J.*, **87**, 424); 630, 1940 (*Ap. J.*, **91**, 503); 652 (*Ap. J.*, **94**, 396); 692, 1944 (*Ap. J.*, **100**, 55).

[2] G. P. Kuiper, *Pub. A.S.P.*, **47**, 307, n. 3, 1935.

[3] P. W. Merrill, *Pub. A.S.P.*, **50**, 350, 1938.

[4] A. van Maanen, *Mt. W. Contr.*, No. 630; *Ap. J.*, **91**, 505, 1940.

TABLE 1

STELLAR PARALLAXES DETERMINED AT MOUNT WILSON

Object	α 1900	δ 1900	m_{pg}	Spectrum*	Relative Parallax	μ_α Rel.	P.E.	No. Exposures	Instrument
Ross 548	$1^h31^m13^s$	$-11°51'$	13.5	A0	$-0''.012$	$+0''.437$	8 21	16	100″
Ross 10	1 31 54	+56 45	13.3	M5	+ .091	−0.204	5 4	18	60
L 1159-19	1 59 12	+12 22	14.5	.....	+ .033	+0.535	7 15	12	100
L 1305-10	2 27 54	+24 30	14.8	.....	+ .130	+0.069	7 6	14	100
Wolf 1450	5 24 54	− 3 31	13.5	.....	+ .045	−0.302	4 1	14	100
Ross 42	5 26 42	+ 9 45	12.4	M5	+ .077	−0.170	4 3	18	60
BD+32°1398A	6 39 36	+32 39	10.	.....	+ .049	−0.458	6 3	16	100
BD+32°1398B	6 39 42	+32 39	14.	.....	+ .051	−0.449	8 4	16	100
Ross 986	7 03 18	+38 43	13.4	M5	+ .149	−0.405	4 3	16	60
BD+36°1638	7 25 24	+36 26	12.3	M3	+ .083	−0.247	8 7	12	60
Ross 989	7 25 24	+36 26	13.7	M5	+ .087	−0.252	7 7	12	60
Ross 882	7 39 24	+ 3 48	var.†	M4e	+ .145	−0.348	5 4	16	100
Radcl. 13, 309	10 59 13	+60 13	14.6	.....	+ .024	−0.277	9 2	16	60
Wolf 364	11 04 57	− 2 14	13.2	.....	+ .019	+0.162	8 6	16	100
Radcl. 56, 27	11 57 16	+29 09	14.7	.....	+ .054	−0.784	6 2	16	60
Wolf 1435	12 04 31	+ 8 56	14.7	.....	+ .013	−0.621	11 1	12	100
Radcl. 80, 158	12 10 37	+15 01	15.6	.....	+ .007	+0.524	12 3	16	100
Ross 486A	13 23 12	− 1 50	13.3	M5	+ .084	+0.151	11 10	12	100
Ross 486B	13 23 12	− 1 50	15.7	.....	+ .107	+0.142	7 6	12	100
Ross 476	13 24 54	− 8 11	16.0	.....	+ .043	−1.095	22 2	16	100
L 1338-3	14 18 12	+18 26	14.2	K	+ .030	−0.457	8 5	16	60
Ross 501	14 47 54	−15 22	15.1	.....	+ .029	+0.168	8 2	12	100
Radcl. 83, 163	15 10 50	+14 24	13.9	.....	+ .035	−0.385	5 1	16	60
Ross 802	15 31 30	−13 47	14.3	.....	+ .082	−0.449	4 1	14	100
Ross 1059	17 07 24	+60 45	13.7	.....	− .006	+0.006	6 6	18	60
Merrill's star	19 07 00	+16 40	11.0	WN7	− .029	+0.002	8 4	18	60
Wolf 1122‡	19 53 06	+51 00	13.3	.....	+ .046	+0.478	2 1	20	60
Ross 766	20 39 12	+35 09	12.5	M2	+0.032	−0.172	3 7	12	60

* The spectra are, in general, by M. L. Humason or G. P. Kuiper; that for Ross 882 is by A. H. Joy, and that for the Wolf-Rayet star by P. W. Merrill.

† m_{pg} varies from 11.8 to 13.3.

‡ Also designated as Ross 1069a.

THE ECLIPSING STAR RT ANDROMEDAE

CECILIA PAYNE-GAPOSCHKIN
Harvard College Observatory
Received February 2, 1946

ABSTRACT

The dwarf eclipsing system RT Andromedae is studied on the basis of its light-curves and velocity-curve. It consists of a pair of dwarf stars (G0 and K1), the former rather smaller than the sun, the latter rather larger. The G0 star has 1.5 times the solar mass; the K1 star is equal in mass to the sun.

A well-known dwarf eclipsing system, RT Andromedae has been studied principally by visual observers;[1,2] a photographic light-curve was obtained by F. C. Jordan.[3] The present paper contains an account of a discussion of 1579 Harvard patrol plates and of 25 spectrograms made at the McDonald Observatory.

I. PHOTOMETRIC DATA

a) Photographic observations.—The observations were made by Dr. S. Gaposchkin, who also re-estimated all plates within primary minimum. The plates were made with the 1-inch Cooke (AC), the 2-inch Zeiss Tessar (AY), the 2-inch Ross-Zeiss Tessar (AX), the 3-inch Ross (RH), and the 1½-inch Cooke (CA) instruments; the final light-curve was derived from AC plates only. The position of RT Andromedae for 1900 is $23^h6^m42^s$, $+52°29'.0$; and it was measured on plates centered at $+45°$: 22^h, 23^h, and 0^h, and at $+60°$: 22^h, 23^h, and 0^h. Systematic corrections for instrument and center will be discussed later.

TABLE 1

COMPARISON STARS FOR RT ANDROMEDAE

BD	HARVARD		JORDAN PG. MAG.	GADOMSKI	
	Step	Pg. Mag.		Vis. Mag.	Vis. Mag. (Rev.)
+51°3545	a 5.5	9.08 blue	.....	.....	.....
52 3394	b 5.0	9.08* red star	.....	.....	.....
52 3380	b′ 2.5	9.45† bluish	8.95	9.61	9.11
52 3382	c 0	9.84 bluish	9.20	10.08	9.58
+52 3384	d −0.5	9.92 bluish	9.31	10.01	9.51

* Red; not used in reduction, possibly variable.
† Has a close companion.

b) Magnitude standards.—The estimates were made directly in steps relative to the comparison stars of Table 1. The photographic magnitudes were determined with reference to the well-established magnitudes of the comparison stars for SX Cassiopeiae.[4]

Three of these comparison stars were also used by Jordan, and his magnitudes are given in the table. Evidently Jordan's magnitudes differ from ours in zero point and

[1] Gadomski, *Acta Astr.*, **1**, 21, 1928.
[2] Sternberk, *Prague Pub.*, **2**, Part VII, 10, 1927.
[3] *Allegheny Pub.*, **7**, 160, 1929.
[4] S. Gaposchkin, *Ap. J.*, **100**, 213, 1944.

scale. The visual magnitudes used by Gadomski were revised in zero point on the basis of their colors.

c) Systematic corrections.—The photographic estimates were examined for systematic errors depending on instrument and plate center. The 462 AC plates centered at 23^h, $+45°$ (nearest to the variable), were used to form a standard curve, from which deviations for other centers were measured. The results are summarized in Table 2, which contains the correction to be applied for each center and the probable error of one estimate at that center. The final column gives the angular distance from the variable to the plate center.

The systematic corrections given in Table 2 are small but appreciable, and they were applied to the deduced magnitudes. Evidently, they increase with distance from the plate center.

The deviations of the estimates from plates of other series were examined in a similar way. These plates are far less numerous than the AC plates; and the systematic deviations are less certain, though they appear to be small. The accidental errors, however, are larger than for the AC plates, ± 0.19 for the AY plates, and comparable for the others—predictable results of the known color equations or greater image strengths. It was decided to use only measures of AC plates for the final light-curve, since plates made

TABLE 2

SYSTEMATIC CORRECTIONS FOR PLATE CENTER (AC PLATES)

Center	Systematic Correction	P.E.	Distance
$22^h+60°$	$+0^m03$	$\pm 0^m13$	12°.15
23 +60	0.00	.12	8.02
0 +60	+0.02	.16	10.95
22 +45	+0.02	.15	12.91
23 +45	Standard	.....	7.02
0 +45	$+0^m01$	± 0.16	11.30

with other cameras would have increased the material by about 25 per cent at the expense of introducing larger errors. The observations made with other cameras were, however, used in the determination of the period.

The double estimation of points in the primary minimum provides another measure of precision. From independent estimates of 233 plates, made at an interval of two months, the difference was found to be $0^m00 \pm 0^m15$ (p.e.); there was no systematic difference over the interval, and the error of one estimate is similar to those of Table 2.

By far the most serious systematic error that affects the present measures is that introduced by the exposure time. The average exposure of the patrol plates is over an hour (and has been increased in recent years). For RT Andromedae, with a period of about 16 hours, the consequent distortion of the light-curve is serious and can be corrected only approximately. Let it be assumed (although it is known to be untrue) that all parts of the exposure are equally effective in blackening the star image. Over portions of the light-curve where the change of brightness is linear, the correction is zero. If the light-curve displays curvature during the exposure, the recorded blackening will not represent the brightness at mid-exposure. The necessary correction was determined graphically, by integrating the light numerically over the appropriate intervals before and after a hundred points equally spaced along the curve. A table of corrections was thus formed, giving the corrections as functions of phase and exposure time. Each estimate was then corrected. A rough check would be given by correcting an uncorrected mean light-curve for an average exposure time (about 70 minutes); but this would leave,

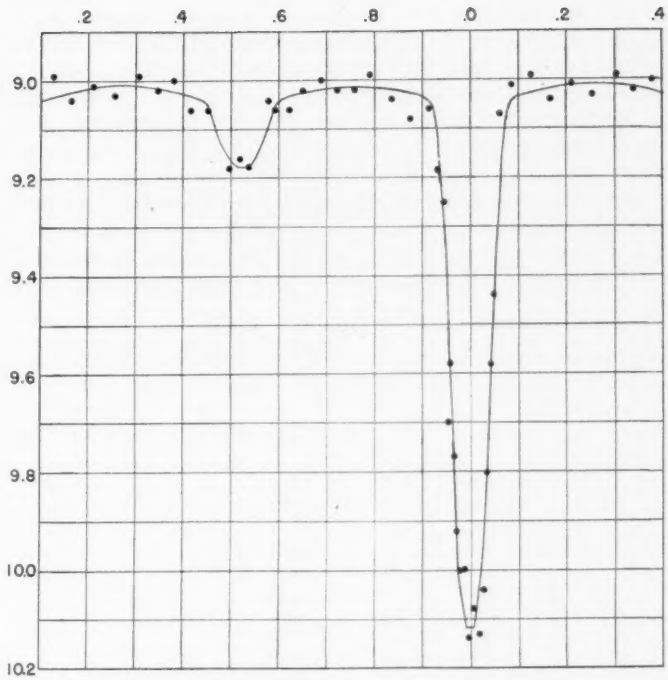

FIG. 1.—Computed light-curve of RT Andromedae

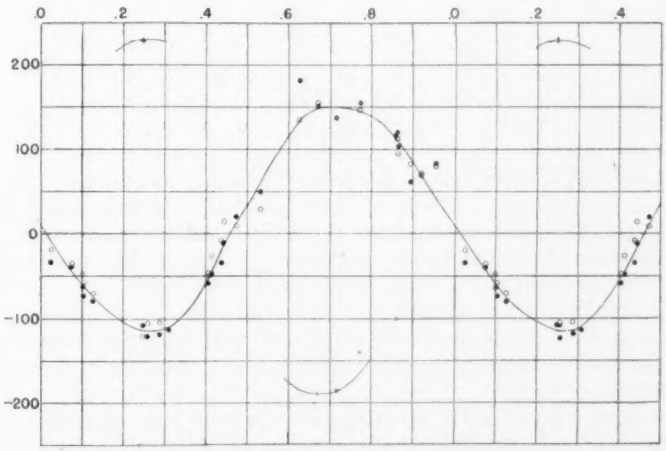

FIG. 2.—Velocity-curve of RT Andromedae

in the final light-curve, a disproportionate effect of large errors, which (at a given phase) would all have the same sign and would magnify the exposure distortion.

It is known that the first part of an exposure is the most effective, but no attempt has been made to allow for this; the effect levels off over exposures as long as those considered; and, since the estimates are differential, not absolute, it would enter only in the second order. If the equal-blackening assumption led to a serious error, we should expect it to produce an asymmetry in the light-curve, with too high a "shoulder" on the way down into primary minimum. The light-curve does, indeed, show an asymmetry, but in the opposite direction; and a similar asymmetry is shown by Jordan's photographic light-curve, made with 4-minute exposures, for which the distortion should be negligible.

d) *The period.*—Several determinations of the period of RT Andromedae, relating to different short intervals and differing slightly, have been published. In discussing our

TABLE 3

MEAN PHOTOGRAPHIC LIGHT-CURVE OF RT ANDROMEDAE (AC PLATES)

Phase	IPg	No. of Obs.	Phase	IPg	No. of Obs.
0.0052	10.079	10	0.5364	9.039	50
.0157	10.128	10	.5748	9.060	50
.0252	10.044	10	.6148	9.057	50
.0333	9.798	10	.6479	9.028	50
.0424	9.581	10	.6889	9.001	50
.0487	9.439	10	.7238	9.020	50
.0619	9.067	20	.7566	9.015	50
.0850	9.014	50	.7928	8.991	50
.1276	8.989	50	.8339	9.035	50
.1683	9.037	50	.8742	9.076	50
.2131	9.009	50	.9120	9.051	30
.2577	9.029	50	.9343	9.184	10
.3001	8.988	59	.9450	9.249	10
.3388	9.021	50	.9508	9.578	10
.3755	9.004	50	.9566	9.697	10
.4153	9.056	50	.9666	9.770	10
.4382	9.056	20	.9736	9.921	10
.4532	9.182	20	.9820	10.012	10
.4794	9.158	40	.9895	10.008	10
0.5072	9.182	22	0.9963	10.143	10

estimates, the period $0^d.62893364$, given by A. A. Nijland,[5] was first used; but it appeared to be slightly too long. Mean light-curves were formed for thousand-day intervals, beginning from JD 14,000, and from times of primary minimum a constant period of $0^d.62893249$ was deduced. The secondary minimum is slightly displaced and falls before the mid-point between primary minima. Individual mean light-curves were formed for the intervals JD 14,000–18,999, 19,000–27,999, and 28,000–31,999. There was no appreciable difference in the time of secondary minimum. The material is thus not adequate to determine whether the displacement is variable, and in forming the mean light-curve it has been treated as constant.

e) *The light-curves.*—The final light-curve, derived from 1252 estimates on AC plates, is given in Table 3. Phases are reckoned from primary minimum. Fifty-point means are generally given outside minima, ten-point means within primary minima. From the errors of estimation mentioned earlier, the probable error of one point outside minimum is $\pm 0^m.02$; and inside minimum, $\pm 0^m.05$.

[5] *B.A.N.*, No. 217, 1931.

f) The photometric elements.—A uniform solution by Russell's method was made for the photometric elements. The ellipticity constant z was determined graphically to be 0.080. The light-curve was rectified, and after some trials it was decided that the best representation is given for a total eclipse with ratio of radii 0.52 (uniform solution).

The average residual from the computed uniform curve is $0^m.020$; within primary minimum it is $0^m.059$; for each group of residuals separately the systematic difference is zero. In consideration of the probable errors of the normal points, the agreement is not worse than could be expected.

Elements derived from Jordan's photographic light-curve have been obtained by N. Tchudovitchev;[6] they differ considerably from ours. Jordan's magnitudes were obtained by a very arbitrary process, and without reduction his light-curves are unsuited to discussion. If corrections were applied to his magnitudes as estimated from Table 2, his range of $0^m.92$ would be increased by about $0^m.3$, to a value even greater than ours. The difference in the photometric solutions is largely a result of the magnitude scales.

TABLE 4

MEAN VISUAL LIGHT-CURVE OF RT ANDROMEDAE

Phase	Vis. Mag.	Phase	Vis. Mag.	Phase	Vis. Mag.
0.005	9.80	0.131	8.98	0.695	8.94
.017	9.69	.230	9.02	.801	8.90
.029	9.52	.384	8.90	.900	9.10
.041	9.36	.463	9.16	.940	9.16
.054	9.16	.487	9.19	.973	9.61
.061	9.10	.514	9.21	.985	9.75
0.083	9.06	0.557	9.19	0.995	9.78

These results assume that the larger star is in front at primary minimum. If the smaller were in front at that time, the limits of k would be 1.00 and 0.83. These values are too large to be compatible with the observed light-curve, and we therefore conclude that the smaller star is eclipsed at the primary minimum.

The photometric elements are not of high precision, principally because of the exposure-time correction necessitated by the shortness of the period. Unfortunately, this correction strongly influences the slope of the primary minimum and tends, in addition, to make difficult a satisfactory determination of the ellipticity constant.

A photometric solution was derived from the 238 visual observations of Gadomski, Kordylewski, Pagaczewski, and Witkowski.[7] The mean visual light-curve is given in Table 4. The elements are given in Table 5; they are to be regarded as of lower weight than those based on the photographic curve.

II. THE SPECTROGRAPHIC DATA

a) The observations and reductions.—The 25 spectrograms of RT Andromedae now discussed were obtained by Dr. S. Gaposchkin with the Cassegrain quartz spectrograph at the 82-inch reflector of the McDonald Observatory during a stay in December, 1944. We are greatly indebted to the director, Dr. Otto Struve, for making available the facilities of the observatory, for assistance in the observing, and for permitting the discussion of the spectrograms.

[6] *Engelhardt Obs. Bull.*, No. 1, 1934.

[7] *Acta Astr.*, C, 1, 21, 1928.

A single spectrum is visible on most of the plates. On 5 plates at elongation it was possible, with some difficulty, to measure lines attributed to the second component. The brighter star, eclipsed at primary minimum, is of spectral class G0, on the basis of 8 plates, estimating the ratios of intensities of several lines: 4045, Hγ, 4226, 4063, Hδ, 4325. For the second component a spectral class K1 has been adopted from 2 plates. The spectrum K2 was given by Miss Cannon.[8]

Table 6 contains the spectrographic material: successive columns give the plate number, the Julian Day, exposure time, phase (in terms of period), plate quality, average velocity from G0 spectrum, number of lines measured, average velocity from hydrogen, and velocity from second spectrum.

TABLE 5

PHOTOMETRIC ELEMENTS OF RT ANDROMEDAE

	Photographic	Visual
Period	$0^d62893249$	$0^d62893249$ (adopted)
Maximum	9^m01 (obs.) 9^m010(rect.)	8^m94(obs.) 8^m94(rect.)
Minimum$_1$	10^m12 (obs.) 10^m070(rect.)	9^m79(obs.) 9^m74(rect.)
Minimum$_2$	9^m177(obs.) 9^m127(rect.)	9^m22(obs.) 9^m17(rect.)
A_1	1^m110(obs.) 1^m060(rect.)	0^m85(obs.) 0^m80(rect.)
A_2	0^m167(obs.) 0^m117(rect.)	0^m28(obs.) 0^m23(rect.)
$1-\lambda_1$	0.6233	0.5214
$1-\lambda_2$	0.1021	0.1909
J_2/J_1	6.20	2.73
Ratio of radii	0.52	0.60
$\sin^2\theta'$	0.2501	0.2487
$\sin^2\theta''$	0.0098	0.0020
Ellipticity constant	0.08	0.08
Major semi-axis, larger star	0.347	0.329
Minor semi-axis, larger star	0.333	0.316
Major semi-axis, smaller star	0.180	0.197
Minor semi-axis, smaller star	0.173	0.190
Eccentricity of meridian section	0.284	0.284
Inclination of orbit plane	82°.7	82°.8
Least apparent distance of centers	0.127	0.126
Spectrum, larger star	K1	.....
Spectrum, smaller star	G0	.....
L_1	0.37	0.50
L_2	0.63	0.50
Δm	0^m58	.....

The plates were measured singly by Dr. S. Gaposchkin on the Gaertner engine loaned to the Harvard Observatory by the Maria Mitchell Observatory; the reductions were made by C. Payne-Gaposchkin independently, using the standard tables provided by the McDonald Observatory, a copy of which was kindly supplied by Dr. Struve.

b) *The spectrographic elements.*—The velocities were discussed by the method of Lehmann-Filhés, as described by R. G. Aitken.[9] The results are given in Table 7.

III. PHYSICAL DIMENSIONS

A combination of the photometric and spectrographic information yields the physical dimensions given in Table 8. The greatest uncertainty is occasioned by the adopted spectral class of the second component.

[8] *Harvard Bull.*, No. 897, 1934.

[9] *The Binary Stars*, chap. vi, New York: McGraw-Hill Book Co., 1935.

TABLE 6

RADIAL VELOCITIES OF RT ANDROMEDAE

Plate No.	JD	Exp.	Phase	Quality	Mean V	No. of Lines	Mean H	Mean V'	No. of Lines
CQ 4035..	31428.661	60^m	0.9530	Good, faint	+79	12	+82	.....	.....
4071..	31433.638	60	.8664	Medium	+95	11	+104	.....	.....
4072..	31433.672	60	.9205	Good	+72:	7	+69.5	.....	.....
4077..	31435.543	70	.8954	Good	+82	11	+61	.....	.....
4079..	31435.674	60	.1037	Good	−58	7	−74	.....	.....
4081..	31435.803	70	.3088	Medium	−116	4	−115.5	.....	.....
4088..	31437.552	90	.0997	Good	−48	8	−63	.....	.....
4091..	31437.677	60	.2884	Good	−105	8	−118	.....	.....
4093..	31437.751	60	.4061	Good	−47:	8	−59.5	.....	.....
4100..	31438.546	60	.6702	Good	+155	8	+151	−190:	2
4103..	31438.664	60	.8578	Good, dark	+114.5	8	+113.5	.....	.....
4106..	31438.769	90	.0247	Good	−19	9	−34	.....	.....
4111..	31439.545	58	.2586	Good	−105	9	−122	.....	.....
4114..	31439.660	67	.4414	Good	+14	8	−11.5	.....	.....
4115..	31439.718	74	.5336	Good	+28.5	9	+48	.....	.....
4123..	31440.555	74	.8644	Good	+120	8	+112.5	−100:	2
4127..	31440.689	60	.0775	Good	−35	9	−39.5	.....	.....
4136..	31441.545	60	.4386	Good	−8	8	−34.5	.....	.....
4143..	31441.754	60	.7709	Good, fuzzy	+147	9	+155	−140:	2
4167..	31442.603	60	.1258	Good	−71	9	−80	.....	.....
4178..	31443.606	60	.7155	Good	+135	.....	+136	−185:	2
4215..	31446.559	70	.4108	Good, fuzzy	−26	8	−48.5	.....	.....
4236..	31448.584*	60	.6258	Medium	+135:	8	+182	.....	.....
4256..	31454.633	100	.2484	Medium	−120	7	−109	+228:	2
4282..	31458.548	55	0.4732	Good	+9	9	+20	.....	.....

* Poor plate.

TABLE 7

SPECTROGRAPHIC ORBIT OF RT ANDROMEDAE

Period (adopted) = $0^d62893249$
T = 2431441.536
e = 0.089
$\omega = -77°50'$
K_1 = 132.5 km/sec
K_2 = 205? km/sec
V = +20 km/sec
$(a_1 + a_2) \sin i = 2.91 \times 10^6$ km = $4.18\odot$
$(m_1 + m_2) \sin^3 i = 2.480\odot$

TABLE 8

ABSOLUTE DIMENSIONS OF RT ANDROMEDAE

	Photographic		Visual	
Spectrum	G0	K1	G0	K1
Temperature (adopted)	5750°	4280°	5750°	4830°
Radius:				
Major axis	0.75⊙	1.45⊙	0.82⊙	1.38⊙
Minor axis	0.72⊙	1.39⊙	0.79⊙	1.32⊙
Mean axis	0.73⊙	1.41⊙	0.80⊙	1.34⊙
Mass	1.50⊙	0.99⊙	1.50⊙	0.99⊙
Mean density	2.70⊙	0.35⊙	2.05⊙	0.41⊙
Absolute visual magnitude	+5.73	+6.06	+5.53	+5.43
Absolute photographic magnitude	+6.34	+7.10	+6.14	+6.28

The absolute magnitudes were derived from the formulae:

$$M_{vis} = \frac{29{,}500}{T} - 5 \log R - 0.08$$

and

$$M_{pg} = \frac{36{,}700}{T} - 5 \log R - 0.72 .$$

The temperature for the hotter (G0) star was adopted at 5750°. The temperatures used for the cooler star were derived from the relative surface brightnesses (Table 5) and the adopted temperature of the G0 star, using the data[10] of *Harvard Reprint 201*. The spectral classes deduced from these temperatures are G8 for the visual and K3 for the photographic curve. The absolute photographic magnitudes of Table 9 are in general agreement with the relative visibility of the two spectra.

The components of RT Andromedae appear, from the present study, to fall somewhat below the mass-luminosity curve.

[10] S. Gaposchkin, *Proc. Amer. Phil. Soc.*, **82**, 298, Table 2, 1940.

THE SYSTEM OF RX CASSIOPEIAE

CECILIA PAYNE-GAPOSCHKIN
Harvard College Observatory
Received February 2, 1946

ABSTRACT

The Harvard photographic observations of RX Cassiopeiae are discussed in detail. The principal conclusions relative to this unusual system are: (1) there is a regular intrinsic variation in a period of 517 days, and this may be ascribed to variation of the blue component with a range of 0.6 mag.; (2) the photometric elements of the eclipsing pair, derived at the times of the maximum, mean, and minimum of the long-period curve, are sensibly similar, except in the ratios of surface brightness; and (3) the relative luminosities of the components, derived from the long-period variations and from the photometric elements, are in agreement.

The general photometric features of RX Cassiopeiae have already been described.[1] Taken in conjunction with the spectroscopic elements derived at the McDonald Observatory,[2] these features are so unusual that a more complete presentation of the material is desirable.

The 2037 estimates on Harvard plates were made by S. Gaposchkin. The steps used in the estimation are related to magnitudes (see Paper I, Table 1) by the linear formula:

$$\text{Magnitude} = 10.550 - 0.095\ \text{Step}\ .$$

The phases were calculated with the period 32.315 days. Epochs and phases were reckoned from JD 2,400,000. The plates and plate centers used are enumerated in the accompanying tabulation.

Plates	Centers	
AC: 1-inch Cooke	0^h +75°	1^h30^m+60°
AI: 1¼-inch Ross Xpres	2 +75	3 60
RH: 3-inch Ross	4 +75	4 60
		5 +60

In discussing the observations and the derivation of light-curves, the following factors were taken into account: (*a*) errors depending on instrument, (*b*) errors depending on plate center, and (*c*) intrinsic variations of the whole light-curve. In regard to systematic errors depending on the instrument, the comparison between the mean photographic light-curves, derived separately from AC and AI plates (see Paper I), shows them to be small. The average deviation of the normal points, derived for AI plates, from the curve drawn through the normal points for AC plates is +0.01 mag. (the AI magnitudes being slightly brighter). The probable error of a single estimate on AI plates is deduced, from the same residuals, to be 0.20 mag. As this is larger than the usual value (0.15 mag.) for estimates from AC plates, it was decided to use the latter only in the final light-curve. As stated in the previous paper, the AI plates furnish valuable corroboration of the peculiar form of the mean photographic light-curve and place the exaggerated "periastron effect" beyond doubt.

[1] S. Gaposchkin, *Ap. J.*, **100**, 230, 1944. Hereafter referred to as "Paper I."

[2] O. Struve, *Ap. J.*, **99**, 295, 1944.

Systematic errors, depending on plate center, have been exhaustively studied in a recent paper[3] on the eclipsing variable RT Andromedae. These errors never exceed 0.03, and they are so much smaller than the effects encountered in the intrinsic variations of RX Cassiopeiae that they have not been considered for the present material, from which it would have been very difficult to evaluate them.

The most important deviations from the average light-curve for RX Cassiopeiae are those arising from the obvious intrinsic variations of the light-curve. There was nothing arbitrary in the process by which the various mean light-curves were derived in Paper I. The material bearing on the intrinsic variation will now, however, be presented in greater detail.

A mean light-curve was first obtained from all the estimates. The observations within each cycle, from No. 451 to No. 963, were compared with this curve; and the deviation

TABLE 1

SECONDARY VARIATION OF RX CASSIOPEIAE

Phase	Step-Difference	No. of Obs.	Mean Mag.	Mag. A5 Star*
0.015	+0.67	19	10.062	10.642
.076	+0.77	18	10.052	10.624
.141	+1.41	23	9.991	10.524
.198	+1.52	15	9.981	10.505
.230	+1.44	14	9.988	10.518
.271	+0.80	12	10.049	10.619
.327	+1.12	22	10.018	10.568
.391	+1.11	21	10.019	10.569
.447	+0.25	15	10.102	10.712
.481	+0.18	14	10.109	10.724
.520	−0.75	15	10.198	10.886
.578	−0.66	20	10.189	10.869
.639	−0.54	21	10.178	10.850
.697	−2.13	13	10.330	11.151
.734	−1.42	15	10.262	11.012
.769	−1.78	17	10.297	11.083
.826	−1.25	21	10.246	10.980
.890	−0.12	19	10.137	10.774
.948	−0.34	17	10.159	10.814
0.970	+0.26	7	10.101	10.710

* G6 constant, 11.012 mag.

from the mean curve (in steps) was determined for each cycle. Phases in the long-period light-curve were computed with the period 517.6 days (which is almost sixteen times the eclipsing period, 32.315 days), referred to Epoch 0 (JD 2,400,000) as zero. The apparent mean light-curve was obtained from the step-differences by taking unweighted means of the deviations for twenty equal intervals in the phase of the long-period curve. The result is summarized in Table 1. The first, second, third, and fourth columns give the mean phase, the mean step-difference, the number of cycles involved, and the "apparent" magnitude at maximum for the mean light-curve, deduced from the second column by the relation:

$$\text{Mag.} = 10^{\text{m}}.126 - 0.095 \text{ Step} .$$

The value 10.126 mag. is that finally adopted as the maximum brightness of the mean light-curve.

[3] C. Payne-Gaposchkin, *Ap. J.*, **103**, 291, 1946.

We now anticipate a result to be obtained from the discussion of the light-curve: at the brightness represented by the mean light-curve the A5 star is 0.258 mag. brighter than the G6 star. If it is assumed that the A5 star is responsible for the long-period variation, it is now possible to obtain a light-curve of the A5 star, freed from the light of the G6 component (supposedly constant). This light-curve is given in the fifth column of Table 1.

The light-curve of Table 1 and Figure 1 is a sensibly regular and symmetrical curve with a range of six-tenths of a magnitude. The star from which it comes is a variable of unusual properties; it is the only star of its kind known to the writer.

In Paper I the variations of the light-curve were illustrated, and the mean light-curve was discussed by approximate methods. It is the present purpose to analyze the light-curves further, in order to draw more definite conclusions from them. For any such discussion, and particularly for so peculiar a light-curve, objectivity in method, with a minimum of arbitrary adjustments, is essential.

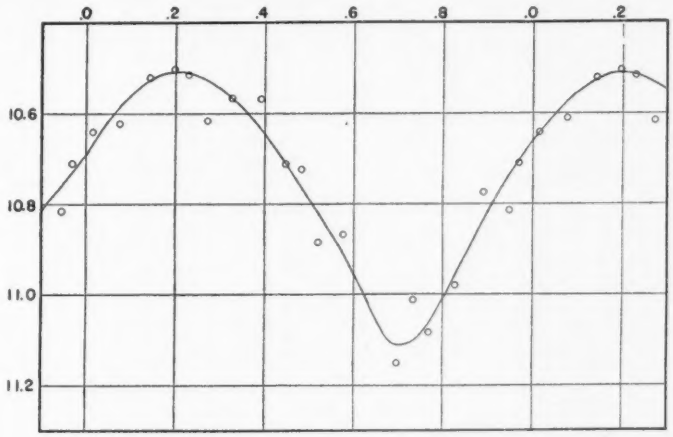

FIG. 1.—Variation of blue component of RX Cassiopeiae (see Table 1)

Discussion will be limited to three mean light-curves: the curve obtained from all observations from AC plates; the curve for maximum brightness of mean light; and the curve for minimum (curves *I* and *III* of Figure 3 of Paper I). All three curves were deduced directly from the observations, without adjustment or correction.

The mean curve was simply deduced from all the (AC) observations. It would not have been appreciably changed if the AI observations had been included, with weight appropriate to their smaller number and lower precision. The "bright" and "faint" curves were obtained from uncorrected estimates at the maximum and minimum of the long-period light-curve. As the periodicity and regularity of this curve have been established, this amounts to selection as a function of phase (using the period 514.7 days), a procedure not at all arbitrary, and depending on one parameter only. The "maximum" curve runs from phase 0.990 to 0.410 of the long-period curve; the "minimum," from 0.620 to 0.840. The two groups of observations thus selected were formed into light-curves without adjustment.

The "mean" light-curve has already been published in Paper I. Curves *I* and *III* are given in Tables 2 and 3. Phases are given in degrees and reckoned from primary minimum.

The large variations of the light-curve introduce uncertainties into the mean curves of Tables 2 and 3, even though these were formed from restricted parts of the long-

period curve. As a check, therefore, the individual observations were corrected according to phase of the long-period curve, and mean curves were formed from the corrected estimates.

As stated previously, the "maximum" curve included phases from 0.990 through 0.410 of the long-period curve; the "minimum," phases from 0.620 through 0.840. The corrections applied to the step estimates are summarized in Table 4.

The data on "corrected" mean light-curves, *I* and *III*, are given in Tables 5 and 6. The curves of Tables 2 and 5 are compared in Figure 2; those of Tables 3 and 6, in Figure 3. The general similarity of the two pairs of curves justifies the further discussion

TABLE 2

RX CASSIOPEIAE, CURVE *I*

Phase θ	IPg	Phase θ	IPg	Phase θ	IPg
5.08	11.016	119.88	9.952	256.18	10.165
10.94	10.364	133.52	9.970	264.92	10.104
20.27	10.184	138.85	10.018	270.68	10.075
31.82	10.093	144.94	9.975	278.32	10.132
40.82	9.966	154.08	10.089	287.71	9.999
45.58	9.970	162.43	10.165	299.66	9.094
53.24	9.990	171.25	10.118	306.40	10.132
61.13	10.108	182.56	10.160	314.06	10.066
69.19	9.970	191.99	10.122	324.94	10.061
76.54	9.956	198.00	10.160	336.38	10.127
83.23	10.051	205.70	10.142	339.80	10.236
89.50	9.985	217.76	9.994	345.92	10.598
94.57	9.990	233.46	10.289	357.12	10.992
101.16	9.961	242.06	10.061		
108.40	10.004	252.76	10.222		

TABLE 3

RX CASSIOPEIAE, CURVE *III*

Phase θ	IPg	Phase θ	IPg	Phase θ	IPg
0.72	11.234	139.28	10.213	275.54	10.426
2.81	10.987	144.61	10.251	282.28	10.446
7.56	10.778	151.74	10.298	287.68	10.545
12.10	10.560	159.26	10.441	294.01	10.512
18.54	10.479	170.64	10.412	299.05	10.393
28.37	10.364	178.74	10.559	304.81	10.431
39.60	10.384	187.34	10.507	309.28	10.484
46.40	10.388	196.60	10.498	315.00	10.350
57.06	10.151	203.98	10.431	325.73	10.522
69.30	10.260	212.40	10.422	335.02	10.436
78.88	10.180	220.54	10.426	340.27	10.493
87.98	10.122	230.76	10.260	345.38	10.987
97.02	10.184	239.22	10.360	349.27	11.054
106.96	10.118	245.66	10.274	352.73	11.196
114.91	10.118	252.47	10.336	356.83	11.092
121.90	10.142	259.49	10.417		
131.51	10.256	268.38	10.279		

TABLE 4

CORRECTION FOR LONG-PERIOD VARIATION

MAXIMUM

Phase	Correction (Steps)	Phase	Correction (Steps)	Phase	Correction (Steps)	Phase	Correction (Steps)
0.99	−0.3	0.08	−1.0	0.17	−1.4	0.33	−1.2
.00	0.5	.09	1.1	.18–25	1.5	.34	1.1
.01	0.6	.10	1.1	.26	1.5	.35	1.0
.02	0.6	.11	1.2	.27	1.4	.36	1.0
.03	0.7	.12	1.3	.28	1.4	.37	0.9
.04	0.7	.13	1.3	.29	1.4	.38	0.8
.05	0.8	.14	1.4	.30	1.3	.39	0.8
.06	0.8	.15	1.4	.31	1.3	.40	0.7
0.07	−0.9	0.16	−1.4	0.32	−1.2	0.41	−0.6

MINIMUM

Phase	Correction (Steps)	Phase	Correction (Steps)	Phase	Correction (Steps)	Phase	Correction (Steps)
0.62	+1.5	0.68	+1.8	0.74	+1.9	0.80	+1.5
.63	1.6	.69	1.9	.75	1.9	.81	1.4
.64	1.7	.70	1.9	.76	1.8	.82	1.3
.65	1.7	.71	1.9	.77	1.8	.83	1.2
.66	1.8	.72	1.9	.78	1.7	0.84	+1.1
0.67	+1.8	0.73	+1.9	0.79	+1.6		

TABLE 5

MAXIMUM CURVE, CORRECTED FOR LONG-PERIOD VARIATION

Phase	Step	Mag.	No. of Obs.	Phase	Step	Mag.	No. of Obs.
0.0042	4.538	10.119	51	0.8012	3.500	10.217	30
.0701	4.134	10.157	50	.8354	2.32	10.330	10
.1334	4.742	10.100	50	.8467	0.57	10.496	10
.2014	4.786	10.095	50	.8573	−3.29	10.862	10
.2800	4.822	10.092	50	.8851	−5.58	11.080	10
.3463	3.300	10.236	50	.8963	−5.80	11.101	10
.4325	2.102	10.350	50	.9099	−6.38	11.156	10
.5114	3.190	10.247	50	.9180	−1.56	10.698	10
.5921	2.720	10.292	50	.9354	1.41	10.416	10
.6697	3.600	10.208	50	.9516	1.89	10.370	10
0.7358	3.674	10.201	50	0.9658	3.03	10.262	10

TABLE 6

MINIMUM CURVE, CORRECTED FOR LONG-PERIOD VARIATION

Phase	Step	Mag.	No. of Obs.	Phase	Step	Mag.	No. of Obs.
0.0057	3.816	10.188	25	0.7381	3.372	10.178	25
.0868	5.160	10.060	25	.7801	3.233	10.243	15
.1804	5.432	10.044	25	.7993	3.340	10.217	15
.2608	5.256	10.051	25	.8422	1.00	10.455	5
.3066	3.787	10.190	15	.8562	−2.72	10.808	5
.3705	2.107	10.350	15	.8690	−4.04	10.934	5
.4287	1.773	10.382	15	.8884	−4.28	10.957	5
.4899	2.100	10.350	15	.9000	−5.12	11.036	5
.5554	4.764	10.097	25	.9126	−1.24	10.668	5
.6164	4.108	10.160	25	0.9494	2.607	10.302	15
0.6828	4.424	10.130	25				

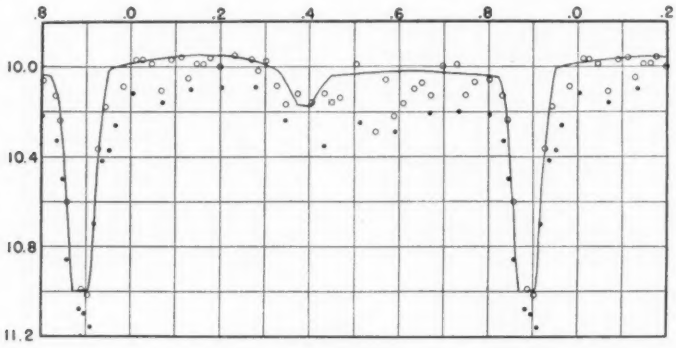

FIG. 2.—Maximum light-curve (*I*). Circles, mean maximum curve (Table 2); dots, maximum curve corrected for long-period variation (Table 5). The curve corresponds to the elements of Table 12.

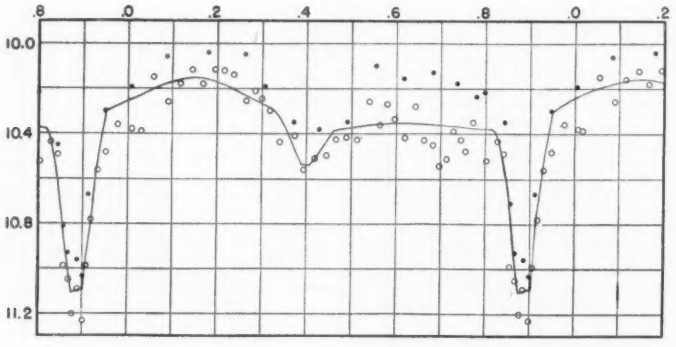

FIG. 3.—Minimum light-curve (*III*). Circles, mean minimum curve (Table 3); dots, minimum curve corrected for long-period variation (Table 6). The curve corresponds to the elements of Table 12.

of curves *I* and *III*. The "corrected" curves are not discussed because the bodily corrections have falsified the ranges; there is evidence that the corrections do not apply during primary minimum, and, indeed, it would be surprising if they did so.

We proceed to examine the uncorrected mean curves: the average from all observations (*M*); the "maximum" curve (*I*); and the "minimum" curve (*III*). The peculiarities of the curves between eclipses are difficult to eliminate. In order to remove them as objectively as possible, the following procedure was adopted.

The conspicuous periastron effect was first removed. To do this, each maximum was reflected separately about a phase midway between minima; and smooth curves were drawn freehand to represent two of the maxima separately. The limits of the minima are obvious upon inspection. The magnitudes reached at each maximum were read from these plots; and by halving their differences, the coefficients of the terms in sin θ for the three curves were determined to be:

Curve *I*	0.039
Curve *M*	.085
Curve *III*	0.095

The points on the reflected maxima were corrected for periastron effect in accordance with these coefficients, and eight or nine normal points outside eclipse were obtained. Their values are given in Table 7. For the "mean" curve, the AI points were included

TABLE 7

MAXIMA CORRECTED FOR PERIASTRON EFFECT

Curve *I*		Curve *M*		Curve *III*	
Phase	IPg	Phase	IPg	Phase	IPg
33°.44	10.104	33°.19	10.183	42°.23	10.419
42.52	10.056	47.77	10.166	54.54	10.273
55.22	10.070	66.13	10.137	69.16	10.255
72.43	10.048	82.15	10.123	83.26	10.252
84.24	10.070	215.75	10.198	219.85	10.348
219.60	10.064	231.84	10.179	236.52	10.271
237.38	10.048	246.96	10.160	249.12	10.317
253.73	10.065	261.29	10.120	262.51	10.302
275.65	9.924				

at this stage, in the hope of eliminating some of the raggedness of the secondary maximum. Phases are expressed in degrees and reckoned from primary minimum.

The magnitudes of Table 7 were used as the basis of least-squares solutions of the form

$$l = a + b \cos \theta + c \cos^2 \theta .$$

The values of the constants for the three curves are given in Table 8.

TABLE 8

LEAST-SQUARES SOLUTIONS

	Curve *I*	Curve *M*	Curve *III*
a	0.9958±0.0151	0.9895±0.0024	0.9719±0.0156
b	.0041± .0190	.0135± .0026	.0017± .0196
c	0.0856±0.0402	0.0884±0.0059	0.1646±0.0512

TABLE 9

RECTIFIED LIGHT-CURVES OF RX CASSIOPEIAE

CURVE *I*

Phase	Mag.	Phase	Mag.	Phase	Mag.	Phase	Mag.
0.17	10.940	86.28	10.089	174.30	10.075	273.73	10.036
8.13	10.963	92.55	10.024	185.61	10.109	281.37	10.092
13.99	10.308	97.62	10.028	195.44	10.066	290.76	9.958
23.42	10.127	104.21	9.997	201.05	10.103	302.71	9.948
34.87	10.037	111.45	10.036	208.75	10.085	309.45	10.084
43.87	9.963	122.93	9.973	220.81	9.939	317.11	10.014
48.63	9.974	136.57	9.976	236.51	10.241	327.99	10.006
56.29	10.004	141.85	10.016	245.11	10.015	339.43	10.069
64.18	10.131	147.99	9.965	255.31	10.181	342.85	10.179
72.24	10.001	157.13	10.066	259.23	10.124	348.97	10.541
79.59	9.991	166.48	10.132	267.97	10.065		

CURVE *M*

Phase	Mag.	Phase	Mag.	Phase	Mag.	Phase	Mag.
0.17	11.035	54.89	10.157	202.49	10.214	338.21	10.289
2.71	11.079	67.85	10.191	214.73	10.214	340.01	10.301
4.13	11.042	78.65	10.129	228.77	10.098	341.81	10.233
7.01	10.997	89.09	10.125	241.01	10.176	343.25	10.364
8.81	10.740	99.89	10.153	250.01	10.126	344.69	10.485
10.25	10.673	112.13	10.145	260.09	10.085	347.49	10.487
12.05	10.576	123.28	10.110	270.89	10.115	349.01	10.890
14.57	10.541	134.81	10.129	281.69	10.115	351.89	10.784
17.09	10.366	144.17	10.140	291.41	10.145	355.13	10.928
18.89	10.350	153.17	10.170	300.77	10.186	358.01	11.002
26.09	10.235	165.77	10.243	309.77	10.237		
35.45	10.156	179.45	10.256	319.49	10.168		
44.09	10.174	193.49	10.270	331.01	10.134		

CURVE *III*

Phase	Mag.	Phase	Mag.	Phase	Mag.	Phase	Mag.
3.77	11.137	110.01	10.201	215.45	10.303	307.86	10.323
5.86	10.894	117.96	10.188	223.59	10.311	312.33	10.373
10.61	10.694	124.95	10.196	233.81	10.150	318.05	10.236
15.15	10.486	134.56	10.286	241.27	10.254	328.78	10.403
21.59	10.422	142.33	10.221	248.71	10.173	338.07	10.317
31.42	10.335	147.66	10.243	255.51	10.238	343.32	10.375
42.65	10.388	154.79	10.269	262.54	10.321	348.43	10.872
49.45	10.413	162.31	10.389	271.43	10.184	352.32	10.942
60.11	10.204	173.69	10.333	278.59	10.332	355.78	11.088
72.35	10.338	181.79	10.463	285.33	10.352	359.88	10.988
81.93	10.270	190.39	10.399	290.73	10.447		
91.03	10.217	199.65	10.382	297.06	10.410		
100.07	10.277	207.03	10.313	299.10	10.288		

The values of rectified maximum magnitude for the three curves are, respectively, $9^m.983 \pm 0^m.016$, $10^m.126 \pm 0^m.003$, and $10^m.258 \pm 0^m.017$. There is no evidence for a sensible reflection effect; and the term for ellipticity is largest for curve *III* (as is evident from an inspection).

The three light-curves, rectified by means of the coefficients just given, are given in Table 9.

The intrinsic variations of the star and the peculiarities of its light-curve make it unwise to overdiscuss the star. Nevertheless, it seems worth while to examine the conclu-

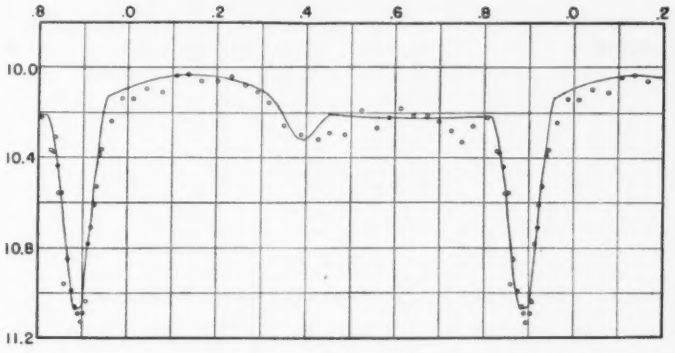

FIG. 4.—Mean light-curve, taken from Paper I. The curve corresponds to the elements of Table 11

TABLE 10

PHOTOMETRIC DATA FOR RX CASSIOPEIAE

	Curve *I*	Curve *M*	Curve *III*
Maximum	9.983 ±0.016	10.126 ±0.003	10.258 ±0.017
Minimum 1	10.950 ±0.045	11.020 ± .009	11.000 ± .048
Minimum 2	10.110 ±0.045	10.270 ± .009	10.430 ± .048
Amplitude 1	0.967 ±0.048	0.894 ± .009	0.742 ± .051
Amplitude 2	0.127 ±0.048	0.144 ± .009	0.172 ± .051
$1-\lambda_1$	0.5898±0.0182	0.5610± .0036	0.4952± .0238
$1-\lambda_2$	0.1103±0.0394	0.1242± .0072	0.1465± .0401
k, larger in front	0.519 ±0.046	0.532 ± .009	0.539 ± .041
k, smaller in front	0.814 ±0.018	0.800 ± .003	0.762 ± .019
J_2/J_1	5.36 ±1.93	4.52 ±0.26	3.38 ±0.94

sions to which the light-curves point. The probable errors of the minimum magnitudes for the three light-curves were deduced from the probable errors at maximum by considering the relative numbers of estimates involved. The probable errors of the amplitudes and $1 - \lambda$ follow. The probable errors of the other quantities in Table 10 are calculated from the standard formulae for the errors of quotients.

Since the eclipses are total, two values of the ratio of radii k are possible; from the spectrographic observations it seems probable that the G6 star, in front at primary minimum, is the larger. Then it appears that, within the limits of uncertainty, the value 0.53 for k will represent all three light-curves. If the smaller star were in front at primary minimum, this would not be so, the value of k from curve *III* differing sensibly from the other two.

The ratio of surface brightness would appear to differ in the three cases, though its value for curve *I* is very uncertain, because of the shallowness of the rectified secondary minimum.

Only rough photometric elements can be derived from the present data. The mean light-curve (*M*) is entitled to the greatest weight, and from it the solution of Table 11 is derived. The other two light-curves (*I* and *III*) present greater difficulties. Quite independently treated, they yield the approximate elements given in Table 12.

TABLE 11

PHOTOMETRIC ELEMENTS, MEAN LIGHT-CURVE

Ratio of radii	0.53	a_2	0.157
$\sin^2\theta'$	0.1765	b_2	0.150
$\sin^2\theta''$	0.0011	ϵ	0.298
i	82°.6	J_1/J_2	4.52
$\cos i$	0.129	L_1	0.56
a_1	0.296	L_2	0.44
b_1	0.283		

TABLE 12

PHOTOMETRIC ELEMENTS FOR CURVES *I* AND *III*

	Curve *I*	Curve *III*		Curve *I*	Curve *III*
Ratio of radii	0.53	0.54	a_2	0.142	0.158
$\sin^2\theta'$	0.1461	0.1660	b_2	0.133	0.144
$\sin^2\theta''$	0.0123	0.0038	ϵ	0.365	0.418
i	86°.3	83°.9	J_1/J_2	5.78	3.38
$\cos i$	0.0645	0.1063	L_1	0.62	0.49
a_1	0.268	0.293	L_2	0.38	0.51
b_1	0.250	0.266			

TABLE 13

	Curve *I*	Curve *III*
Observed:		
G6–A5 (Table 1)	.....	.....
Extreme	$+0^m.60$	$-0^m.05$
Mean	$+0^m.51$	$+0^m.04$
Computed (Table 12):		
L_1 (A5)	+0.62	−0.49
L_2 (G6)	+0.38	−0.51
dm_{pg}	$+0^m.53$	$-0^m.04$

As they stand, the elements given in Table 12 cannot be said to differ sensibly from those of Table 11, except in the relative luminosities, which depend directly on the relative surface brightness. The relative luminosities given in Table 12 can be directly compared with the relative magnitudes of Table 1, which were obtained in quite a different manner. The comparison is given in Table 13.

The entries in the last column of Table 1 were obtained on the supposition that the A5 component is responsible for the long-period variation. The decrease in relative sur-

face brightness of the A5 star, which coincides with the deduced decrease in its total brightness, strengthens this assumption; and the fact that the bluer component is peculiar and unstable spectroscopically increases its probability further.

The elements of Tables 11 and 12, taken together, are unsatisfactory in detailed agreement. The inclination should, of course, be equal for the three solutions; and there is no basis for supposing that the ratio of radii differs sensibly. On the other hand, the values of the ellipticity appear to differ significantly; and this exposes the unreality of the detailed solutions and the inadvisability of further discussion. The fact that the ellipticity appears greatest when the blue component is relatively faintest suggests markedly different ellipticities for the two components. It may be noted that the ellipticity determined by D. Martinoff[4] from his visual light-curve has the still larger value 0.424, an effect that points in the same direction. Obviously, the detailed differences in dimensions derived under these restrictions have no real significance.

[4] *Trudi Obs. U. Kasan*, No. 26, p. 18, 1930.

ON THE NATURE OF THE ECLIPSES OF ζ AURIGAE

ZDENĚK KOPAL
Harvard College Observatory
Received February 7, 1946

ABSTRACT

An analysis of the light-changes observed photoelectrically during the ingress of the 1939 minimum of the eclipsing system of ζ Aurigae leads to the following conclusions:

1. The ratio of radii k of its B and K components can be determined with considerable accuracy from the fractional loss of light during totality. The ensemble of photoelectric observations made at different effective wave lengths leads to $k = 0.0145 \pm 0.0003$, which renders the K supergiant sixty-nine nine times as large as its companion. This ratio appears to be relatively the most dependable characteristic of the system that can so far be inferred from its light-changes.

2. The observed duration of the disappearance of the B star, coupled with the foregoing value of k, excludes the possibility of the orbital inclination i being less than 78°, this latter value corresponding to an eclipse of two sharp-edged disks. The actual light-curve at the respective phases bears, however, little resemblance to any theoretical light-curve of a bodily eclipse, whatever the limb darkening on the apparent disk of the B star may be.

3. If $i > 78°$, the apparent distance by which the B star gets displaced by orbital motion between the first and the second contact of the eclipse exceeds the diameter of the B star, which suggests that this eclipse may have been partly due to the extinction of the B light in a semitransparent envelope surrounding the K supergiant. In order to analyze the situation, a theory of eclipses of stellar disks of finite relative dimensions by semitransparent outer layers of their mates has been developed, and equations are set up which relate the observed loss of light with variable absorption coefficient of these layers. The practical problem has been reduced to the solution of a pair of integral equations, one of which admits of a formal inversion, while the other must be solved by numerical means.

4. An application of this type of analysis to the light-changes of ζ Aurigae exhibited during the gradual disappearance of the B component shows that the orbital inclination must be very close to 90° in order to make a solution possible. A detailed interpretation of the light-changes leads us to conclude that, at the beginning of the eclipse, the B star must have been obscured, first, by an almost completely opaque cloud of a width equal roughly to $0.5r_B$, followed by a nearly transparent region $0.6r_B$ wide, before disappearing ultimately behind the limb of the K star, which, as far as we can tell, may have been quite sharp. Assuming that the depth of the cloud along the line of sight was equal to its width and that its continuous absorption was due to metallic ions, we find the density necessary to produce the observed effects to be of the order of 10^{11} ions per cubic centimeter—i.e., a quantity of the same order of magnitude as the density of solar prominences.

5. The absolute radii of the K and B components of ζ Aurigae should be approximately 200 and 2.8 ⊙; and their masses, 22 and 10 ⊙, respectively. The observational errors of quantities from which these elements were derived make these radii and masses uncertain by about 10 per cent.

I. INTRODUCTION

The system of ζ Aurigae, recognized as a spectroscopic binary by Campbell[1] and discovered as an eclipsing variable by Bottlinger,[2] can be regarded as the prototype of a rapidly growing group of eclipsing systems in which a late-type supergiant is attended by an early-type main-sequence star. The principal characteristic of such systems is a conspicuous disparity in radii of the two components. In ζ Aurigae, which consists of a supergiant of spectral class K5 accompanied by an apparently late-type B star, this disparity is such that the radius of the B component may be regarded as small, not only in comparison with its mate but perhaps even with the extent of the atmosphere surrounding the K star. In consequence, the phenomena exhibited when the narrow beam of light emitted by the B component penetrates through the outer layers of its giant mate might provide a rather unique opportunity for investigating the structure of the atmosphere of the K star to a greater detail than has hitherto proved possible for any

[1] *Lick Obs. Bull.*, **5**, 62, 1908.

[2] *A.N.*, **226**, 239, 1926.

other star except the sun. Such an opportunity is, however, but rarely given. A single revolution of both components in the system of ζ Aurigae lasts almost 973 days—out of which the actual disappearance or reappearance of the B star, before or after totality, takes place in a little more than 24 hours. In 1932, during the first epoch at which Bottlinger's prediction was tested, the partial phase of the eclipse was missed altogether. In 1934, things went better; but it was not until at subsequent eclipses in 1937 and especially in 1939–40 that astronomers succeeded in covering satisfactorily this rather elusive phenomenon. In the meantime, the photometric as well as the spectroscopic data accumulated during these eclipses have given rise to a great number of investigations in an attempt to explain the nature of the observed phenomena. The literature on this subject is too extensive to be quoted here in full.[3] In most such investigations, however, one question stood in the forefront and—so long as it remained unanswered—kept blocking further progress in the exploration of the structure of the atmosphere surrounding the K star: Are the light-changes exhibited by ζ Aurigae during partial phases before or after totality due to bodily or atmospheric eclipses?

Spectroscopic observations in 1934 and later have established beyond any doubt that when, in the neighborhood of superior conjunction, the B star passes behind the atmosphere of its K mate, new absorption lines appear in the B spectrum several days before the totality sets in, and their strength increases proportionally with increasing proximity of the limb of the K star. Is, then, the gradual disappearance of the B component due merely to an increasing dim-out as its light passes progressively through denser layers of the extended atmosphere surrounding the K star, or is the continuous absorption of this atmosphere too weak to produce any noticeable effect on the light-curve, so that the loss of light does not become apparent until the B star eventually passes behind the (possibly diffuse) photosphere of the K supergiant? In contrast to an initially conservative approach of German astronomers,[4] an interpretation of the eclipse as an extinction phenomenon was put forward by Menzel.[5] A discussion of a series of photographic observations made in the 1934 minimum by Miss Swope[6] led Menzel to conclude: "There is no eclipse in the ordinary sense. The B star sinks into obscurity behind the K, like a planet setting in a smoky atmosphere, disappearing before it reaches the horizon."[7] On the other hand, Christie,[8] in examining the ensemble of observations secured in 1939, arrived at conclusions wholly opposite to Menzel's, contending that "the observations can be well represented by a light-curve computed on the assumption that the B star is undarkened at limb and that the limb of the K star can be considered a straight occulting edge" and hence that "general absorption of the light of the B star by the atmosphere of the K star is almost negligible at heights exceeding a small fraction of the diameter of the B star." More recently still, Roach[9] rediscussed selected photoelectric observations of ζ Aurigae made during ingress of the same minimum and concluded that both hypotheses, Menzel's and Christie's, are almost equally compatible with the observations.

Such a deadlock, if real, would be bound to lessen seriously the importance attached to the changes of light exhibited by ζ Aurigae at the critical phases, bringing all hopes for a detailed investigation of the structure of outer layers of its K component virtually to a standstill. These prospects have prompted the present writer to reopen the question *de novo*, with the aim of ascertaining, first, whether or not any such ambiguity in the

[3] For a fairly complete survey cf., e.g., Wellmann, *Veröff. Berlin.-Babelsberg*, **12**, No. 4, 104, 1939.

[4] For Guthnick, Schneller, and Hachenberg (*Abh. preuss. Akad. Wiss., Phys.-math. Kl.*, No. 1, 1935): "Stillschweigende Voraussetzung ist natürlich, dass die K5-Komponente trotz ihrer sehr geringen Dichte optisch scharf begrenzt ist, eine Voraussetzung, deren theoretische Möglichkeit gegeben zu sein scheint und die allem Anschein nach auch hinreichend erfüllt ist" (p. 34).

[5] *Harvard Circ.*, No. 417, 1936.

[6] *Harvard Circ.*, No. 399, 1935.

[7] *Op. cit.*, p. 6.

[8] *Ap. J.*, **92**, 392, 1940.

[9] *Ap. J.*, **93**, 1, 1941.

interpretation of the respective light-changes really exists, and, if not, precisely what information can be extracted from their analysis. As often happens, the truth turned out to be rather intermediate between the positions taken by Menzel and by Christie; and the problem appears to be the more complex, the deeper one looks into it. The conclusions reached in the course of this investigation have already been summarized in the abstract; and in what follows we are going to substantiate them by presenting our argument in detail.

II. OBSERVATIONAL DATA

Of all the photometric evidence available thus far, the observations of ζ Aurigae secured during the ingress of the recent eclipse in December, 1939, represented by far the most complete record of its light-changes during partial phases. Since the egress in January, 1940, was but meagerly observed and since it is difficult to combine data from different eclipses because of the intrinsic variability in light (and perhaps in radius) of the K component, the ingress observations will hereafter be discussed exclusively. Of these, moreover, we shall single out the photoelectric observations alone to form the real basis of our investigation. The photographic observations,[10] though valuable, are not numerous enough to compensate for their inferior accuracy; and their effective wave length differs considerably from that of the photoelectric observations.

The ensemble of photoelectric measures of light of ζ Aurigae made during the ingress of 1939 has already been discussed by Roach,[9] who attempted also to account for minor differences in effective wave lengths between the series made by different observers.[11] In what follows we shall adopt their results as reduced by Roach to a common effective wave length of 4520 A. We shall, however, also include the observations by Brück and Green,[12] which were disregarded by Roach on account of the fact that these observers failed to record the light of ζ Aurigae out of eclipse or during totality. This, though certainly a handicap, does not, however, seem to provide a sufficient reason for rejecting the observations. We may notice that the Cambridge observations were made barely 6 minutes before Roach started with his own series; and since it is unlikely that the luminosity of ζ Aurigae could have changed appreciably during such a short interval, the zero point of the Cambridge observations with respect to Roach's may be readily determined. There exists, indeed, no possibility of checking on the scale of the Cambridge observations; but the effective wave length of a potassium-hydride cell mounted on a Sheepshanks telescope could not have been very different from 4520 A; and any slight discrepancy would be of little consequence because of the small amplitude of measured light-changes (0.075 mag.). Thus, we are going to reduce the magnitude-differences Δm as measured at Cambridge to Roach's system merely by setting the latter equal to $3^m139 - \Delta m$.

Table 1 then summarizes the observational data, collected in 25 normal points, which will serve as a basis for our investigation. Its successive columns indicate: (1) the Julian date of the respective observation; (2) the observer; (3) and (4) the mean anomaly M and the true anomaly v at each respective phase, computed on the basis of an orbital eccentricity $e = 0.43 \pm 0.01$ and the longitude of periastron $\omega = 328° \pm 1°$, as given by the ensemble of available spectrographic orbits.[13] The period of ζ Aurigae was assumed to be 972^d24 (Christie); the time of mid-primary minimum $T_0 = \text{JD } 2429637.14$ (a mean of independent determinations by Christie and Roach); and the adopted true anomaly of mid-primary minimum was 302°. Column (5) then gives the ratios, at the

[10] Christie, *op. cit.*, p. 392; Walter, *I.A.U. Circ.*, No. 808, 1940.

[11] Guthnick and Schneller, *I.A.U. Circ.*, No. 808, 1940; Kron, *Pub. A.S.P.*, **52**, 124, 1940; Roach, *op. cit.*

[12] *I.A.U. Circ.*, No. 807, 1940.

[13] For their discussion cf. Hopmann, *Leipzig Veröff.*, No. 6, p. 62, 1936.

respective moment, of the instantaneous radius-vector r to the semi-major axis a of the relative orbit; while column (6) contains the fractional losses of light which α of the B star suffered at any particular phase and defined by

$$\alpha = \frac{1-l}{1-\lambda}, \tag{1}$$

where l stands, as usual, for the fractional instantaneous luminosity of the system as a whole, and λ for that during totality. The observed amplitude of light-changes at the effective wave length of 4520 A amounts, according to Roach, to $0^m.472$, which, translated in the intensity units, yields $\lambda = 0.6474$—a value which we shall hereafter adopt.

TABLE 1

(1) JD 2,429,000+	(2) Observer*	(3) M	(4) v	(5) r/a	(6) α	(7) δ	(8) p	(9) α^U	(10) α^D
617.459	B and G	329°.499	288.189	0.71866	0.026	0.22861	+0.967	0.003	0.001
.470	B and G	.503	.196	.71862	.057	.22854	+ .945	.008	.002
.518	B and G	.521	.228	.71847	.105	.22821	+ .844	.036	.017
.529	B and G	.525	.235	.71844	.150	.22814	+ .823	.043	.022
.535	B and G	.527	.238	.71842	.150	.22811	+ .814	.046	.025
.583	B and G	.545	.270	.71829	.218	.22779	+ .716	.088	.054
.585	B and G	.546	.272	.71828	.213	.22777	+ .710	.090	.057
.589	R	.547	.273	.71827	.218	.22775	+ .704	.091	.059
.624	R	.560	.296	.71817	.261	.22753	+ .636	.123	.087
.690	K	.584	.338	.71798	.308	.22710	+ .505	.192	.153
.693	R	.586	.341	.71796	.296	.22707	+ .496	.198	.158
.726	R	.598	.363	.71786	.326	.22685	+ .428	.235	.197
.733	K	.600	.366	.71784	.340	.22682	+ .419	.240	.204
.778	R	.617	.397	.71771	.363	.22634	+ .272	.327	.300
.846	R	.642	.440	.71751	.457	.22607	+ .190	.378	.358
.862	K	.648	.450	.71748	.485	.22598	+ .162	.397	.378
.885	R	.657	.466	.71740	.492	.22582	+ .113	.427	.414
.920	R	.670	.489	.71730	.545	.22558	+ .040	.473	.469
.956	R	.683	.511	.71720	.599	.22536	− .028	.517	.519
618.250	G and S	.792	.703	.71634	.934	.22345	− .612	.863	.901
.273	G and S	.800	.717	.71628	.934	.22331	− .655	.884	.921
.295	G and S	.808	.731	.71621	.944	.22316	− .701	.906	.939
.318	G and S	.817	.747	.71614	.964	.22301	− .746	.924	.955
.357	G and S	.831	.771	.71603	.973	.22276	− .823	.952	.977
.369	G and S	329.836	288.780	0.71599	0.977	0.22268	−0.847	0.965	0.983

* B and G = Brück and Green; G and S = Guthnick and Schneller; K = Kron; and R = Roach.

With these data on hand, we now find ourselves confronting the question: Was the gradual disappearance of the B star during the ingress of 1939 an eclipse or an extinction phenomenon? The simplest way to answer this question would be to investigate whether or not the observed light-changes could be produced by an eclipse of two sharp-edged disks; and to this end we must first attempt to determine the ratio of radii of the two components. It is known that for systems exhibiting total eclipses this can be effected in a simple and straightforward way. Let L_B and L_K denote the fractional luminosities of the respective components of ζ Aurigae, expressed in terms of the combined light of the system out of eclipse. Since at the time of the minimum the B component suffers a total eclipse and it becomes totally eclipsed by its mate, it follows immediately that $L_K = \lambda$ and $L_B = 1 - \lambda$, or

$$\frac{L_B}{L_K} = \frac{1-\lambda}{\lambda}. \tag{2}$$

On the other hand,

$$\frac{L_B}{L_K} = \left(\frac{r_B}{r_K}\right)^2 \frac{J_B}{J_K}, \tag{3}$$

where r_B and r_K denote the radii of both components, and J_B and J_K their mean surface brightnesses. Setting $r_B/r_K = k$ and combining equation (2) with equation (3), we readily obtain

$$k^2 = \frac{1-\lambda}{\lambda}\frac{J_K}{J_B}. \tag{4}$$

Of the quantities entering in this latter equation, λ can be inferred directly from photometric measures of ζ Aurigae in full light and during totality, and the ratio J_K/J_B may be predicted by means of Planck's formula and the temperatures appropriate to the spectral types of the respective component. Both λ and J_K/J_B will generally depend on the wave length; and a check upon the correctness of the adopted temperatures is afforded by the requirement that the value of k, as it results from equation (4), be frequency-independent. In conformity with Menzel and other previous investigators, we shall adopt $T_K = 3200°$ K and $T_B = 15{,}000°$ K as effective temperatures of the respective components and shall take the depths of the minima observed photoelectrically at effective wave lengths between 4400 and 6100 A from a recent compilation by Hall.[14] The actual figures are compiled in Table 2, the successive columns of which indicate (1)

TABLE 2

λ	Author	Δm	L_K	L_B/L_K	J_B/J_K	k
4450.....	Guthnick	0.559	0.598	0.673	3089	0.0148
4520.....	Roach	.472	.647	.545	2752	.0141
4950.....	Guthnick	.274	.777	.287	1434	.0141
5900.....	Guthnick	.105	.908	.101	486.5	.0144
6100.....	Walter	0.095	0.916	0.091	405.3	0.0150

the effective wave length; (2) the author (exact sources are quoted in Hall's paper just referred to); (3) the observed amplitude of light-changes (in magnitudes); (4) the fractional luminosity of the K component; (5) the ratio L_B/L_K; (6) the black-body ratio of surface brightnesses J_B/J_K computed from Planck's formula for the respective frequency of light and the adopted temperatures of both stars; and (7) the value of k as defined by the foregoing dada by means of equation (4). A straight mean of the individual determinations turns out to be

$$k = 0.0145 \pm 0.0003\,,$$

which renders the K star 69 ± 2 times as large as the B star.[15]

Now let us assume, for the sake of argument, that the K supergiant appears in projection as a perfectly sharp disk and that the minimum is consequently due to a bodily eclipse. The elements of such an eclipse may then be approximated from the observed duration of the partial phase as follows. Let, as usual, $-\theta = v + \omega - 270°$ denote the

[14] *Ap. J.*, **90**, 317, 1939.

[15] Hopmann and Schaub (*Leipzig Veröff.*, No. 6, p. 41, 1936), on the basis of more extensive but less accurate observational data, arrived at a somewhat lower ratio of $r_K/r_B = 61$; whereas Guthnick, Schneller, and Hachenberg (*op. cit.*) previously had deduced $r_K/r_B = 73$.

Professor Russell (private communication) regards the uncertainty of the best estimate that can be made of T_K to be at least 300°, and of T_B as more like 2000°, since the spectrum is so badly blended and the subclass of the B star is only very roughly estimable. Furthermore, it is unlikely that the huge K component or the B star with absorption at the Balmer limit would radiate exactly like a black body. In view of this, Russell estimates the actual uncertainty of the adopted value of k to be about 10 per cent.

conventional phase angle reckoned from the moment of conjunction, and i the inclination of orbital plane of ζ Aurigae to the celestial sphere. Then it can be shown by simple geometry that

$$\left(\frac{r}{a}\right)' (1 - \cos^2 \theta' \sin^2 i)^{1/2} = r_K (1 + k) \qquad (5.0)$$

and

$$\left(\frac{r}{a}\right)'' (1 - \cos^2 \theta'' \sin^2 i)^{1/2} = r_K (1 - k), \qquad (5.1)$$

where the fractional radius r_K of the larger component has been expressed in terms of the semi-major axis of the relative orbit, which will hereafter be taken as our unit of length; and where the single and double primes refer to values of the appropriate quantities at the moment of the first and second contact, respectively.

A plot of the individual observations (see Fig. 1) suggests that the first contact oc-

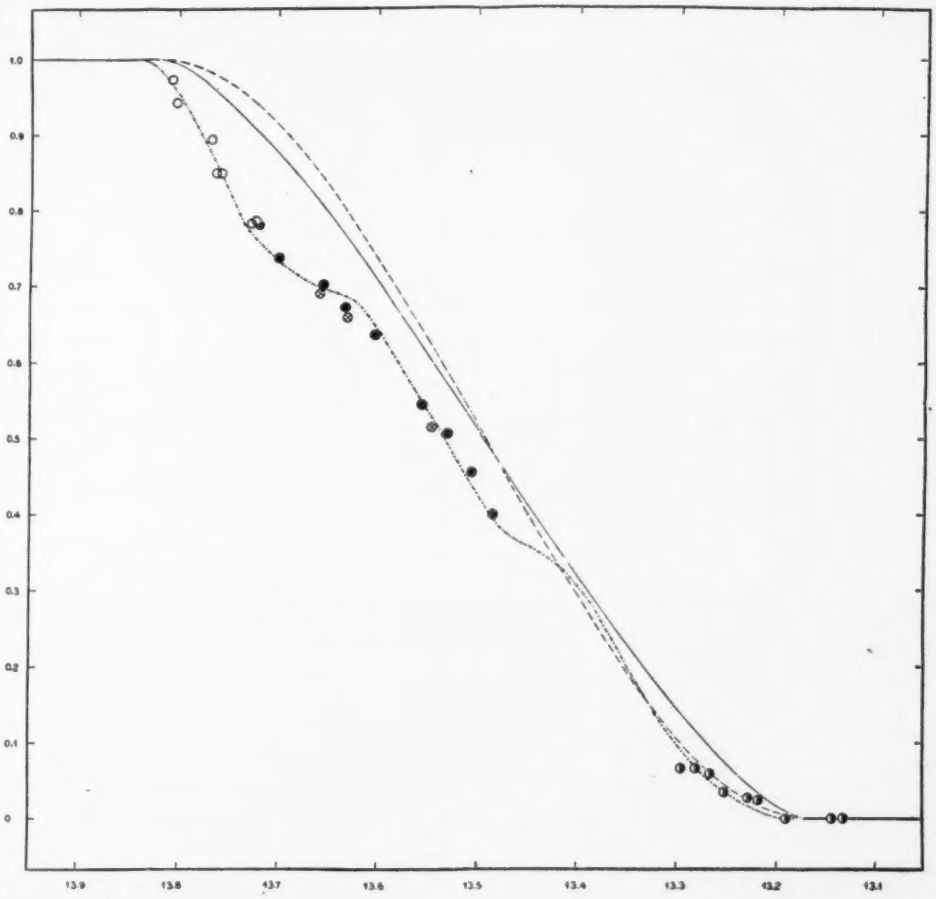

FIG. 1.—The fractional loss of light $(1 - \alpha)$ of the B component (*abscissae*) is plotted against the phase-angle $\theta = 270° - (v + \omega)$ (*ordinates*). Full line represents the theoretical light-curve corresponding to a "uniform" solution for a bodily eclipse; the broken line, to a "completely darkened" one. The dotted-and-dashed curve corresponds to the hypothesis of an atmospheric eclipse described in Section IV. The measurements made by different observers are marked as follows: ○ = Brück and Green; ◑ = Guthnick and Schneller; ⊗ = Kron; ● = Roach.

curred, very approximately, at $\theta' = 13^{\circ}.822$ and the second contact at $\theta'' = 13^{\circ}.168$, when $(r/a)' = 0.71870$ and $(r/a)'' = 0.71577$. These values, coupled with the already known ratio of the radii k and inserted in equations (5), yield

$$r_K = 0.22545\,, \qquad r_B = 0.00327\,, \qquad i = 77^{\circ}.496\,,$$

as elements of the hypothetical bodily eclipse. The apparent separations δ of the centers of the two components at any moment during such an eclipse then follow from

$$\delta = \frac{r}{a}(1 - \cos^2\theta \sin^2 77^{\circ}.496)^{1/2} \tag{6}$$

and are given in column (7) of Table 1. Column (8) of the same table contains the geometrical depth, $p = (\delta - r_K)/r_B$; while columns (9) and (10) indicate the respective

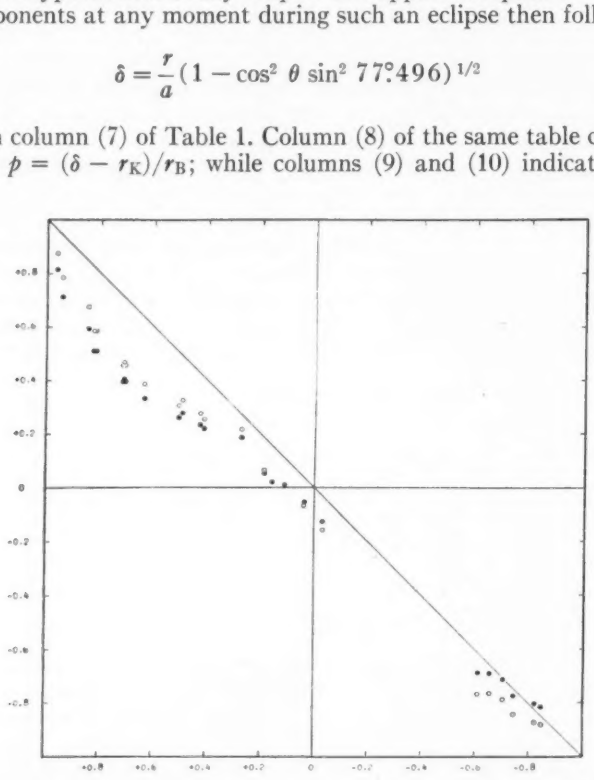

FIG. 2.—The geometrical depth $p(k, \alpha)$ corresponding to the fractional loss of light of observations listed in Table 1 (*abscissae*) plotted against $(\delta - r_K)/r_B$ (*ordinates*). The values of $p(k, \alpha)$ appropriate for uniform disks (*full circles*) as well as those for disks completely darkened at limb (*open circles*) have been taken from Zessewitsh's tables.

fractional losses of light, $\alpha^U(k, p)$ and $\alpha^D(k, p)$, which the B star would suffer if its apparent disk were uniformly bright or (what is unlikely for a star of such an early spectral type) if it were completely darkened at limb. Figure 1 then shows diagrammatically both the "uniform" and the "darkened" theoretical light-curves, together with the observed normal points.

A glance at this diagram will reveal at once that *the actual light-variation of ζ Aurigae exhibited during gradual disappearance of its B component is very different from any theoretical light-curve computed under the assumption that the eclipsing component possesses a sharp limb*—so different that it seems futile to try improving the fit by an arbitrary variation of the adopted values of θ' or θ''. This situation is further illustrated in Figure 2, where the values of p of column (8), Table 1, are plotted against the geometrical depths $p(k, \alpha)$ inferred from the observed losses of light under the assumption of uniform

disks as well as those completely darkened at limb.[16] Were the light-changes of ζ Aurigae due to bodily eclipses, the "geometrical" and "photometric" p's would be the same for every normal within the limits of observational errors. Their plot would therefore define a straight line passing through the origin and bisecting the angle between the axes. A glance at Figure 2 reveals, however, that this is by no means the case. The hump between $0.8 > p > 0.4$ is particularly conspicuous; and the fact that it is corroborated independently by four observers (Brück and Green, Kron, Roach) working at three different stations leaves little room for doubt as to its reality. In brief, the form of the light-changes of ζ Aurigae observed during the ingress of 1939 appears to be peculiar and suggests that the gradual disappearance of the B component may have been due partly or wholly to the extinction of its light in the atmosphere of the K star or merely to the fact that the limb of this supergiant does not appear in projection as perfectly sharp. Sound physical reasons can be listed[17] why should we indeed expect this to be the case; and it appears a priori not unlikely that a pertinent analysis of the respective light-changes could throw considerable light on the structure of the semitransparent layers enveloping the K component.

A type of analysis required for the solution of such a problem was first outlined by Menzel.[5] His pioneer investigation appears, however, to be no longer sufficiently general in scope. First, Menzel (and, following him, Roach) assumed the atmospheric opacity to be a simple exponential function of the height and limited himself to a determination of constants specifying this exponential—whereas our aim should be to infer the *form* of the opacity variation from the observed light-changes without biasing it by any a priori assumptions from the outset. Second, the theory as developed by Menzel presumes that the component undergoing eclipse may be regarded as a luminous point—an assumption which seemed harmless enough in a system like ζ Aurigae but which, on closer scrutiny, will prove to be treacherous. Here we shall develop a new and more general theory of atmospheric eclipses, which is entirely free from the above-mentioned limitations. It still presumes the eclipsing component to be so large in comparison with its mate that, for the study of the eclipse, the matter in its semitransparent regions can be regarded as stratified in parallel layers;[18] but it does not suppose that the center of light of the star undergoing eclipse projects itself constantly on the geometrical center of its apparent disk, and it makes no a priori assumptions as to the variation of opacity in stellar atmospheres. In the following section this theory will be developed in some detail.

III. INTERPRETATION OF ATMOSPHERIC ECLIPSES

Let us abandon for a while ζ Aurigae and consider, quite generally, an eclipsing system whose one (say the primary) component is surrounded by a radially symmetrical envelope of gradually increasing opacity and is thus semitransparent at the limb. When, in the neighborhood of superior conjunction, its companion begins to project itself behind such semitransparent layers, a loss of light occurs, which we shall refer to as an "atmospheric eclipse." Furthermore, let $\mathfrak{L}(\delta)$ denote the instantaneous luminosity of the secondary component and J the true distribution of brightness over its apparent disk of a fractional radius r_2. If this disk is divided into elements by circles concentric with the primary star, the light emitted by all parts of an element lying between the radii r and $r + dr$ and passing through the envelope surrounding the primary compo-

[16] The numerical values of $p(0.0145, a)$ for uniform or darkened disks were taken from tables published by Zessewitsh in *Bull. Inst. Astr. Leningrad*, No. 45, 1939, and No. 50, 1940.

[17] Cf., e.g., Unsöld, *Physik der Sternatmosphären*, pp. 394–95, Berlin, 1938.

[18] This assumption is one of convenience rather than of necessity, as it should come close to reality in the practical case we have presently in mind and offers some analytical simplifications. A development of the theory which is free from this assumption is being postponed to a separate paper.

nent at a distance r from its center[19] will emerge with its original intensity reduced by the factor $e^{-\tau}$, where τ denotes the optical depth of the semitransparent layers along the line of sight. In other words, a passage of light of the secondary component through semitransparent layers of its mate will cause the *apparent* distribution of brightness as seen by a distant observer *through* such layers to be, not J, but $Je^{-\tau}$. Let us, for the sake of simplicity, also regard the secondary component as a sphere with intrinsically uniform distribution of brightness ($J = 1$). The isophotes over its apparent disk as seen through the obscuring medium will then form a one-parameter family of circles depending on r alone. If, furthermore, the primary component happens to be so large in comparison with its mate that the curvature of its limb may be ignored, the family of isophotes will degenerate into a grid of straight lines normal to the line joining the centers of the two components. Under such circumstances, it can be proved by simple geometry that

$$\pi r_2^2 \mathfrak{L}(\delta) = 2\int_{\delta - r_2}^{\delta + r_2} \Lambda(r)\, \sqrt{r_2^2 - (\delta - r)^2}\, dr\,, \tag{7.0}$$

where $\Lambda(r) \equiv \exp(-\tau)$. A substitution $\delta - r = r_2 x$ reduced this to[20]

$$\mathfrak{L}(\delta) = \frac{2}{\pi}\int_{-1}^{+1} \Lambda(\delta - r_2 x)\, \sqrt{1 - x^2}\, dx\,, \tag{7.1}$$

which represents the first fundamental integral equation of our problem, relating the observed luminosity $\mathfrak{L}(\delta)$ with its unknown transform $\Lambda(r)$.

The physical meaning of this transform can also be described in the following terms: $\Lambda(r)$ represents the remaining light of a point-source, of luminosity equal to that of the secondary component, at a distance r from the center of the primary star. It is obvious that if $r_2 = 0$, then $r = \delta$ and equations (7.0) and (7.1) admit, indeed, of a trivial solution $\mathfrak{L}(\delta) = \Lambda(\delta)$. We should, however, bear well in mind that a mere numerical smallness of r_2 in comparison with the photospheric "radius" of the opaque core of the primary component still offers by itself no guaranty that the $\mathfrak{L}$- and Λ-functions are identical. What equally matters is the steepness of the density gradient in the semitransparent outer layers of the primary star—i.e., the fact as to *whether or not* $\Lambda(r)$ *would react appreciably to a change of its argument by a quantity of the order of* $\pm r_2$. This, in turn, depends as much on the properties of the obscuring layers as on the secondary's size; and, since the former are not known beforehand, it appears necessary to put the observed light-curve through the mill of equation (7.1) in every practical case.

Before we outline a method for solving such an equation, it may be pointed out that the remaining light of the secondary component can be expressed by equations (7.0) and (7.1), irrespective of whether the eclipse is bodily or atmospheric. Should the eclipsing component possess a perfectly sharp limb at $r =$ (say) r_1, the solution of equations (7.0) and (7.1) would obviously reduce to $\Lambda(r) = 1$ or $\Lambda(r) = 0$, according to whether $r \gtrless r_1$. In other words, *the* Λ*-transform of the light-changes due to a bodily eclipse is discontinuous at* $r = r_1$. Should, however, the primary's limb appear diffuse, $\Lambda(r)$ will be a continuous function which will, in general, run its course more rapidly than $\mathfrak{L}(\delta)$—the

[19] Refraction of rays within the envelope is assumed to be negligible, so that their paths are straight lines.

[20] Professor H. N. Russell pointed out in correspondence with the writer that as long as the curvature of the eclipsing limb can be ignored, equation (7.1) may be re-written symmetrically as

$$\mathfrak{L}(\delta) = \int_{-1}^{+1} \Lambda(\delta + r_2 p)\, \frac{\partial \alpha}{\partial p}\, dp\,, \tag{7.2}$$

where α is the fractional loss of light (for any degree of darkening) of the component undergoing eclipse and p, the geometrical depth of this eclipse.

more so, the smaller the fraction of r in which the atmospheric effect runs from transparency to complete opacity.[21]

The first task confronting us in our analysis of atmospheric eclipses is, then, to devise a method for deducing $\Lambda(r)$ from the observed light-changes $\mathfrak{L}(\delta)$. In order to do so, we replace the integral on the right-hand side of equation (7.1) by a summation of a finite number of terms by means of some formula for approximate numerical integration. In this particular case we find it convenient to employ a summation formula, due to Mehler,[22] which asserts that if $f(x)$ is a function of degree not in excess of $2n-1$, then

$$\int_{-1}^{+1} f(x)\,\sqrt{1-x^2}\,dx = \frac{\pi}{n+1}\sum_{i=1}^{n} \sin^2\frac{\pi i}{n+1}\, f\left(\cos\frac{\pi i}{n+1}\right). \tag{8}$$

By virtue of this, equation (7.1) can be approximately re-written as

$$\mathfrak{L}(\delta) \doteq \frac{2}{n+1}\sum_{i=1}^{n} \sin^2\frac{\pi i}{n+1}\,\Lambda\left(\delta - r_2\cos\frac{\pi i}{n+1}\right), \tag{9}$$

where the unknown function no longer occurs behind the integral sign, as the integral has been replaced by a weighted sum of particular values of our Λ-function corresponding to n discrete values of its argument. An equation of the form (9) can be set up from every observed normal. Since the argument of Λ in equation (7.1) involves δ, the discrete values of Λ occurring in each such equations will *not*, however, be identical; and if we regard them as unknown, a set of m such equations will represent a diophantine system containing $m \times n$ unknowns.

This indeterminacy can, however, be removed in the following manner: A representation of the integral in equation (7.1) by a weighted sum of n unequally spaced ordinates tacitly presumes that the Λ-transform is a polynomial of degree not exceeding $2n-1$. Suppose, now, that, out of the array of $m \times n$ ordinates of the diophantine system, *we single out* 2n *of them as unknowns and express all remaining ones in terms of this selected set of pivotal points by means of an interpolation polynomial of the* (2n − 1)*th degree.* This is indeed admissible, for the Λ-transform is supposed to be continuous; and though the magnitude of each ordinate is unknown, its position with respect to any other one is specified as soon as δ and r_2 are fixed.

Let $\Lambda(r)$ be a polynomial of degree $2n-1$, which for arbitrarily spaced values $a_0, a_1, a_2, \ldots, a_{2n-1}$ of the argument r admits of the values $\Lambda(a_0), \Lambda(a_1), \ldots, \Lambda(a_{2n-1})$. A $\Lambda(r)$ appropriate for any particular value of r may then be found, for instance, from Lagrange's interpolation formula of the form[23]

$$\left.\begin{aligned}\frac{\Lambda(r)}{(r-a_0)(r-a_1),\ldots,(r-a_{2n-1})} &= \frac{\Lambda(a_0)}{(r-a_0)(a_0-a_1)(a_0-a_2),\ldots,(a_0-a_{2n-1})}\\ &+\frac{\Lambda(a_1)}{(r-a_1)(a_1-a_0)(a_1-a_2),\ldots,(a_1-a_{2n-1})}\\ &+\ldots+\frac{\Lambda(a_{2n-1})}{(r-a_{2n-1})(a_{2n-1}-a_0),\ldots,(a_{2n-1}-a_{2n-2})},\end{aligned}\right\} \tag{10}$$

[21] The writer owes this remark to Professor Russell (private communication).

[22] *J. f. Math.*, **63**, 152, 1863. This formula is but a generalization of the well-known Gauss's method for numerical integration.

[23] Cf., e.g., Whittaker and Robinson, *The Calculus of Observations*, p. 29, London, 1944.

which is suitable for computation and which will permit us to reduce the originally indeterminate system to a set of m linear equations containing $2n$ discrete values of Λ which correspond to known arguments. If $m = 2n$, the system will possess a unique solution; if $m > 2n$, the system becomes overdeterminate and may be solved by the method of least squares. When values of the unknown function are inserted back in the interpolation polynomial (10), the latter will represent an nth approximation to $\Lambda(r)$, whose accuracy may be arbitrarily increased by taking n sufficiently large.

The above-described method for a solution of the first fundamental equation of our problem consists, in brief, in replacing the original integral equation (7.1) by an equivalent system of linear algebraic equations by means of a convenient summation formula and in reducing subsequently the number of the unknowns by expressing $(m - 2)n$ of them as interpolates in terms of $2n$ pivotal points. This procedure requires the unknown function to be continuous within the whole domain concerned; for, if so, both approximate steps represented by equations (9) and (10) are easily justified and the process can be shown to lead to a rigorous solution when n is allowed to increase beyond any limit.[24] In practice, however, even a moderate number of terms (i.e., a low value of n) should, as a rule, give a good approximation; for the method has been so adjusted as to give the best possible fit with the smallest number of terms.

The physical advantages of the transformation we have just effected will be immediately apparent. In passing from $\mathfrak{L}(\delta)$ to $\Lambda(r)$, we have replaced a distended beam of light emitted by the secondary component and emerging from semitransparent layers of its mate by an equivalent beam of a point-source, which, unlike $\mathfrak{L}(\delta)$, can be related with the absorption coefficient κ_ν of the obscuring atmosphere by a series of purely analytical operations. It follows, then, from the definition of the optical depth that

$$\Lambda = e^{-\tau} = \exp\left[-\int_{\sqrt{r_A^2-\delta^2}}^{\sqrt{r_A^2-\delta^2}} \kappa_\nu \, ds\right], \tag{11}$$

where r_A denotes the extent of absorbing atmosphere of the primary component and ds, the element of the line of sight. As the reader can easily visualize, $s^2 = r^2 - \delta^2$. If we eliminate s for r by means of this relation and take logarithms, equation (11) readily assumes the form

$$\log \Lambda = -2\int_\delta^{r_A} \frac{\kappa_\nu r \, dr}{\sqrt{r^2 - \delta^2}} . \tag{12.0}$$

If, furthermore, we set

$$r_A^2 - \delta^2 = c$$

and

$$r_A^2 - r^2 = x$$

and introduce new auxiliary functions $\psi(x)$ and $\sigma(c)$, related with κ_ν and Λ by

$$\kappa_\nu = \frac{d\psi}{dx} \quad \text{and} \quad \log \Lambda = -\sigma(c),$$

then equation (12.0) assumes the alternative form,

$$\sigma(c) = \int_0^c \frac{d\psi}{dx} \frac{dx}{\sqrt{c - x}}. \tag{12.1}$$

Equation (12.0) or its equivalent (12.1) represents the second fundamental equation of our problem, which relates the Λ-transform with the absorption coefficient κ_ν. In

[24] The numerical process itself works, however, regardless of whether or not $\Lambda(r)$ is a continuous function; for if it were not (as in the case of a bodily eclipse), the behavior of successive approximations would give us a sufficient warning that we are trying to interpolate over a discontinuity.

order to solve it, this time we do not need to resort to any approximate procedure; for equation (12.1) will be easily recognized as an integral equation of Abel's type, whose inversion yields

$$\psi(x) = \frac{1}{\pi}\int_0^x \frac{\sigma(c)\,dc}{\sqrt{x-c}}. \tag{13}$$

Next integrate the right-hand side of equation (13) by parts. Since, by definition, the extinction vanishes at $r = r_A$ and hence $\Lambda = 1$ for $c = 0$, the integrated part must disappear, and we are left with

$$\psi(x) = \frac{2}{\pi}\int_0^x \frac{d\sigma}{dc}\sqrt{x-c}\;dc\,. \tag{14}$$

Ultimately differentiating equation (14) with respect to x, we obtain

$$\frac{d\psi}{dx} = \frac{1}{\pi}\int_0^x \frac{d\sigma}{dc}\frac{dc}{\sqrt{x-c}} \tag{15}$$

or, reverting to our original functions and variables,

$$\kappa_\nu = \frac{1}{\pi}\int_r^{r_A} \frac{d}{d\delta}(\log\Lambda)\frac{d\delta}{\sqrt{\delta^2-r^2}}. \tag{16}$$

This last equation expresses κ_ν explicitly as a function of r in terms of Λ; and since this latter function can be deduced from the observed light-changes by methods developed earlier in this section, the solution of our problem is thus complete. It may be reiterated

TABLE 3

i	δ'	δ''	$\Delta\delta$	r_K	r_B	$\Delta\delta - d_B$
90°	0.17170	0.16308	0.00862	0.166	0.00240	+0.00382
85°	.18215	.17402	.00813	.177	.00256	+ .00301
80°	.21016	.20308	.00708	.206	.00299	+ .00110
75°	0.24922	0.24318	0.00604	0.247	0.00358	−0.00112

that the whole derivation of κ_ν involves nothing that would bias its variation with the altitude in any way; for, as the reader can easily verify, our whole method consists of a series of purely mathematical operations and is therefore free from any physical assumptions of speculative nature.[25]

IV. DISCUSSION OF THE OBSERVATIONS

Having completed an outline of a general theory of atmospheric eclipses, let us return to ζ Aurigae and consider the light-changes exhibited in the course of a gradual disappearance of its B component in 1939. We found earlier in this paper that the consequences of a bodily-eclipse hypothesis were definitely at variance with the observed facts, and this led us to conjecture that the limb of the eclipsing K component may be semitransparent. If so, however, the value of $i = 77°.5$ as deduced earlier (Sec. II) from the well-determined ratio of the radii k and the observed duration of the light-changes represents merely a *lower limit* of the orbital inclination, whose actual value may now be anywhere between 77°.5 and 90°.

Table 3 summarizes the pertinent geometrical data, computed again with the pre-

[25] A notoriously ill-determinate character of r_A is not really troublesome in this connection; for, beyond certain limiting value of δ, $\log\Lambda$ and hence the integrand in eq. (16) become effectively zero. Any increase in the upper limit of our integral would then add nothing to its numerical value. We could, for all practical purposes, set $r_A = \infty$ without affecting the numerical results to any appreciable degree.

viously adopted values of θ', θ'', and k. Its successive columns indicate (1) the orbital inclination (assumed); (2) the apparent separation δ' of both components at the moment of the observed first contact ($\theta' = 13^{\circ}.822$); (3) the separation δ'' at the beginning of totality ($\theta'' = 13^{\circ}.168$); (4) the displacement $\Delta\delta = \delta' - \delta''$ of the secondary component by orbital motion during its disappearance; (5) and (6) the fractional radii of the K and B components, computed on the assumption that the inner contact marks the complete disappearance of the B star—i.e., that $\delta'' = r_K - r_B$, in which case

$$r_K = \frac{\delta''}{1-k} \quad \text{and} \quad r_B = \frac{k\,\delta''}{1-k}. \tag{17}$$

The seventh column ultimately gives the difference between $\Delta\delta$ and the diameter d_B of the B star—a quantity which represents the permissible extent, under given conditions, of the semitransparent limb of the K component. The semi-major axis of the relative orbit of ζ Aurigae has been taken throughout as our unit of length.

As the reader can easily verify, the difference $\Delta\delta - d_B$ is indeed zero for $i = 77^{\circ}.5$ but increases thereafter with i until, for $i = 90^{\circ}$, it may well exceed the radius (though not the diameter) of the B star. Should the orbital plane of ζ Aurigae happen to be normal to the celestial sphere, the maximum admissible thickness of the semitransparent limb of the K component would amount to 2.3 per cent of its photospheric radius—or approximately 3×10^6 km. This value is, indeed, of the order of magnitude to be expected from the theory of photospheric layers of the stars, but it is by no means comparable with the spectroscopically detected dimensions of the extended calcium atmosphere enveloping the K component. This leaves but little room for doubt that *this atmosphere must be for the most part practically transparent to light of effective wave length around 4500 A;* for the actual loss of light does not become apparent until the B star has closely approached the limb of its mate and lasts only a very short time.

The fact that the limb of the K component appears to change from transparency to complete opacity within a width which is *less* than the diameter of the B star makes it obvious that *at no moment, during eclipse, will the center of light of the B component coincide, even approximately, with the geometrical center of its apparent disk* and that it is, therefore, not correct to regard the star undergoing eclipse as a luminous point. This invalidates, unfortunately, the outcome of the investigations of atmospheric structure of ζ Aurigae by Menzel and Roach, which were based on this unverified assumption.[26] Menzel and Roach failed to notice that the actual size of the B component, which they thought to be indeterminate, can be deduced with relative accuracy from the fractional loss of light during totality without any appeal to the duration or the form of the partial phases and that this size, coupled with the observed duration of the ingress, imposes severe restrictions on the possible extent of the semitransparent limb of the K star. On the other hand, Christie's contention that the general absorption of the K atmosphere is almost negligible at heights exceeding a few tens of thousands of kilometers at most appears to have run to the other extreme. We have seen above that, in 1939, the height at which this absorption set in may have exceeded 3,000,000 km if i is close to 90°, though the exact height is bound to remain uncertain as long as the inclination is unknown.

[26] Moreover, H. N. Russell has pointed out to the writer that Roach's Table 4, giving solutions for a sharp edge, is vitiated by errors. Roach's values of R_B and R_B/R_K give the same R_K for all values of the inclination i, whereas R_B should vary as cos b and R_K as sec b, b being the latitude at which the track of the B star crosses the K disk. The correct version of the first three columns of Roach's Table 4 (according to his data) is as follows:

i	b	R_B/R_K
90°	0°	0.035
87.8	15	.033
84.7	30	.027
80.9	45	.017
74.0	60	0.0087

Under such circumstances, in order to investigate the structure of semitransparent layers surrounding the K component of ζ Aurigae, it seems necessary to resort to the complete analysis developed in the preceding section and, as the first step, to solve equation (7.1) for $\Lambda(r)$. In doing so, we run, however, into a significant fact at the very outset: namely, *it turns out to be impossible to satisfy the observed light-changes with a Λ-transform which remains positive for all values of its argument between* $\delta + r_B$, *unless the orbital inclination is considerably higher than* 78°.[27] But a transform assuming negative values is clearly inconceivable from the physical point of view; hence the above-mentioned fact merely restricts the possible location of i to the neighborhood of 90°. Professor Russell has, indeed, pointed out to the writer that a positive transform of the observed light-changes can be obtained if $i = 90°$ or very nearly so. Then it is possible to represent the observed light-variation, as shown in Figure 1, to every detail; but in doing so we are led to the conclusion that, *at the beginning of the eclipse, the B star must first have been obscured by an almost completely opaque strip (or cloud) of a width equal to roughly* 0.5 r_B, *followed by an almost transparent region* 0.6 r_B *wide, before disappearing ultimately behind the limb of the K star*, which, so far as we can tell, appears to have been quite sharp. A theoretical light-curve corresponding to such a composite eclipse is also diagrammatically shown on Figure 1 (dots and dashes).[28]

A postulate of the existence of a heavy dark cloud in a stellar atmosphere, with a clear space of a couple of million kilometers underneath it, may appear, at first sight, to be so unusual that, before we proceed to discuss its implications, we should consider the possibility that something might, perhaps, be wrong with the underlying observational data. The evidence for rapid loss of light following the first contact, which is the crux of the matter, is based mainly (though *not* wholly) on the Cambridge series of photoelectric observations made by Brück and Green,[12] who failed to record with their instrument the luminosity of ζ Aurigae either in full light or during totality. For these reasons both the scale and the zero point of their series remain theoretically uncertain—though, as we have pointed out in Section II, the zero point can be fixed satisfactorily by a comparison with almost simultaneous observations by Roach; and because of the smallness of the observed light-changes the scale does not matter a great deal. Moreover, a rapid decrease of light following the first contact is also borne out by photographic observations made by Christie;[29] and Christie's own light-curve (*op. cit.*), based on more extensive but less homogeneous data relative to the ingress of 1939, exhibits this feature so well that it would certainly be unwise to ignore it.

We have seen, however, that in this case no conventional type of eclipse can account for the observed light-curve. This leaves us with two alternatives: either the B component is very much smaller in comparison with its mate than our accepted value of k would indicate (and then the orbital inclination may be largely uncertain), or this component must have been obscured in the course of its gradual disappearance in 1939 by clouds in the atmosphere of the K star in addition to a photospheric eclipse (and the orbital inclination could not then deviate sensibly from 90°). The first alternative is being mentioned here only for completeness; for the determination of k as outlined in Section II above is so simple and straightforward that anyone who wishes to dispute it must do so at his own risk. The second alternative appears to the writer to be definitely more probable—the more so, the closer we come to consider it. Menzel pointed out to the writer that the eclipses of the B component of ζ Aurigae may aptly be termed as "chromospher-

[27] This may, indeed, have been anticipated; for in Sec. II we found that, with $i = 77°.5$, the light of the B star decreases during the ingress more rapidly than it should if the limb of the eclipsing component were perfectly sharp; and an atmospheric eclipse (semitransparent limb) would naturally bring about a still more gradual decrease.

[28] Professor Russell first computed this light-curve by a "cut-and-try" method of his own. Subsequent calculations carried out by the writer along the lines developed in Sec. III have essentially confirmed Russell's outcome.

[29] *Op. cit.*

ic." When we recall the variability of solar chromosphere and its activities, it should not be too difficult to surmise that analogous activities are probably characteristic of other stars as well and of supergiants like the K component of ζ Aurigae, surrounded by huge atmospheres, in particular. Our present hunch is, however, based on more than a mere analogy. Let us assume, reasonably enough, that the continuous absorption of the cloud which we invoked to explain the particular features of the light-curve of ζ Aurigae during the ingress in 1939 was due to metallic ions. Using Menzel's formula,[30] which relates the extinction with the number of absorbing particles per unit of space, we find that *the density necessary to give rise to the observed drop of light turns out to be a quantity of the order of 10^{11} ions per cubic centimeter* if the depth of the cloud along the line of sight is to be equal to its width, which is of the *same* order of magnitude as the densities of solar prominences. The same is true of the respective electron pressures as well. The hypothetical cloud in the atmosphere of the K component of ζ Aurigae turns out, in brief, to differ from analogous solar phenomena in magnitude rather than in kind. It may simply have been a prominence—a giant prominence, to be sure, judged by solar standards; but in comparison with the size of the K supergiant it need not have been any more conspicuous than an average-sized prominence of the sun.

If this explanation is correct, a passage of the B component of ζ Aurigae behind a prominence of its mate during the ingress of 1939 and the consequent peculiar form of the light-curve were probably a matter of chance—perhaps a rare chance which may not occur again for several cycles. Whether or not this is so only future eclipses can decide; but the moral which can be derived from such cases is obvious: Rare and fleeting phenomena like the eclipses of ζ Aurigae can never be observed with too great accuracy and care while they happen.

V. CONCLUDING REMARKS

In preceding sections of the present investigation of the system of ζ Aurigae we have established the fact that its K component is approximately sixty-nine times as large as the B star and that the orbital inclination lies somewhere between 78° and 90°, but probably very close to the latter. This opens the way for a determination of the absolute dimensions of both components of this system. Spectroscopic determinations of the semi-major axis of the relative orbit of ζ Aurigae are still subject to some uncertainty because of our inaccurate knowledge of the mass-ratio m_K/m_B of both components, the published values of which range from $m_K/m_B = 1.85$ (Christie and Wilson[31]) to $m_K/m_B = 2.47$ (Guthnick, Schneller, and Hachenberg[32]). A rediscussion of all original data by Hopmann[33] has shown that a value of $m_K/m_B = 2.15 \pm 0.11$ seems consistent with both the Mount Wilson and the Babelsberg radial velocities within the limits of their observational errors. The corresponding projection of the semi-major axis $a_K \sin i$ of absolute orbit of the K component was found to be $(271 \pm 6) \times 10^6$ km, and hence

$$a = a_K \left(1 + \frac{m_K}{m_B}\right) \csc i = 854 \csc i \times 10^6 \text{ km}.$$

This is the absolute value of our unit of length, in terms of which the fractional radii of both components (fifth and sixth cols. of Table 3) were expressed. Since the orbital inclination i is probably close to 90°, the radius of the K component of the eclipsing system ζ Aurigae should be in the neighborhood of 200$\odot$ and that of the B star around 2.8$\odot$. The masses of these components are then approximately 22 and 10$\odot$, respectively. Both the radii and the masses just quoted are subject to an uncertainty of at least 10 per cent.

[30] *Op. cit.*, eqs. (1) and (2).

[31] *Ap. J.*, **81**, 426, 1935.

[32] *Op. cit.*

[33] *Op. cit.*, pp. 62–66.

A detailed interpretation of the light-changes exhibited by ζ Aurigae during a gradual disappearance of its B component in 1939 led to a rather unexpected conclusion that the "photospheric" eclipse must have been preceded by a partial obscuration due to a cloud of approximately 10^6 km in diameter and of density comparable with that of solar prominences, sustained at an altitude of some 1.7×10^6 km above the photosphere of the K star. Unless the observations near first contact are systematically vitiated by some unexplained error, the changes of light exhibited during the ingress of 1939 do not seem to admit of any alternative explanation.

It should be clearly pointed out, however, that the entire extent of the atmosphere surrounding the K component did not fall within the scope of our investigation. Spectroscopic observations have shown that the envelope of the K star must extend to at least 50×10^6 km above its photosphere; for a selective absorption begins to manifest itself at least a week before the ultimate disappearance of the B component. A line absorption may naturally be insufficient to affect the combined light of the system to any appreciable degree. The actual loss of light does not become apparent until the B star has merged deep behind relatively dense inner layers of the atmosphere and lasts not much longer than a day. This makes it evident that an exploration of the upper atmosphere of the K component is bound to depend for a long time solely on studies of the "absorption flash" in the B spectrum. On the other hand, the present investigation has demonstrated—at least in theory—that an analysis of the light-changes exhibited during an atmospheric eclipse is likely to reveal the structure and physical properties of the semitransparent layers of the eclipsing component to much greater detail and with much greater accuracy than spectroscopic observations alone could ever hope to attain.

The particular duration of the crucial light-changes of ζ Aurigae, which does not differ much from 24 hours, makes it well-nigh impossible to follow their whole course from a single observing station and invites strong international co-operation. No plea for it can be more eloquent than a brief review of events during the ingress of 1939. The series of photoelectric observations on which the present study was based started with Brück and Green in Cambridge, England, in the evening hours of December 17. Shortly after 2 A.M. local time of the next day, their observations were interrupted by the vagaries of English weather; but, fortunately, not more than 6 minutes after the skies clouded up in Cambridge the series was resumed by Roach at Tucson, Arizona; and he, in turn, was joined 2 hours and 25 minutes later by Kron at Mount Hamilton. The American observers then followed the star through the rest of the night, and there our series temporarily ends. The reader has undoubtedly noticed a tantalizing lack of observations (of any kind!) during the next 6 hours—i.e., at the time of daylight in the Western Hemisphere. Observations made in Japan or any other place in eastern Asia would have admirably filled the gap, but unfortunately none were forthcoming; and so it happened that only the last glimpse of the eclipse was caught by Guthnick and Schneller in central Europe the next evening.

As to subsequent eclipses, the one in September, 1942, passed almost unnoticed; and there was very little chance that the recent eclipse in May, 1945, fared any better. The first really favorable eclipse will not occur until January, 1948—at the time when ζ Aurigae will be observable for many hours of night. Let us hope that this event will find astronomers of all nations around the globe back at their instruments, ready to record for posterity the details of this important and elusive phenomenon.

In conclusion, the writer takes pleasure in expressing his indebtedness to Professor (now Commander, U.S.N.R.) Donald H. Menzel and, in particular, to Professor Henry Norris Russell for constructive criticisms and stimulating suggestions. In point of fact, it was Professor Russell's insistence on putting the observed light-changes through the mill of equation (7) that gave this investigation its present form.

APPLICATION OF THE MULTIPLIER PHOTOTUBE TO ASTRONOMICAL PHOTOELECTRIC PHOTOMETRY*

GERALD E. KRON
Lick Observatory
Received March 13, 1946

ABSTRACT

The type 1P21 multiplier phototube, manufactured by the Radio Corporation of America, has been found to be well adapted to photoelectric photometry. Signal-to-noise ratios and other characteristics are given and discussed. The 1P21 is many times superior to light-sensitive units previously used for photometry in the blue region of the spectrum.

The technique of photoelectric photometry was pioneered in this country by Professor Joel Stebbins, who, in 1907, exposed a selenium cell to moonlight[1] and observed a galvanometer deflection. The selenium cell, though useful, proved to be unsuitable for astronomical photometry and was supplanted entirely by the superior photoelectric cell. Sinclair Smith[2] has shown that the theoretical limiting magnitude for photoelectric photometry can be achieved by connecting a perfect photoelectric cell directly to a Hoffmann electrometer. Prior to 1932, photometry was done by means of comparatively inefficient electrometers, which were rugged enough to be carried by the telescope.

In 1932 Whitford[3] introduced the electronic amplifier and applied the constant-deflection method. This new type of equipment is more sensitive and more convenient to use than the old, but the combination of the electronic amplifier with a photoelectric cell does not utilize the latter with its optimum effectiveness. The vacuum-tube amplifier brings in extraneous signals of its own in the form of "shot-noise" in its grid current; and, if a grid resistor is used in order to invoke the constant-deflection principle, a comparatively large amount of unavoidable "thermal noise" is introduced in addition. The natural shot-noise of the photocurrent is thus masked for faint levels of illumination, and the signal-to-noise ratio is therefore inferior to that achieved with the best electrometer.

The principle of the electron multiplier suggests itself as a means of reaching the ultimate signal-to-noise ratio without the use of an electrometer. By means of the multiplier principle,[4] very large amplification of the original photocurrent can be accomplished previous to the introduction into the circuit of a measuring device. Thus, if a noise-free amplification factor of, say, 1,000 can be obtained before a vacuum tube and its accompanying grid resistor need to be employed, then the ratio of signal to externally introduced noise will generally be increased a thousand fold, and the primary shot-noise of the photocurrent may then be predominant. It is clear that, from a theoretical point of view, the photomultiplier should make possible the achievement of a high signal-to-noise ratio without the use of delicate and impractical equipment.

Among the first to use an electron multiplier for astronomical purposes were Whitford and Kron,[5] who employed a primitive form of the instrument in the construction of some auxiliary equipment for a telescope. Experience with this multiplier indicated that it was inferior to a photocell because of the low efficiency of the sensitive surfaces; hence, at the time, little interest was stimulated. Considerable developmental work has been done on the multiplier since this early model was tested, however, and it seems that the use of

* *Contributions from the Lick Observatory*, Ser. II, No. 13.

[1] *Ap. J.*, **26**, 326, 1907.

[2] *Ap. J.*, **76**, 1, 1932.

[3] *Ap. J.*, **76**, 213, 1932.

[4] V. K. Zworykin, G. A. Morton, and L. Malter, *Proc. I.R.E.*, **24**, 351, 1936.

[5] *Rev. Sci., Inst.*, **8**, 78, 1937.

the new antimony-caesium type of sensitive surface[6,7] marks a real advance in the performance of such tubes. The appearance of the R.C.A. type 931 multiplier phototube convinced the writer that the possibility of using multipliers for astronomical photometry should be reconsidered. Work on this project, barely begun in 1941, was interrupted by the war. During this period several new types of multiplier phototubes appeared on the market. The most notable of these is the R.C.A. type 1P21, which is intended expressly for the purpose of measuring faint light.

As indicated in the foregoing discussion, the fundamental quantity which determines the effectiveness of a light-sensitive unit for measuring faint sources is the signal-to-noise ratio. Before undertaking the determination of signal-to-noise ratios for multipliers, a standard light-source had to be adopted, and some method had to be devised for measuring the effective (root-mean-square) value of the noise level. Inasmuch as the Lick Observatory has a 12-inch refractor and since this instrument is usually available, a convenient light-standard was provided by a number of stars, whose brightnesses were reduced to the equivalent of the image of a 6.0-mag. star. Because determinations of signal-to-noise ratios need not be done with high precision, no corrections for lens absorption or atmospheric extinction were made. The data given here may, therefore, be taken as representative of the performance of multipliers as used with a typical 12-inch refracting telescope. Laboratory measurements were facilitated by using a tungsten source, maintained at constant intensity by an electronic control. Although the artificial source was calibrated against the primary standard, most data given here depend upon direct observation of the primary standard.

Values for noise level must be expressed in terms of the frequency band-width, or a related quantity such as the time-constant. In the present investigation, band-width is, for convenience, expressed in terms of the time-constant derived from a resistance-capacity product, with a value of 2 seconds adopted as standard. This selection is based on previous experience, for most present-day photometers employ a grid resistance of $R = 10^{11}$ ohms and have an input circuit capacity of about $C = 20 \times 10^{-12}$ farads, which gives an RC of about 2 seconds. Adoption of this standard value makes convenient a direct comparison of data given here with the performance reported for other comparable devices. All measurements were made with 90 volts between the secondary electrodes of the multipliers and with 45 volts on the anode electrode. These voltages were conveniently provided by compact 45-volt hearing-aid batteries. To obtain an appropriate amplification, a load resistor of the proper value was placed in the anode circuit. A multiple-contact switch made possible the selection of any one of ten load resistors, varying in factors of approximately 2 from 0.187 to 100 megohms. The multiplier output was direct-coupled into a low-grid-current power amplifier having an effective transconductance of 3,100 micromhos. The power amplifier drove a 0–1 milliampere Esterline-Angus recording meter, which recorded noise and signal at measurable amplitude for all cells when its own mechanical time-constant of 0.28 seconds was the band-width limiting factor. Noise was evaluated from the records by determining the mean axis of a representative sample, by measuring twenty equally spaced ordinates, and then by determining the root-mean-square ordinate. This value was first reduced to that for a 2-second time-constant by dividing by 2.7, and then to R.M.S. current in the load resistor for comparison with the signal in similar units.

Data for four multiplier phototubes are given in Table 1. The first column contains the name of the multiplier and the second column the dark-current measured at the output. This current is composed partly of base leakage between the anode and the cathode pins and partly of amplified spontaneous emission from cathode and secondary-emission electrodes. The leakage is appreciable because a potential difference of 855 volts exists

[6] Gorlich and Meyer, *Zs. f. Ap.*, **16**, 343, 1938.

[7] P. Gorlich, *J. Opt. Soc. Amer.*, **31**, 504, 1941.

between two closely spaced socket pins. Data quoted in Table 1 are for stock tubes; but the leakage may be cut to a negligible quantity by breaking the anode pin from the base, by unsoldering it from the anode lead-wire, and by insulating this lead from the near-by base structure by means of a sleeve of insulating material. Such precautions are very necessary if the multipliers are to be used at optimum performance in a humid atmosphere. The third column gives the sensitivity in terms of output current on the standard light-source, which is a 6.0-mag. class A0 star at the focus of the 12-inch refractor. The fourth column contains the R.M.S. "dark-noise" at the output, and the fifth column gives the signal-to-dark-noise ratio, which may be compared with those given for photocells in Table 2. The sensitivity of the cathode surface was determined for three of the multipliers by using the cathode and the first dynode element as the two electrodes of a photo-

TABLE 1

PERFORMANCE DATA FOR MULTIPLIER PHOTOTUBES

Type of Multiplier Phototube	Dark-Current (Amp.)	Over-all Sensitivity (Amp.)	Dark-Noise (Amp.)	Signal/Noise	Sensitivity (Amp.)	Amplification per Stage
931	5×10^{-9}	0.66×10^{-9}	2.0×10^{-11}	33	0.9×10^{-14}	3.5
931*A*	6×10^{-9}	0.23×10^{-7}	2.2×10^{-11}	1,050	1.3×10^{-14}	4.9
1P21(*a*)	3×10^{-9}	1.2×10^{-7}	0.6×10^{-11}	20,000	.....	.....
1P21(*b*)	2×10^{-9}	1.6×10^{-7}	1.3×10^{-11}	12,000	3.3×10^{-14}	5.5

TABLE 2

PERFORMANCE DATA FOR PHOTOCELLS

Type of Cell	Vacuum Sens. (Amp.)	Gas-Ampl. Factor	Serv. Sens. (Amp.)	Maximum Signal/Noise
Kunz (*K-H*)	0.13×10^{-14}	85	11.1×10^{-14}	700
D97087(*CsO-Ag*)	$.26\times10^{-14}$	11	2.9×10^{-14}	61
929* (*Sb-Cs*)	3.3×10^{-14}	1	3.3×10^{-14}	200

*Base removed, press cavity filled with ceresin wax. This cell was the better of two selected at random.

cell, with a potential of $10\frac{1}{2}$ volts. This sensitivity, in amperes, is shown in the sixth column. From these data the amplification per multiplier stage, given in the last column, can be computed.

Table 2 gives corresponding data for a quartz potassium hydride photocell, made about 1918 by the late Professor Jakob Kunz, for a Western Electric type D97087 caesium-oxide-on-silver photocell and for an R.C.A. type 929 photocell.[8] The first two cells were investigated because they represent those types which, in the past, have provided nearly all the useful photometric observations, while the 929 was included because it is representative of a photocell with the same type of sensitive surface found in the multipliers. The D97087 must be used at the temperature of dry ice, and it should be borne in mind that this cell operates at a disadvantage on the bluish light of an A0 star.

In Table 2 the first column gives the name of the cell and the second column the vacuum sensitivity; the latter is the output in amperes given by the standard source when the cathode voltage is too low ($22\frac{1}{2}$ volts) to cause appreciable ionization of the inert gas in the photocell. The third column gives the gas amplification for maximum

[8] A. M. Glover and R. B. James, *Electronics*, **13**, No. 8, 26, 1940.

signal-to-noise ratio with the photocell used with a 10^{11}-ohm load resistor, with a capacity of 20×10^{-12} farads, and with a Victoreen type VW-41 electrometer tube. For both gas-filled cells the limit of stable gas amplification is defined as that amplification which causes cell dark-noise to be equal to the thermal noise of the load resistor. The service sensitivities are given in the fourth column, and the maximum signal-to-noise ratio in the fifth column. These service sensitivities compare well with those reported by Stebbins and Whitford,[9] which are 14.6×10^{-14} amp. and 2.16×10^{-14} amp. for a Kunz cell and for a D97087, respectively, when proper allowance is made for the fact that their values are for a 4.0-mag. A0 star and a 60-inch reflecting telescope.

The dark-noise output of a multiplier phototube is a function of the interelectrode voltage, of the temperature, and of the cathode area. When the anode lead of 1P21(*b*) was well insulated from near-by high-voltage conductors, an output dark-current of 1.4×10^{-9} amp. and an R.M.S. noise level of 1.2×10^{-11} amp. were measured. For a total multiplication factor of $(5.5)^9$, the theoretical shot-noise output, for a time-constant of 2 seconds and the observed dark-current, is computed to be 1.65×10^{-11} amp., which is in reasonable agreement with the observed noise 1.3×10^{-11} amp. It is evident, therefore, that the dark-noise level of the 1P21 is set by the shot component of its dark-current and that the signal-to-dark-noise ratios are near the maximum possible.

The noise values in Table 1 are for a temperature of about 5° C, such as exists in the dome on an average winter night at Mount Hamilton. If a multiplier is cooled to the temperature of dry ice (−78° C) and the output is examined by means of a cathode-ray oscilloscope with sufficient time resolution, the dark-current may be observed as a series of sharp pulses, probably the records of initial release of small groups or possibly of individual electrons. These pulses are of all amplitudes, which indicates that dark emission takes place from the secondary surfaces throughout the amplifying labyrinth, as well as from the photosurface. The tallest pulses, presumably caused by electrons from the photosurface, are observed at rates of from 5 to 10 per second, while the total pulse output takes place at the rate of 100–200 per second. Electrons released from stages beyond the second contribute but little to the effective noise current, because of the relatively small average amplification to which they have been subjected.

Our experience has shown that maximum signal-to-noise ratio is developed for multipliers only after they have been "dark-aged" with voltage applied for 1 or more hours, depending upon their previous history. Exposure to strong light or application of too much voltage will put a tube into a temporary state of great noisiness, which may require several hours to subside. Figure 1 shows a typical dark-current versus time record for a 1P21 which had been exposed to room light at no applied voltage; the dark-noise behaves in a fashion similar to the dark-current.

The antimony-caesium photosurfaces have been used successfully for color measurements by V. Nikonov.[10] Figure 2, *a* and *b* gives color-sensitivity data for multiplier 1P21 (*a*). Figure 2, *a* gives the absolute color sensitivity in amperes for a number of stars of various spectral types in the comparison list of Stebbins and Huffer.[11] The magnitudes were taken from the *Henry Draper Catalogue*, and the deflections were reduced to those to be expected from a 6.0-mag. star. It should be noted that the 1P21, when used with a refracting telescope and no color filter, yields magnitudes referred to an effective wavelength slightly to the red of that for the photographic system of the *Henry Draper Catalogue*. Figure 2, *b* shows a comparison with Stebbins and Huffer of a color scale established by the writer with the use of blue and yellow filters with 1P21 (*a*). The blue filter was Corning Glass No. 5850, 5.0 mm thick; and the yellow filter was Corning Glass No. 3385, 1.0 mm thick. The color scale thus established is less open than that of Nikonov, but it

[9] *Ap. J.*, **98**, 21, 1943; *Mt. W. Contr.*, No. 680.

[10] *Bull. Acad. Sci. Georgian S.S.R.*, **5**, Part III, No. 6, 511, 1942.

[11] *Pub. Washburn Obs.*, **15**, Part V, 217, 1934.

is still superior to the best one possible with the potassium hydride photocell. It would be possible to use a denser yellow filter with the 1P21, but the stability of the color scale would then depend to a high degree upon the stability of the extreme red-sensitive end of the 1P21 color-response curve. Owing to the high violet-sensitive peak at 3750 A[12] the 1P21, when used with a reflector, will doubtless yield magnitudes referred to a shorter effective wave length than that for normal photographic magnitudes determined with a reflector.

It is evident that astronomy now has at hand a device for photoelectric photometry which is more convenient to use, and which is from ten to twenty-five times more sensitive than any heretofore employed. Our photometer consists of the multiplier and battery voltage supply, a small and simple D.C. amplifier, and an indicating meter. Sensitivity is controlled by changing the anode load resistor, as described above. With this equipment, we could do satisfactory photometry on stars of the sixteenth magnitude with the 36-inch refractor, with the "seeing" accuracy limit[13] occurring at about the elev-

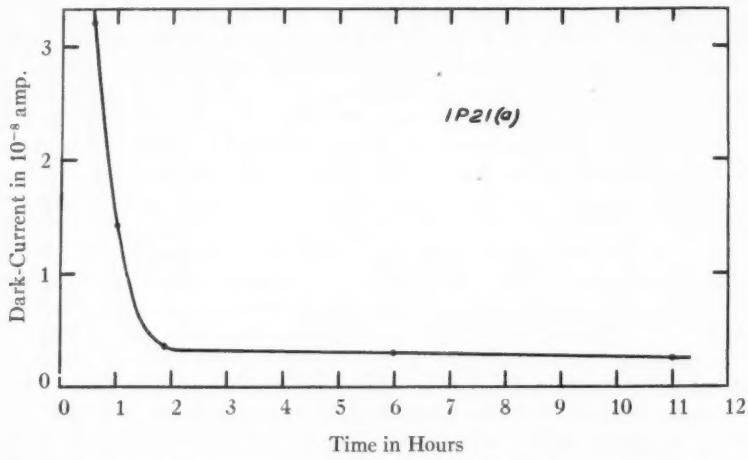

FIG. 1.—Variation of dark current with time after application of voltage, for a 1P21 multiplier phototube.

enth magnitude. With no further refinement of technique, it would be possible to reach the nineteenth magnitude with the 100-inch reflector.

A 1P21 may be operated by using a galvanometer directly connected in series with its anode circuit. We can attain the eleventh magnitude this way with a Leeds and Northrup type R galvanometer used with the 36-inch refractor. While the use of a galvanometer, because of its insufficient sensitivity, does not achieve the best in the multiplier, the simplicity of the arrangement is appealing, and it has many applications. The conveniences offered by the multiplier will not fail to impress workers in the field of photoelectric photometry. There need be no storage batteries and no bulky, heavy equipment on the telescope. In addition, the trouble of maintaining vacuums is avoided, and the annoyance of continual and unpredictable drift of the zero is all but eliminated.

In conclusion, it may be of interest to speculate on the possibility of using an ideal multiplier under ideal conditions. Our multiplier will be constructed with a quartz envelope for best insulation of the anode, and it will have a cathode area only one-fifth that of the 1P21, in order to reduce the dark-current by a factor of 5; there will still be sufficient

[12] *Technical Data for 1P21 Multiplier Phototube* (Radio Corporation of America).

[13] G. E. Kron, *Pub. A.S.P.*, **52**, 250, 1940.

area to receive all the light from a star or faint nebula. The multiplier will have only three or four stages for the sake of simplicity of construction, but it will operate at a multiplication factor of 12 per stage, to reduce the effects of emission from the secondary surfaces. Such a multiplier, when operated at the temperature of dry ice, will have a dark emission from the photosurface of about 1 electron per second; the sensitivity, on the other hand, will be about 4.4×10^5 electrons per second from light of the standard source (6.0-mag. A0 star) collected with a 12-inch reflecting telescope. The quartz envelope of the multiplier will transmit more radiation from the deep-blue and near-ultraviolet region of the spectrum, so that the sensitivity will be increased by a factor of approximately 2 when a reflector is used. A simple calculation shows that a star of 21.4 mag. at the focus of the 100-inch telescope would give a current of 20 electrons per second from the primary surface of our ideal multiplier. We will now make our observations by counting electrons with one of the new commercially available pulse-counters and will operate the counter so that it will not respond to pulses unless they are of such amplitude that they originate

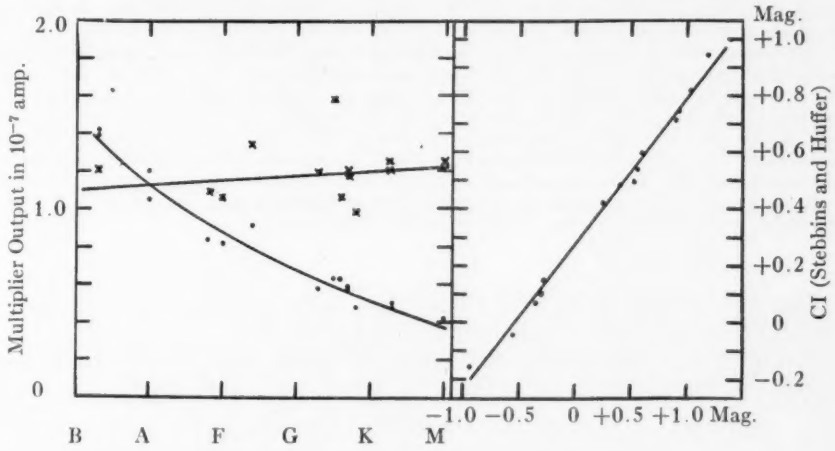

a) Spectral Class *b*) CI (Kron)

FIG. 2. —*a*) Absolute sensitivity of 1P21 (*a*) to stars of different colors reduced to a common brightness of 6.0 mag. The crosses are for the photographic system, the dots for the visual system of the *Draper Catalogue*. *b*) A two-filter color scale compared with that of Stebbins and Huffer.

from the photosurface. The lesser-amplified dark-current electrons emitted from the secondary surfaces will thus not be counted at all, and they need not be considered further. Inasmuch as the electrons are emitted in a random fashion, we shall have to count 1000 of them to make an observation having an accuracy of ± 3 per cent, and this will require 50 seconds. The dark-current emission, if constant, needs to be checked only at rare intervals, so that in practice we may neglect the time required for its determination.

In a recent publication, W. Baade reports[14] photography of stars of 21.0 photographic magnitude with exposure times of 90 minutes. We may conclude, therefore, that the photoelectric method, when used under the ideal conditions stated above, can equal at least, and possibly may exceed, the photographic emulsion in sensitivity.

This investigation was supported principally by a grant from the Henry Draper Fund of the National Academy of Sciences. I am indebted to Mr. Harold Johnson for helpful suggestions and stimulating discussion during the course of this work and for assistance with the observations.

[14] *Ap. J.*, **100**, 141, 1944; *Mt. W. Contr.*, No. 696.

NEAR THERMODYNAMIC RADIATIVE EQUILIBRIUM

L. G. HENYEY
Yerkes Observatory
Received February 7, 1946

ABSTRACT

Deviations from the excitation and ionization conditions existing in thermodynamic equilibrium, together with the resulting deviations from Kirchhoff's law, are considered. Complete radiative equilibrium is assumed; hence the deviations mentioned arise from the nonblack-body nature of the radiation field. The problem is approached from the point of view of first-order perturbations to the conditions of strict thermodynamic equilibrium.

The solution of the equations for a steady state is discussed, allowance being made for the finite breadths of the discrete energy states. It is shown that, under the assumption of near thermodynamic equilibrium, the problem reduces to the solution of a set of linear algebraic equations, one for each energy state, the unknowns being the average deviations of the populations of states as a whole from their values in strict equilibrium. The deviations over the breadth of a state follow from the solution in a relatively simple way. The general level of ionization is taken care of in the same way as are the discrete states. However, the details of the ionization are handled by supposing that the free electrons are distributed according to a Maxwell formula with an appropriate electron temperature. This temperature is fixed by the condition that there can exist no net exchange of energy between matter and radiation. The resulting expressions for the various radiative parameters involve a part which is the equilibrium value of the parameter and a new part. This latter is made up of a linear combination of the deviations, in intensity, from black-body values over the entire spectrum and of a term arising from the difference between the electron temperature and the reference, or approximate, temperature.

I

Investigations of the transfer of radiation have made extensive use of the two concepts of local thermodynamic equilibrium and of scattering.

The first of these involves, in the first place, the notion of a temperature, T, defined at each point in the medium, and, in the second place, the use of Kirchhoff's law:

$$j_\nu = \alpha_\nu B_\nu(T)\,. \tag{1}$$

This expression relates the emission coefficient, j_ν, and the absorption coefficient, α_ν, to the Planck function, $B_\nu(T)$, at the appropriate frequencies, ν, in the spectrum. The usual procedure, furthermore, is to compute α_ν on the assumption of strict thermodynamic equilibrium at the local temperature. Expression (1) has been used in treatments of the continuous spectrum.

The notion of scattering, on the other hand, involves the use of the relationship

$$j_\nu = \alpha_\nu J_\nu \equiv \alpha_\nu \int I_\nu \frac{d\omega}{4\pi}. \tag{2}$$

Here the ratio of the emission and the absorption coefficients is determined by the mean value, J_ν, of the specific intensity, I_ν, taken over all directions.

The theory of the formation of absorption lines uses a combination of the two concepts in the form

$$j_\nu = \alpha_\nu[\,\lambda_\nu B_\nu + (1-\lambda_\nu)J_\nu\,]\,. \tag{3}$$

The presence of the term $\lambda_\nu B_\nu$ is considered as arising partly from the action of the continuous absorption coefficient and, in the case of lines originating from a ground level, partly from the depopulation of the upper level, involved in the line, by processes distinct from the radiative transitions in the line itself. B. Strömgren[1] has discussed the important case in which the process is dominantly controlled by fluorescence involving free electrons.

[1] *Zs. f. Ap.*, **10**, 237, 1935.

While equation (3) appears suitable for the treatment of resonance lines or lines originating from a ground level, it quite certainly is inadequate for subordinate lines in general. Its validity depends primarily on the extent to which the radiation in the line itself controls the population of the upper level. In the case of subordinate lines, this criterion is generally not met; in fact, the populations may be governed by other lines, and scattering from one line to another should be allowed for. Such interlocking or cyclical effects were first considered by S. Rosseland,[2] who considered the problem from the point of view of the static equilibrium of the populations of the energy levels of an atom under the influence of radiation, through the balancing of all transitions to and from a level. One may hope that ultimately a general treatment of radiative processes based on this picture may be developed in order to obtain a rigorous description of the formation of subordinate lines and to go beyond the assumptions involved in the use of the concept of local thermodynamic equilibrium.

At present, the mathematical complexities involved in a rigorous treatment of radiative processes based on the microscopic conditions for a steady state appear somewhat formidable, although the physical principles are entirely straightforward. It would appear that an approximate discussion may prove, at this time, to give a useful approach to the problem of subordinate lines and to the justification or improvement of the method of local thermodynamic equilibrium. This paper is concerned with a discussion in which it is assumed that the excitation in a gas is nearly that obtaining in strict thermodynamic equilibrium with allowance, in a first-order manner, for departures from it. For the present we content ourselves with a discussion, on this basis, of the case of pure radiative transfer and, in part, to the case of negligibly weak contributions by collisions.

II

This section is concerned with certain general remarks about the form in which the first-order deviations from thermal equilibrium appear in the equation of transfer under the conditions of pure radiative transfer of energy through a medium. The discussion leads to the introduction of certain parameters, which are again encountered in the next section, from a consideration of the microscopic conditions of a steady state for radiative equilibrium. For the purposes of this section we suppose that the exciting radiation deviates from strict equilibrium values by quantities of the first order. Actually, as we see in the next section, it is sufficient in the derivation of the formalism to assume that it is the excitation of the gas which deviates from that encountered in strict equilibrium, i.e., that given by Boltzmann's distribution and the Saha formula, by first-order effects. From a strict mathematical point of view the two assumptions are equivalent; yet from a practical point of view it is conceivable that fairly large deviations, of a random or irregular character, of the radiation from black-body values may entail but small deviations of the excitation from equilibrium values, provided that the reference temperature is properly chosen. Here the term "reference temperature" refers to the parameter describing the approximate excitation.

If the transfer of energy is purely radiative, the excitation must be determined by the local values in the radiation field. While it may be that the direct agencies which operate in the excitation of the atoms include collisions of the first and second kinds, yet ultimately their influence must be expressible, in principle, in terms of the radiative intensities. This being so, we may express the facts mathematically thus:

$$j_\nu = a_\nu \mathfrak{J}_\nu (J_{\nu'}) . \tag{4}$$

This expression simply states that j_ν/a_ν, at each frequency ν, is some function of the intensities, $J_{\nu'}$, over the entire spectrum. The function $\mathfrak{J}_\nu$ must depend on the density and chemical composition of the gas and on the kinds of excitation processes operating.

[2] *Ap. J.*, **63**, 218, 1926.

Here we assume that j_ν is independent of direction and that $\mathfrak{J}_\nu$ involves only the mean values, $J_{\nu'}$, of the specific intensities taken over all directions. These assumptions are not valid in Doppler cores in the presence of Doppler broadening,[3] where a separate treatment would be necessary.

From the known properties of matter and radiation in thermodynamic equilibrium, the function $\mathfrak{J}_\nu$ must have the important property that

$$\mathfrak{J}_\nu(B_{\nu'}) = B_\nu . \tag{5}$$

In the presence of small deviations from strict equilibrium we must include correction terms in $J_{\nu'} - B_{\nu'}$ for each ν'. For this purpose we may write, for the first-order terms,

$$\mathfrak{J}_\nu(J_{\nu'}) = B_\nu + \int_0^\infty \left\{\frac{\partial \mathfrak{J}_\nu}{\partial (J_{\nu'} d\nu')}\right\}^{(0)} (J_{\nu'} - B_{\nu'})\, d\nu' . \tag{6}$$

Here the zero superscript indicates that the derivative is evaluated for $J_{\nu'} = B_{\nu'}$, that is, for thermodynamic equilibrium. We may then write

$$j_\nu = a_\nu B_\nu + \int_0^\infty \omega_{\nu,\nu'} (J_{\nu'} - B_{\nu'})\, d\nu' . \tag{7}$$

Here

$$\omega_{\nu,\nu'} = a_\nu^{(0)} \left\{\frac{\partial \mathfrak{J}_\nu}{\partial (J_{\nu'} d\nu')}\right\}^{(0)} . \tag{8}$$

In this formula we carry only the equilibrium value of the absorption coefficient, $a_\nu^{(0)}$, since its rigorous value would add some superfluous higher-order terms. We do, however, carry the absorption coefficient in the first term on the right-hand side of equation (7) beyond the accuracy given by $a_\nu^{(0)}$.

The equation of transfer in its most general form is as follows:

$$\frac{dI_\nu}{\rho ds} = -a_\nu I_\nu + j_\nu . \tag{9}$$

Substituting our value for the emission coefficient as given by equation (7) in the equation of transfer, we have

$$\frac{dI_\nu}{\rho ds} = -a_\nu (I_\nu - B_\nu) + \int_0^\infty \omega_{\nu,\nu'} (J_{\nu'} - B_{\nu'})\, d\nu' . \tag{10}$$

This expression represents the formal way in which the concept of near thermodynamic radiative equilibrium enters the equation of transfer.

In spite of the generality of this discussion so far, we may deduce two identities involving $\omega_{\nu,\nu'}$ and representing two important properties of our approximations.

In the first place, consider a black-body radiation field characterized by a temperature $T + dT$, differing slightly from our standard, or reference, temperature. It is obviously possible to describe the excitation and, consequently, j_ν/a_ν at this new temperature as a special case of the preceding representation. Hence, in equation (6) we may substitute the following:

$$\left.\begin{aligned} J_{\nu'} &= B_{\nu'} + \frac{\partial B_{\nu'}}{\partial T}\, dT , \\ \mathfrak{J}_\nu &= B_\nu + \frac{\partial B_\nu}{\partial T}\, dT . \end{aligned}\right\} \tag{11}$$

[3] L. G. Henyey, *Proc. Nat. Acad.*, **26**, 50, 1940.

With a little manipulation, the resulting expression assumes the following form:

$$a_\nu^{(0)} \frac{\partial B_\nu}{\partial T} = \int_0^\infty \omega_{\nu,\nu'} \frac{\partial B_{\nu'}}{\partial T} \, d\nu' . \tag{12}$$

This is our first identity.

The second identity is concerned with the original hypothesis of pure radiative transfer of energy. The net rate of exchange of energy between matter and radiation of frequency ν is obtained by integrating the equation of transfer over all solid angles. Using equation (10), we find this process leading to the following:[4]

$$\frac{1}{4\pi\rho}\left(\frac{\partial F_{\nu,x}}{\partial x}+\frac{\partial F_{\nu,y}}{\partial y}+\frac{\partial F_{\nu,z}}{\partial z}\right) = -a_\nu (J_\nu - B_\nu) + \int_0^\infty \omega_{\nu,\nu'} (J_{\nu'} - B_{\nu'}) \, d\nu' . \tag{13}$$

The net rate of exchange of energy between matter and radiation at all frequencies is obtained by integrating over all frequencies. After this is done, the right-hand side of equation (13) becomes

$$-\int_0^\infty a_\nu (J_\nu - B_\nu) \, d\nu + \int_0^\infty d\nu \int_0^\infty \omega_{\nu,\nu'} (J_{\nu'} - B_{\nu'}) \, d\nu' . \tag{14}$$

Apropos of our assumption of radiative transfer, this expression must vanish; and, if for a_ν we put $a_\nu^{(0)}$, it must vanish identically. This is apparent from the following considerations. Let J_ν differ from B_ν by an infinitesimal amount, but let the difference be arbitrary in so far as dependence on ν is concerned. Then the term $a_\nu (J_\nu - B_\nu)$ is substantially $a_\nu^{(0)} (J_\nu - B_\nu)$. Since $\omega_{\nu,\nu'}$ is evaluated under the assumption of radiative transfer, equation (14) must vanish, whatever $J_\nu - B_\nu$ may be. Because $a_\nu^{(0)}$ and $\omega_{\nu,\nu'}$ are independent of $J_\nu - B_\nu$, it then follows that the coefficient of $J_\nu - B_\nu$ must vanish. Hence

$$a_\nu^{(0)} = \int_0^\infty \omega_{\nu',\nu} d\nu' . \tag{15}$$

This is the second identity. It should be noted that the integrations in the two identities are over different subscripts.

In this discussion we have been carrying the absorption coefficient correct to within second-order terms. In this approximation we have

$$a_\nu = a_\nu^{(0)} + a_\nu^{(1)} , \tag{16}$$

where the second term is clearly of the form

$$a_\nu^{(1)} = \int_0^\infty \beta_{\nu,\nu'} (J_{\nu'} - B_{\nu'}) \, d\nu' . \tag{17}$$

Such a procedure is desirable if the conjecture already mentioned is correct, namely, that fairly large values of $J_\nu - B_\nu$ may produce only small deviations of excitation from thermodynamic equilibrium. In that case, from the vanishing of equation (14) we have

$$\int_0^\infty a_\nu^{(1)} (J_\nu - B_\nu) \, d\nu = 0 . \tag{18}$$

In effect, this condition serves to determine the reference temperature.

In the event that the conjecture is not valid, equation (18) is a condition only on a portion of the terms of the second order in $J_\nu - B_\nu$, since such terms have been dropped in j_ν/a_ν. While equation (18) may still be a good way of determining the temperature, it should be pointed out that the condition of radiative transfer must be satisfied identically in the second order when all terms of this order are included. We can then obtain an identity, similar to equation (15), involving the second-order coefficients. However,

[4] Cf. E. A. Milne, *Handb. d. Ap.*, 3, Part I, 100, Berlin: Springer, 1929.

if large values of $J_\nu - B_\nu$ lead to large values of the deviations in excitation from equilibrium conditions, neither of the methods of local or of near thermodynamic equilibrium is applicable.

The determination of the temperature by equation (18) may, in certain problems (particularly when $a_\nu^{(1)}$ is negligible compared to $a_\nu^{(0)}$), be undesirable. Rather, it may prove more advantageous in actual computations to allow a small error in equation (14), in order to represent certain other features more closely.

III

We turn now to a consideration of the problem from the point of view of the microscopic conditions for a steady state. At this stage we suppose that the excitation is purely radiative, thereby neglecting the influence of collisions of the first and second kinds. We also disregard the influence of the Doppler effect in the broadening of spectral lines.

The computation of the excitation of a gas, in a steady state, is based on the consideration that, in 1 second and in 1 gm of gas, the number of transitions from any given state to the totality of other states is equal to the number of transitions into that state from all the others. The transition rates being proportional to the populations of the states from which the transitions originate, it is then possible, in principle, to compute the populations to within a constant factor of proportionality.

In speaking of states and of populations of states, the following points must be considered: In order to obtain a correct picture of the processes of emission and absorption it is necessary to consider each so-called "discrete" state as being, in fact, a narrow continuum of states. We have, then, to concentrate our attention not only on the total population of the state but on the population of each element of the state, applying to each of these the conditions for a steady state.

In addition to the discrete states, we must allow for the continuum of states involving one or more free electrons. These states will participate in transitions to and from discrete states, as well as other free states. The condition of a steady state cannot be applied to each element of the continuum, that is, to each velocity of the free electrons, without considering the influence of collisions in modifying the velocity distribution of the electrons. In so far as the radiative processes go, the condition of a steady state can only determine, first, the total number of ions and electrons (and only in terms of a velocity distribution to be determined otherwise) and, second, the total rate of exchange of energy between matter and radiation. In the present investigation we avoid the general problem of the velocity distribution by supposing it to be Maxwellian with a parametric temperature $T^{(e)}$. This electron temperature serves to determine the rate at which energy is exchanged between the electrons and the radiation field, or, conversely, it is determined by this rate of exchange. We need to account only for the total energy, without any reference to its spectral distribution, since we wish to determine the single parameter $T^{(e)}$.

In the following discussion we express the energies of states in frequency units, using the symbol ϵ. Thus the true energy of a state described by ϵ is $h\epsilon$.

In discussing radiative processes involving broadened discrete levels, the following factors must be considered:[5]

a) To each element of state $(\epsilon, \epsilon + d\epsilon)$, in a state k, must be assigned a statistical weight, given by

$$g_k \psi_k(\epsilon)\, d\epsilon \equiv \frac{g_k \gamma_k d\epsilon}{\pi} \frac{1}{(\epsilon - \epsilon_k)^2 + \gamma_k^2}. \tag{19}$$

Here g_k is the total statistical weight of the state, ϵ_k its normal position, and γ_k its half-width. The definition of $\psi_k(\epsilon)$ is such that

$$\int_{-\infty}^{\infty} \psi_k(\epsilon)\, d\epsilon = 1\,. \tag{20}$$

[5] We follow the picture developed, most completely, by Weisskopf and Wigner, *Zs. f. Phys.*, **63**, 54, 1930.

b) The rate at which radiative transitions take place is governed by the Einstein transition probabilities.

c) Any transition probability, describing a transition from a discrete state, depends only on the state as a whole and not on the part of the state from which the transition originates.

d) Any transition probability, describing a transition into a discrete state, is proportional to the statistical weight of the element of state into which the transition passes.

Let $N_k(\epsilon)d\epsilon$ be the number of atoms per gram of gas in the element of state $(\epsilon, \epsilon + d\epsilon)$, of the discrete state k. In thermodynamic equilibrium $N_k(\epsilon)$ has the value $N_k^{(0)}(\epsilon)$, where

$$N_k^{(0)}(\epsilon) \sim g_k \psi_k(\epsilon)\, e^{-h\epsilon/kT}\,. \tag{21}$$

Over the narrow breadth of the state we may neglect the variation of the exponential factor. Hence, if $N_k^{(0)}$ is the total number of atoms in k, we have

$$N_k^{(0)}(\epsilon) = N_k^{(0)} \psi_k(\epsilon)\,. \tag{22}$$

It is convenient for our purposes to represent $N_k(\epsilon)$ in terms of a deviation from thermodynamic equilibrium by the formula

$$\frac{N_k(\epsilon)}{N_k^{(0)}(\epsilon)} = 1 + \xi_k(\epsilon)\,. \tag{23}$$

It is also convenient to describe the population of the state as a whole in the same way, i.e.,

$$\frac{N_k}{N_k^{(0)}} = \frac{1}{N_k^{(0)}} \int_{-\infty}^{\infty} N_k(\epsilon)\, d\epsilon = 1 + \xi_k\,. \tag{24}$$

We may readily verify the fact that

$$\xi_k = \int_{-\infty}^{\infty} \xi_k(\epsilon)\, \psi_k(\epsilon)\, d\epsilon\,. \tag{25}$$

The degree of ionization of an atom usually enters our formulas through the product $N_i N_e$, where N_i is the number of ions, of the kind considered, per gram of gas, while N_e is the number of electrons per gram. We use, for the ionized states, a formula similar to equation (24), that is,

$$\frac{N_i N_e}{N_i^{(0)} N_e^{(0)}} = 1 + \xi_\infty\,. \tag{26}$$

Here the zero superscripts refer, as usual, to the evaluation of the symbols in thermodynamic equilibrium.

Since the values of the various N's depend in varying degrees on the density, as well as on the temperature, it is clear that, to have small ξ's in near thermodynamic equilibrium, we should compute each $N^{(0)}$ at the given density.

As has been stated, the condition for a steady state involves only ratios of the various N's. This implies, to the first order, the occurrence only of the differences of the ξ's in the formulas. It is convenient to remove the mathematical indeterminacy by the use of the following substitutions:

$$\left.\begin{aligned} \xi_k(\epsilon) &= \xi_\infty + \zeta_k(\epsilon)\,, \\ \xi_k &= \xi_\infty + \zeta_k\,. \end{aligned}\right\} \tag{27}$$

It may be verified that relation (25) is also valid for the ζ's.

The deviation of J_ν from the black-body intensity, B_ν, we express as follows:

$$J_\nu = B_\nu(1 + \eta_\nu)\,. \tag{28}$$

We now consider transitions between two discrete states. Let $(\epsilon', \epsilon' + d\epsilon')$ be the element of the lower state, k, and $(\epsilon'', \epsilon'' + d\epsilon'')$ the element of the upper state, l, involved in the transition. The number of transitions, per second and per gram, from the lower to the upper state we denote by $N_{kl}(\epsilon', \epsilon'')d\epsilon' d\epsilon''$, and from the upper to the lower by $N_{lk}(\epsilon'', \epsilon')d\epsilon' d\epsilon''$. The rate at which the upward transitions progress is proportional to

$$N_k(\epsilon')J_{\epsilon''-\epsilon'},$$

and the downward rate to

$$N_l(\epsilon'')\left(1+\frac{J_{\epsilon''-\epsilon'}}{\sigma_{\epsilon''-\epsilon'}}\right).$$

Here σ_ν is $2h\nu^3/c^2$. The second term in the latter expression includes the effect of stimulated emission. Each of these expressions must be multiplied by appropriate transition probabilities, which are independent of the physical state of the gas and the radiation field. We intend to express these rates in terms of their values in thermodynamic equilibrium. We then have

$$N_{kl}(\epsilon', \epsilon'') = N_{kl}^{(0)}(\epsilon', \epsilon'')\frac{N_k(\epsilon')}{N_k^{(0)}(\epsilon')}\frac{J_{\epsilon''-\epsilon'}}{B_{\epsilon''-\epsilon'}}.$$

For the equilibrium rate we may write

$$N_{kl}^{(0)}(\epsilon', \epsilon'') = N_{kl}^{(0)}\psi_k(\epsilon')\psi_l(\epsilon''). \tag{29}$$

where $N_{kl}^{(0)}$ is the equilibrium rate of transitions from the whole of k to the whole of l. Using equations (23), (28), and (29), we have

$$N_{kl}(\epsilon', \epsilon'') = N_{kl}^{(0)}\psi_k(\epsilon')\psi_l(\epsilon'')[1+\xi_k(\epsilon')][1+\eta_{\epsilon''-\epsilon'}]. \tag{30}$$

For the downward transitions we proceed in a similar fashion. The equilibrium rate is exactly the same as before, owing to the presence of detailed balancing in equilibrium. We then have

$$N_{lk}(\epsilon'', \epsilon') = N_{kl}^{(0)}\psi_k(\epsilon')\psi_l(\epsilon'')[1+\xi_l(\epsilon'')]\left[1+\frac{\eta_{\epsilon''-\epsilon'}B_{\epsilon''-\epsilon'}}{\sigma_{\epsilon''-\epsilon'}+B_{\epsilon''-\epsilon'}}\right]. \tag{31}$$

Consider, next, the transitions between a discrete state and a continuous state. Let $N_{k\infty}(\epsilon', \epsilon'')d\epsilon' d\epsilon''$ be the number of transitions, per second and per gram, from $(\epsilon', \epsilon' + d\epsilon'$ in state k to $(\epsilon'', \epsilon'' + d\epsilon'')$ in the continuum. In thermodynamic equilibrium we may write

$$N_{k\infty}^{(0)}(\epsilon', \epsilon'') = N_{k\infty}^{(0)}(\epsilon'')\psi_k(\epsilon'), \tag{32}$$

which is analogous to equation (29), $N_{k\infty}^{(0)}(\epsilon'')$ being the rate of transition from the whole of k to ϵ''. The transitions progress, in general, with a rate proportional to

$$N_k(\epsilon')J_{\epsilon''-\epsilon'}.$$

Hence

$$N_{k\infty}(\epsilon', \epsilon'') = N_{k\infty}^{(0)}(\epsilon'')\psi_k(\epsilon')[1+\xi_k(\epsilon')][1+\eta_{\epsilon''-\epsilon'}]. \tag{33}$$

For the downward transitions we make use of the assumption of the existence of an electron temperature $T^{(e)}$. The distribution of the free electrons over the parameter ϵ is given by the expression:

$$f^{(e)}(\epsilon) = 2\left(\frac{h^3}{\pi k^3 T^3}\epsilon\right)^{\frac{1}{2}} e^{-h\epsilon/kT}. \tag{34}$$

The constants, in this expression, are such as to give the value unity to the integral of $f^{(e)}$ from 0 to ∞. Let $N_{\infty k}(\epsilon'', \epsilon')d\epsilon' d\epsilon''$ be the number of transitions, per second and per

gram, from $(\epsilon'', \epsilon'' + d\epsilon'')$ in the continuum to $(\epsilon', \epsilon' + d\epsilon')$ in state k. In thermodynamic equilibrium this transition rate is equal to the rate of upward transitions, and it may be expressed as in the right-hand side of equation (32). The downward rate is, in general, proportional to

$$N_i N_e f^{(e)}(\epsilon'')\left(1+\frac{J_{\epsilon''-\epsilon'}}{B_{\epsilon''-\epsilon'}}\right).$$

Expressing it in terms of its value in thermodynamic equilibrium, we have

$$N_{\infty k}(\epsilon'', \epsilon') = N_{k\infty}^{(0)}(\epsilon'')\psi_k(\epsilon')\frac{N_i N_e}{N_i^{(0)} N_e^{(0)}}\frac{f^{(e)}(\epsilon'')}{f^{(0)}(\epsilon'')}\frac{\sigma_{\epsilon''-\epsilon'}+J_{\epsilon''-\epsilon'}}{\sigma_{\epsilon''-\epsilon'}+B_{\epsilon''-\epsilon'}}.$$

Here $f^{(0)}(\epsilon'')$ is the distribution function, given in equation (34), evaluated for temperature T. Let us introduce the notation

$$\frac{N_i N_e}{N_i^{(0)} N_e^{(0)}}\frac{f^{(e)}(\epsilon)}{f^{(0)}(\epsilon)} = 1 + \xi_\infty(\epsilon)\,. \tag{35}$$

It is readily seen that

$$\int_0^\infty f^{(0)}(\epsilon)\,\xi_\infty(\epsilon)\,d\epsilon = \xi_\infty\,, \tag{36}$$

where ξ_∞ is given by equation (26). Using equations (36) and (28), we have

$$N_{\infty k}(\epsilon'', \epsilon') = N_{k\infty}^{(0)}(\epsilon'')\psi_k(\epsilon')\left[1+\xi_\infty(\epsilon'')\right]\left[1+\frac{\eta_{\epsilon''-\epsilon'}B_{\epsilon''-\epsilon'}}{\sigma_{\epsilon''-\epsilon'}+B_{\epsilon''-\epsilon'}}\right]. \tag{37}$$

We find it convenient to introduce $\zeta_\infty(\epsilon)$, in analogy with equation (27), by the definition

$$\xi_\infty(\epsilon) = \xi_\infty + \zeta_\infty(\epsilon)\,. \tag{38}$$

From equation (35) we have

$$\zeta_\infty(\epsilon) = \frac{N_i N_e}{N_i^{(0)} N_e^{(0)}}\frac{f^{(e)}(\epsilon) - f^{(0)}(\epsilon)}{f^{(0)}(\epsilon)}.$$

For sufficiently small deviations from equilibrium we may readily verify

$$\zeta_\infty(\epsilon) \simeq \frac{T^{(e)} - T}{T}\left(\frac{h\epsilon}{kT} - \frac{3}{2}\right). \tag{39}$$

This shows that $\zeta_\infty(\epsilon)$ is dominantly given by the difference between the electron temperature and the reference temperature.

We are now in a position to apply the condition for a steady state to the determination of the ξ's. In order that an element of state $(\epsilon', \epsilon' + d\epsilon')$ in state k may have an unvarying population, it is necessary that the following condition be satisfied:

$$\left.\begin{aligned}\sum_l \int_{-\infty}^{\infty} N_{kl}(\epsilon', \epsilon'')\,d\epsilon'' + \int_0^\infty N_{k\infty}(\epsilon', \epsilon'')\,d\epsilon'' = \sum_l \int_{-\infty}^{\infty} N_{lk}(\epsilon'', \epsilon')\,d\epsilon' \\ + \int_0^\infty N_{\infty k}(\epsilon'', \epsilon')\,d\epsilon''.\end{aligned}\right\} \tag{40}$$

The summations are carried over all possible states, while the integrations are carried over the whole of each of the discrete states (taken from $-\infty$ to $+\infty$ for simplicity) and over the continuum, regarded as starting at 0 and extending upward to ∞. The character

of the terms in the sums are different according to whether l is less, or greater, than k. We may combine the terms in the sums which have similar subscripts, and we have the following combinations, evaluated by means of equations (30), (31), (33), and (37), where for brevity we have put $\nu = |\epsilon'' - \epsilon'|$:

$$\left.\begin{aligned}
N_{kl}(\epsilon', \epsilon'') - N_{lk}(\epsilon'', \epsilon') &= N_{kl}^{(0)}\psi_k(\epsilon')\psi_l(\epsilon'')\left\{\xi_k(\epsilon') - \xi_l(\epsilon'')\right. \\
&\qquad \left. - \eta_\nu\left[\frac{\sigma_\nu}{\sigma_\nu + B_\nu} + \xi_l(\epsilon'') - \xi_k(\epsilon')\frac{B_\nu}{\sigma_\nu + B_\nu}\right]\right\}, \qquad (l < k); \\
N_{kl}(\epsilon', \epsilon'') - N_{lk}(\epsilon'', \epsilon') &= N_{kl}^{(0)}\psi_k(\epsilon')\psi_l(\epsilon'')\left\{\xi_k(\epsilon') - \xi_l(\epsilon'')\right. \\
&\qquad \left. + \eta_\nu\left[\frac{\sigma_\nu}{\sigma_\nu + B_\nu} + \xi_k(\epsilon') - \xi_l(\epsilon'')\frac{B_\nu}{\sigma_\nu + B_\nu}\right]\right\}, \qquad (l > k); \\
N_{k\infty}(\epsilon', \epsilon'') - N_{\infty k}(\epsilon'', \epsilon') &= N_{k\infty}^{(0)}(\epsilon'')\psi_k(\epsilon')\left\{\xi_k(\epsilon') - \xi_\infty(\epsilon'')\right. \\
&\qquad \left. + \eta_\nu\left[\frac{\sigma_\nu}{\sigma_\nu + B_\nu} + \xi_k(\epsilon') - \xi_\infty(\epsilon'')\frac{B_\nu}{\sigma_\nu + B_\nu}\right]\right\}.
\end{aligned}\right\} \tag{41}$$

In accordance with the assumption of near thermodynamic equilibrium, we now neglect the second and third terms in each of the expressions in brackets, considering them as being small compared to the first. In order to see more fully the character of the approximation, we may re-write the expression in the bracket in the first equation as follows:

$$(1 - e^{-h\nu/kT}) + \xi_l(\epsilon'') - \xi_k(\epsilon')\, e^{-h\nu/kT}\,. \tag{42}$$

The last term arises from the effect of stimulated emission and, except in the infrared, is small both for that reason and because of the smallness of ξ_k. The first term also becomes small in the infrared, where it may become of the order of the second term. However, the error introduced in this event is inconsequential, since the transition probabilities are also small, relatively, making the contributions of such transitions to the equilibrium correspondingly small.

The expressions in equation (41) may now be substituted in equation (40), in their approximate form, and hence we have, dropping the common factor $\psi_l(\epsilon')$,

$$\left.\begin{aligned}
&\sum_l N_{kl}^{(0)}\{\xi_k(\epsilon') - \xi_l\} + \int_0^\infty N_{k\infty}^{(0)}(\epsilon'')\{\xi_k(\epsilon') - \xi_\infty(\epsilon'')\}\,d\epsilon'' \\
&- \sum_{l(<k)} \int_0^\infty N_{kl}^{(0)}\psi_l(\epsilon' - \nu)\,\eta_\nu \frac{\sigma_\nu}{\sigma_\nu + B_\nu}\,d\nu + \sum_{l(>k)} \int_0^\infty N_{kl}^{(0)}\psi_l(\epsilon' + \nu)\,\eta_\nu \frac{\sigma_\nu}{\sigma_\nu + B_\nu}\,d_\nu \\
&\qquad + \int_{-\epsilon'}^\infty N_{k\infty}^{(0)}(\epsilon' + \nu)\,\eta_\nu \frac{\sigma_\nu}{\sigma_\nu + B_\nu}\,d_\nu = 0\,.
\end{aligned}\right\} \tag{43}$$

The coefficient of $\xi_k(\epsilon')$ in this expression is

$$\sum_l N_{kl}^{(0)} + \int_0^\infty N_{k\infty}^{(0)}(\epsilon'')\,d\epsilon''\,.$$

But this is the total rate at which radiative transitions leave state k, in 1 second and 1 gm, in thermodynamic equilibrium at temperature T. It is proportional to $N_k^{(0)}$, the total equilibrium population of state k. The factor of proportionality is the reciprocal of the

radiative lifetime of state k in equilibrium at temperature T. Denoting this lifetime by $\tau_k^{(0)}$ we have

$$\sum_l N_{kl}^{(0)} + \int_0^\infty N_{k\infty}^{(0)}(\epsilon'')\, d\epsilon'' = \frac{N_k^{(0)}}{\tau_k^{(0)}}. \tag{44}$$

It is convenient to divide equation (43) through by this expression. For this reason we introduce the following definitions:

$$\left.\begin{aligned} N_{kl}^{(0)} &= \frac{N_k^{(0)}}{\tau_k^{(0)}}\, p_{kl}, \\ N_{k\infty}^{(0)}(\epsilon'') &= \frac{N_k^{(0)}}{\tau_k^{(0)}}\, p_{k\infty}(\epsilon''). \end{aligned}\right\} \tag{45}$$

These new symbols, p, have an interesting and important physical meaning. They represent the probability that an atom, anywhere in state k, will, when it makes a transition, choose the state designated by the second subscript or, for the continuum, by ϵ'' as the end-state of the transition. The transitions are regarded as taking place in equilibrium at temperature T. Clearly,

$$\sum_l p_{kl} + \int_0^\infty p_{k\infty}(\epsilon'')\, d\epsilon'' = 1. \tag{46}$$

Further, these symbols satisfy the following relations, which depend on the existence of detailed balancing in equilibrium:

$$\frac{N_k^{(0)}}{\tau_k^{(0)}}\, p_{kl} = \frac{N_l^{(0)}}{\tau_l^{(0)}}\, p_{lk}. \tag{47}$$

Another modification which is desirable is the replacement of each ξ in equation (43) by the corresponding ζ, as given by equations (27) and (38). This serves the purpose of isolating, in the first place, the effect of the electron temperature from the degree of ionization as given by ξ_∞. When this is done, it then appears that only the differences among the set, $\xi_k(\epsilon)$ and ξ_∞, appear in equation (43). The second reason for the substitution of the ζ's is the removal, in a formal way, of the indeterminacy.

For conciseness in the following discussion we define the quantity $\phi_k(\epsilon')$ through the equation:

$$\left.\begin{aligned} \phi_k(\epsilon') = {} & \sum_{l(<k)} p_{kl} \int_0^\infty \psi_l(\epsilon' - \nu)\, \frac{\eta_\nu \sigma_\nu}{\sigma_\nu + B_\nu}\, d\nu - \sum_{l(>k)} p_{kl} \int_0^\infty \psi_l(\epsilon' + \nu)\, \frac{\eta_\nu \sigma_\nu}{\sigma_\nu + B_\nu}\, d\nu \\ & - \int_{-\epsilon'}^\infty p_{k\infty}(\epsilon' + \nu)\, \frac{\eta_\nu \sigma_\nu}{\sigma_\nu + B_\nu}\, d\nu + \int_{-\epsilon'}^\infty p_{k\infty}(\epsilon' + \nu)\, \zeta_\infty(\epsilon' + \nu)\, d\nu. \end{aligned}\right\} \tag{48}$$

We regard the functions $\phi_k(\epsilon')$ as known, for the present, and endeavor to evaluate each ζ in terms of them. We also use the notation

$$\phi_k = \int_{-\infty}^\infty \phi_k(\epsilon')\, \psi_k(\epsilon')\, d\epsilon'. \tag{49}$$

Equation (43) may now be written as follows:

$$\zeta_k(\epsilon') = \sum_l p_{kl} \zeta_l + \phi_k(\epsilon'). \tag{50}$$

This represents the fundamental equation of the problem.

While, ultimately, each ζ should be expressible in terms of $J_\nu - B_\nu$ over the spectrum, the immediate physical interpretation of equation (50) is as follows: The fractional deviation from thermodynamic equilibrium in the population of a bound level, expressed in a relative way by $\zeta_k(\epsilon')$, originates in two ways: (*a*) it depends on the presence of a similar deviation in levels communicating with it by a single transition, and (*b*) it depends on the nonblack-body character of radiation in each such transition. As is appropriate to the first-order approximation we are using, each of these effects is considered as operating as if the other were absent. The effects of type (*a*) are expressed by the first term in equation (50), as well as by the term in $\zeta_\infty(\epsilon' + \nu)$ in $\phi_k(\epsilon')$. A fundamentally important property of these is that their influence on $\zeta_k(\epsilon')$ is independent of ϵ'. Dependence on ϵ' enters only through effects (*b*) and then in a known way.

We proceed with the formal solution of equation (50). Take the average of each member by multiplying by $\psi_k(\epsilon')$ and integrating over the level. Then

$$\zeta_k = \sum_l p_{kl}\zeta_l + \phi_k . \tag{51}$$

The formal solution of these equations may be carried out as follows. Define the quantities q_{jk} by the relations

$$\sum_k q_{jk}p_{kl} = q_{jl} - p_{jl} . \tag{52}$$

The solution of equation (51) then is

$$\zeta_j = \phi_j + \sum_k q_{jk}\phi_k . \tag{53}$$

This may be verified by multiplying equation (51) through by q_{jk}, summing for k, and applying equation (52).

Since the numerical solution depends on the determination of the matrix q_{jk}, its properties are of considerable importance. Denote the set q_{jk} by $\boldsymbol{Q}$, and the set p_{kl} by $\boldsymbol{P}$. Then equation (52) may be written as follows:

$$\boldsymbol{QP} = \boldsymbol{Q} - \boldsymbol{P} . \tag{54}$$

This is equivalent to the equation

$$(\mathbf{1} + \boldsymbol{Q})(\mathbf{1} - \boldsymbol{P}) = \mathbf{1} . \tag{55}$$

In other words, $\mathbf{1} + \boldsymbol{Q}$ and $\mathbf{1} - \boldsymbol{P}$ are reciprocal matrices. Hence

$$(\mathbf{1} - \boldsymbol{P})(\mathbf{1} + \boldsymbol{Q}) = \mathbf{1}$$

or

$$\boldsymbol{PQ} = \boldsymbol{Q} - \boldsymbol{P} . \tag{56}$$

This indicates that $\boldsymbol{P}$ and $\boldsymbol{Q}$ commute.[6]

Equation (55) implies that

$$(\mathbf{1} + \boldsymbol{Q}) = (\mathbf{1} - \boldsymbol{P})^{-1} = \mathbf{1} + \boldsymbol{P} + \boldsymbol{P}^2 + \ldots .$$

or that

$$\boldsymbol{Q} = \boldsymbol{P} + \boldsymbol{P}^2 + \ldots . \tag{57}$$

This series corresponds to the solution of equation (51) by a reiteration process and represents a possible numerical method of evaluating $\boldsymbol{Q}$. It will be noted that the matrix $\boldsymbol{P}$ contains zero diagonal elements, i.e., we regard p_{kk} as being zero. Contrasted with this, we note that $\boldsymbol{Q}$ has nonzero diagonal elements.

[6] For an explanation of the technique and terminology of matrix algebra see some standard textbook on matrices or higher algebra.

The expressions in equation (47) are also valid for the q's:

$$\frac{N_k^{(0)}}{\tau_k^{(0)}}\, q_{kl} = \frac{N_l^{(0)}}{\tau_l^{(0)}}\, q_{lk}. \tag{58}$$

These may be verified as follows: Equation (56) may be written in expanded form thus:

$$\sum_k p_{ik} q_{kj} = q_{ij} - p_{ij}. \tag{59}$$

Multiply by $N_l^{(0)}/\tau_l^{(0)}$ and apply equation (47). Then

$$\sum_k \frac{N_k^{(0)}}{\tau_k^{(0)}}\, q_{kj} p_{kl} = \frac{N_l^{(0)}}{\tau_l^{(0)}}\, q_{lj} - \frac{N_j^{(0)}}{\tau_j^{(0)}}\, p_{jl},$$

or

$$\sum_k \left(\frac{N_k^{(0)}}{\tau_k^{(0)}}\, q_{kl}\, \frac{\tau_j^{(0)}}{N_j^{(0)}}\right) p_{kl} = \left(\frac{N_l^{(0)}}{\tau_l^{(0)}}\, q_{lj}\, \frac{\tau_j^{(0)}}{N_j^{(0)}}\right) - p_{jl}.$$

This expression shows that the quantities

$$\frac{N_k^{(0)}}{\tau_k^{(0)}}\, q_{kl}\, \frac{\tau_j^{(0)}}{N_j^{(0)}}$$

satisfy equation (52), where they replace the set q_{ik}. But they must be equal to the q_{ik} set, since there can be only one solution for the latter. This proves equation (58).

Substitute the value of the ζ's given by equation (51) in the right-hand side of equation (49) and reduce the result, using equation (59). We then obtain the final solution as follows:

$$\zeta_k(\epsilon') \equiv \xi_k(\epsilon') - \xi_\infty = \phi_k(\epsilon') + \sum_l q_{kl}\phi_l. \tag{60}$$

In order to complete the solution we should now compute ξ_∞. To do this we use the fact that the known total concentration, or abundance, of any element is equal to the sum of the partial concentrations in its various discrete states and the concentration of its ions. Further, the total concentration of the electrons is equal to the total concentration of all positive ions of all elements. While these considerations serve to determine ξ_∞, we omit the details, which are not needed in the following discussion.

The next step in our discussion is the computation of the rates of emission and absorption, arising from transitions between discrete states, using equations (60).

Equation (31) gives the rate at which downward transitions, $l \rightarrow k$, progress. The ordinary emission transitions are represented by dropping the J_ν in the last bracket in this expression. The contribution to the emission coefficient by the elements of state indicated is, then,

$$\frac{h\nu}{4\pi}\, N_{kl}^{(0)} \psi_k(\epsilon')\, \psi_l(\epsilon'')\, [1 + \xi_l(\epsilon'')]\, \frac{\sigma_\nu}{\sigma_\nu + B_\nu}.$$

Similarly, the upward transitions are represented by equation (30). To obtain the absorption of energy from a single direction we must replace J_ν by $I_\nu/4\pi$ and multiply by $h\nu$. We then have, for the elements of state indicated, the following:

$$\frac{h\nu}{4\pi}\, N_{kl}^{(0)} \psi_k(\epsilon')\, \psi_l(\epsilon'')\, [1 + \xi_k(\epsilon')]\, \frac{I_\nu}{B_\nu}.$$

The stimulated emission contributions may be isolated from equation (31) in the same way to give

$$\frac{h\nu}{4\pi} N_{kl}^{(0)} \psi_k(\epsilon') \psi_l(\epsilon'') [1 + \xi_l(\epsilon'')] \frac{I_\nu}{\sigma_\nu + B_\nu}.$$

In each of these expressions $\nu = \epsilon'' - \epsilon'$. Counting the stimulated emissions as negative absorptions, we have for the absorption coefficient

$$a_{kl,\nu} = \frac{h\nu N_{kl}^{(0)}}{4\pi B\nu} \int_{-\infty}^{\infty} \psi_k(\epsilon') \psi_l(\epsilon' + \nu) \left[\frac{\sigma_\nu}{\sigma_\nu + B_\nu} + \xi_k(\epsilon') - \xi_l(\epsilon' + \nu) \frac{B_\nu}{\sigma_\nu + B_\nu} \right] d\epsilon'. \quad (61)$$

The emission coefficient is

$$j_{kl,\nu} = \frac{h\nu\sigma_\nu N_{kl}^{(0)}}{4\pi(\sigma_\nu + B_\nu)} \int_{-\infty}^{\infty} \psi_k(\epsilon') \psi_l(\epsilon' + \nu) [1 + \xi_l(\epsilon' + \nu)] d\epsilon'. \quad (62)$$

From these two expressions we may also write the following:

$$j_{kl,\nu} - a_{kl,\nu} B_\nu = \frac{h\nu N_{kl}^{(0)}}{4\pi} \int_{-\infty}^{\infty} \psi_k(\epsilon') \psi_l(\epsilon' + \nu) [\xi_l(\epsilon' + \nu) - \xi_k(\epsilon')] d\epsilon'. \quad (63)$$

We are interested in this last combination for comparison with equation (7). It appears in the equation of transfer, written as in equation (10) with the term in $I_\nu - B_\nu$.

The absorption coefficient consists of a part independent of ξ, which is clearly $a_\nu^{(0)}$, and a part involving the ξ's. This latter we denote by $a_\nu^{(1)}$, as in equation (16). The so-called "natural" shape of the line, which gives the run of the absorption coefficient with frequency for thermodynamic equilibrium, is determined by the well-known integral

$$\psi_{kl}(\nu) = \int_{-\infty}^{\infty} \psi_k(\epsilon') \psi_l(\epsilon' + \nu) d\epsilon' = \frac{\gamma_k + \gamma_l}{\pi} \frac{1}{(\nu - \nu_{kl})^2 + (\gamma_k + \gamma_l)^2}. \quad (64)$$

The variation, with frequency, of $a_\nu^{(1)}$ is more complex. From equation (61) we see that it may be written

$$a_{kl,\nu}^{(1)} = a_{kl,\nu}^{(0)} \xi_\infty + \frac{h\nu N_{kl}^{(0)}}{4\pi} \int_{-\infty}^{\infty} \psi_k(\epsilon') \psi_l(\epsilon' + \nu) \left[\frac{\zeta_k(\epsilon')}{B_\nu} - \frac{\zeta_l(\epsilon' + \nu)}{\sigma_\nu + B_\nu} \right] d\epsilon'. \quad (65)$$

The first term represents an effect which may be considered as one of abundance, since it affects all lines of a given atom in the same ratio and without altering the dependence on frequency.

Equation (63) may be re-written with the appropriate ζ's, ξ_∞ canceling out exactly:

$$j_{kl,\nu} - a_{kl,\nu} = \frac{h\nu N_{kl}^{(0)}}{4\pi} \int_{-\infty}^{\infty} \psi_k(\epsilon') \psi_l(\epsilon' + \nu) [\zeta_l(\epsilon' + \nu) - \zeta_k(\epsilon')] d\epsilon'. \quad (66)$$

In both equations (65) and (66) we need to evaluate the following two expressions:

$$U_{kl,\nu} = \frac{h\nu N_{kl}^{(0)}}{4\pi} \int_{-\infty}^{\infty} \psi_k(\epsilon' - \nu) \psi_l(\epsilon') \zeta_l(\epsilon') d\epsilon', \quad (67)$$

and

$$L_{kl,\nu} = \frac{h\nu N_{kl}^{(0)}}{4\pi} \int_{-\infty}^{\infty} \psi_k(\epsilon') \psi_l(\epsilon' + \nu) \zeta_k(\epsilon') d\epsilon'. \quad (67')$$

In terms of these we have the following:

$$a_{kl,\nu} = a^{(0)}_{kl,\nu}(1+\xi_\infty) + L_{kl,\nu}/B_\nu - U_{kl,\nu}/(\sigma_\nu + B_\nu) \tag{68}$$

and

$$j_{kl,\nu} - a_{kl,\nu}B_\nu = U_{kl,\nu} - L_{kl,\nu}\,. \tag{68'}$$

The evaluation of U and L in terms of the radiative intensities and of the electron temperature may be carried out conveniently by considering the two terms on the right-hand side of equation (60) separately and, further, by breaking up the contributions of each of these according to the origin of the effects. The manner in which we do this should become apparent as we proceed.

Consider, first, those contributions to U and L which depend on the second term in equation (60) and come from a spectral line defined by states m and n, where $m < n$. The contribution to ϕ_ν is, from equation (48),

$$-p_{mn}\int_0^\infty \psi_{mn}(\nu')\,\eta_{\nu'}\,\frac{\sigma_{\nu'}}{\sigma_{\nu'}+B_{\nu'}}\,d\nu'\,,$$

and to ϕ_n,

$$p_{nm}\int_0^\infty \psi_{mn}(\nu')\,\eta_{\nu'}\,\frac{\sigma_{\nu'}}{\sigma_{\nu'}+B_{\nu'}}\,d\nu'\,.$$

Here ψ_{mn} is given by equation (64). Each of these contributes to both U_{kl} and L_{kl}. Using a single prime to denote these, we have, using equation (45),

$$\left.\begin{aligned} U'_{kl,\nu} &= \frac{h\nu N^{(0)}_l}{4\pi\tau^{(0)}_l}\,p_{lk}\psi_{kl}(\nu)\sum_{m,n(>m)}\int_{-\infty}^{\infty}\psi_m(\nu')\,\frac{\eta_{\nu'}\sigma_{\nu'}}{\sigma_{\nu'}+B_{\nu'}}(q_{ln}p_{nm}-q_{lm}p_{mn})\,d\nu'\,,\\ L'_{kl,\nu} &= \frac{h\nu N^{(0)}_k}{4\pi\tau^{(0)}_l}\,p_{kl}\psi_{kl}(\nu)\sum_{m,n(>m)}\int_{-\infty}^{\infty}\psi_{mn}(\nu')\,\frac{\eta_{\nu'}\sigma_{\nu'}}{\sigma_{\nu'}+B_{\nu'}}(q_{kn}p_{nm}-q_{km}p_{mn})\,d\nu'\,. \end{aligned}\right\} \tag{69}$$

We now introduce the equilibrium absorption coefficient in the line (m, n):

$$a^{(0)}_{mn,\nu'} = \frac{h\nu'\sigma_{\nu'}}{4\pi B_{\nu'}(\sigma_{\nu'}+B_{\nu'})}\,\frac{N^{(0)}_m}{\tau^{(0)}_m}\,p_{mn} = \frac{h\nu'\sigma_{\nu'}}{4\pi B_{\nu'}(\sigma_{\nu'}+B_{\nu'})}\,\frac{N^{(0)}_n}{\tau^{(0)}_n}\,p_{nm}\,. \tag{70}$$

Using this, we have, with the aid of equations (58) and (28),

$$\left.\begin{aligned} U'_{kl,\nu} &= \psi_{kl}(\nu)\,p_{lk}\sum_{m,n(>m)}(q_{nl}-q_{ml})\int_{-\infty}^{\infty}\frac{\nu}{\nu'}\,a^{(0)}_{mn,\nu'}(J_{\nu'}-B_{\nu'})\,d\nu'\,,\\ L'_{kl,\nu} &= \psi_{kl}(\nu)\,p_{kl}\sum_{m,n(>m)}(q_{nk}-q_{mk})\int_{-\infty}^{\infty}\frac{\nu}{\nu'}\,a^{(0)}_{mn,\nu'}(J_{\nu'}-B_{\nu'})\,d\nu'\,. \end{aligned}\right\} \tag{71}$$

If these are substituted in the second equation of equations (68) and the result is compared with equation (7), we find that we have determined a contribution to $\omega_{\nu,\nu'}$:

$$\omega'_{kl;\nu,\nu'} = \frac{\nu}{\nu'}\,\psi_{kl}(\nu)\sum_{m,n(>m)}a^{(0)}_{mn,\nu'}[\,p_{lk}(q_{nl}-q_{ml})+p_{kl}(q_{mk}-q_{nk})]\,. \tag{72}$$

In addition to the interactions between spectral lines of the type just discussed, there exist those depending on the first term in equation (60). These involve integrals over the

product of three ψ-functions. The most general integral of this type we may write as follows:

$$W_{klm}(\nu, \nu', \nu'') = \int_{-\infty}^{\infty} \psi_k(\epsilon - \nu)\psi_l(\epsilon - \nu')\psi_m(\epsilon - \nu'')\, d\epsilon. \tag{73}$$

Using this notation and substituting for ζ_l and ζ_k the first two terms of equation (48) in each of the two parts of equation (67), we obtain the remaining contributions from spectral lines as follows:

$$U''_{kl,\nu} = \frac{h\nu N_l^{(0)}}{4\pi\tau_l^{(0)}} p_{lk} \left\{ \sum_{m(<l)} p_{lm} \int_{-\infty}^{\infty} W_{klm}(\nu, 0, \nu')\, \eta_{\nu'} \frac{\sigma_{\nu'}}{\sigma_{\nu'} + B_{\nu'}}\, d\nu' \right.$$
$$\left. - \sum_{m(>l)} p_{lm} \int_{-\infty}^{\infty} W_{klm}(\nu, 0, -\nu')\, \eta_{\nu'} \frac{\sigma_{\nu'}}{\sigma_{\nu'} + B_{\nu'}}\, d\nu' \right\},$$

$$L''_{kl,\nu} = \frac{h\nu N_k^{(0)}}{4\pi\tau_k^{(0)}} p_{kl} \left\{ \sum_{m(<k)} p_{km} \int_{-\infty}^{\infty} W_{klm}(0, -\nu, \nu')\, \eta_{\nu'} \frac{\sigma_{\nu'}}{\sigma_{\nu'} + B_{\nu'}}\, d\nu' \right.$$
$$\left. - \sum_{m(>k)} p_{km} \int_{-\infty}^{\infty} W_{klm}(0, -\nu, -\nu')\, \eta_{\nu'} \frac{\sigma_{\nu'}}{\sigma_{\nu'} + B_{\nu'}}\, d\nu' \right\}.$$

These expressions may be put in a different form by introducing the equilibrium absorption coefficient for ν'. When we do this, we have, with the aid of equation (47),

$$\left.\begin{aligned} U''_{kl,\nu} &= \sum_{m(<l)} p_{lk} \int_{-\infty}^{\infty} \frac{\nu}{\nu'} \frac{W_{klm}(\nu, 0, \nu')}{\psi_{ml}(\nu')}\, a^{(0)}_{ml,\nu'} (J_{\nu'} - B_{\nu'})\, d\nu' \\ &\quad - \sum_{m(>l)} p_{lk} \int_{-\infty}^{\infty} \frac{\nu}{\nu'} \frac{W_{klm}(\nu, 0, -\nu')}{\psi_{lm}(\nu')}\, a^{(0)}_{lm,\nu'} (J_{\nu'} - B_{\nu'})\, d\nu', \\ L''_{kl,\nu} &= \sum_{m(<k)} p_{kl} \int_{-\infty}^{\infty} \frac{\nu}{\nu'} \frac{W_{klm}(0, -\nu, \nu')}{\psi_{mk}(\nu')}\, a^{(0)}_{mk,\nu'} (J_{\nu'} - B_{\nu'})\, d\nu' \\ &\quad - \sum_{m(>k)} p_{kl} \int_{-\infty}^{\infty} \frac{\nu}{\nu'} \frac{W_{klm}(0, -\nu, -\nu')}{\psi_{km}(\nu')}\, a^{(0)}_{km,\nu'} (J_{\nu'} - B_{\nu'})\, d\nu'. \end{aligned}\right\} \tag{74}$$

These new terms may now be substituted in equation (68). The second expression reveals a new contribution to $\omega_{\nu,\nu'}$, which we write as follows:

$$\left.\begin{aligned} \omega''_{kl;\nu,\nu'} = \frac{\nu}{\nu'} \Bigg\{ &\sum_{m(<l)} p_{lk} \frac{W_{klm}(\nu, 0, \nu')}{\psi_{ml}(\nu')}\, a^{(0)}_{ml,\nu'} - \sum_{m(>l)} p_{lk} \frac{W_{klm}(\nu, 0, -\nu')}{\psi_{lm}(\nu')}\, a^{(0)}_{lm,\nu'} \\ &- \sum_{m(<k)} p_{kl} \frac{W_{klm}(0, -\nu, \nu')}{\psi_{mk}(\nu')}\, a^{(0)}_{mk,\nu'} + \sum_{m(>k)} p_{kl} \frac{W_{klm}(0, -\nu, -\nu')}{\psi_{km}(\nu')}\, a^{(0)}_{km,\nu'} \Bigg\}. \end{aligned}\right\} \tag{75}$$

In either equation (74) or equation (75) the summation includes a term representing the influence of the line on itself.

The properties associated with the function W have been discussed by Weisskopf,[7] Spitzer,[8] and Wooley.[9] If anyone of the ratios of W_{klm} to ψ, occurring in equation (75), is denoted by $P(\nu', \nu)$, it may be shown quite readily that in all cases

$$\int_{-\infty}^{\infty} P(\nu', \nu)\, d\nu' = 1.$$

[7] *Observatory*, **56**, 305, 1933. [8] *M.N.*, **96**, 794, 1936. [9] *M.N.*, **98**, 627, 1938.

For an explicit expression giving W, the following identity may be useful:

$$\left.\begin{aligned}\frac{\gamma_1\gamma_2\gamma_3}{\pi^3}\int_{-\infty}^{\infty}&\frac{dt}{[\gamma_1+(t-x)^2][\gamma_2+(t-y)^2][\gamma_3+(t-z)^2]}=\frac{\gamma_1\gamma_2\gamma_3}{\pi^2}\\ \times&\frac{4(\gamma_1+\gamma_2+\gamma_3)}{[(\gamma_1+\gamma_2)^2+(x-y)^2][(\gamma_2+\gamma_3)^2+(y-z)^2][(\gamma_3+\gamma_1)^2+(z-x)^2]}\\ &+\frac{\gamma_1\gamma_2}{\pi^2}\frac{1}{[(\gamma_2+\gamma_3)^2+(y-z)^2][(\gamma_3+\gamma_1)^2+(z-x)^2]}\\ &+\frac{\gamma_2\gamma_3}{\pi^2}\frac{1}{[(\gamma_3+\gamma_1)^2+(z-x)^2][(\gamma_1+\gamma_2)^2+(x-y)^2]}\\ &+\frac{\gamma_3\gamma_1}{\pi^2}\frac{1}{[(\gamma_1+\gamma_2)^2+(x-y)^2][(\gamma_2+\gamma_3)^2+(y-z)^2]}.\end{aligned}\right\}\quad(76)$$

The derivation of this formula is rather lengthy and is omitted. It may be carried out by the method of partial fractions or by reducing the path of integration to a contour in the complex plane consisting of three circles of infinitesimal radii surrounding the three points $x+i\gamma_1$, $y+i\gamma_2$, $z+i\gamma_3$. It is clear that the result of the integration is unchanged (1) if the signs of x, y, and z are all changed and (2) if the same number is added to each of these variables, the integral being a function only of the differences between them. In using the explicit form (76), it should be remembered that the set (ν, ν', ν'') is not the same as the set (x, y, z) in W_{klm} but differs by the set $(\epsilon_k, \epsilon_l, \epsilon_m)$. For instance, in evaluating $W_{klm}(\nu, 0, \nu')$ in the first term of equation (75), we must take $x=\nu+\epsilon_k$, $y=\epsilon_l$, and $z=\nu'+\epsilon_m$.

Consider, next, the terms in equation (67) derived from the continuum, i.e., from the third term in equation (48). Here the distinction as to whether the contribution arises from the first or the second term in equation (60) need not be made, as far as the line shape is concerned. The point is that the variation of the continuous spectrum over a frequency interval as small as the width of a line can be neglected. We may take for these terms ϕ_k in place of $\phi_k(\epsilon')$ in equation (60) or, more conveniently, take the sum

$$\sum_l(\delta_{kl}+q_{kl})\phi_l,$$

where δ_{kl} is 1 or 0, depending on whether k and l are, or are not, equal. In effect, we replace q_{kl} by $\delta_{kl}+q_{kl}$. Clearly, with this modification, the final result must be analogous to equation (71):

$$\left.\begin{aligned}U'''_{kl,\nu}&=-\psi_{kl}(\nu)\,p_{lk}\sum_m(\delta_{ml}+q_{ml})\int_{-\epsilon_m}^{\infty}\frac{\nu}{\nu'}\,a^{(0)}_{m,\nu'}(J_{\nu'}-B_{\nu'})\,d\nu',\\ L'''_{kl,\nu}&=-\psi_{kl}(\nu)\,p_{kl}\sum_m(\delta_{mk}+q_{mk})\int_{-\epsilon_m}^{\infty}\frac{\nu}{\nu'}\,a^{(0)}_{m,\nu'}(J_{\nu'}-B_{\nu'})\,d\nu'.\end{aligned}\right\}\quad(77)$$

Here, $a^{(0)}_{m,\nu'}$ is the absorption coefficient in the mth continuum, computed in equilibrium at temperature T.

We have, finally, to consider the contributions of the last term in equation (48). Comparing this with the preceding term, we see that we can derive the result by replacing, in equation (77), $J_{\nu'}-B_{\nu'}$ by

$$-\frac{B_{\nu'}(\sigma_{\nu'}+B_{\nu'})}{\sigma_{\nu'}}\zeta_\infty(\epsilon_m+\nu').$$

Hence the final parts of U and L are the following:

$$\left.\begin{aligned} U''''_{kl,\nu} &= \psi_{kl}(\nu)\, p_{lk} \sum_m (\delta_{ml} + q_{ml}) \int_{-\epsilon_m}^{\infty} \frac{\nu}{\nu'} a^{(0)}_{m,\nu'} \frac{B_{\nu'}}{1 - e^{-h\nu'/kT}} \zeta_\infty(\epsilon_m + \nu')\, d\nu', \\ L''''_{kl,\nu} &= \psi_{kl}(\nu)\, p_{kl} \sum_m (\delta_{mk} + q_{mk}) \int_{-\epsilon_m}^{\infty} \frac{\nu}{\nu'} a^{(0)}_{m,\nu'} \frac{B_{\nu'}}{1 - e^{-h\nu'/kT}} \zeta_\infty(\epsilon_m + \nu')\, d\nu'. \end{aligned}\right\} \quad (78)$$

Equations (77) determine a third contribution to $\omega_{\nu,\nu'}$, which is as follows:

$$\omega'''_{kl;\nu,\nu'} = \frac{\nu}{\nu'} \psi_{kl}(\nu) \sum_m a_{m,\nu'} [\, p_{kl}(\delta_{mk} + q_{mk}) - p_{lk}(\delta_{ml} + q_{ml})\,]. \quad (79)$$

As far as equations (78) are concerned, we may derive another contribution to $\omega_{\nu,\nu'}$ only if $\zeta_\infty(\epsilon_m + \nu')$ is expressed, to the first order, in terms of $J_\nu - B_\nu$ over the entire spectrum.

We turn, now, to a consideration of the continuous emission and absorption coefficients in near thermodynamic equilibrium and of the determination of the electron temperature. First, we discuss the bound-free transitions.

Here we no longer need consider the structure of the discrete states but may regard them as perfectly sharp. In analogy with equation (61) we may write for the absorption coefficient in the kth continuum the following:

$$a_{k,\nu} = \frac{h\nu N^{(0)}_{k\infty}(\epsilon_k + \nu)}{4\pi B_\nu} \left[\frac{\sigma_\nu}{\sigma_\nu + B_\nu} + \xi_k - \xi_\infty(\epsilon_k + \nu) \frac{B_\nu}{\sigma_\nu + B_\nu} \right]. \quad (80)$$

This may be written thus:

$$a_{k,\nu} = a^{(0)}_{k,\nu} + a^{(1)}_{k,\nu}, \quad (81)$$

where

$$a^{(1)}_{k,\nu} = a^{(0)}_{k,\nu} \xi_\infty + \frac{h\nu N^{(0)}_{k\infty}(\epsilon_k + \nu)}{4\pi B_\nu} \zeta_k - \frac{B_\nu}{\sigma_\nu} a^{(0)}_{k,\nu} \zeta_\infty(\epsilon_k + \nu). \quad (82)$$

Analogous to equation (62) we have, for the kth continuous emission coefficient,

$$j_{k,\nu} = \frac{h\nu\sigma_\nu N^{(0)}_{k\infty}(\epsilon_k + \nu)}{4\pi(\sigma_\nu + B_\nu)} [\, 1 + \xi_\infty(\epsilon_k + \nu)\,]. \quad (83)$$

From these expressions we may also derive the following:

$$j_{k,\nu} - a_{k,\nu} B_\nu = -\frac{h\nu N^{(0)}_{k\infty}(\epsilon_k + \nu)}{4\pi} \zeta_k + \frac{B_\nu}{1 - e^{-h\nu/kT}} a^{(0)}_{k,\nu} \zeta_\infty(\epsilon_k + \nu). \quad (84)$$

The terms involving ζ_k, in equations (82) and (84), are similar to $L_{kl,\nu}$ for the case of bound-bound transitions and may be evaluated in the same way. The final result is

$$\left.\begin{aligned} \frac{h\nu N^{(0)}_{k\infty}(\epsilon_k + \nu)}{4\pi} \zeta_k = p_{k\infty}(\epsilon_k + \nu) \Bigg[& \sum_{m,\, n(>m)} (\delta_{nk} + q_{nk} - \delta_{mk} - q_{mk}) \\ \times \int_0^\infty \frac{\nu}{\nu'} a^{(0)}_{mn,\nu'} (J_{\nu'} - B_{\nu'})\, d\nu' & - \sum_m (\delta_{mk} + q_{mk}) \int_{-\epsilon_m}^{\infty} \frac{\nu}{\nu'} a^{(0)}_{m,\nu'} (J_{\nu'} - B_{\nu'})\, d\nu' \\ & + \sum_m (\delta_{mk} + q_{mk}) \int_{-\epsilon_m}^{\infty} \frac{\nu}{\nu'} a^{(0)}_{m,\nu'} \frac{B_{\nu'}}{1 - e^{-h\nu'/kT}} \zeta_\infty(\epsilon_m + \nu')\, d\nu'. \end{aligned}\right\} \quad (85)$$

From this expression we may again obtain contributions to $\omega_{\nu,\nu'}$, namely

$$\left.\begin{aligned}\omega'_{k;\nu,\nu'} = \frac{\nu}{\nu'} p_{k\infty}(\epsilon_k+\nu)\Bigg[\sum_{m,\,n(>m)} (\delta_{nk}+q_{mk}-\delta_{nk}-q_{nk})\, a^{(0)}_{mn,\nu'} \\ + \sum_m (\delta_{mk}+q_{mk})\, a^{(0)}_{m,\nu'}\Bigg].\end{aligned}\right\} \quad (86)$$

So far, free-free transitions have not entered our discussion, since they have no direct bearing on the populations of the discrete states. Through their contribution to the radiative processes in the continuum, however, they do influence the equilibrium of the free electrons, represented by the electron temperature in the present picture, and, in consequence, have an indirect effect on the discrete states. We now write down the radiative parameters, in our notation, for transitions between states ϵ and $\epsilon+\nu$. This we do without any detailed derivation, the forms of the expressions being apparent from an analogy with previous formulas, say, those for bound-free transitions. Let $N^{(0)}(\epsilon, \epsilon+\nu)$ be the transition rate at temperature T, $a_{\epsilon,\nu}$ the absorption coefficient, and $j_{\epsilon,\nu}$ the emission coefficient. Then

$$a_{\epsilon,\nu} = \frac{h\nu N^{(0)}(\epsilon,\epsilon+\nu)}{4\pi B_\nu}\left[\frac{\sigma_\nu}{\sigma_\nu+B_\nu}+\xi_\infty(\epsilon)-\xi_\infty(\epsilon+\nu)\frac{B_\nu}{\sigma_\nu+B_\nu}\right]. \quad (87)$$

This may be written thus:

$$a_{\epsilon,\nu} = a^{(0)}_{\epsilon,\nu}(1+\xi_\infty)+a^{(0)}_{\epsilon,\nu}\left[\frac{\zeta_\infty(\epsilon)}{1-e^{-h\nu/kT}}-\frac{\zeta_\infty(\epsilon+\nu)}{e^{h\nu/kT}-1}\right]. \quad (88)$$

For the emission coefficient we have

$$j_{\epsilon,\nu} = \frac{h\nu\sigma_\nu N^{(0)}(\epsilon,\epsilon+\nu)}{4\pi(\sigma_\nu+B_\nu)}\left[1+\xi_\infty(\epsilon+\nu)\right]. \quad (89)$$

From equations (87) and (89) we also have

$$j_{\epsilon,\nu}-a_{\epsilon,\nu}B_\nu = \frac{a^{(0)}_\nu B_\nu}{1-e^{-h\nu/kT}}\left[\zeta_\infty(\epsilon+\nu)-\zeta_\infty(\epsilon)\right]. \quad (90)$$

We may now summarize our results as they stand at the present point in the discussion. Owing to the presence of the so far undetermined electron temperature in the various radiative coefficients, the present form of the equation of transfer differs from that given in equation (10). We have, instead, the following:

$$\frac{dI_\nu}{\rho d\,s} = -a_\nu(I_\nu-B_\nu)+\int_0^\infty \omega^*_{\nu,\nu'}(J_{\nu'}-B_{\nu'})\,d\nu'+g_\nu(T^{(e)}). \quad (91)$$

Here a_ν is computed as the total contribution of all chemical constituents of the gas, which individually contribute as follows: In the continuous spectrum a_ν is the sum of all contributions of the form of equation (81), given in detail by the substitution of equation (85) in equation (82), and of all contributions of the form (88), the former being summed over all values of k and the latter integrated over all continuous values of ϵ. In discrete spectral lines we have, in addition, the contribution of equation (68) as given by equations (69), (74), (77), and (78). Likewise, $\omega^*_{\nu,\nu'}$ is made up of a combination of equations (72), (75), (79), and (86), all summed over all constituents of the gas. Finally, $g_\nu(T^{(e)})$ is the sum of those terms in equation (68) given by equation (78), the second term on the right-hand side of equation (84), and the whole of equation (90)—all further summed over all constituents of the gas. This last is a function of $T^{(e)}$.

The form of the condition of radiative equilibrium appropriate to equation (91) is, then,

$$\left.\begin{aligned} -\int_0^\infty a_{\nu'}(J_{\nu'}-B_{\nu'})\,d\nu' + \int_0^\infty d\nu'' \int_0^\infty \omega^*_{\nu'',\nu'}(J_{\nu'}-B_{\nu'})\,d\nu' \\ + \int_0^\infty g_\nu(T^{(e)})\,d\nu = 0\,. \end{aligned}\right\} \tag{92}$$

This one condition on $T^{(e)}$ serves to determine it in principle. Since $T^{(e)}$ enters equation (92) in a complicated way, it may be preferable to consider the approximate but more tractable form obtained by computing g_ν, using the approximate form of $\zeta_\infty(\epsilon)$ as given in equation (39). Putting ΔT for $T^{(e)} - T$, it is clear that

$$g_\nu(T^{(e)}) = \frac{\Delta T}{T} G_\nu\,, \tag{93}$$

where G_ν, as defined by this expression, is independent of $T^{(e)}$. Let

$$G = \int_0^\infty G_\nu d\nu\,. \tag{94}$$

Then equation (92) takes the form

$$\frac{\Delta T}{T} = \frac{1}{G}\int_0^\infty (J_{\nu'}-B_{\nu'})\,d\nu'\left[a_{\nu'} - \int_0^\infty \omega^*_{\nu'',\nu'}d\nu''\right]. \tag{95}$$

We may now put equation (91) in the form

$$\frac{dI_\nu}{\rho ds} = -a_\nu(I_\nu - B_\nu) + \int_0^\infty \omega_{\nu,\nu'}(J_{\nu'}-B_{\nu'})\,d\nu'\,, \tag{96}$$

where

$$\omega_{\nu,\nu'} = \omega^*_{\nu,\nu'} + \frac{G_\nu}{G}\left[a_{\nu'} - \int_0^\infty \omega^*_{\nu'',\nu'}d\nu''\right]. \tag{97}$$

We may verify the fact that

$$\int_0^\infty \omega_{\nu,\nu'} = a_{\nu'}\,, \tag{98}$$

which is similar to equation (15). It should be pointed out that the earlier equation contains only first-order terms, while both equation (97) and equation (98) include the second-order terms included in the absorption coefficient. If the expression (18) is used to determine T, we may remove the term in $a_\nu^{(1)}$ in equation (95) and recover the form of equation (96), provided we now use the new definition:

$$\omega_{\nu,\nu'} = \omega^*_{\nu,\nu'} + \frac{G_\nu}{G}\left[a^{(0)}_{\nu'} - \int_0^\infty \omega^*_{\nu'',\nu'}d\nu''\right]. \tag{99}$$

Then $\omega_{\nu,\nu'}$ satisfies equation (15) exactly.

The proper handling of the second-order terms must await a numerical consideration of the orders of magnitude of the various parameters. This is deferred, pending an extension of the formal theory to include the effects of collisions as they influence both the excitation and the breadth of the discrete states.

Since the determination of the electron temperature must depend on continuous radiative processes, we may expect that the contributions to $\omega^*_{\nu'',\nu'}$, arising from discrete spectral lines in ν', are irrelevant. That this is the case may be verified by a lengthy computation not given here. It will be found that in

$$\int_0^\infty \omega^*_{\nu'',\nu'}d\nu''$$

all effects which arise when ν' lies in a spectral line cancel out identically.

ON THE RADIATIVE EQUILIBRIUM OF A STELLAR ATMOSPHERE. X

S. CHANDRASEKHAR
Yerkes Observatory
Received February 12, 1946

ABSTRACT

In this paper a detailed theory of the radiative equilibrium of an atmosphere in which the Thomson scattering by free electrons governs the transfer of radiation is developed. In particular, allowance has been made for the polarization of the scattered radiation; and the equations of transfer for the intensities I_l and I_r, referring, respectively, to the two states of polarization in which the electric vector vibrates in the meridian plane and at right angles to it, are separately formulated. The equations of transfer are found to be

$$\mu \frac{dI_l}{d\tau} = I_l - \frac{3}{8}\left\{2\int_{-1}^{+1} I_l(\tau, \mu')(1 - \mu'^2)d\mu' + \mu^2 \int_{-1}^{+1} I_l(\tau, \mu')(3\mu'^2 - 2)d\mu' + \mu^2 \int_{-1}^{+1} I_r(\tau, \mu')d\mu'\right\}$$

and

$$\mu \frac{dI_r}{d\tau} = I_r - \frac{3}{8}\left\{\int_{-1}^{+1} I_r(\tau, \mu')d\mu' + \int_{-1}^{+1} I_l(\tau, \mu')\mu'^2 d\mu'\right\}.$$

These equations have been solved in a general nth approximation, and their explicit numerical forms have been found in the second and the third approximations.

It is found that the theory predicts different laws of darkening for the two states of polarization distinguished by I_l and I_r. The emergent radiation is therefore polarized, and it is further predicted that the degree of polarization must vary from zero at the center of the disk to 11 per cent at the limb.

1. *Introduction.*—It is now generally recognized that the Thomson scattering by free electrons must play an important role in the transfer of radiation in the atmospheres of the early-type stars.[1] Thus, it has been suggested by J. L. Greenstein[2] that the absolute-magnitude effect among the early-types stars shown by the discontinuity at the head of the Balmer series is probably to be attributed to the increased importance of electron scattering as we go to the more luminous stars. But it does not seem to have been observed so far that, if electron scattering is as major a factor as there appears to be evidence for, then there is an associated effect which should be detectable, namely, the polarization of the continuous radiation. It is the object of this paper to analyze this effect theoretically and to show that it is within the possibilities of detection. The detailed theory of radiative transfer in an atmosphere in which electron scattering plays the principal part, developed in this paper, predicts a degree of polarization to the extent of 11 per cent at the limb. In practice, this effect may be partially masked by other sources of continuous opacity; but it would seem, from all the available evidence, that the effect is probably present in detectable amounts in the early-type stars. Moreover, it would appear that the most favorable conditions under which the phenomenon could be observed are during the phases close to the primary minimum in an eclipsing binary, one component of which is an early-type star.

On the theoretical side, the problem discussed in this paper provides the first example in which the equations of transfer for the two states of polarization have been explicitly formulated and solved.[3]

[1] A. Unsöld, *Zs. f. Ap.*, **21**, 229, 1942; M. Rudkjøbing, *Zs. f. Ap.*, **21**, 254, 1942.

[2] *Ap. J.*, **95**, 299, 1942.

[3] The method of solution adopted is those of the earlier papers of this series. Familiarity with papers II and III (*Ap. J.*, **100**, 76, 117, 1944) is necessary to follow the analysis of this paper.

2. *The equations of transfer for the two components of polarization in an atmosphere in which the scattering by free electrons governs the transfer of radiation.*—We shall consider the radiative equilibrium of a semi-infinite plane-parallel atmosphere with a constant net flux of radiation and in which the transfer of radiation takes place in accordance with Thomson's laws of scattering by free electrons. It is apparent that under these conditions we can characterize the field of radiation by the intensities $I_l(z, \vartheta)$ and $I_r(z, \vartheta)$ at height z and inclined at an angle ϑ to the positive normal and referring to the states of polarization in which the electric vectors vibrate along the principal meridian and at right angles to it, respectively. And we require to write down the equations of transfer for the two components separately. For this purpose we shall first formulate the laws of scattering in the form we shall need them.

According to Thomson's classical theory[4] of the scattering by free electrons, the amount of radiation (initially unpolarized) which is scattered (per unit time) in a direction inclined at an angle Θ to the direction of incidence, and confined to an element of solid angle $d\omega'$ and per free electron, is given by

$$\frac{8\pi}{3}\frac{e^4}{m^2c^4} I\left\{\tfrac{3}{4}(1+\cos^2\Theta)\frac{d\omega'}{4\pi}\right\}, \tag{1}$$

where I denotes the intensity[5] of the incident radiation, e the charge of the electron, m its mass, and c the velocity of light. Moreover, the scattered radiation is polarized with the direction of the electric vector perpendicular to the *plane of scattering*.[6] For our purposes, however, we need a more detailed formulation of the law of scattering which will allow us to take into account a partial polarization of the incident light. We shall formulate these more detailed laws in the following manner:

Let $I_\perp$ denote the intensity of radiation plane-polarized with the electric vector perpendicular to the plane of scattering. Then the amount of radiation scattered in a direction inclined at an angle Θ to direction of $I_\perp$ and confined to an element of solid angle $d\omega'$ and per free electron is

$$\frac{8\pi}{3}\frac{e^4}{m^2c^4} I_\perp\left(\frac{3}{2}\frac{d\omega'}{4\pi}\right). \tag{2}$$

The scattered radiation is also polarized with the electric vector perpendicular to the plane of scattering. On the other hand, if the incident light is polarized with the electric vector parallel to the plane of scattering, then the scattered radiation is also polarized in the same way, but its amount is now given by (cf. eq.[2])

$$\frac{8\pi}{3}\frac{e^4}{m^2c^4} I_{\parallel}\left(\frac{3}{2}\cos^2\Theta\frac{d\omega'}{4\pi}\right), \tag{3}$$

where $I_\parallel$ denotes the intensity of the incident polarized radiation. More generally, if the incident light is plane-polarized with its electric vector inclined to the plane of scattering by an angle α, then the amount of scattered radiation (under the same circumstances to which equations [2] and [3] refer) is given by

$$\frac{8\pi}{3}\frac{e^4}{m^2c^4} I\left\{\tfrac{3}{2}(\sin\alpha+\cos\alpha\cos\Theta)^2\frac{d\omega'}{4\pi}\right\}, \tag{4}$$

[4] Cf. A. H. Compton and S. K. Allison, *X-Rays in Theory and Experiment*, pp. 117–119, New York: D. Van Nostrand, 1935.

[5] Since the Thomson scattering coefficient is independent of wave length, we can directly consider the intensity I integrated over all the frequencies.

[6] This is the plane which contains the directions of the incident and the scattered light.

while its plane of polarization is such that the electric vector is inclined to the plane of scattering by an angle

$$\beta = \tan^{-1}(\tan \alpha \sec \Theta) . \tag{5}$$

Thus there is, in general, a "turning" of the plane of polarization. We shall now show how, with the laws of scattering formulated in this manner, we can obtain the equations of transfer for the two components of polarization distinguished by I_l and I_r.

It is first evident that the equations of transfer must be expressible in the forms

$$\cos \vartheta \frac{dI_l}{d\tau} = I_l - \mathfrak{J}_{l,l}(\tau, \vartheta) - \mathfrak{J}_{r,l}(\tau, \vartheta) \tag{6}$$

and

$$\cos \vartheta \frac{dI_r}{d\tau} = I_r - \mathfrak{J}_{l,r}(\tau, \vartheta) - \mathfrak{J}_{r,r}(\tau, \vartheta) , \tag{7}$$

where τ denotes the optical depth, measured in terms of the Thomson scattering coefficient

$$\sigma = \frac{8\pi}{3} \frac{e^4}{m^2 c^4} N_e . \tag{8}$$

with N_e denoting the number of electrons per unit mass. Further, in equation (6), $\mathfrak{J}_{l,l}$ and $\mathfrak{J}_{r,l}$ are the contributions to the source function for the radiation in a particular direction and polarized with the electric vector in the meridian plane, arising from the scattering from all other directions of radiations polarized with the electric vectors parallel, respectively, perpendicular to the appropriate meridian planes. Similarly, in equation (7), $\mathfrak{J}_{l,r}$ and $\mathfrak{J}_{r,r}$ are the contributions to the source function for the radiation in a particular direction polarized with the electric vector perpendicular to the meridian plane, arising from the scattering from all other directions of radiations polarized with the electric vectors parallel, respectively, perpendicular to the appropriate meridian planes.

To evaluate $\mathfrak{J}_{l,l}(\tau, \vartheta)$ and $\mathfrak{J}_{l,r}(\tau, \vartheta)$, we consider the contributions to these source functions for the radiation in the direction $(\vartheta, 0)$, say, arising from the scattering of radiation of intensity $I_l(\tau, \vartheta')$ in the direction (ϑ', φ') and polarized with the electric vector in the meridian plane through (ϑ', φ'). Let ξ_l denote a quantity proportional to the amplitude of the electric vector such that

$$I_l = \xi_l^2 . \tag{9}$$

(We shall refer, quite generally, to ξ's defined in this manner as simply the *amplitude*.) The components of the amplitude that are parallel, respectively, perpendicular to the plane of scattering, are

$$\xi_l \cos i_1 \quad \text{and} \quad \xi_l \sin i_1 , \tag{10}$$

where i_1 denotes the angle between the meridian plane OZP_1 through $P_1 = (\vartheta', \varphi')$ and the plane of scattering OP_1P_2 ($P_2 = [\vartheta, 0]$) (see Fig. 1). When this radiation is scattered into the direction OP_2, the components of the scattered amplitude that are parallel, respectively, perpendicular to the plane OP_1P_2, are proportional to

$$\xi_l \cos i_1 \cos \Theta \quad \text{and} \quad \xi_l \sin i_1 , \tag{11}$$

while the amplitudes in the meridian plane OZX through P_2, and at right angles to it, are, respectively, proportional to

$$\xi_l (\sin i_1 \sin i_2 - \cos i_1 \cos i_2 \cos \Theta) \tag{12}$$

and

$$-\xi_l (\sin i_1 \cos i_2 + \sin i_2 \cos i_1 \cos \Theta) . \tag{13}$$

where i_2 denotes the angle between the planes OZX and OP_1P_2. The contributions to the source functions $\mathfrak{J}_{l,l}(z, \vartheta, 0)$ $(= \mathfrak{J}_{l,l}(z, \vartheta))$ and $\mathfrak{J}_{l,r}(z, \vartheta, 0)$ $(= \mathfrak{J}_{l,r}(z, \vartheta))$, arising from the scattering of the radiation $I_l(z, \vartheta', \varphi')$ $(= I_l(z, \vartheta'))$ in the direction (ϑ', φ') and confined to an element of solid angle $d\omega'$ are, therefore,

$$d\mathfrak{J}_{l,l} = \tfrac{3}{2} I_l(\tau, \vartheta') (\sin i_1 \sin i_2 - \cos i_1 \cos i_2 \cos \Theta)^2 \frac{d\omega'}{4\pi} \tag{14}$$

and

$$d\mathfrak{J}_{l,r} = \tfrac{3}{2} I_l(\tau, \vartheta') (\sin i_1 \cos i_2 + \sin i_2 \cos i_1 \cos \Theta)^2 \frac{d\omega'}{4\pi}. \tag{15}$$

Hence,

$$\mathfrak{J}_{l,l} = \frac{3}{8\pi} \int_0^{\pi} \int_0^{2\pi} I_l(\tau, \vartheta') (\sin i_1 \sin i_2 - \cos i_1 \cos i_2 \cos \Theta)^2 \sin \vartheta' d\vartheta' d\varphi' \tag{16}$$

and

$$\mathfrak{J}_{l,r} = \frac{3}{8\pi} \int_0^{\pi} \int_0^{2\pi} I_l(\tau, \vartheta') (\sin i_1 \cos i_2 + \sin i_2 \cos i_1 \cos \Theta)^2 \sin \vartheta' d\vartheta' d\varphi'. \tag{17}$$

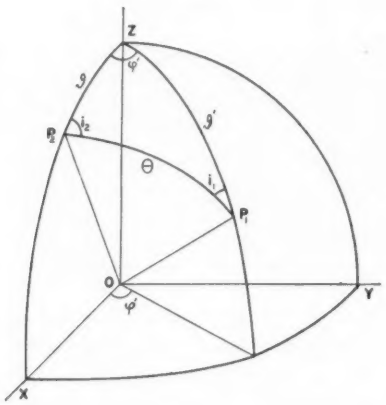

FIG. 1

On the other hand, from the spherical triangle ZP_1P_2 we have

$$\sin \varphi' \cos \vartheta' = \cos i_2 \sin i_1 + \sin i_2 \cos i_1 \cos \Theta . \tag{18}$$

Equation (17) accordingly reduces to the form

$$\mathfrak{J}_{l,r} = \frac{3}{8\pi} \int_0^{\pi} \int_0^{2\pi} I_l(\tau, \vartheta') \sin^2 \varphi' \cos^2 \vartheta' \sin \vartheta' d\vartheta' d\varphi'; \tag{19}$$

or, in view of the axial symmetry of the radiation field about the z-axis, in our problem, we can write

$$\mathfrak{J}_{l,r}(\tau, \mu) = \frac{3}{8} \int_{-1}^{+1} I_l(\tau, \mu') \mu'^2 d\mu', \tag{20}$$

where we have used μ and μ' to denote $\cos \vartheta$ and $\cos \vartheta'$, respectively.

From equations (16) and (17) we have

$$\mathfrak{J}_{l,l} + \mathfrak{J}_{l,r} = \frac{3}{8\pi} \int_0^{\pi} \int_0^{2\pi} I_l(\tau, \vartheta') (\sin^2 i_1 + \cos^2 i_1 \cos^2 \Theta) \sin \vartheta' d\vartheta' d\varphi'; \tag{21}$$

or, since

$$\left.\begin{aligned}\sin^2 i_1 + \cos^2 i_1 \cos^2\Theta &= 1 - \cos^2 i_1 \sin^2\Theta \\ &= 1 - (\cos\vartheta \sin\vartheta' - \sin\vartheta \cos\vartheta' \cos\varphi')^2 ,\end{aligned}\right\} \quad (22)$$

we have

$$\mathfrak{J}_{l,l} + \mathfrak{J}_{l,r} = \frac{3}{8}\int_{-1}^{+1} I_l(\tau, \mu')\,[2 - \mu'^2 + \mu^2(3\mu'^2 - 2)]\,d\mu' . \quad (23)$$

From equations (20) and (23) we now obtain

$$\mathfrak{J}_{l,l}(\tau, \mu) = \frac{3}{8}\int_{-1}^{+1} I_l(\tau, \mu')\,[2(1 - \mu'^2) + \mu^2(3\mu'^2 - 2)]\,d\mu' . \quad (24)$$

To determine the source functions $\mathfrak{J}_{r,l}$ and $\mathfrak{J}_{r,r}$, we proceed along similar lines, considering radiation of intensity $I_r(\tau, \vartheta', \varphi')$ $(= I_r(\tau, \vartheta'))$ in the direction (ϑ', φ') and polarized with the electric vector perpendicular to the meridian plane OZP_1 and evaluating its contribution to the source function for the radiation in the direction $(\vartheta, 0)$. Let ξ_r denote the amplitude corresponding to the intensity $I_r(\tau, \vartheta', \varphi')$. Its components, parallel, respectively, perpendicular to the scattering plane, are

$$\xi_r \sin i_1 \quad \text{and} \quad \xi_r \cos i_1 . \quad (25)$$

When this radiation is scattered into the direction OP_2, the components of the scattered amplitude, parallel, respectively, perpendicular to the plane OP_1P_2, are proportional to

$$\xi_r \sin i_1 \cos\Theta \quad \text{and} \quad \xi_r \cos i_1 . \quad (26)$$

The amplitudes in the meridian plane OZX and at right angles to it are, respectively, proportional to

$$\xi_r(\sin i_1 \cos i_2 \cos\Theta + \cos i_1 \sin i_2) = \xi_r \sin\varphi' \cos\vartheta \quad (27)$$

and

$$\xi_r(\sin i_1 \sin i_2 \cos\Theta - \cos i_1 \cos i_2) = \xi_r \cos\varphi' . \quad (28)$$

Accordingly, the contributions to the source functions $\mathfrak{J}_{r,l}(\tau, \vartheta, 0)$ and $\mathfrak{J}_{r,r}(\tau, \vartheta, 0)$, arising from the scattering of the radiation $I_r(\tau, \vartheta', \varphi')$ in the direction (ϑ', φ') and confined to an element of solid angle $d\omega'$, are given by

$$d\mathfrak{J}_{r,l} = \tfrac{3}{2} I_r(\tau, \vartheta')(\sin i_1 \cos i_2 \cos\Theta + \cos i_1 \sin i_2)^2 \frac{d\omega'}{4\pi} \quad (29)$$

and

$$d\mathfrak{J}_{r,r} = \tfrac{3}{2} I_r(\tau, \vartheta')\cos^2\varphi' \frac{d\omega'}{4\pi} . \quad (30)$$

Hence,

$$\mathfrak{J}_{r,r} = \frac{3}{8\pi}\int_0^{\pi}\int_0^{2\pi} I_r(\tau, \vartheta')\cos^2\varphi' \sin\vartheta' d\vartheta' d\varphi' , \quad (31)$$

or

$$\mathfrak{J}_{r,r}(\tau, \mu) = \frac{3}{8}\int_{-1}^{+1} I_r(\tau, \mu')\,d\mu' . \quad (32)$$

On the other hand (cf. eqs. [27] and [28]),

$$\mathfrak{J}_{r,r} + \mathfrak{J}_{r,l} = \frac{3}{8\pi}\int_0^{\pi}\int_0^{2\pi} I_r(\tau, \vartheta')(\sin^2 i_1 \cos^2\Theta + \cos^2 i_1)\sin\vartheta' d\vartheta' d\varphi' ; \quad (33)$$

or, since

$$\sin^2 i_1 \cos^2\Theta + \cos^2 i_1 = 1 - \sin^2 i_1 \sin^2\Theta = 1 - \sin^2\vartheta \sin^2\varphi' . \quad (34)$$

we have

$$\mathfrak{J}_{r,r}+\mathfrak{J}_{r,l}=\frac{3}{8}\int_{-1}^{+1}I_r(\tau,\mu')(1+\mu^2)\,d\mu'. \tag{35}$$

From equations (32) and (35) we now obtain

$$\mathfrak{J}_{r,l}(\tau,\mu)=\tfrac{3}{8}\mu^2\int_{-1}^{+1}I_r(\tau,\mu')\,d\mu'. \tag{36}$$

Combining equations (6), (24), and (36) and similarly equations (7), (20), and (32), we obtain

$$\left.\begin{aligned}\mu\frac{dI_l}{d\tau}=I_l-\tfrac{3}{8}\Big\{2\int_{-1}^{+1}I_l(\tau,\mu')(1-\mu'^2)\,d\mu'+\mu^2\int_{-1}^{+1}I_l(\tau,\mu')(3\mu'^2-2)\,d\mu'\\ +\mu^2\int_{-1}^{+1}I_r(\tau,\mu')\,d\mu'\Big\}\end{aligned}\right\} \tag{37}$$

and

$$\mu\frac{dI_r}{d\tau}=I_r-\tfrac{3}{8}\Big\{\int_{-1}^{+1}I_r(\tau,\mu')\,d\mu'+\int_{-1}^{+1}I_l(\tau,\mu')\mu'^2d\mu'\Big\}, \tag{38}$$

which are the required equations of transfer for I_l and I_r.

We may note here that, for radiation initially unpolarized, the source functions for radiations polarized in the two ways can be obtained from equations (20), (24), (32), and (36) by setting $I_l = I_r = \frac{1}{2}I$. Thus,

$$\mathfrak{J}_l=\frac{3}{16}\Big\{2\int_{-1}^{+1}I(\tau,\mu')(1-\mu'^2)\,d\mu'+\mu^2\int_{-1}^{+1}I(\tau,\mu')(3\mu'^2-1)\,d\mu'\Big\} \tag{39}$$

and

$$\mathfrak{J}_r=\frac{3}{16}\int_{-1}^{+1}I(\tau,\mu')(1+\mu'^2)\,d\mu', \tag{40}$$

which agree with A. Schuster's well-known formulae.[7]

In terms of the quantities J and K, defined in the usual manner (cf. paper III, eq. [6]), we can re-write the equations of transfer (37) and (38) in the following forms:

$$\mu\frac{dI_l}{d\tau}=I_l-\tfrac{3}{4}\Big\{2(J_l-K_l)+\mu^2(3K_l-2J_l+J_r)\Big\} \tag{41}$$

and

$$\mu\frac{dI_r}{d\tau}=I_r-\tfrac{3}{4}(J_r+K_l). \tag{42}$$

From the equations of transfer in the foregoing forms we can readily establish the flux integral

$$F_l+F_r=F=2\int_{-1}^{+1}[\,I_l(\tau,\mu)+I_r(\tau,\mu)\,]\mu\,d\mu=\text{constant} \tag{43}$$

and the "K-integral"

$$K_l+K_r=\tfrac{1}{4}F(\tau+Q) \tag{44}$$

where Q is a constant.

3. *The general solution of the equations of transfer in the* n*th approximation.*—In solving equations (37) and (38) we shall follow the method developed in the earlier papers of this series and replace the various integrals which occur on the right-hand sides of the equations by sums according to Gauss's formula for numerical quadratures. Thus, in

[7] *M.N.*, **40**, 35, 1879; see also M. Minnaert, *Zs. f. Ap.*, **1**, 209, 1930, and H. Zanstra, *M.N.*, **101**, 250, 1941.

the nth approximation, equations (37) and (38) are replaced by the following system of $4n$ linear equations:

$$\left.\begin{aligned}\mu_i \frac{dI_{l,i}}{d\tau} = I_{l,i} - \tfrac{3}{8}\left[2\Sigma a_j I_{l,j}(1-\mu_j^2) + \mu_i^2\{\Sigma a_j I_{l,j}(3\mu_j^2-2) + \Sigma a_j I_{r,j}\}\right] \\ (i = \pm 1, \ldots, \pm n)\end{aligned}\right\} \quad (45)$$

and

$$\mu_i \frac{dI_{r,i}}{d\tau} = I_{r,i} - \tfrac{3}{8}(\Sigma a_j I_{r,j} + \Sigma a_j I_{l,j}\mu_j^2) \qquad (i = \pm 1, \ldots, \pm n), \quad (46)$$

where the μ_i's ($i = \pm 1, \ldots, \pm n$) are the zeros of the Legendre polynomial of order $2n$ and the a_i's are the appropriate Gaussian weights. Further, in equations (45) and (46) we have written $I_{l,i}$ and $I_{r,i}$ for $I_l(\tau, \mu_i)$ and $I_r(\tau, \mu_i)$, respectively.

We shall now find the different linearly independent solutions of equations (45) and (46) and later, by combining these, obtain the general solution.

First, we seek a solution of equations (45) and (46) of the form

$$I_{l,i} = g_i e^{-k\tau} \quad \text{and} \quad I_{r,i} = h_i e^{-k\tau} \qquad (i = \pm 1, \ldots, \pm n), \quad (47)$$

where the g_i's, h_i's, and k are constants, for the present unspecified. Substituting the foregoing forms for $I_{l,i}$ and $I_{r,i}$ in equations (45) and (46), we obtain

$$g_i(1+\mu_i k) = \tfrac{3}{8}\left[2\Sigma a_j g_j(1-\mu_j^2) + \mu_i^2\{\Sigma a_j g_j(3\mu_j^2-2) + \Sigma a_j h_j\}\right] \quad (48)$$

and

$$h_i(1+\mu_i k) = \tfrac{3}{8}\left[\Sigma a_j g_j \mu_j^2 + \Sigma a_j h_j\right]. \quad (49)$$

Equations (48) and (49) imply that g_i and h_i must be expressible in the forms

$$g_i = \frac{\alpha\mu_i^2 + \beta}{1+\mu_i k} \quad \text{and} \quad h_i = \frac{\gamma}{1+\mu_i k} \qquad (i = \pm 1, \ldots, \pm n), \quad (50)$$

where α, β, and γ are certain constants, independent of i. Inserting the solution (50) back into equations (48) and (49), we find

$$\left.\begin{aligned}\alpha\mu_i^2 + \beta = \tfrac{3}{8}\left[2\{\alpha(D_2 - D_4) + \beta(D_0 - D_2)\} + \mu_i^2\{\alpha(3D_4 - 2D_2)\right. \\ \left. + \beta(3D_2 - 2D_0) + \gamma D_0\}\right]\end{aligned}\right\} \quad (51)$$

and

$$\gamma = \tfrac{3}{8}(\alpha D_4 + \beta D_2 + \gamma D_0), \quad (52)$$

where we have introduced the quantities D_0, D_2, and D_4, defined according to the formula

$$D_m = \Sigma \frac{a_j \mu_j^m}{1+\mu_j k}. \quad (53)$$

Since equations (51) and (52) are valid for all i, we must require that

$$\tfrac{8}{3}\alpha = \alpha(3D_4 - 2D_2) + \beta(3D_2 - 2D_0) + \gamma D_0, \quad (54)$$

$$\tfrac{4}{3}\beta = \alpha(D_2 - D_4) + \beta(D_0 - D_2), \quad (55)$$

and

$$\tfrac{8}{3}\gamma = \alpha D_4 + \beta D_2 + \gamma D_0. \quad (56)$$

It is seen that equations (54), (55), and (56), together, represent a system of homogeneous linear equations for α, β, and γ. The determinant of this system must, therefore, be required to vanish. Thus,

$$\begin{vmatrix} 3D_4 - 2D_2 - \frac{8}{3} & 3D_2 - 2D_0 & D_0 \\ D_2 - D_4 & D_0 - D_2 - \frac{4}{3} & 0 \\ D_4 & D_2 & D_0 - \frac{8}{3} \end{vmatrix} = 0 . \tag{57}$$

Expanding this determinant by the elements of the last column, we find, after some minor reductions, that

$$D_0(\tfrac{4}{3} - D_0 + 2D_2 - D_4) - (\tfrac{32}{9} - \tfrac{8}{3}D_0 + \tfrac{16}{3}D_2 - 4D_4 + D_0D_4 - D_2^2) = 0 . \tag{58}$$

To simplify equation (58) still further, we must make use of certain relations which can be derived from the recursion formulae[8]

$$D_{2m} = \frac{1}{k^2}\left(D_{2m-2} - \frac{2}{2m-1}\right) \tag{59}$$

and

$$D_{2m-1} = -kD_{2m}, \tag{60}$$

which the D's satisfy. From equation (59) we infer, in particular, that

$$D_2 = \frac{1}{k^2}(D_0 - 2) \tag{61}$$

and

$$D_4 = \frac{1}{k^2}(D_2 - \tfrac{2}{3}) = \frac{1}{k^4}(D_0 - 2) - \frac{2}{3k^2}. \tag{62}$$

A further relation which follows from equations (61) and (62) is

$$D_2(D_2 - \tfrac{2}{3}) = D_4(D_0 - 2), \tag{63}$$

or

$$D_0D_4 - D_2^2 = 2D_4 - \tfrac{2}{3}D_2 . \tag{64}$$

By using equation (64), equation (58) reduces to

$$D_0(\tfrac{4}{3} - D_0 + 2D_2 - D_4) - (\tfrac{32}{9} - \tfrac{8}{3}D_0 + \tfrac{16}{3}D_2 - 2D_4) = 0 . \tag{65}$$

Now, substituting for D_2 and D_4 according to equations (61) and (62) in terms of D_0 in equation (65), we find, after some simplification, that

$$\frac{1}{k^4}(D_0 - 2)^2 - \frac{2}{k^2}(D_0 - 2)^2 + D_0^2 - 4D_0 + \tfrac{32}{9} = 0 . \tag{66}$$

Again using equations (61) and (62), we can re-write the foregoing equation in the form

$$D_2^2 - 2D_2(D_0 - 2) + D_0^2 - 4D_0 + \tfrac{32}{9} = 0 \tag{67}$$

or

$$(D_0 - D_2)^2 - 4(D_0 - D_2) + \tfrac{32}{9} = 0 . \tag{68}$$

[8] Cf. *Ap. J.*, **101**, 328, 1945 (eqs. [54] and [56]).

Equation (68) is equivalent to

$$(D_0 - D_2 - \tfrac{8}{3})(D_0 - D_2 - \tfrac{4}{3}) = 0 . \tag{69}$$

In other words, either

$$D_0 - D_2 = \Sigma \frac{a_j(1-\mu_j^2)}{1+\mu_j k} = \frac{8}{3} \qquad \text{(case 1)} \tag{70}$$

or

$$D_0 - D_2 = \Sigma \frac{a_j(1-\mu_j^2)}{1+\mu_j k} = \frac{4}{3} \qquad \text{(case 2)} . \tag{71}$$

Equations (70) and (71) can be written alternatively in the forms

$$\sum_{j=1}^{n} \frac{a_j(1-\mu_j^2)}{1-\mu_j^2 k^2} = \frac{4}{3} \qquad \text{(case 1)} \tag{72}$$

and

$$\sum_{j=1}^{n} \frac{a_j(1-\mu_j^2)}{1-\mu_j^2 k^2} = \frac{2}{3} \qquad \text{(case 2)} . \tag{73}$$

And k^2 must be a root of either of the two foregoing equations.

Equation (72) is of order n in k^2 and admits $2n$ distinct nonvanishing roots for k which occur in pairs as

$$\pm k_\alpha \qquad (\alpha = 1, \ldots, n) . \tag{74}$$

On the other hand, equation (73), though of order $2n$ in k^2, admits of only $(2n - 2)$ distinct nonvanishing roots for k, since $k^2 = 0$ is a root.[9] However, these $2n - 2$ roots also occur in pairs, which we shall denote by

$$\pm \kappa_\beta \qquad (\beta = 1 \ldots, n-1) , \tag{75}$$

to distinguish them from the roots of equation (72).

Case 1: k^2 *a root of equation* (72).—In this case, $D_0 - D_2 = 8/3$; and from equations (61) and (62) we readily find that

$$D_0 = \frac{2}{3}\frac{4k^2-3}{k^2-1}; \qquad D_2 = \frac{2}{3(k^2-1)}; \qquad D_4 = \frac{2}{3k^2}\frac{2-k^2}{k^2-1}. \tag{76}$$

With these values for D_0, D_2, and D_4, equations (55) and (56) lead to

$$\alpha = -k^2\beta \tag{77}$$

and

$$\gamma = -(k^2-1)\beta . \tag{78}$$

Accordingly, equations (45) and (46) allow $2n$ linearly independent integrals of the form

$$\left.\begin{aligned} I_{l,i} &= \text{constant}\,(1 \mp k_\alpha \mu_i)\, e^{\mp k_\alpha \tau} \\ I_{r,i} &= -\,\text{constant}\,\frac{k_\alpha^2 - 1}{1 \pm k_\alpha \mu_i}\, e^{\mp k_\alpha \tau} \end{aligned}\right\}, \qquad \left\{\begin{matrix}(i = \pm 1, \ldots, \pm n) \\ (\alpha = 1, \ldots, n)\end{matrix}\right\} . \tag{79}$$

[9] Note that $\sum_{j=1}^{n} a_j(1-\mu_j^2) = \frac{8}{3}$.

Case 2: κ^2 a root of equation (73).—In this case, $D_0 - D_2 = 4/3$; and equations (61) and (62) now give

$$D_0 = \frac{2}{3}\frac{2\kappa^2 - 3}{\kappa^2 - 1}; \qquad D_2 = D_4 = -\frac{2}{3(\kappa^2 - 1)}. \tag{80}$$

With these values of D_0, D_2, and D_4 it is seen that equation (55) is satisfied identically, while the consideration of equations (54) and (56) leads to the result that

$$\alpha = -\beta \qquad \text{and} \qquad \gamma = 0\,. \tag{81}$$

Accordingly, equations (45) and (46) admit of $(2n - 2)$ linearly independent integrals of the form

$$I_{l,i} = \text{constant}\,\frac{1-\mu_i^2}{1\pm\mu_i\kappa_\beta}\,e^{\mp\kappa_\beta\tau} \qquad \left\{\begin{array}{l}(i = \pm 1, \ldots, \pm n)\\ (\beta = 1, \ldots, n-1)\end{array}\right\} \tag{82}$$

and

$$I_{r,i} \equiv 0 \qquad (i = \pm 1, \ldots, \pm n)\,. \tag{83}$$

To complete the solution, we verify that equations (45) and (46) also admit the solution

$$I_{l,i} = I_{r,i} = b(\tau + \mu_i + Q) \qquad (i = \pm 1, \ldots, \pm n)\,, \tag{84}$$

where b and Q are arbitrary constants.

Combining the solutions (79), (82), (83), and (84), we observe that the general solution of the system of equations (45) and (46) can be written in the forms

$$\left.\begin{aligned} I_{l,i} = b\Big\{\tau + \mu_i + Q + (1-\mu_i^2)\sum_{\beta=1}^{n-1}\Big(\frac{L_\beta e^{-\kappa_\beta\tau}}{1+\mu_i\kappa_\beta} + \frac{L_{-\beta}e^{+\kappa_\beta\tau}}{1-\mu_i\kappa_\beta}\Big)\\ + \sum_{\alpha=1}^{n} M_\alpha(1-k_\alpha\mu_i)\,e^{-k_\alpha\tau} + \sum_{\alpha=1}^{n-1} M_{-\alpha}(1+k_\alpha\mu_i)\,e^{+k_\alpha\tau}\Big\}\\ (i = \pm 1, \ldots, \pm n)\end{aligned}\right\} \tag{85}$$

and

$$\left.\begin{aligned} I_{r,i} = b\Big\{\tau + \mu_i + Q - \sum_{\alpha=1}^{n} M_\alpha\frac{(k_\alpha^2-1)}{1+\mu_i k_\alpha}\,e^{-k_\alpha\tau} - \sum_{\alpha=1}^{n} M_{-\alpha}\frac{(k_\alpha^2-1)}{1-\mu_i k_\alpha}\,e^{+k_\alpha\tau}\Big\}\\ (i = \pm 1, \ldots, \pm n)\,,\end{aligned}\right\} \tag{86}$$

where $L_{\pm\beta}$ $(\beta = 1, \ldots, n-1)$, $M_{\pm\alpha}$ $(\alpha = 1, \ldots, n)$, b, and Q are the $4n$ constants of integration.

4. *The solution satisfying the necessary boundary conditions.*—The boundary conditions for the astrophysical problem on hand are that none of the I_i's tend to infinity exponentially as $\tau \to \infty$ and that there is no radiation incident on the surface $\tau = 0$. The first of these conditions implies that in the general solution (85) and (86) we omit all terms in $\exp(+k_\alpha\tau)$ and $\exp(+\kappa_\beta\tau)$. We are thus left with

$$\left.\begin{aligned} I_{l,i} = b\Big\{\tau + \mu_i + Q + (1-\mu_i^2)\sum_{\beta=1}^{n-1}\frac{L_\beta e^{-\kappa_\beta\tau}}{1+\mu_i\kappa_\beta} + \sum_{\alpha=1}^{n} M_\alpha(1-k_\alpha\mu_i)\,e^{-k_\alpha\tau}\Big\}\\ (i = \pm 1, \ldots, \pm n)\end{aligned}\right\} \tag{87}$$

and

$$I_{r,i} = b\Big\{\tau + \mu_i + Q - \sum_{\alpha=1}^{n}\frac{M_\alpha(k_\alpha^2-1)}{1+\mu_i k_\alpha}\,e^{-k_\alpha\tau}\Big\} \qquad (i = \pm 1, \ldots, \pm n)\,. \tag{88}$$

Next, the nonexistence of any radiation incident on $\tau = 0$ requires that

$$I_{l,i} = I_{r,i} = 0 \quad \text{at} \quad \tau = 0 \quad \text{and for} \quad i = -1, \ldots, -n; \tag{89}$$

or, according to equations (86) and (87),

$$(1-\mu_i^2)\sum_{\beta=1}^{n-1}\frac{L_\beta}{1-\mu_i\kappa_\beta}+\sum_{\alpha=1}^{n}M_\alpha(1+k_\alpha\mu_i)-\mu_i+Q=0 \qquad (i=1,\ldots,n) \tag{90}$$

and

$$\sum_{\alpha=1}^{n}\frac{M_\alpha(k_\alpha^2-1)}{1-\mu_i k_\alpha}+\mu_i-Q=0 \qquad (i=1,\ldots,n). \tag{91}$$

These are the $2n$ equations which determine the $2n$ constants L_β ($\beta = 1, \ldots, n-1$), M_α ($\alpha = 1, \ldots = n$), and Q.[10] The constant b is left arbitrary and is related to the constant net flux of radiation in the atmosphere.

For, defining the net flux in terms of F_l and F_r where

$$F_q = 2\int_{-1}^{+1} I_q \mu\, d\mu \simeq 2\Sigma a_i I_{q,i}\mu_i \qquad (q = l, r), \tag{92}$$

we have, according to equations (87) and (88),

$$F_l = 2b\left\{\frac{2}{3}+\sum_{\beta=1}^{n-1}L_\beta[\,D_1(\kappa_\beta)-D_3(\kappa_\beta)\,]\,e^{-\kappa_\beta\tau}-\frac{2}{3}\sum_{\alpha=1}^{n}M_\alpha k_\alpha e^{-k_\alpha\tau}\right\} \tag{93}$$

and

$$F_r = 2b\left\{\frac{2}{3}-\sum_{\alpha=1}^{n}M_\alpha(k_\alpha^2-1)\,D_1(k_\alpha)\,e^{-k_\alpha\tau}\right\}. \tag{94}$$

On the other hand, from equations (60), (76), and (80) we conclude that

$$D_1(k_\alpha) = -k_\alpha D_2(k_\alpha) = -\frac{2}{3}\frac{k_\alpha}{k_\alpha^2-1} \tag{95}$$

and

$$D_1(\kappa_\beta)-D_3(\kappa_\beta) = -\kappa_\beta[\,D_2(\kappa_\beta)-D_4(\kappa_\beta)\,] = 0\,. \tag{96}$$

Hence,

$$F_l = \tfrac{4}{3}b\left(1-\sum_{\alpha=1}^{n}M_\alpha k_\alpha e^{-k_\alpha\tau}\right) \tag{97}$$

and

$$F_r = \tfrac{4}{3}b\left(1+\sum_{\alpha=1}^{n}M_\alpha k_\alpha e^{-k_\alpha\tau}\right). \tag{98}$$

From the two preceding equations we infer the constancy of the net flux. More particularly,

$$F = F_l + F_r = \tfrac{8}{3}b = \text{constant}\,. \tag{99}$$

[10] Adding equations (90) and (91), we obtain the equation

$$\sum_{\alpha=1}^{n}\frac{M_\alpha k_\alpha^2}{1-\mu_i k_\alpha}+\sum_{\beta=1}^{n}\frac{L_\beta}{1-\mu_i\kappa_\beta}=0 \qquad (i=1,\ldots,n),$$

which together with equation (91) is more convenient for the practical determination of these constants.

We can, therefore, re-write the solution (85) and (86) in the form

$$I_{l,i} = \tfrac{3}{8}F\left\{\tau + \mu_i + Q + (1-\mu_i^2)\sum_{\beta=1}^{n-1}\frac{L_\beta e^{-\kappa_\beta\tau}}{1+\mu_i\kappa_\beta} + \sum_{\alpha=1}^{n} M_\alpha(1-k_\alpha\mu_i)\,e^{-k_\alpha\tau}\right\} \quad (i=\pm 1, \ldots, \pm n) \tag{100}$$

and

$$I_{r,i} = \tfrac{3}{8}F\left\{\tau + \mu_i + Q - \sum_{\alpha=1}^{n}\frac{M_\alpha(k_\alpha^2-1)}{1+\mu_i k_\alpha}\,e^{-k_\alpha\tau}\right\} \qquad (i=\pm 1, \ldots, \pm n). \tag{101}$$

In terms of the foregoing solutions for $I_{l,i}$ and $I_{r,i}$ we can readily establish the following formulae

$$J_l = \tfrac{1}{2}\Sigma a_j I_{l,j} = \tfrac{3}{8}F\left(\tau + Q + \frac{2}{3}\sum_{\beta=1}^{n-1} L_\beta e^{-\kappa_\beta\tau} + \sum_{\alpha=1}^{n} M_\alpha e^{-k_\alpha\tau}\right), \tag{102}$$

$$K_l = \tfrac{1}{2}\Sigma a_j I_{l,j}\mu_j^2 = \tfrac{1}{8}F\left(\tau + Q + \sum_{\alpha=1}^{n} M_\alpha e^{-k_\alpha\tau}\right), \tag{103}$$

$$J_r = \tfrac{3}{8}F\left(\tau + Q - \frac{1}{3}\sum_{\alpha=1}^{n} M_\alpha[\,4k_\alpha^2 - 3\,]\,e^{-k_\alpha\tau}\right), \tag{104}$$

and

$$K_r = \tfrac{1}{8}F\left(\tau + Q - \sum_{\alpha=1}^{n} M_\alpha e^{-k_\alpha\tau}\right). \tag{105}$$

Now the source functions $\mathfrak{J}_l(\tau,\mu)$ and $\mathfrak{J}_r(\tau,\mu)$ for I_l and I_r are (cf., eqs. [41] and [42])

$$\mathfrak{J}_l(\tau,\mu) = \tfrac{3}{4}[\,2(J_l - K_l) + \mu^2(3K_l - 2J_l + J_r)\,] \tag{106}$$

and

$$\mathfrak{J}_r(\tau,\mu) = \tfrac{3}{4}(J_r + K_l); \tag{107}$$

or, substituting for J_l, K_l, J_r, and K_r from equations (102)–(105), we find

$$\mathfrak{J}_l(\tau,\mu) = \tfrac{3}{8}F\left\{\tau + Q + (1-\mu^2)\sum_{\beta=1}^{n-1} L_\beta e^{-\kappa_\beta\tau} + \sum_{\alpha=1}^{n} M_\alpha(1-k_\alpha^2\mu^2)\,e^{-k_\alpha\tau}\right\} \tag{108}$$

and

$$\mathfrak{J}_r(\tau,\mu) = \tfrac{3}{8}F\left\{\tau + Q - \sum_{\alpha=1}^{n} M_\alpha(k_\alpha^2 - 1)\,e^{-k_\alpha\tau}\right\}. \tag{109}$$

With the explicit forms for the source functions now found, we can readily obtain formulae for the intensity distribution of the emergent radiation. For, since quite generally

$$I(0,\mu) = \int_0^\infty \mathfrak{J}(\tau,\mu)\,e^{-\tau/\mu}\frac{d\tau}{\mu}, \tag{110}$$

we have, in our present case,

$$I_l(0,\mu) = \tfrac{3}{8}F\left\{\mu + Q + (1-\mu^2)\sum_{\beta=1}^{n-1}\frac{L_\beta}{1+\kappa_\beta\mu} + \sum_{\alpha=1}^{n} M_\alpha(1-k_\alpha\mu)\right\} \tag{111}$$

and

$$I_r(0, \mu) = \tfrac{3}{8}F\left\{\mu + Q - \sum_{a=1}^{n}\frac{M_a(k_a^2 - 1)}{1 + k_a\mu}\right\}. \tag{112}$$

It is to be particularly noted that the foregoing expressions for $I_l(0, \mu)$ and $I_r(0, \mu)$ agree with the solution (100) and (101) for $\tau = 0$ at the points of the Gaussian division.

This completes the solution of the problem in the nth approximation.

5. *The numerical forms of the solution in the second and the third approximations; the degree of polarization of the emergent radiation.*—The consideration of the solution obtained in the preceding section in the first approximation is of no special interest except possibly to emphasize the importance of having a method which gives solutions to any desired degree of accuracy. For, in the first approximation ($n = 1$) there are no L's; and, though there is an M, this is also seen to be zero; and the only nonvanishing constant of integration is Q, which has the value $1/\sqrt{3}$. Accordingly, in this approximation (cf. II, eq. [35], and III eq. [72])

$$I_l(0, \mu) = I_r(0, \mu) = \tfrac{3}{8}F\left(\mu + \frac{1}{\sqrt{3}}\right). \tag{113}$$

It is, therefore, seen that the first approximation is far too crude to disclose the essentially finer features of our problem. We therefore proceed to the higher approximations.

i) *Second approximation.*—In this approximation it is found that

$$\kappa_1 = \sqrt{\tfrac{7}{3}}\,; \qquad k_1 = \sqrt{5}; \qquad \text{and} \qquad k_2 = \sqrt{\tfrac{7}{6}}\,. \tag{114}$$

Further, the constants L_1, M_1, M_2, and Q have the values

$$\left.\begin{aligned} L_1 = -0.19265\,; \qquad M_1 = +0.021830\,; \qquad M_2 = -0.029516\,; \\ Q = +0.69638\,; \end{aligned}\right\} \tag{115}$$

and the laws of darkening for the emergent radiation in the two states of polarization take the forms

$$\left.\begin{aligned} I_l(0, \mu) = \tfrac{3}{8}F\left\{\mu + 0.69638 - (1-\mu^2)\frac{0.19265}{1 + 1.5275\mu}\right. \\ \left. + 0.021830(1 - 2.23607\mu) - 0.029516(1 - 1.08012\mu)\right\} \end{aligned}\right\} \tag{116}$$

and

$$I_r(0, \mu) = \tfrac{3}{8}F\left\{\mu + 0.69638 - \frac{0.0873215}{1 + 2.23607\mu} + \frac{0.0049193}{1 + 1.08012\mu}\right\}. \tag{117}$$

Values of $I_l(0, \mu)$ and $I_r(0, \mu)$ obtained[11] from the preceding formulae are given in Table 1.

ii) *Third approximation.*—In this approximation the characteristic equations for κ^2 and k^2 are

$$\kappa^4 - 8.64\kappa^2 + 9.24 = 0 \tag{118}$$

and

$$k^6 - 14.82k^4 + 36.12k^2 - 23.1 = 0\,. \tag{119}$$

The characteristic roots are

$$\left.\begin{aligned} \kappa_1 = 2.718381\,; \qquad \kappa_2 = 1.118216\,; \qquad k_1 = 3.458589\,; \\ k_2 = 1.327570\,; \qquad \text{and} \qquad k_3 = 1.046766\,. \end{aligned}\right\} \tag{120}$$

[11] I am indebted to Mrs. Frances H. Breen for assistance with these calculations.

The constants of integration L_1, L_2, Q, M_1, M_2, and M_3 are found to have the values

$$\left.\begin{aligned} &L_1 = -0.1402646\,; \quad L_2 = -0.06791696\,; \quad Q = +0.705927\,, \\ &M_1 = +0.00718392\,; \quad M_2 = +0.01861255\,; \quad M_3 = -0.0328664\,; \end{aligned}\right\} \tag{121}$$

and the laws of darkening for the emergent radiation in the two states of polarization take the forms

$$\left.\begin{aligned} I_l(0, \mu) = \tfrac{3}{8}F \Big\{ &\mu + 0.705927 - (1-\mu^2)\Big[\frac{0.1402646}{1+2.718381\mu} \\ &+ \frac{0.06791696}{1+1.118216\mu}\Big] + 0.00718392(1-3.458589\mu) \\ &+ 0.01861255(1-1.327570\mu) - 0.0328664(1-1.046766\mu) \Big\} \end{aligned}\right\} \tag{122}$$

TABLE 1

THE LAW OF DARKENING IN THE EMERGENT RADIATION IN THE TWO STATES OF POLARIZATION GIVEN BY THE SECOND APPROXIMATION

μ	$I_l(0, \mu)/F$	$I_r(0, \mu)/F$	$I_l(0, \mu)/I_l(0, 1)$	$I_r(0, \mu)/I_r(0, 1)$
0.	0.1860	0.2302	0.2967	0.3673
0.1	.2331	.2735	0.3718	0.4363
0.2	.2789	.3150	0.4448	0.5025
0.3	.3238	.3554	0.5165	0.5670
0.4	.3681	.3951	0.5871	0.6303
0.5	.4119	.4344	0.6570	0.6929
0.6	.4553	.4733	0.7263	0.7549
0.7	.4985	.5119	0.7952	0.8166
0.8	.5415	.5504	0.8637	0.8779
0.9	.5843	.5887	0.9320	0.9391
1.0	0.6269	0.6269	1.0000	1.0000

and

$$\left.\begin{aligned} I_r(0, \mu) = \tfrac{3}{8}F \Big\{ &\mu + 0.705927 - \frac{0.0787490}{1+3.458589\mu} - \frac{0.01419099}{1+1.327570\mu} \\ &+ \frac{0.00314593}{1+1.0467659\mu} \Big\}. \end{aligned}\right\} \tag{123}$$

Values of $I_l(0, \mu)$ and $I_r(0, \mu)$ obtained from the foregoing formulae are given in Table 2. Comparison with the values given in Table 1 indicates that the solution obtained in the third approximation is probably accurate to within 1 per cent over the entire range of the variables.

In Figure 2 we have illustrated the laws of darkening on the third approximation for the intensities $I_l(0, \mu)$ and $I_r(0, \mu)$. It is seen that, while they are equal at the center of the disk ($\mu = 1$), they differ by about 25 per cent at the limit ($\mu = 0$). The theory, therefore, predicts a polarization of the emergent radiation. And the degree of polarization $\delta(\mu)$, defined by

$$\delta(\mu) = \frac{I_r(0, \mu) - I_l(0, \mu)}{I_r(0, \mu) + I_l(0, \mu)}, \tag{124}$$

varies from 0 at $\mu = 1$ to 11 per cent at $\mu = 0$ (see Table 2). It is not impossible that this predicted polarization of the radiation of the early-type stars (in which scattering

by free electrons is believed to play an important part in the transfer of radiation) could be detected under suitably favorable conditions.

One further comparison is of interest. In an earlier paper (paper III) we have worked out the theory of radiative transfer in an atmosphere in which radiation is scattered in accordance with Rayleigh's phase function. This is not a strictly correct procedure, inasmuch as no allowance is made for the polarization of the existing radiation field. However, a comparison (see Table 2) of the emergent intensity $I(0, \mu)/F$ derived on the theory of transfer incorporating Rayleigh's phase function with the total emergent in-

TABLE 2

THE LAWS OF DARKENING IN THE TWO STATES OF POLARIZATION GIVEN BY THE THIRD APPROXIMATION; THE DEGREE OF POLARIZATION OF THE EMERGENT RADIATION; COMPARISON OF THE TOTAL INTENSITIES GIVEN BY THE THEORY IGNORING THE POLARIZATION OF THE EXISTING FIELD OF RADIATION BUT INCORPORATING RAYLEIGH'S PHASE FUNCTION

μ	$\frac{I_l(0,\mu)}{F}$	$\frac{I_r(0,\mu)}{F}$	$\frac{I_l(0,\mu)}{I_l(0,1)}$	$\frac{I_r(0,\mu)}{I_r(0,1)}$	$\frac{I_r(0,\mu)}{I_l(0,\mu)}$	$\delta(\mu)$	$\frac{I_l(0,\mu)+I_r(0,\mu)}{F}$	$\frac{I(0,\mu)}{F}$ for Rayleigh's Phase Function
0.....	0.1840	0.2310	0.2914	0.3659	1.2557	0.1134	0.4151	0.4195
0.1.....	.2354	.2767	0.3728	0.4382	1.1753	.0806	0.5120	0.5175
0.2.....	.2832	.3190	0.4486	0.5053	1.1264	.0594	0.6023	0.6076
0.3.....	.3291	.3598	0.5213	0.5699	1.0932	.0445	0.6890	0.6937
0.4.....	.3738	.3997	0.5921	0.6330	1.0691	.0334	0.7735	0.7773
0.5.....	.4178	.4390	0.6616	0.6953	1.0508	.0248	0.8567	0.8593
0.6.....	.4611	.4779	0.7303	0.7569	1.0364	.0179	0.9390	0.9402
0.7.....	.5041	.5165	0.7983	0.8181	1.0247	.0122	1.0206	1.0203
0.8.....	.5467	.5549	0.8659	0.8789	1.0150	.0075	1.1017	1.0998
0.9.....	.5891	.5932	0.9331	0.9396	1.0069	0.0034	1.1824	1.1789
1.0.....	0.6314	0.6314	1.0000	1.0000	1.0000	0	1.2628	1.2576

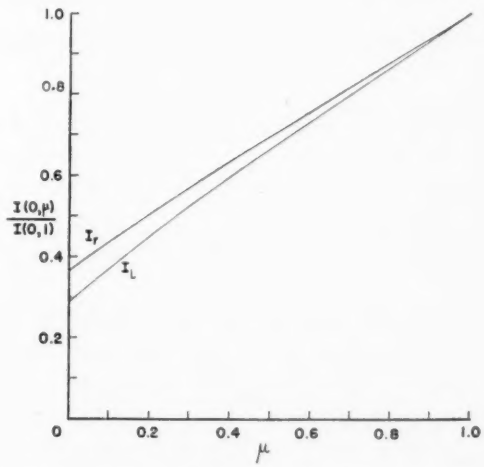

FIG. 2.—The laws of darkening in the two states of polarization. The symbol I_l refers to the component polarized with the electric vector in the meridian plane, while I_r refers to the component polarized with the electric vector at right angles to the meridian plane.

tensity $[I_l(0, \mu) + I_r(0, \mu)]/F$ given by our present more exact theory shows that the errors made in the *total intensities* by ignoring the polarization of the radiation field are small.

6. *The reduction of the laws of darkening in the two states of polarization to certain closed forms.*—In § 4 we derived expressions for the angular distribution of the emergent radiation in the two states of polarization (eqs. [111] and [112]). These expressions involve certain constants of integration ($2n$ of them in the nth approximation), and it would appear that these have to be evaluated before the solutions can be brought to their numerical forms. However, we shall now show how, for the purposes of characterizing the emergent radiation, we can avoid the necessity of solving explicitly for these constants by expressing the laws of darkening in forms in which they require only a knowledge of characteristic roots k_α and κ_β.

First, we may observe that equations (90) and (91), which determine the constants of integration, can be re-written as

$$S_l(\mu_i) = 0 \qquad \text{and} \qquad S_r(\mu_i) = 0 \qquad (i = 1, \ldots, n), \tag{125}$$

where

$$S_l(\mu) = (1 - \mu^2) \sum_{\beta=1}^{n-1} \frac{L_\beta}{1 - \mu\kappa_\beta} + \sum_{\alpha=1}^{n} M_\alpha (1 + k_\alpha \mu) - \mu + Q \tag{126}$$

and

$$S_r(\mu) = -\mu + Q - \sum_{\alpha=1}^{n} \frac{M_\alpha (k_\alpha^2 - 1)}{1 - \mu\kappa_\alpha}. \tag{127}$$

In terms of these same functions the angular distribution of the emergent radiation in the two states of polarization can also be expressed. For, according to equations (111) and (112), we can write

$$I_l(0, \mu) = \tfrac{3}{8} F S_l(-\mu) \qquad \text{and} \qquad I_r(0, \mu) = \tfrac{3}{8} F S_r(-\mu). \tag{128}$$

We shall now show how explicit expressions for the functions $S_l(\mu)$ and $S_r(\mu)$ can be obtained.

First, we shall define the functions $R(\mu)$, $R_\alpha(\mu)$, $\rho(\mu)$ and $\rho_\beta(\mu)$ according to the formulae

$$R(\mu) = \prod_{\alpha=1}^{n} (1 - k_\alpha \mu); \qquad R_\alpha(\mu) = \prod_{a \neq \alpha} (1 - k_a \mu), \tag{129}$$

and

$$\rho(\mu) = \prod_{\beta=1}^{n-1} (1 - \kappa_\beta \mu); \qquad \rho_\beta(\mu) = \prod_{b \neq \beta} (1 - \kappa_b \mu). \tag{130}$$

Considering, now, the function $S_l(\mu)$, we see that $R(\mu)S_l(\mu)$ is a polynomial of degree n in μ which vanishes for $\mu = \mu_i$ $(i = 1, \ldots, n)$. We must, accordingly, have a relation of the form

$$S_l(\mu) = \sigma \frac{P(\mu)}{\rho(\mu)}, \tag{131}$$

where σ is a constant and

$$P(\mu) = \prod_{i=1}^{n} (\mu - \mu_i). \tag{132}$$

The function $S_l(\mu)$ is therefore determinate apart from a constant of proportionality. Apart from this same constant of proportionality, the constants L_β can also be determined. For, according to equations (126) and (131),

$$\left(1-\frac{1}{\kappa_\beta^2}\right)L_\beta=\sigma\frac{P(1/\kappa_\beta)}{\rho_\beta(1/\kappa_\beta)}\qquad(\beta=1,\ldots,n-1).\quad(133)$$

Moreover, setting $\mu=+1$, respectively, -1, in equations (126) and (131) we obtain

$$S_l(+1)=\sum_{\alpha=1}^{n}M_\alpha(1+k_\alpha)-1+Q=\sigma\frac{P(1)}{\rho(1)},\qquad(134)$$

and

$$S_l(-1)=\sum_{\alpha=1}^{n}M_\alpha(1-k_\alpha)+1+Q=\sigma\frac{P(-1)}{\rho(-1)}.\qquad(135)$$

Adding and subtracting these two equations, we have

$$\sum_{\alpha=1}^{n}M_\alpha=\alpha\sigma-Q\qquad(136)$$

and

$$\sum_{\alpha=1}^{n}M_\alpha k_\alpha=\beta\sigma+1,\qquad(137)$$

where we have written

$$\alpha=\frac{1}{2}\left[\frac{P(1)}{\rho(1)}+\frac{P(-1)}{\rho(-1)}\right]\quad\text{and}\quad\beta=\frac{1}{2}\left[\frac{P(1)}{\rho(1)}-\frac{P(-1)}{\rho(-1)}\right].\qquad(138)$$

Considering, next, the function $S_r(\mu)$, we observe that we must have a proportionality of the form

$$R(\mu)S_r(\mu)\propto P(\mu)(\mu+c),\qquad(139)$$

where c is a constant, since the quantity on the right-hand side is a polynomial of degree $n+1$ in μ and has the zeros $\mu=\mu_i$ $(i=1,\ldots,n)$. The constant of proportionality in equation (139) can be found from a comparison of the coefficients of the highest powers of μ on either side. In this manner we find that

$$S_r(\mu)=(-1)^{n+1}k_1\ldots k_n\frac{P(\mu)}{R(\mu)}(\mu+c).\qquad(140)$$

From equations (127) and (140) we now conclude that

$$M_\alpha=(-1)^n k_1\ldots k_n\frac{P(1/k_\alpha)}{R_\alpha(1/k_\alpha)(k_\alpha^2-1)}\left(\frac{1}{k_\alpha}+c\right)\qquad(\alpha=1,\ldots,n).\quad(141)$$

Also, setting $\mu=0$ in equations (127) and (140), we have

$$\sum_{\alpha=1}^{n}M_\alpha(k_\alpha^2-1)-Q=k_1\ldots k_n\mu_1\ldots\mu_n c.\qquad(142)$$

On the other hand, from the characteristic equation (72) for k we infer that

$$k_1 \ldots . k_n \mu_1 \ldots . \mu_n = \frac{1}{\sqrt{2}} . \tag{143}$$ [12]

Hence,

$$\sum_{a=1}^{n} M_a (k_a^2 - 1) = Q + \frac{c}{\sqrt{2}} . \tag{144}$$

Adding equations (136) and (144), we have

$$\sum_{a=1}^{n} M_a k_a^2 = a\sigma + \frac{c}{\sqrt{2}} . \tag{145}$$

Finally, substituting for M_a according to equation (141), we can re-write equations (136) and (137) in the forms

$$\xi_{-1} + c\,\xi_0 = a\sigma - Q , \tag{146}$$

$$\xi_0 + c\,\xi_1 = \beta\sigma + 1 , \tag{147}$$

and

$$\xi_1 + c\,\xi_2 = a\sigma + \frac{c}{\sqrt{2}} , \tag{148}$$

where

$$\xi_m = (-1)^n k_1 \ldots . k_n \sum_{a=1}^{n} \frac{P(1/k_a)\, k_a^m}{R_c(1/k_a)(k_a^2 - 1)} \qquad (m = -1, 0, 1, 2) . \tag{149}$$

To evaluate the sum occurring on the right-hand side of equation (149), we introduce the function

$$f_m(x) = \sum_{a=1}^{n} \frac{P(1/k_a)\, k_a^m}{R_a(1/k_a)(k_a^2 - 1)} R_a(x) \qquad (m = -1, 0, 1, 2) , \tag{149a}$$

and express ξ_m in terms of it. Thus,

$$\xi_m = (-1)^n k_1 \ldots . k_n f_m(0) . \tag{150}$$

[12] This relation follows most readily from the characteristic equation written in the form

$$\sum_{j=0}^{n} p_{2j} \Delta_{2j} = 0 ,$$

where the p_{2j}'s are the coefficients of μ^{2j} in the Legendre polynomial $P_{2n}(\mu)$ and

$$\Delta_{2j} = \sum_{i=1}^{n} \frac{a_i (1 - \mu_i^2) \mu_i^{2j}}{1 - k^2 \mu_i^2} .$$

The Δ's defined in this manner satisfy the recursion formula

$$\Delta_{2j} = \frac{1}{k^2} \left(\Delta_{2j-2} - \frac{2}{4j^2 - 1} \right) .$$

For the characteristic equation (72), $\Delta_0 = \frac{1}{3}$ and $\Delta_2 = 2/3k^2$. From the recursion formula we therefore conclude that Δ_{2n} starts with $2/3k^{2n}$. The equation for k must accordingly have the form

$$\tfrac{1}{3} p_0 k^{2n} + \ldots . + \tfrac{2}{3} p_{2n} = 0 .$$

Hence,

$$k_1^2 \ldots . k_n^2 = \frac{(-1)^n p_{2n}}{2 p_0} = \frac{1}{2 \mu_1^2 \ldots . \mu_n^2} .$$

Now, $f_m(x)$ defined as in equation (149) is a polynomial of degree $(n-1)$ in x, which takes the values

$$\frac{P(1/k_a)\,k_a^m}{k_a^2-1} \tag{151}$$

for $x = 1/k_a$, $(a = 1, \ldots, n)$. In other words,

$$(1-x^2)\,f_m(x) - x^{2-m}P(x) = 0 \quad \text{for} \quad x = \frac{1}{k_a} \quad \text{and} \quad a = 1, \ldots, n. \tag{152}$$

The polynomial on the right-hand side of equation (152) must therefore divide $R(x)$. There must, accordingly, exist a relation of the form

$$(1-x^2)\,f_m(x) - x^{2-m}P(x) = R(x)\Psi(x), \tag{153}$$

where $\Psi(x)$ is a polynomial of degree 3, 2, 1, or 1 in x for $m = -1, 0, 1$, or 2, respectively. To determine $\Psi(x)$ more explicitly we must consider each case separately. We shall illustrate the procedure for the case $m = -1$.

For $m = -1$, equation (153) becomes

$$(1-x^2)\,f_{-1}(x) - x^3P(x) = R(x)(A_{-1}x^3 + B_{-1}x^2 + C_{-1}x + D_{-1}), \tag{154}$$

where A_{-1}, B_{-1}, C_{-1}, and D_{-1} are certain constants to be determined. The constants A_{-1} and B_{-1} readily follow from a comparison of the coefficients of x^{n+3} and x^{n+2} on either side of equation (154). In this manner we find

$$A_{-1} = \frac{(-1)^{n+1}}{k_1 \ldots k_n} \quad \text{and} \quad B_{-1} = \frac{(-1)^n}{k_1 \ldots k_n}\left(\sum_{j=1}^{n}\mu_j - \sum_{a=1}^{n}\frac{1}{k_a}\right). \tag{155}$$

Next, putting $x = +1$, respectively -1, in equation (154), we have

$$A_{-1} + B_{-1} + C_{-1} + D_{-1} = -\frac{P(1)}{R(1)}, \tag{156}$$

and

$$-A_{-1} + B_{-1} - C_{-1} + D_{-1} = +\frac{P(-1)}{R(-1)}. \tag{157}$$

These equations determine the remaining constants C_{-1} and D_{-1}. In particular,

$$D_{-1} = f_{-1}(0) = -b + \frac{(-1)^{n+1}}{k_1 \ldots k_n}\left(\sum_{j=1}^{n}\mu_j - \sum_{a=1}^{n}\frac{1}{k_a}\right), \tag{158}$$

where (cf. eq. [138])

$$b = \frac{1}{2}\left[\frac{P(1)}{R(1)} - \frac{P(-1)}{R(-1)}\right]. \tag{159}$$

From equation (150) we now conclude that

$$\xi_{-1} = (-1)^{n+1}k_1 \ldots k_n b - \left(\sum_{j=1}^{n}\mu_j - \sum_{a=1}^{n}\frac{1}{k_a}\right). \tag{160}$$

The evaluation of ξ_0, ξ_1, and ξ_2 proceeds along similar lines. We find

$$\xi_0 = (-1)^{n+1}k_1 \ldots k_n a + 1, \tag{161}$$

$$\xi_1 = (-1)^{n+1}k_1 \ldots k_n b, \tag{162}$$

and

$$\xi_2 = (-1)^{n+1}k_1 \ldots k_n a + \frac{1}{\sqrt{2}}. \tag{163}$$

In equations (161) and (163) a stands for (cf. eq. [138])

$$a = \frac{1}{2}\left[\frac{P(1)}{R(1)} + \frac{P(-1)}{R(-1)}\right]. \tag{164}$$

With the foregoing expressions for ξ's, equations (147) and (148) become

$$a + bc = \frac{(-1)^{n+1}}{k_1 \ldots . k_n}\beta\sigma, \tag{165}$$

and

$$b + ac = \frac{(-1)^{n+1}}{k_1 \ldots . k_n}\alpha\sigma. \tag{166}$$

These equations determine c and σ. We find

$$c = -\frac{\alpha a - \beta b}{\alpha b - \beta a}, \tag{167}$$

and

$$\sigma = (-1)^n k_1 \ldots . k_n \frac{a^2 - b^2}{\alpha b - \beta a}. \tag{168}$$

Equation (146) now determines Q. After some minor reductions we find that

$$Q = -c + \sum_{j=1}^{n}\mu_j - \sum_{\alpha=1}^{n}\frac{1}{k_\alpha}. \tag{169}$$

Finally, substituting for c and σ according to equations (167) and (168) in equations (131) and (140), we obtain

$$S_l(\mu) = \frac{1}{\sqrt{2}}\frac{a^2 - b^2}{\alpha b - \alpha\beta}\frac{(-1)^n}{\mu_1 \ldots . \mu_n}\frac{P(\mu)}{\rho(\mu)}, \tag{170}$$

and

$$S_r(\mu) = \frac{1}{\sqrt{2}}\frac{(-1)^{n+1}P(\mu)}{\mu_1 \ldots . \mu_n R(\mu)}\left(\mu - \frac{\alpha a - \beta b}{\alpha b - \beta a}\right). \tag{171}$$

The laws of darkening now follow according to equation (128).

We may note here that in the third approximation

$$\sigma = -3.3351 \quad \text{and} \quad c = -0.87134.$$

7. *Concluding remarks.*—The successful solution of a specific problem in theory of radiative transfer distinguishing the different states of polarization justifies the hope that it will be possible to solve other astrophysical problems in which polarization plays a significant role. Thus it may be expected that a theory of diffuse reflection along the lines of an earlier paper of this series[13] but incorporating the polarization of the existing field of diffuse radiation will account, in a general way, for the remarkable observations of Lyot[14] on the polarization of the reflected light from Venus. We hope to return to these and similar essentially more difficult problems in the theory of radiative transfer in the near future.

I am indebted to Dr. G. Herzberg for helpful discussions on some of the physical aspects of the problem considered in this paper.

Note added May 6: The problem of diffuse reflection from a semi-infinite plane-parallel atmosphere, allowing for the partial polarization of the diffuse radiation has now been solved. It is hoped to publish the results of this investigation in the near future.

[13] *Ap. J.*, **103**, 165, 1946.

[14] *Ann. Obs. Meudon* (Paris), **8**, 66, 1929.

THE SPECTRUM OF CLUSTER-TYPE CEPHEIDS

GUIDO MÜNCH[1] AND LUIS RIVERA TERRAZAS
Yerkes Observatory
Received February 4, 1946

ABSTRACT

The spectral variations of the cluster cepheid RR Lyrae throughout its light-curve have been investigated. It is found that the spectrum of the variable is peculiar at all phases, in the sense that the hydrogen lines are too weak for the spectral types indicated by the *Ca* II K line and the metallic lines; the latter indicate types of F0 at minimum light and A2 slightly before maximum. These spectral types are in agreement with the color of the variable at the corresponding phases. The hydrogen lines alone would indicate a spectral type of F0 at maximum brightness and F6 at minimum. The luminosity criteria give for the variable about the same absolute magnitude as that of a normal giant. Among ten other objects of the RR Lyrae class, seven were found to be also peculiar, in a manner similar to RR Lyrae.

I. INTRODUCTION

In a recent article that summarizes the present knowledge on the spectra of cepheid variables, O. Struve[2] has drawn attention to the convenience of locating the stars of the short end of the period-luminosity relation in the two-dimensional classification system of Morgan, Keenan, and Kellman. The object of the present work is to present the results of the study of a series of spectrograms covering the light-curve of RR Lyrae, the brightest of the members of the class. One or two spectrograms of each of ten other variables of this class have been obtained, at undetermined phases of their light-oscillation, and for only one of them, SW Andromedae, exposures at maximum and minimum light were secured. The spectrograms of all the variables, as well as of the comparison stars, were obtained on Eastman 103*a*-O plates with the small one-prism spectrograph used in the preparation of the *Atlas of Stellar Spectra*.

II. THE SPECTRAL VARIATIONS OF RR LYRAE

The total number of spectrograms obtained for RR Lyrae is forty-six, each one of which is represented in Figure 1 by a dot drawn on the mean photographic light-curve of the variable by Hertzsprung.[3] The epoch of median increasing brightness,

$$T_0 = \text{July } 29.386,\ 1945 \pm 0^d.007\ (\text{C.S.T.}), \qquad (1)$$

was determined by eye estimates at the finders of the telescope during the rise of the variable on the nights of July 29–30 and August 3–4, 1945. The observations in other parts of the light-curve were made on the nights of July 6–7, 7–8, and 26–27 and were reduced to one cycle by the use of Sterne's mean constant period, namely, $0^d.56684186$. It is true that this procedure is not entirely correct on account of the departures of the period of the variable from a mean value; but since, according to Sterne,[4] such departures cannot be accurately predicted, we neglected them altogether, inasmuch as in the descending branch of the light-curve the changes in spectral type are quite slow.

It has been shown before[5] that the spectrum of RR Lyrae is peculiar and cannot be located uniquely in a spectral-classification system, because the hydrogen lines are much too weak for the spectral type indicated by the intensity of the *Ca* II K line or of the

[1] Latin-American Fellow of the John Simon Guggenheim Memorial Foundation.

[2] *Observatory*, **65**, 227, 1944.

[3] *B.A.N.*, **1**, 139, 1922.

[4] *Harvard Circ.* No. 387, p. 16, 1934.

[5] Morgan, Keenan, and Kellman, *An Atlas of Stellar Spectra*, Pl. 33, Chicago, 1943.

metallic lines. In general, we have found that this is true throughout the whole light-curve (Pl. XIII) and, moreover, that, disregarding the peculiar behavior of the hydrogen lines, the variable can be classified following the criteria established for giant stars. The actual description of the spectral changes can be made as follows:

a) The spectrum appears to be earliest on plates taken at phases 0.021 P and 0.024 P, that is, about 30 minutes before maximum light. From the intensity of the metallic lines and of the K line we assign a spectral type of A2, by comparing with the standard ζ Ursae Majoris (br). The hydrogen lines alone would indicate a spectral type of around F0.

b) At maximum light the K and metallic lines indicate a spectral type of A3.

c) The spectral type derived from the K and metallic lines in exposures at phases 0.190 P and 0.227 P is A5. Applying to these spectra the luminosity criteria of the system used, we obtain the same absolute magnitude as β Trianguli (A5 III).

d) At phases 0.574 P, 0.576 P, and 0.611 P the K and metallic lines give a spectral type and a luminosity equal to that of γ Bootis (A7 III).

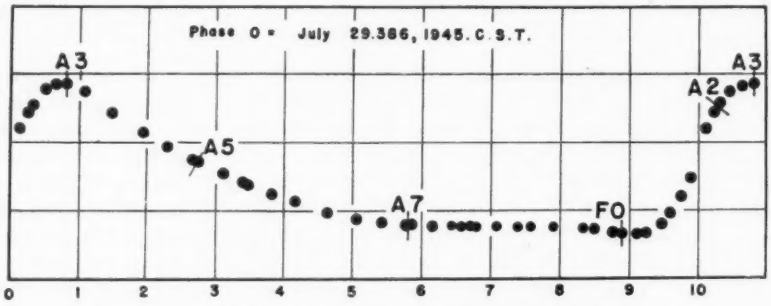

FIG. 1.—Spectral types of RR Lyrae throughout its light-curve

e) At minimum light the K and metallic lines indicate a spectral type close to that of ζ Leonis (F0 III). The luminosity derived corresponds again to that of a normal giant. The hydrogen lines alone would give a spectral type of around F6.

f) Finally, the changes in the K line of *Ca* II and in the metallic lines in the ascending branch of the light-curve are first noticed in a plate of phase 0.942 P, where they resemble again the spectrum of γ Bootis. At phase 0.958 P they approach closely to those of β Trianguli and from there on rapidly decrease to their minimum intensity described under *a*.

In connection with these results, it is of interest to recall that the range of variation in spectral type generally adopted for RR Lyrae is the one given by Shapley,[6] namely, from B9 to F2. Since these types are in the HD system, we wish to point out that none of our plates taken near maximum light shows a trace of the line *He* I λ 4026, and instead they show metallic lines with an intensity that does not correspond to a spectral type earlier than A2.

III. THE COLOR EQUIVALENTS OF RR LYRAE

In order to find out whether the spectral type indicated by the K and metallic lines or that indicated by the hydrogen lines corresponds to the intensity distribution in the continuous spectrum of RR Lyrae, the color equivalents of the variable were determined at maximum and minimum light. For this purpose we have followed a modification of the Tikhoff method worked out by W. W. Morgan. Accordingly, we have obtained, on the Eastman 103*a*-E emulsion, a series of exposures of the field of the variable

[6] *Ap. J.*, **43**, 217, 1916.

PLATE XIII

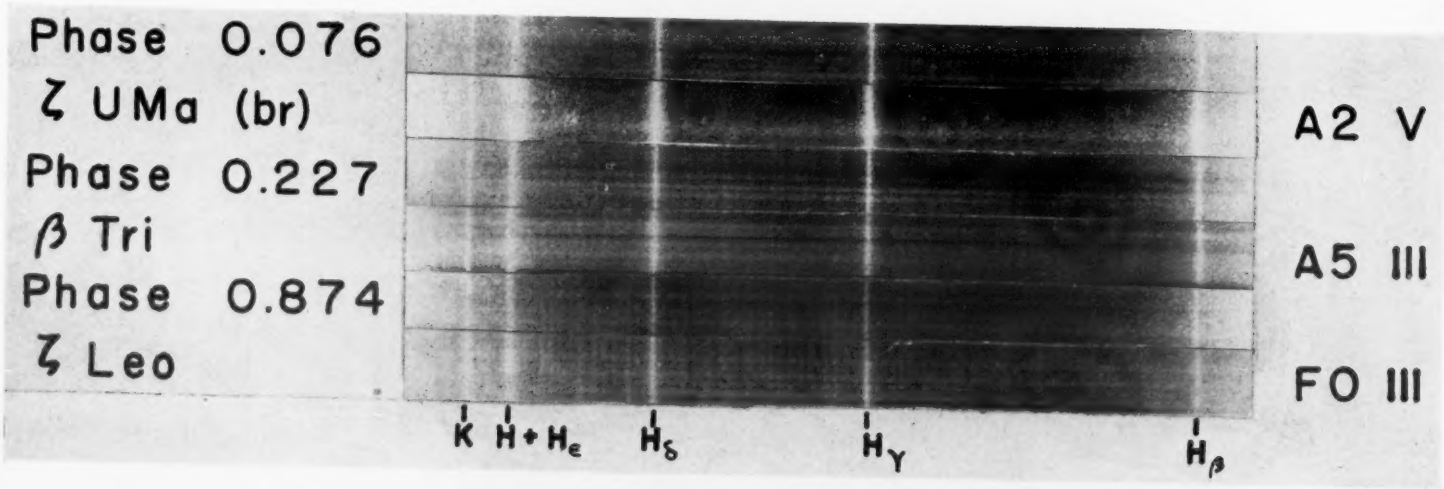

SPECTRA OF RR LYRAE AND COMPARISON STARS

Phases are measured from the time of median increasing brightness in units of the mean period

PLATE XIV

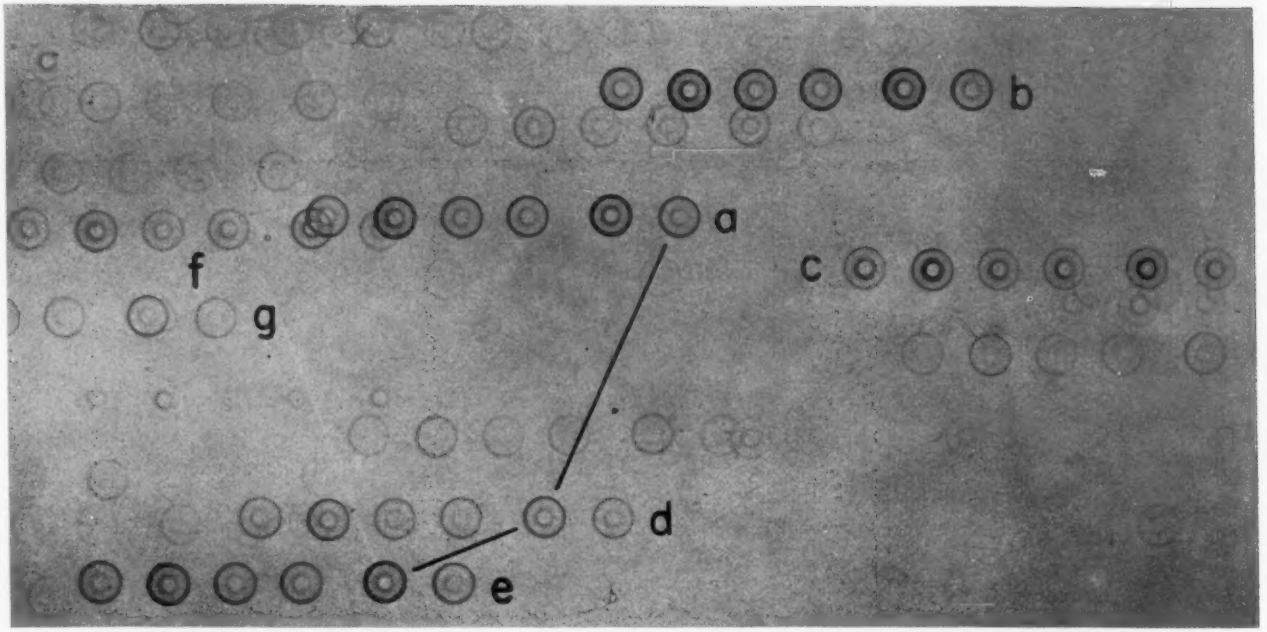

(*a*) RR Lyrae; (*b*) HD 182487, $m = 6.92$, AO; (*c*) HD 182054, $m = 7.18$, KO(HD); (*d*) HD 183125, $m = 7.7$, K line A3, metallic lines F2; (*e*) HD 183383, $m = 7.42$, AO; (*f*) HD 183473, $m = 8.6$, GO(HD); (*g*) HD 183787, $m = 8.8$, A5. (The visual magnitudes are taken from the HD catalogue.) The image at the right was taken at maximum light of RR Lyrae on October 9, 1945, with 4^m exposure. The succeeding images were exposed 8^m, 4^m, 4^m, 8^m, and 4^m, respectively. The plate was obtained with the 10-inch Bruce telescope on the Eastman 103 a-E emulsion. A central stop of 8 inches in diameter was placed in front of the lens. The inner ring is due to red light, the outer to blue. The red rings of the images of *a*, *d*, and *e* connected with lines are approximately equal, while the blue ring is strongest for the AO star. The difference in color index between *d* and *e* is about 0.30 mag.

through the 10-inch Bruce telescope, with the center of the lens covered by an 8-inch circular diaphragm. Under these conditions, if the plate is placed 5 mm outside the blue focus, a stellar image appears as two concentric rings, the outer one formed by light of effective wave length around λ 4300; the inner one with λ_{eff} near 6000 A. To illustrate the appearance of the images obtained, a section of one of the plates secured is reproduced in Plate XIV. The relative intensities of the blue and red rings of the star considered, when compared with those of stars of previously determined color, fixes the color equivalent of the star very simply and quite accurately. Following this procedure, we observed RR Lyrae during a rise from minimum to maximum light. The epoch T_0 of median increasing brightness was estimated from the intensity of the blue rings of the different exposures of the variable, when compared with the corresponding rings of field stars with known photographic magnitude. It was found that

$$T_0 = \text{Oct. } 9.945,\ 1945 \pm 0^d.005\ (\text{C.S.T.}). \qquad (2)$$

Since between this epoch and the one given by (1) there is a difference of 73 days, an interval that represents, roughly, twice the short-term oscillation of the period of the variable from a mean value, a check of our epoch (1) is provided by the more accurate one (2), when reduced with Sterne's mean constant period referred to above. Actually, we

TABLE 1

Star	Date	Type	Star	Date	Type
XZ Cyg	1945 May 31.055	A5	T Sex	1945 Jan. 4.130	A2
VY Ser	July 2.958	A7	RR Cet	Sept. 7.125	A5
VX Her	July 15.956	F0	RX Eri	Oct. 3.197	A3
RZ Cep	Aug. 4.121	A2	SU Dra	Nov. 5.204	A2

found both epochs to be in agreement within the mean errors with which they have been fixed.

As a final result we found that at minimum the variable has about the same color as BD+42°3340, which is a metallic-line star, with a K line of type A3 and metallic lines of type F2. As it is now known that the metallic-line stars have a color corresponding to the spectral type indicated by the metallic lines, we can say that, at minimum, RR Lyrae has a color equivalent of approximately f2. Similarly, it was found that at maximum light the variable is slightly redder than BD+41°3352, the spectrum of which is A0 V. It seems fairly certain that any selective interstellar absorption effect is very small. In addition, the distances of RR Lyrae and the A0 comparison star is of the same order of magnitude (around 200 parsecs), and any possible slight effect of selective absorption would be similar for the two objects. As a consequence, we may conclude that the oscillation in effective temperature of the variable is compatible with the derived oscillation in spectral type, if indicated by the intensity of the metallic lines and K.

IV. SPECTRAL TYPES FOR TEN OTHER CLUSTER CEPHEIDS

With the purpose of finding out whether the peculiarity of the spectrum of RR Lyrae is characteristic of all cluster cepheids, it was decided to obtain some individual exposures of other members of the class. The objects selected for observation were taken from the list given by C. Payne Gaposchkin and S. Gaposchkin.[7] Of the nine stars observed, seven show a spectrum that can be compared with that of RR Lyrae at a certain phase. These stars are given in Table 1, together with the date of exposure in C.S.T. and the spectral type as derived from the intensity of the K and metallic lines.

[7] *Variable Stars*, Harvard Mono. No. 5, pp. 185–186, 1938.

Stars that do not show the same kind of spectrum as RR Lyrae are discussed below.

SW Andromedae.—Exposures secured on August 17.067 and September 2.062 show a spectrum close to that of a giant of type F6, with hydrogen lines apparently of normal intensity for such a class. However, in a plate taken immediately after the afore-mentioned, on September 2.144, the spectrum looks peculiar, the K and metallic lines giving a spectrum around A7; but the hydrogen lines are somewhat weaker than in a normal star of such type, although the effect is not so pronounced as in RR Lyrae. On the night of September 2 it was noticed that the variable increased from minimum to maximum light, but the time when the rise began was missed. Therefore, it is very likely that the exposure showing the earliest spectrum is a combination of the maximum and the minimum.

AR Persei.—On two exposures (September 15.067 and October 3.075) the spectrum looks like that of a normal star of class F6. However, owing to the faintness of this object, the plates are underexposed, and therefore the estimation of spectral type is not so accurate as is that of the stars listed above.

It is a pleasure to record our indebtedness to Dr. W. W. Morgan for suggesting the problem, for his advice, and for permitting us to use his spectrograms of some standard stars and of T Sextantis.

NOTES

MICROWAVE RADIATION FROM THE SUN AND MOON*

G. C. Southworth[1] has reported the measurement of microwave radiation from the sun with a conventional superheterodyne receiver and a large parabolic antenna. This note is to report similar measurements made with a microwave radiometer, which was designed primarily for the measurement of the atmospheric absorption of water vapor by observing the thermal radiation emitted by the atmosphere.[2] The instrument has also been used to observe the microwave radiation from the sun and moon. These astronomical measurements are quite incomplete because of the pressing demands of war research. It was decided, however, to report them now, since it seems unlikely that the authors will be able to continue this work.

The radiometer[3] measured the thermal radiation in a small band (0.06 per cent) of wave lengths at a wave length of 1.25 cm. Its sensitivity was such that it could detect a change of $\frac{1}{2}$° C in the temperature of a black body. Stated more exactly, the root-mean-square fluctuation in the indicating meter was about $\frac{1}{2}$° C when expressed in temperature units.

For the astronomical measurements the radiometer was provided with a parabolic-reflector antenna (18-inch diameter). This antenna had a measured half-power beam width of 2° and a measured gain of 6.0×10^3 times that of an isotropic radiator. The radiometer was calibrated by replacing the antenna by an artificial black body (mounted in a wave-guide), which could be heated to known temperatures. Three series of astronomical measurements were made, all at Cambridge, Massachusetts. These will be described below.

a) The microwave radiation from the sun was observed during the partial eclipse of July 9, 1945. The results are shown as points in Figure 1. The radiation intensities are expressed in arbitrary units but have been corrected for atmospheric absorption, using the results of thermal-radiation measurements made at the same time, which gave an absorption of 0.46 db/atmosphere (i.e., 0.46 db total absorption for a vertical path through the atmosphere). The curve of Figure 1 is the calculated intensity during the eclipse, assuming a uniform sun disk of optical size and the optical percentage of eclipse. It is arbitrarily adjusted to fit the measured points under the above assumptions. The agreement between this curve and the measured points indicates that the size of the sun's disk at $\lambda = 1.25$ cm is not greatly different from that at optical wave lengths. The ordinate of Figure 1 may be put into absolute units by a knowledge of the sensitivity of the radiometer and the antenna gain. The results of such a calculation are indicated in Figure 1 by the length of the arrow labeled 1.0×10^4° K. It is seen that the best fit with the observations is obtained with an effective black-body temperature for the sun of 1.0×10^4° K.

b) On July 12, 1945, the microwave radiation from the sun was measured in a similar manner. The atmospheric absorption at that time was 0.38 db/atmosphere. The effective black-body temperature of the sun was found to be 1.1×10^4° K.

c) On October 19, 1945, at 10:25 P.M., E.S.T., the effective black-body temperature of the nearly full moon was measured to be 292° K. It was assumed that the moon's disk

* This paper is based on work done for the Office of Scientific Research and Development under Contract OEMsr-262 with the Massachusetts Institute of Technology.

[1] *J. Frank Inst.*, 239, 285, 1945.

[2] To appear shortly in *Phys. Rev.*

[3] Details of the device will appear shortly in the *Rev. Sci. Inst.*

was a uniform radiator subtending an angle of 32′ along a diameter. The measured atmospheric absorption at that time was 0.24 db/atmosphere.

The only known sources of large error in these measurements are the calibration of the radiometer and the measurement of the antenna gain. The radiometer calibration is a direct comparison between the radiation received by the antenna and that emitted by a black body at a known temperature. The antenna gain was measured several times

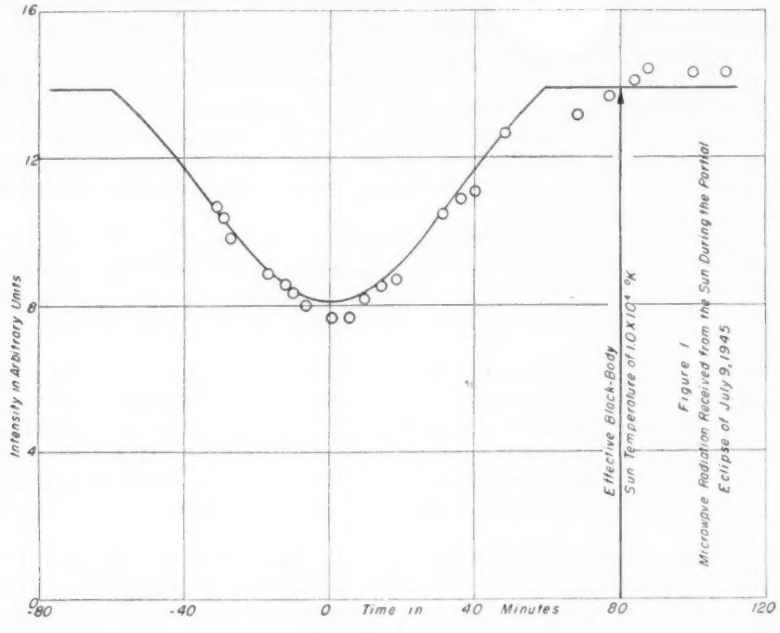

FIG. 1

by two different methods[4] and is believed to be reliable. The probable error in the effective black-body temperatures of the sun and moon is believed to be about ± 10 per cent.

ROBERT H. DICKE
ROBERT BERINGER

PALMER PHYSICAL LABORATORY
PRINCETON UNIVERSITY
SLOAN PHYSICS LABORATORY
YALE UNIVERSITY
March 30, 1946

THE NEAR-ECLIPSING SPECTROSCOPIC BINARIES AS A MEANS FOR STUDYING PECULIAR PHENOMENA IN CLOSE DOUBLE STARS

In recent years much excellent research has been devoted to elucidating some of the puzzling phenomena in close binary systems. There remain, however, several unexplained peculiarities, of which the skewness of light- and velocity-curves is one example. The

[4] These measurements were kindly made for us by members of the antenna group of this laboratory.

light-variation of an eclipsing binary may be thought of as consisting of a number of components attributable to such phenomena as eclipse, ellipticity, gravity-brightening, and reflection. The term "skewness" is used to describe components which contribute to the asymmetry observed in the light-curves of many eclipsing variables.[1] Kopal[2] has suggested as a possible method of explaining skewness a careful study of the line profiles of such stars as U Cephei. But there is available another, perhaps less powerful but still valuable, method of investigation. This is the precise photometric study of that neglected class of spectroscopic binaries which have high orbital inclinations but no eclipses. Photometry of such objects may yield observations of the skew components largely unaffected by the much greater light-variations caused by an eclipse.

A theory of the origin of the skew components of light-variation is needed, among other reasons, to aid the precise analysis of several available accurate photoelectric light-curves. For instance, the writer has an unpublished light-curve for AR Lacertae, which should be analyzed for darkening coefficients. This curve shows strong skewness; and, if reliable darkening coefficients are to be derived, a practicable theory for skewness is required.

One criterion for selection of suitable spectroscopic binaries for investigations of skewness evidently is a short period, probably under 3 days. For example, J. B. Irwin[3] did not find appreciable skewness in photoelectric light-curves in two colors for the eclipsing binary U Sagittae, which has a period of 3.38 days, and no skewness was detected by the writer[4] in either the blue or the red light-curves for YZ Cassiopeiae, which has a period of 4.47 days. On the other hand, skewness is present in both the velocity- and the light-curves of U Cephei ($P = 2.49$ days) and in the light-curve of AR Lacertae ($P = 1.98$ days). An inspection of Baker's[5] photoelectric light-curve for u Herculis ($P = 2.05$ days) indicates that a slight amount of skewness accompanies the small asymmetry of the radial velocity-curve. In general, then, favorable cases seem to be those with short periods, and possibly with large ratios of the diameters of the binary components. Among the stars which satisfy these criteria are Nos. 67, 113, 123, 176, and 286 in Moore's *Fourth Catalogue of Spectroscopic Binaries*.[6] No. 286 (HD 176853) is of particular interest because it has been found by S. Gaposchkin[7] to be an eclipsing binary with minima only 0.08 mag. in depth. The possibility exists that a considerable fraction of this light-variation may be caused by effects other than those due to eclipse and that any variation to be expected from skewness is not seriously distorted by a grazing eclipse.

A precise photometric study of the near-eclipsing variables may also throw additional light upon the nature of stars having peculiarities attributable to extended atmospheres; two such examples are SX Cas and the Wolf-Rayet eclipsing binary, HD 193576. Precise light-curves for several Wolf-Rayet spectroscopic binaries, such as HD 152270,[8] might also disclose significant variations not attributable to an eclipse.

GERALD E. KRON

LICK OBSERVATORY
April 17, 1946

[1] P. H. Taylor, *Ap. J.*, **94**, 46, 1941.

[2] *Ap. J.*, **99**, 239, 1944.

[3] Dissertation, unpublished.

[4] *Lick Obs. Bull.*, **19**, 59, 1939 (No. 499); *Ap. J.*, **96**, 173, 1942; *Contr. Lick Obs.*, Ser. II, No. 5.

[5] *Lick Obs. Bull.*, **12**, 130, 1926.

[6] *Lick Obs. Bull.*, **18**, 1, 1936, (No. 483).

[7] *Harvard Bull.*, No. 917, p. 5, 1943.

[8] O. Struve, *Ap. J.*, **100**, 384, 1944.

NEW *Hα* EMISSION STARS

The spectra of the following stars (Table 1) have been found to have the *Hα* line in emission on an objective-prism plate obtained with the Schmidt telescope at the Case School of Applied Science in Cleveland on October 15, 1944. The photovisual magnitudes are rough estimates, based on Gaposchkin's sequence for the variable Z Lacertae (*Harvard Ann.*, Vol. **108,** No. 1). The estimates in the last column of Table 1 are on an arbitrary scale of 1 to 3.

TABLE 1

NEW EMISSION-LINE STARS

No.	Star	α (1900)	δ (1900)	Pv. Mag.	Int. *Hα* Emission
1	AC+57°57939	22h10m 8s	+56°44′.4	11.6	2
2	AC+57°57718	22 10 56	56 17.5	11.0	2
3	AC+57°59236	22 14 30	57 2.6	11.5	2
4	AC+57°59172	22 16 12	56 54.3	11.2	2
5	BD+55°2725	22 16 37	55 53.1	10.1	2
6	BD+57°2510	22 18 0	57 51.4	10.7	1
7	AC+59°54029	22 18 0	58 7.9	11.6	1
8	Anon.	22 20 14	58 40.2	11.7	3
9	BD+57°2525	22 21 23	57 20.0	10.2	3
10	Anon.	22 21 37	58 32.9	12.2	2
11	AC+57°59246	22 22 17	57 2.2	11.3	1
12	AC+57°59089	22 23 19	56 36.9	10.7	1
13	AC+55°64276	22 24 42	55 30.2	10.8	3
14	AC+59°54351	22 25 26	58 7.9	11.8	2
15	AC+59°54421	22 25 37	58 24.4	11.9	3
16	AC+57°60526	22 27 34	57 56.8	11.1	3
17	AC+57°60196	22 27 56	57 8.8	11.2	1
18	AC+57°60492	22 33 44	57 48.8	11.2	3
19	AC+55°64300	22 35 44	55 32.8	12.0	1
20	AC+57°61154	22 35 49	57 10.4	11.5	3
21	AC+59°54453	22 36 34	58 27.1	11.5	3
22	Anon.	22 37 29	58 50.1	11.3	2
23	AC+55°65968	22 38 52	55 58.5	12.0	2
24	AC+57°61488	22 40 7	57 58.8	11.4	2
25	AC+57°60603	22 40 13	56 4.5	10.8	3
26	AC+57°60716	22 41 12	56 16.9	10.6	3
27	AC+57°61129	22 42 39	57 5.8	11.4	2
28	BD+57°2615	22 43 50	57 37.2	9.9	3
29	AC+57°61101	22 44 20	57 1.3	11.0	2
30	Anon.	22 44 59	57 11.1	12.1	2

It is fairly certain that as a group these stars are of class Be. The thirty stars listed are included within a range of approximately 2 mag.; it seems very likely, therefore, that they are in the same general region in space. Since the area of the plate is around 20 square degrees, the frequency of all the emission-line stars in this region is of the order of two per square degree, including known Be and Wolf-Rayet stars. The extent of the area rich in Be stars is not known, since plates of adjoining regions were not available.

We are indebted to Dr. J. J. Nassau, director of the Warner and Swasey Observatory, for permission to obtain the plate used.

W. W. MORGAN
W. P. BIDELMAN

YERKES OBSERVATORY
April 1946

PLATE XV

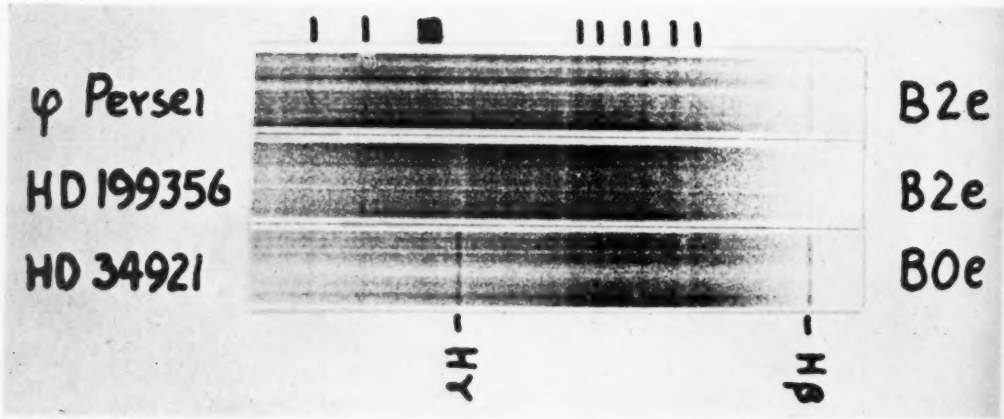

EMISSION LINES OF FE II IN THE SPECTRA OF HD 199356 AND HD 34921
The spectrum of φ PERSEI is shown for comparison

UNIV. OF MICH.

Be STARS SHOWING BRIGHT LINES OF *Fe* II

The following Be stars (Table 1) have recently been found to have spectra similar to that of φ Persei in the characteristic of bright lines of *Fe* II. The strength of the iron emission lines has been estimated on a scale such that intensity 1 corresponds to the faintest emission considered definitely present, and 3 to an intensity similar to φ Persei. It is possible that the iron emission lines vary in intensity in 59 Cygni; on September 4, 1942, they were definitely present, while on July 30, 1943, they were weak or absent. The presence of iron emission lines at λ 4233 and λ 4585 was suspected by McLaughlin[1] in the spectrum of 105 Tauri.

TABLE 1

NEW IRON EMISSION STARS

Star HD No.	MWC	α (1900)	δ (1900)	m	Sp HD	Sp MKK	*Fe* Int.
232552	19	$1^h45^m.9$	+54° 50′	8.2	B0	B0::	2
56 Eri	89	4 39.3	− 8 41	5.87	B5	B2e	2
105 Tau	98	5 2.0	+21 34	5.95	B3p	B2e	1
33152	99	5 3.2	+36 53	7.8	B2	B2e	2
34921	107	5 15.8	+37 35	7.39	B0	B0e	2–3
37657	118	5 35.1	+43 0	6.99	B3	B3e	1
37967	122	5 37.2	+23 10	6.06	B3	B3e	1
44458	138	6 16.8	−11 44	5.49	B2p	B2e	2
45314	140	6 21.6	+14 57	7.09	Oe5	B1e::	1
50083	156	6 46.5	+ 5 13	6.76	B2p	B2e	1
o Pup	186	7 43.9	−25 42	4.59	B2	B2e	2
161306	271	17 39.7	− 9 46	8.31	B	B2e:	2
183362	318	19 24.1	+37 44	6.36	B2	B3e	1
187567	322	19 45.5	+ 7 39	6.39	B3	B3e	1:
193009	336	20 12.9	+32 4	7.02	B0p	B2e	2
199356	357	20 51.6	+39 55	7.02	B0p	B2e	2–3
59 Cyg	359	20 56.4	+47 8	4.86	B0p	B1e	1

The plates were obtained with a small spectrograph attached to the 40-inch telescope and have a dispersion of around 125 A/mm at $H\gamma$. The spectra were greatly widened during exposure to insure maximum visibility of faint, broad features. Plate XV shows spectrograms of HD 34921 and HD 199356, together with φ Persei for comparison.

W. W. MORGAN
IRENE HANSEN

YERKES OBSERVATORY
April 1946

[1] *Pub. Obs. U. Michigan*, **4**, 181, 1932.

ON THE POLARIZATION OF THE CONTINUOUS RADIATION OF EARLY-TYPE STARS

A program has been undertaken at the Yerkes Observatory to determine whether the polarization of the continuous radiation of early-type stars, as predicted by S. Chandrasekhar,[1] can be detected observationally. As the theory shows that the maximum degree of polarization is to be expected only in early-type stars and, further, that it varies from zero at the center to about 11 per cent at the limb, it was necessary to select an early-type eclipsing variable. The system U Sagittae appears to satisfy the necessary requirements. The spectrum of U Sagittae has been classified by A. H. Joy[2] as B9n, and the light-curve shows a deep minimum when the B9n star is eclipsed by the gG2 star. This is the only system which has been investigated so far.

For preliminary observations a Wollaston prism was made and attached to a rotatable plateholder. Plates were then taken at the 40-inch telescope, while the plateholder was rotated during the times just preceding and following the period of totality. Plates were also obtained in a similar fashion of a near-by star to determine the degree of instrumental errors.

A comparison of the differences in intensities of the two beams with the change in angle as shown by U Sagittae and the near-by star gives evidence that there is a discernible amount of polarization at the limb of U Sagittae. As this amount varies with both time and angle, further observations are being undertaken to ascertain the direction and amount of maximum polarization. Similar observations are also planned for Z Vulpeculae, which should also be a good case.

EDITH M. JANSSEN

YERKES OBSERVATORY
June 5, 1946

[1] *Ap.J.*, **103**, 363, 1946.

[2] *Ap.J.*, **71**, 336, 1930.

REVIEWS

Tables of Associated Legendre Functions. Prepared by MATHEMATICAL TABLES PROJECT, NATIONAL BUREAU OF STANDARDS. New York: Columbia University Press, 1945. Pp. 46+306. $5.00.

There are fourteen principal and five supplementary tables. For example, Table I gives the values of $P_n^m(\cos\theta)$ for values of n from 1 to 10, of m from 1 to 4 ($m \leqslant n$), and of θ from 0° to 90° in intervals of 1°; results are given to six significant figures. Also tabulated are $dP_n^m(\cos\theta)/d\theta$, $P_n^m(x)$, $1 \leqslant x \leqslant 10$; $Q_n^m(x)$, $1 \leqslant x \leqslant 10$; its derivative; and other variations of these functions involving pure imaginary arguments and half-integral values of n. There is also a valuable Bibliography.

Table of Arc Sin x. Prepared by MATHEMATICAL TABLES PROJECT, NATIONAL BUREAU OF STANDARDS. New York: Columbia University Press, 1945. Pp. 19+124. $3.50.

The principal table lists the values of arc sin x to twelve decimal places at intervals of 0.0001 for the range $0 \leqslant x \leqslant 0.9890$, and at intervals of 0.00001 for $0.9890 \leqslant x \leqslant 1$. The second central difference is also tabulated. The methods and accuracy of interpolation are discussed in the Introduction. There are six short auxiliary tables, which facilitate interpolation.

The Theory of Eclipses. By A. A. MIKHAILOV. (In Russian.) Moscow and Leningrad: Government Publishing House for Technical and Theoretical Literature (Gostekhizdat), 1945. Pp. 199+chart. R. 10.

A methodically arranged and clear presentation of all the essential topics of the theory of solar and lunar eclipses (117 pp.); of occultations of stars and of planets by the moon (27 pp.); of the transits of Mercury and of Venus (26 pp.); and a brief account of the eclipses, occultations, and transits of the satellites of Jupiter and of Saturn (8 pp.). Readers interested in eclipsing binaries or in problems of solar physics connected with total eclipses of the sun are referred to textbooks on astrophysics; a five-page section is, however, devoted to the geometrical aspects of ionospheric and corpuscular eclipses. The Appendixes include nine pages of tables and an alphabetically arranged Bibliography of 139 numbered items. There is a detailed Table of Contents and a good Index. The 56 figures in the text are well reproduced; the typography is good; and the proofreading was done with great care.

A. A. Mikhailov was born in 1888; for more than thirty years he has been contributing to the theory and the computation of eclipses; his *Theory of Solar Eclipses* (in Russian) and his *Tables pour le calcul des éclipses du soleil* appeared in 1925. The book under review reflects the interests of the author—geometrical and analytical methods, tabular and mechanical aids to computation. He devotes a couple of pages to the instruments used for the computation of occultations, giving, incidentally, an illustrated description of A. A. Yakovkin's instrument. In his four-page section on the "Western and Eastern Limits of the Principal Phase," he discusses the "elliptical" curves at the ends of the path of the umbra and gives the formulae for their computation; at the end of the discussion he admits that the computation of these curves is of little practical value. In R. Buchanan's *The Mathematical Theory of Eclipses* (Philadelphia, 1904), the subject of these terminal curves is dismissed (p. 117) in three lines: "The umbral cone, of course, forms small circles of rising and setting curves, similar to those of the penumbra, and surrounding the points K and L on the earth's surface; but they are never computed."

The book under review is very valuable both for students of astronomy and for computers of eclipses, occultations, and transits. All the important topics of the classical theory of solar and lunar eclipses are discussed in sufficient detail in the limited space assigned to them. The author's lack of interest in problems of eclipse statistics and of eclipse classification is, however, reflected in a somewhat inadequate treatment of several topics. Thus, he repeats—echoing the compilers of standard textbooks on astronomy and the editors of articles on eclipses in the best of encyclopaedias—the obsolete data on the number of eclipses in a saros series; these data were acceptable guesses before 1887, but they should have been corrected after the publication of Oppolzer's

Canon der Finsternisse. Some of the statements concerning the saros are objectionable on various grounds.

R. Schram's introduction of the concept of noncentral solar eclipses was a great step forward —threescore years ago—in the classification of eclipses; when the first three signatures of the *Canon der Finsternisse* (pp. 1–24) were already printed, the noncentral eclipses achieved recognition; they constituted only 0.8 per cent of all the solar eclipses, but they soon annexed the partial eclipses, which constitute 35.3 per cent of all the solar eclipses; the unsatisfactory traditional division of solar eclipses into partial and central eclipses was thus superseded by the computationally more satisfactory division into noncentral (36.1 per cent) and central (63.9 per cent) eclipses; the very nature of the eclipse phenomena—produced either by the penumbra or by the umbra—suggests a division into penumbral and umbral eclipses; in the case of solar eclipses, this natural classification puts the troublesome noncentral eclipses (0.8 per cent) in their proper place—among the umbral eclipses, at the ends of the umbral runs in their respective saros series, and not among the partial, i.e., among the penumbral, eclipses. In the case of lunar eclipses, this natural classification gives recognition to the traditionally overlooked penumbral eclipses and puts the partial lunar eclipses where they belong—among the umbral eclipses, at the ends of the umbral runs in their respective saros series. When Mikhailov describes, in his table on page 20, the solar eclipse of −196, February 1, as a "central eclipse near the South pole,"he merely repeats P. V. Neugebauer's mistake (*Astronomische Chronologie*, I, 25); before the Schram reform, this eclipse would have been listed as "partial"; the eclipse is listed in the *Canon* as "total, not central"; it was the first umbral eclipse of its saros series. The lunar eclipse of 2082, February 13, in Mikhailov's table on page 21, is likely to be the first penumbral eclipse of the terminal run of its saros series (*A.J.*, **47**, 47, 1938) and to be omitted from the almanacs for the year 2082, if they should continue to preserve the old tradition of disregarding the existence of penumbral lunar eclipses. Mikhailov's statement (p. 14) that the darkening of the moon by the penumbra is so insignificant that it is not noticeable without exact photometric observations is not supported by published observational and statistical data; of the 40 penumbral lunar eclipses of the first half of our century, 15 are conspicuous (the distance of the moon's limb from the umbra is less than one-fifth of the lunar diameter); the coming penumbral lunar eclipses of 1947, November 28 (in the zenith over the Pacific), and of 1948, October 18 (over the Atlantic), will be very conspicuous. The vague discussions of the frequency of occurrence of solar and lunar eclipses (pp. 23 and 24) will become clear and simple when the unscientific discriminations against penumbral lunar eclipses are abolished and the eclipse mechanism is studied objectively, in its entirety. In the case of lunar eclipses, just as in the case of solar eclipses, there *must* be, near each node, at least one eclipse (either umbral or penumbal), and there *may* be two eclipses (both penumbral); a calendar year *must* have two lunar eclipses and it *may* have three, four, or five lunar eclipses; from a theoretical and from a statistical point of view, a predictable denting of the solar disk by the terrestrial disk, as seen from the moon, is just as important as the encroachment of the lunar disk on the sun, as seen from the Arctic or the Antarctic.

Let us hope that the next edition of *The Theory of Eclipses* will treat the saros series as an important and integral part of the theory of eclipses and that it will present the problems of classification and of statistics of eclipses with the same precision and clarity that characterize the book as a whole. Even in its present imperfect state, this is probably the best book of its size on the theory of eclipses—in any European language.

ALEXANDER POGO

Carnegie Institution of Washington

The Milky Way. By BART J. BOK and PRISCILLA F. BOK. 2d ed. Philadelphia: Blakiston Co., 1945. Pp. vi+224. $2.50.

The principal change from the first edition of 1941 is the addition of a chapter summarizing recent advances in Milky Way research. The book as a whole alternates between the popular and technical points of view.

W. W. MORGAN

Sur la construction d'un spectrographe infra-rouge auto-enregistreur à grand pouvoir de résolution. By M. MIGEOTTE. (In French.) Brussels: Royal Academy of Belgium, 1945. Pp. 107. 26 illus.

In a short review, published in this country in 1944,[1] attention was called to the first results obtained by Migeotte at the University of Liége on the infrared solar spectrum in the region from 1.46 to 1.51μ.

Astrophysicists and industrial spectroscopists, as well as physicists, will be interested in Migeotte's detailed description of his infrared spectrometer, which is one of the best-conceived and equipped instruments of the type. It is to be hoped that a similar instrument will, some day, be installed at the coudé focus of a large reflector. The difficulty arising from the unavoidable variation in slit illumination can be solved by a proper method of amplification. The region from 1 to 15μ would thus be opened to planets and bright stars.

Migeotte also describes his first results on the solar spectrum from 13,440 to 15,293 A. As soon as his instrument can be reinstalled he plans to redetermine the wave lengths by superposition of the second- and third-order spectra of the spectral regions in which the solar wave lengths are accurately known. These new data will then be compared to the direct measures at present published. The latter will be quite useful, especially to the physicists who are interested in the spectrum of water vapor. Circumstances have prevented Migeotte from comparing his data on the water vapor lines with the ones recently published by H. H. Nielsen.

P. SWINGS

Pasadena, California

[1] *Ap. J.*, 99, 118, 1944.

ERRATA

The following corrections should be made in Volume **103:**

On page 209 after λ 3843.05, *Sc* II 3.00 (4) should be deleted and entered with the identifications of the preceding line.

On page 211 after λ 3894.04, *Fe* I 4.00 (2) should be deleted and entered with the identification of the preceding line.

On page 243 after 6475.17, delete *Fe* I 4.61 (1).

NOTICE

Books—war victims.—During the war the libraries of half the world were destroyed in the fires of battle and in the fires of hate and fanaticism. Where they were spared physical damage, they were impoverished by isolation. There is an urgent need—now—for the printed materials which are basic to the reconstruction of devastated areas and which can help to remove the intellectual blackout of Europe and the Orient.

There is need for a pooling of resources, for co-ordinated action, in order that the devastated libraries of the world may be restocked as far as possible with needed American publications. The American Book Center for War Devastated Libraries, Inc., has come into being to meet this need. It is a program that is born of the combined interests of library and educational organizations, of government agencies, and of many other official and nonofficial bodies in the United States.

The American Book Center is collecting and shipping abroad scholarly books and periodicals which will be useful in research and necessary in the physical, economic, social, and industrial rehabilitation and reconstruction of Europe and the Far East.

The Center cannot purchase books and periodicals; it must depend upon gifts from individuals, institutions, and organizations. Each state will be organized to participate in the program through the leadership of a state chairman. Other chairmen will organize interest in the principal subject fields. Co-operation with these leaders or direct individual contributions are welcomed.

What is needed.—Shipping facilities are precious and demand that all materials be carefully selected. Emphasis is placed upon publications issued during the past decade, upon scholarly books which are important contributions to their fields, upon periodicals (even incomplete volumes) of significance, upon fiction and nonfiction of distinction. All subjects—history, the social sciences, music, fine arts, literature, and especially the sciences and technologies—are wanted.

What is not needed.—Textbooks, outdated monographs, recreational reading, books for children and young people, light fiction, materials of purely local interest, popular magazines, such as *Time*, *Life*, *National Geographic*, etc., popular nonfiction of little enduring significance, such as Gunther's *Inside Europe*, Haliburton's *Royal Road to Romance*, etc. Only carefully selected federal and local documents are needed, and donors are requested to write directly to the Center with regard to specific documents.

How to ship.—All shipments should be sent PREPAID via the cheapest means of transportation to THE AMERICAN BOOK CENTER, % THE LIBRARY OF CONGRESS, WASHINGTON 25, D.C. Although the Center hopes that donors will assume the costs of transportation of their materials to Washington, when this is not possible, reimbursement will be made upon notification by card or letter of the amount due. *The center cannot accept material which is sent collect.* Reimbursement cannot be made for packing or for other charges beyond actual transportation. When possible, periodicals should be tied together by volume. It will be helpful if missing issues are noted on incomplete volumes.

K. R. SHAFFER, *Executive Director*

AMERICAN BOOK CENTER, INC.
LIBRARY OF CONGRESS
WASHINGTON 25, D.C.
May 13 1946

INDEX TO VOLUME 103

INDEX TO SUBJECTS

Absorption-Line Contours across the Solar Disc, The Variations of. *Merle Tuberg* . . . 145

Algol Variable SS Boötis, Orbital Elements of the. *Roscoe F. Sanford* 114

η Andromedae, The Spectroscopic Binary. *Katherine C. Gordon* 13

RT Andromedae, The Eclipsing Star. *Cecilia Payne-Gaposchkin* 291

ι Arietis, The Spectroscopic Orbit of. *Katherine C. Gordon* 16

Atomic Lines in the Spectrum of R Leonis. *Paul W. Merrill* 275

ζ Aurigae, On the Nature of the Eclipses of. *Zdeněk Kopal* 310

BD Stars within Five Degrees of the North Pole, Spectra of. *J. J. Nassau and Carl K. Seyfert* 117

Be Stars Showing Bright Lines of *Fe* II. *W. W. Morgan and Irene Hansen* 379

SS Boötis, Orbital Elements of the Algol Variable. *Roscoe F. Sanford* 114

ι Cassiopeiae, The Period of the Spectrum Variable. *Armin J. Deutsch* 99

RX Cassiopeiae, The System of. *Cecilia Payne-Gaposchkin* 299

μ Cephei, Spectrographic Observations of. *Dean B. McLaughlin* 35

U Cephei, Note on the Period of. *John G. Phillips and Arne Slettebak* 251

VW Cephei, A Photoelectric Study of. *C. M. Huffer* 1

Cepheids, The Spectrum of Cluster-Type. *Guido Münch and Luis Rivera Terrazas* . . 371

Continuous Radiation of Early-Type Stars, On the Polarization of the. *Edith M. Janssen* 380

Eclipses of ζ Aurigae, On the Nature of the. *Zdeněk Kopal* 310

Eclipsing Binaries, Spectrographic Observations of Eleven. *Otto Struve* 76

Eclipsing Star RT Andromedae, The. *Cecilia Payne-Gaposchkin* 291

Emission-Line Star near the Orion Nebulae, An Interesting. *W. W. Morgan and Stewart Sharpless* 249

Emission Stars, New *Hα*. *W. W. Morgan and W. P. Bidelman* 378

Emission Regions of the Solar Corona, The Correlation of Magnetic Disturbances with Intense. *A. H. Shapley and W. O. Roberts* 257

Hartree Field of a Hydrogen Atom, The Motion of an Electron in the. *S. Chandrasekhar and Frances Herman Breen* 41

HD 151932, The Spectrum of. *Jorge Sahade* 250

R Hydrae, Measurements in the Spectrum of. *Paul W. Merrill* 6

TT Hydrae, Spectrographic Observations of the Eclipsing Variable. *Jorge Sahade and Carlos U. Cesco* 71

Hα Emission Stars, New. *W. W. Morgan and W. P. Bidelman* 378

Hydrogen Atom, The Motion of an Electron in the Hartree Field of a. *S. Chandrasekhar and Frances Herman Breen* 41

Hydrogen, On the Equation of State of Ionized. *Ralph E. Williamson* 139

R Leonis, Atomic Lines in the Spectrum of. *Paul W. Merrill* 275

Magnetic Disturbances with Intense Emission Regions of the Solar Corona, The Correlation of. *A. H. Shapley and W. O. Roberts* 257

Magnitudes of the North Polar Sequence Stars, Red. *J. J. Nassau and Virginia Burger* 25

Microwave Radiation from the Sun and Moon. *Robert H. Dicke and Robert Beringer* . . 375

Moon, The Infrared Spectrum of the. *Arthur Adel* 19

Moon, Microwave Radiation from the Sun and. *Robert H. Dicke and Robert Beringer* . 375

Multiplier Phototube to Astronomical Photoelectric Photometry, Application of the. *Gerald E. Kron* 326

Orbital Elements of the Algol Variable SS Boötis. *Roscoe F. Sanford* 114

Orion Nebula, An Interesting Emission-Line Star near the. *W. W. Morgan and Stewart Sharpless* 249

Parallaxes with the 60- and 100-Inch Reflectors, The Photographic Determination of Stellar. Twentieth Series. *Adriaan van Maanen* 289

Photoelectric Study of VW Cephei, A. *C. M. Huffer* 1

Photographic Determination of Stellar Parallaxes with the 60- and 100-Inch Reflectors, The. Twentieth Series. *Adriaan van Maanen* 289

Photometry, Application of the Multiplier Phototube to Astronomical Photoelectric. *Gerald E. Kron* 326

Photometry of Stars, Six-Color. IV. The Variation of α Ursae Minoris at Different Wave Lengths. *Joel Stebbins* 108

Polarization of the Continuous Radiation of Early-Type Stars, On the. *Edith M. Janssen* 380

Polar Sequence Stars, Red Magnitudes of the North. *J. J. Nassau and Virginia Burger* 25

Procyon, The Spectrum of: A Typical Star of Class F. *J. W. Swensson* 207

Radiative Equilibrium of a Stellar Atmosphere, On the. IX. *S. Chandrasekhar* . . . 165

Radiative Equilibrium of a Stellar Atmosphere, On the. X. *S. Chandrasekhar* . . . 351

Radiative Equilibrium, Near Thermodynamic. *L. G. Henyey* 332

Reviews:

Beet, Ernest Agar. *A Textbook of Elementary Astronomy* 256

Bok, Bart J., and Priscilla F. Bok. *The Milky Way.* 2d ed. (W. W. Morgan) . . . 382

Bok, Priscilla F., and Bart J. Bok. *The Milky Way.* 2d ed. (W. W. Morgan) . . . 382

Cohen, I. Bernard. *Roemer and the First Determination of the Velocity of Light* (N. Ernest Dorsey) 255

Dugan, R. S., J. Q. Stewart, and H. N. Russell. *Astronomy,* Vol. I 103

Gatterer, A., and J. Junkes, with the collaboration of V. Frodl. *Atlas der Restlinien,* Vol. II: *Spektren der seltenen Erden* (Giorgio Abetti) 252

Herzberg, Gerhard. *Atomic Spectra and Atomic Structure* 103

Hellman, C. Doris. *The Comet of 1577: Its Place in the History of Astronomy* (N. T. Bobrovnikoff) 102

Junkes, J., and A. Gatterer, with the collaboration of V. Frodl. *Atlas der Restlinien,* Vol. II: *Spektren der seltenen Erden* (Giorgio Abetti) 252

Mathematical Tables Project under Sponsorship of National Bureau of Standards. *Table of Arc Sin x* 381

Mathematical Tables Project under Sponsorship of National Bureau of Standards. *Tables of Associated Legendre Functions* 381

Migeotte, M. *Sur la construction d'un spectrographe infra-rouge auto-enregistreur à grand pouvoir de résolution.* (P. Swings) 383

Mikhailov, A. A. *The Theory of Eclipses* (A. Pogo) 381

Papers contributed by the members of the Observatory staff. *One Hundred Years of the Pulkovo Observatory* (A. N. Vyssotsky) 253

Russell, H. N., R. S. Dugan, and J. Q. Stewart. *Astronomy*, Vol. I 103

Stewart, J. Q., H. N. Russell, and R. S. Dugan. *Astronomy*, Vol. I 103

Waldmeier, M. *Sonne und Erde* 103

Solar Corona, The Correlation of Magnetic Disturbances with Intense Emission Regions of the. *A. H. Shapley and W. O. Roberts* 257

Solar Disc, The Variations of Absorption-Line Contours across the. *Merle Tuberg* . . 145

Space Motions of the Cluster Variables, The. *Noah W. McLeod* 134

Spectra of BD Stars within Five Degrees of the North Pole. *J. J. Nassau and Carl K. Seyfert* 117

Spectrographic Observations of μ Cephei. *Dean B. McLaughlin* 35

Spectrographic Observations of the Eclipsing Variable TT Hydrae. *Jorge Sahade and Carlos U. Cesco* 71

Spectrographic Observations of Eleven Eclipsing Binaries. *Otto Struve* 76

Spectroscopic Binary η Andromedae, The. *Katherine C. Gordon* 13

Spectroscopic Binaries as a Means for Studying Peculiar Phenomena in Close Double Stars, The Near-eclipsing. *Gerald E. Kron* 376

Spectroscopic Orbit of ι Arietis, The. *Katherine C. Gordon* 16

Spectrum of Cluster-Type Cepheids, The. *Guido Münch and Luis Rivera Terrazas* . . 371

Spectrum of HD 151932, The. *Jorge Sahade* 250

Spectrum of R Hydrae, Measurements in the. *Paul W. Merrill* 6

Spectrum of R Leonis, Atomic Lines in the. *Paul W. Merrill* 275

Spectrum of the Moon, The Infrared. *Arthur Adel* 19

Spectrum of Procyon, The: A Typical Star of Class F. *J. W. Swensson* 207

Spectrum Variable ι Cassiopeiae, The Period of the. *Armin J. Deutsch* 99

Stellar Atmosphere, On the Radiative Equilibrium of a. IX. *S. Chandrasekhar* . . . 165

Stellar Atmosphere, On the Radiative Equilibrium of a. X. *S. Chandrasekhar* . . . 351

Stellar Models with Partially Degenerate Isothermal Cores and Point-Source Envelopes. *Marjorie Hall Harrison* 193

Sun and Moon, Microwave Radiation from the. *Robert H. Dicke and Robert Beringer* . . 375

Thermodynamic Radiative Equilibrium, Near. *L. G. Henyey* 332

α Ursae Minoris at Different Wave Lengths, Six-Color Photometry of Stars. IV. The Variation of. *Joel Stebbins* 108

Van Maanen, Adriaan. *Ralph E. Wilson* 105

Variables, The Space Motions of the Cluster. *Noah W. McLeod* 134

INDEX TO AUTHORS

ABETTI, GIORGIO. Review of: *Atlas der Restlinien*, Vol. II: *Spektren der seltenen Erden*, A. Gatterer and J. Junkes, with the collaboration of V. Frodl 252

ADEL, ARTHUR. The Infrared Spectrum of the Moon 19

BERINGER, ROBERT, and ROBERT H. DICKE. Microwave Radiation from the Sun and Moon 375

BIDELMAN, W. P., and W. W. MORGAN. New *Hα* Emission Stars 378

BOBROVNIKOFF, N. T.: Review of: *The Comet of 1577: Its Place in the History of Astronomy*, C. Doris Hellman 102

BREEN, FRANCES HERMAN, and S. CHANDRASEKHAR. The Motion of an Electron in the Hartree Field of a Hydrogen Atom 41

BURGER, VIRGINIA, and J. J. NASSAU. Red Magnitudes of the North Polar Sequence Stars 25

CESCO, CARLOS U., and JORGE SAHADE. Spectrographic Observations of the Eclipsing Variable TT Hydrae 71

CHANDRASEKHAR, S. On the Radiative Equilibrium of a Stellar Atmosphere. IX . . . 165

CHANDRASEKHAR, S. On the Radiative Equilibrium of a Stellar Atmosphere. X . . . 351

CHANDRASEKHAR, S., and FRANCES HERMAN BREEN. The Motion of an Electron in the Hartree Field of a Hydrogen Atom 41

DEUTSCH, ARMIN J. The Period of the Spectrum Variable ι Cassiopeiae 99

DICKE, ROBERT H., and ROBERT BERINGER. Microwave Radiation from the Sun and Moon 375

DORSEY, N. ERNEST. Review of: *Roemer and the First Determination of the Velocity of Light*, I. Bernard Cohen 255

GORDON, KATHERINE C. The Spectroscopic Binary η Andromedae 13

GORDON, KATHERINE C. The Spectroscopic Orbit of ι Arietis 16

HANSEN, IRENE, and W. W. MORGAN. Be Stars Showing Bright Lines of *Fe* II . . . 379

HARRISON, MARJORIE HALL. Stellar Models with Partially Degenerate Isothermal Cores and Point-Source Envelopes 193

HENYEY, L. G. Near Thermodynamic Radiative Equilibrium 332

HUFFER, C. M. A Photoelectric Study of VW Cephei 1

JANSSEN, EDITH M. On the Polarization of the Continuous Radiation of Early-Type Stars 380

KOPAL, ZDENĚK. On the Nature of the Eclipses of ζ Aurigae 310

KRON, GERALD E. Application of the Multiplier Phototube to Astronomical Photoelectric Photometry 326

KRON, GERALD E. The Near-eclipsing Spectroscopic Binaries as a Means for Studying Peculiar Phenomena in Close Double Stars 376

McLAUGHLIN, DEAN B. Spectrographic Observations of μ Cephei 35

McLEOD, NOAH W. The Space Motions of the Cluster Variables 134

MERRILL, PAUL W. Atomic Lines in the Spectrum of R Leonis 275

MERRILL, PAUL W. Measurements in the Spectrum of R Hydrae 6

MORGAN, W. W., and W. P. BIDELMAN. New *Hα* Emission Stars 378

MORGAN, W. W., and IRENE HANSEN. Be Stars Showing Bright Lines of *Fe* II . . . 379

MORGAN, W. W. Review of: *The Milky Way*. 2d ed. Bart J. Bok and Priscilla F. Bok . 382

MORGAN, W. W., and STEWART SHARPLESS. An Interesting Emission-Line Star near the Orion Nebula 249

MÜNCH, GUIDO, and LUIS RIVERA TERRAZAS. The Spectrum of Cluster-Type Cepheids . 371

NASSAU, J. J., and VIRGINIA BURGER. Red Magnitudes of the North Polar Sequence Stars 25

NASSAU, J. J., and CARL K. SEYFERT. Spectra of BD Stars within Five Degrees of the North Pole 117

PAYNE-GAPOSCHKIN, CECILIA. The Eclipsing Star RT Andromedae 291

PAYNE-GAPOSCHKIN, CECILIA. The System of RX Cassiopeiae 299

PHILLIPS, JOHN G., and ARNE SLETTEBAK. Note on the Period of U Cephei 251

POGO, A. Review of: *The Theory of Eclipses*, A. A. Mikhailov 381

ROBERTS, W. O., and A. H. SHAPLEY. The Correlation of Magnetic Disturbances with Intense Emission Regions of the Solar Corona 257

SAHADE, JORGE. The Spectrum of HD 151932 250

SAHADE, JORGE, and CARLOS U. CESCO. Spectrographic Observations of the Eclipsing Variable TT Hydrae 71

SANFORD, ROSCOE F. Orbital Elements of the Algol Variable SS Boötis 114

SEYFERT, CARL K., and J. J. NASSAU. Spectra of BD Stars within Five Degrees of the North Pole 117

SHAPLEY, A. H., and W. O. ROBERTS. The Correlation of Magnetic Disturbances with Intense Emission Regions of the Solar Corona 257

SHARPLESS, STEWART, and W. W. MORGAN. An Interesting Emission-Line Star near the Orion Nebula 249

SLETTEBAK, ARNE, and JOHN G. PHILLIPS. Note on the Period of U Cephei 251

STEBBINS, JOEL. Six-Color Photometry of Stars. IV. The Variation of α Ursae Minoris at Different Wave Lengths 108

STRUVE, OTTO. Spectrographic Observations of Eleven Eclipsing Binaries 76

SWENSSON, J. W. The Spectrum of Procyon: A Typical Star of Class F 207

SWINGS, P. Review of: *Sur la construction d'un spectrographe infra-rouge auto-enregistreur à grand pouvoir de résolution*, M. Migeotte 383

TERRAZAS, LUIS RIVERA, and GUIDO MÜNCH. The Spectrum of Cluster-Type Cepheids . 371

TUBERG, MERLE. The Variations of Absorption-Line Contours across the Solar Disc. . 145

VAN MAANEN, ADRIAAN. The Photographic Determination of Stellar Parallaxes with the 60- and 100-Inch Reflectors. Twentieth Series 289

VYSSOTSKY, A. N. Review of: *One Hundred Years of the Poulkovo Observatory.* Papers contributed by the members of the Observatory staff 253

WILLIAMSON, RALPH E. On the Equation of State of Ionized Hydrogen 139

WILSON, RALPH E. Adriaan van Maanen 105

371
145
289
253
139
105